General Disclaimer

One or more of the Following Statements may affect this Document

- This document has been reproduced from the best copy furnished by the organizational source. It is being released in the interest of making available as much information as possible.

- This document may contain data, which exceeds the sheet parameters. It was furnished in this condition by the organizational source and is the best copy available.

- This document may contain tone-on-tone or color graphs, charts and/or pictures, which have been reproduced in black and white.

- This document is paginated as submitted by the original source.

- Portions of this document are not fully legible due to the historical nature of some of the material. However, it is the best reproduction available from the original submission.

Produced by the NASA Center for Aerospace Information (CASI)

E75-10323
CR-142925

"Made available under NASA sponsorship
in the interest of early and wide dis-
semination of Earth Resources Survey
Program information and without liability
for any use made thereof."

AN EVALUATION OF ERTS DATA FOR OCEANOGRAPHIC USES THROUGH GREAT LAKE STUDIES

by
A.E. Strong and H.G. Stumpf

NOAA/NESS

(E75-10323) AN EVALUATION OF ERTS DATA FOR OCEANOGRAPHIC USES THROUGH GREAT LAKES STUDIES Final Report (National Environmental Satellite Service) 254 p HC $8.50 CSCL 08H G3/43

N75-26467

Unclas 00323

1106A

color
Original photography may be purchased from
EROS Data Center
10th and Dakota Avenue
Sioux Falls, SD 57198

AN EVALUATION OF ERTS DATA FOR OCEANOGRAPHIC USES THROUGH GREAT LAKES STUDIES

by

A.E. Strong

and

H.G. Stumpf

Department of Commerce
National Oceanic and Atmospheric Administration
National Environmental Satellite Service
Suitland, Maryland 20233

December 1974

Final Report

Prepared for
GODDARD SPACE FLIGHT CENTER
Greenbelt, Maryland 20771

RECEIVED
JUN 09 1975
SIS/902.6

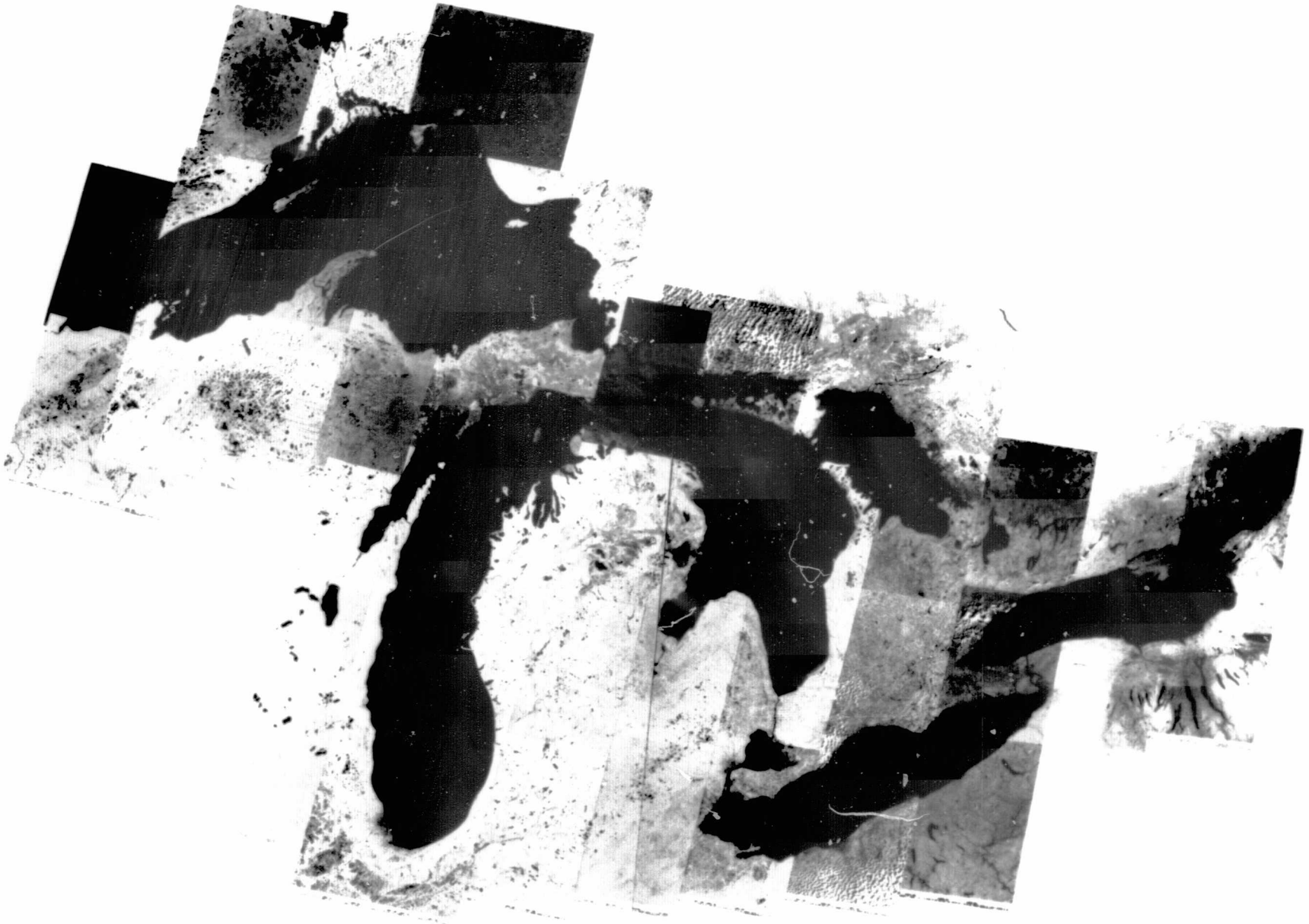

Preface

The main objective of the following ERTS-1 work was to exploit satellite-obtained multispectral data for Great Lakes observations. Near-coincident NOAA-2 satellite data have also been utilized to provide additional information in the thermal-infrared part of the spectrum.

A broad-based approach enabled us to develop techniques for monitoring high concentrations of surface biomass and algal blooms in the Great Lakes during late summer and early fall. Chemical precipitation in the near-surface layer is readily observed by ERTS-1 and was found more extensive than previously believed. These "whitings" have been seen observed as regular summer and fall events in three of the Great Lakes--Lakes Michigan, Erie, and Ontario.

The high resolution of the MSS instrument permitted ice vector movement studies on successive days where overlapping data were available. These opportunities were infrequent in the Great Lakes because of the extensive cloud-cover that normally occurs in the study area during the winter months.

Water color displays a positive correlation with surface water temperature during the spring and early summer months as the surface water becomes increasingly warmer. This correlation reverses for fall and early winter. Since most of the color in the Great Lakes is due to river effluents or shoreline erosion (the lakes were at record high levels during all of our observations), the resulting turbidity is found principally in the nearshore regions. The correlation was anticipated as it is these shallow nearshore waters that respond most quickly to warming in the spring and cooling in the fall.

Of all our ERTS-1 findings the most troubling was the extensive

sunglint contamination. At the latitude of the Great Lakes the effect of glitter was most obvious from April to August. Although contamination of the imagery (water scenes only) is possible for solar elevations below 50° it is most apparent when the sun elevation exceeds 55°. A model is employed to permit a better understanding of these effects. Glint becomes most troublesome at the low wind speeds typical of clear sky conditions, i.e. those needed for ERTS-1 observations.

The final, and most rigorous, study presents a nearly-complete set of circulation charts for five Great Lake areas that revealed numerous natural color tracers: southern Lake Michigan, southern Lake Huron, Lake St. Clair, Lake Erie and Lake Ontario. These charts were further categorized by a weighted three-day resultant wind stress. Whenever possible these derived currents were compared with previous analyses of lake currents.

Our Great Lakes ERTS-1 study resulted in the following recommendations for future investigations:

The ERTS System

(1) Incorporate a thermal-infrared detector as an additional MSS channel.

(2) Consider a sensor-pointing capability to avoid the sunglint problem under high solar elevation,

(3) Add multispectral capability in the blue region (0.45-0.5μm) of the spectrum for better "whiting" and biomass detection.

(4) Provide quantitative radiances.

(5) Develop better calibration techniques to prevent banding in future sensors.

(6) Provide additional amplification for the low radiances typical of water scenes.

(7) Consider an orbit closer to local noon. Geometry permits high solar elevations for better water color data and increased depth penetration capability. A pointable sensor is essential for a noon orbit to avoid sunglint effects along the sub-satellite track.

(8) More frequent coverage is essential for coastal work.

Algal Studies

(1) Further investigate a correlation of surface chlorophyll and biomass with low level variability in 0.7-0.8μm data.

(2) Investigate other lakes and periods for high surface concentrations of algae using the classification developed in the study.

(3) Compare Great Lakes classification signatures with oceanic observations (red tides, etc.).

Chemical Precipitation

(1) Develop a classification technique for monitoring the depth of the upper level of whitings.

(2) Investigate relationship of radiation intensity observed in 0.5-0.6μm data to the concentration of calcium carbonate.

(3) Monitor changes in evolution of whiting events.

(4) Survey other ERTS-1 data for similar classifications in oceanic areas. Whitings reportedly occur in such regions as the Florida Keys and Persian Gulf.

Ice

(1) More frequent coverage is needed to monitor ice movement in the Great Lakes, although in overlapping areas ice motions may be charted over two-day intervals.

(2) Ice condition information is augmented by the multispectral approach (especially the 0.8-1.1μm channel), but could benefit from additional spectral data in the near-infrared (wavelengths up to 2μm).

Sunglint

(1) Calm water areas could be charted readily using images contaminated by sunglint; information on glitter probabilities should be provided all marine and lake investigators.

(2) Oil spills and other pollutants with similar capillary wave damping attributes are easily detected in sunglint highlight areas; more work seems appropriate in this area for automatic classification.

(3) Current boundaries frequently provide contrasting roughness fields that are enhanced by sunglint.

(4) If more quantitative radiance data could be gleaned in sunglint regions, the surface wind field could be calculated.

Circulation Mapping

(1) Some resultant wind stress conditions were not observed in all of the five areas studied. These omitted wind directions should be incorporated as they are observed during subsequent cloud-free overpasses.

(2) Additional areas in the Great Lakes should be monitored for circulation features as conditions permit. Lake Superior was not included in this study; portions of that lake have the extensive turbidity needed for circulation observations.

(3) Refinements of the circulation charts become more tentative in those areas most distant from the wind stations used.

Figure List

		Page
1.	ERTS-1 Great Lakes Coverage Chart	1-2
2.	Chart of western Lake Erie.	2-2
3.	15 October 1972 aircraft multispectral photography.	2-4
4.	Thermal scanner image over the area delimited in Fig. 2.	2-5
5.	Digitally enhanced ERTS-1 data from 15 October 1972.	2-6
6.	False-color enhancement of ERTS-1 MSS-6 data for Kelleys Island test site.	2-8
7.	Kelleys Island 4-channel training on algal bloom.	2-10
8.	Lake Erie algal bloom classification for 15 October 1972.	2-12
9a.	Digitally enhanced MSS-5 ERTS-1 data for 9 September 1972.	2-14
9b.	Digitally enhanced MSS-6 ERTS-1 data for 9 September 1972.	2-14
10.	False-color enhancement of 9 September ERTS-1 MSS-4 data for Point Pelee Test Site.	2-15
11.	Same as Figure 10--MSS-5.	2-16
12.	Same as Figure 10--MSS-6.	2-17
13.	Point Pelee gyre 4-channel training on algal bloom.	2-19
14.	Lake Erie algal bloom classification for 9 September 1972.	2-20
15.	Unbanded classification of Figure 14.	2-22
16.	12 September 1972 ERTS-1 imagery of Utah Lake.	2-24
17.	Surface weather for 21 August 1973 in the Lake Michigan region.	3-3
18.	20 August 1973 NOAA-2 VHRR image.	3-4
19.	21 August 1973 enhanced NOAA-2 VHRR-IR image.	3-6
20.	Analysis of Lake Michigan surface temperatures from Figure 19.	3-7
21.	21 August 1973 NOAA-2 VHRR-VIS image of Lake Michigan.	3-8
22.	21 August 1973 ERTS-1 MSS-4 and MSS-5 imagery.	3-9

Page

23. False-color enhancement of MSS-4 and -6 for Lake Michigan. 3-11

24a. Whiting classification produced for 21 August 1973 "Milwaukee" ERTS imagery 3-13

24b. Whiting classification produced for 21 August 1973 "Chicago" ERTS imagery. 3-14

25. 22 August 1973 NOAA-2 enhanced VHRR-IR image of Lake Michigan. 3-15

26. Analysis of Lake Michigan surface temperatures from Figure 25. 3-16

27. 3 August 1973 ERTS-1 MSS-4 and MSS-5 imagery. 3-17

28. 3 August 1973 NOAA-2 VHRR-IR image of Lake Michigan 3-18

29. Whiting classification for 3 August 1973 for portions of "Chicago" ERTS imagery. 3-19

30. 29 January 1973 NOAA-2 VHRR-VIS image of Great Lakes at initiation of freeze-up on Lake Erie. 4-2

31. 14 February 1973 NOAA-2 VHRR-VIS image of Great Lakes just prior to total ice cover in Lake Erie. 4-4

32. 17 February 1973 NOAA-2 VHRR-VIS enhanced imagery of Great Lakes at time of near-100% ice cover on Lake Erie. 4-5

33. 18 February 1973 NOAA-2 VHRR-VIS image of Great Lakes area. 4-6

34. 17 February 1973 ERTS-1 MSS-5 of Lake Ontario and eastern half of Lake Erie. 4-7

35. 18 February 1973 ERTS-1 MSS-5 of middle portion of Lake Erie. 4-7

36. Ice motions from overlap area of Figures 35 and 36. 4-9

37. 27 March 1973 NOAA-2 VHRR-VIS image of Great Lakes. 4-10

38. 27 March 1973 NOAA-2 VHRR-IR enhanced image coincident with Figure 37. 4-11

39a. 16 July 1973 ERTS-1 MSS-5 image of Lake Michigan. 5-2

39b. 16 July 1973 ERTS-1 MSS-6 image of Lake Michigan. 5-3

Page

40. 16 July 1973 NOAA-2 VHRR-VIS image of Great Lakes area. 5-5

41. Sunglint modelled NOAA-2 brightness patterns for 0·m sec^{-1} wind speed. 5-6

42. Sunglint modelled NOAA-2 brightness patterns for 5·m sec^{-1} wind speed. 5-7

43. Sunglint modelled ERTS-1 brightness patterns for 0·m sec^{-1} wind speed. 5-8

44. Same as Figure 43 for 2 m sec^{-1} wind speed. 5-9

45. Same as Figure 43 for 5 m·sec^{-1} wind speed. 5-10

46. Same as Figure 43 for 10 m sec^{-1} wind speed. 5-11

47. 27 March 1973 ERTS-1 MSS-5 turbidity patterns in Lakes Huron, St. Clair and Erie. 6-2

48. 27 March 1973 NOAA-2 temperature analysis from VHRR-IR. 6-3

49. 29 April 1973 ERTS-1 MSS-4 image of Lake Ontario and eastern Lake Erie. 6-4

50. 29 April 1973 NOAA-2 temperature analysis from VHRR-IR. 6-5

51. 20 May 1973 ERTS-1 MSS-5 image of Lake Huron. 6-7

52. 20 May 1973 NOAA-2 VHRR-IR enhanced image of Great Lakes. 6-9

53. Temperature analysis from VHRR-IR data in Figure 52. 6-10

54. Wind station used for southern Lake Michigan. 7-4

55. Surface current analyses for southern Lake Michigan. 7-9/14

56. Wind station used for southern Lake Huron. 7-17

57. Surface current analyses for southern Lake Huron. 7-24/30

58. Wind stations used for Lake St. Clair. 7-32

59. Surface current analyses for Lake St. Clair. 7-38/43

60. Wind stations used for Lake Erie. 7-45

61. Surface current analyses for Lake Erie. 7-53/60

62. Wind stations used for Lake Ontario. 7-62

63. Surface current analyses for Lake Ontario. 7-70/75

List of Tables

		Page
1.	Kelleys Island Test Site Training---15 October 1972	2-9
2.	Lake Erie Algal Bloom Classification--- 15 October 1972	2-11
3.	Point Pelee Test Site Training---9 September 1972	2-18
4.	Lake Erie Algal Bloom Classification---9 September 1972	2-21
5.	Lake Michigan Whiting Classification---3 and 21 August 1972	3-12
6.	ERTS-1 scenes employed for surface current analysis of southern Lake Michigan	7-5
7.	ERTS-1 scenes employed for surface current analyses of southern Lake Huron	7-18
8.	ERTS-1 scenes employed for surface current analyses of Lake St. Clair.	7-33
9.	ERTS-1 scenes employed for surface current analyses of Lake Erie.	7-46
10.	ERTS-1 scenes employed for surface current analyses of Lake Ontario.	7-63.
A1.	Listing of ERTS cycles used for circulation analyses.	A-2
A2.	Weighted wind analysis for southern Lake Michigan.	A-3
A3.	Weighted wind analysis for southern Lake Huron.	A-4
A4.	Weighted wind analysis for Lake St. Clair.	A-5
A5.	Weighted wind analysis for western Lake Erie.	A-7
A6.	Weighted wind analysis for eastern Lake Erie.	A-11
A7.	Weighted wind analysis for Lake Ontario.	A-13

TABLE OF CONTENTS

Chapter		Page
1.	Introduction	1-1
2.	Algal Blooms	2-1
	a. Introduction	2-1
	b. Observations and Results	2-1
	c. Discussion	2-23
	d. Concluding Remarks	2-26
3.	Chemical Precipitation - $CaCO_3$ Whitings	3-1
	a. Introduction	3-1
	b. Upwelling in Lake Michigan	3-2
	c. Discussion and Conclusions	3-20
4.	Ice	4-1
	a. Using satellite imagery to monitor ice cover	4-1
	1. Freeze-up	4-1
	2. Total ice cover	4-3
	3. Breakup and thaw	4-3
	b. Conclusions	4-8
5.	Sunglint	5-1
6.	Water color vs. water temperatures	6-1
7.	Wind vs. Circulation - Case Studies	7-1
	a. Southern Lake Michigan	7-3
	1. northerly winds	7-3
	2. northeasterly winds	7-6
	3. easterly winds	7-6
	4. southeasterly winds	7-7
	5. southerly winds	7-7

Page

6. southwesterly winds 7-7

7. westerly winds 7-7

8. northwesterly winds 7-15

9. Summary 7-16

b. Southern Lake Huron 7-16

1. northerly winds 7-19

2. northeasterly winds 7-19

3. easterly winds 7-20

4. southeasterly winds 7-20

5. southerly winds 7-21

6. southwesterly winds 7-21

7. westerly winds 7-21

8. northwesterly winds 7-22

9. Summary 7-22

c. Lake St. Clair 7-31

1. northerly winds 7-31

2. northeasterly winds 7-34

3. easterly winds 7-34

4. southeasterly winds 7-34

5. southerly winds 7-34

6. southwesterly winds 7-35

7. westerly winds 7-35

8. northwesterly winds 7-36

9. Summary 7-36

d. Lake Erie 7-44

1. northerly winds 7-44

2. northeasterly winds 7-47

Page

3. easterly winds 7-48

4. southeasterly winds 7-48

5. southerly winds 7-49

6. southwesterly winds 7-49

7. westerly winds 7-50

8. northwesterly winds 7-50

9. Summary 7-51

e. Lake Ontario 7-61

1. northerly winds 7-61

2. northeasterly winds 7-64

3. easterly winds 7-64

4. southeasterly winds 7-64

5. southerly winds 7-64

6. southwesterly winds 7-65

7. westerly winds 7-66

8. northwesterly winds 7-66

9. Summary 7-67

8. References 8-1

Appendix A-1

Chapter 1 INTRODUCTION

The guarded optimism expressed by the oceanographic community prior to the launch of ERTS-A gave way to surprise and elation as the first ERTS-1 images became available during August 1972. The multispectral scanner subsystem (MSS) imagery provided the following during the first few weeks of observations: (1) an image of the Monterey area that pinpointed location and extent of the near-shore kelp beds; (2) an image of Rhode Island Sound that displayed numerous turbidity tracers for surface circulation; and (3) a Great Lakes image that produced the first indication that western Lake Superior was indeed colored red by suspended clay particles (Strong, 1972).

Our original test area was composed of Lakes Erie and Ontario. However, as we quickly became enthusiasts of the ERTS-1 MSS data we felt we were doing the Great Lakes a disservice by not including Lakes Michigan and Huron as well. Lake St. Clair was included for completeness. A chart in Figure 1 provides an overview of the area covered in our ERTS studies. (Chesapeake Bay initially had been included in our proposal to NASA/GSFC, but this study was omitted after finding many other investigators were covering this estuary. We were to have studied ice in Chesapeake Bay; however, due to very mild winters ice was rarely observed in the open bay.)

The ERTS-1 MSS data have been used primarily in their raw (basic) image form for this study. Computer compatible tapes (CCT) have been employed in selected instances to produce printouts, or they were processed for computer enhancement using a NOAA/NESS Digital Muirhead Device (DMD). General Electric's "Image 100" and the Environmental Research Institute of Michigan's (ERIM) multispectral processing equipment were used in some portions of our study.

Figure 1. ERTS-1 Great Lakes Coverage Chart. Stippled area indicates image overlap along individual orbits.

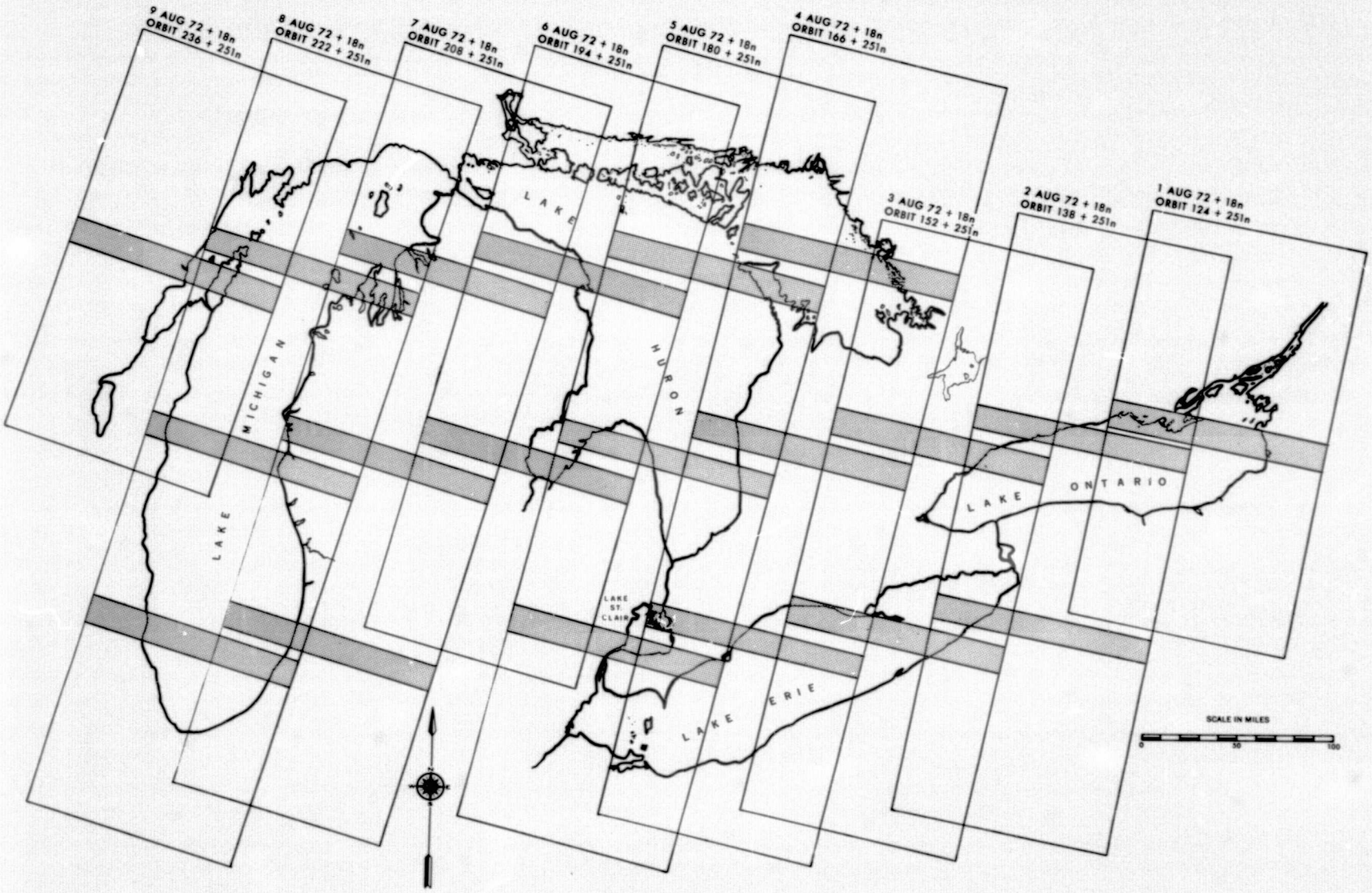
9 AUG 72 + 18n
ORBIT 236 + 251n
8 AUG 72 + 18n
ORBIT 222 + 251n
7 AUG 72 + 18n
ORBIT 208 + 251n
6 AUG 72 + 18n
ORBIT 194 + 251n
5 AUG 72 + 18n
ORBIT 180 + 251n
4 AUG 72 + 18n
ORBIT 166 + 251n
3 AUG 72 + 18n
ORBIT 152 + 251n
2 AUG 72 + 18n
ORBIT 138 + 251n
1 AUG 72 + 18n
ORBIT 124 + 251n
LAKE MICHIGAN
LAKE HURON
LAKE ST. CLAIR
LAKE ERIE
LAKE ONTARIO
SCALE IN MILES
0
50
100

The bulk of our work has been directed toward the production of circulation atlases for the following lakes:

(1) Southern Lake Michigan

(2) Southern Lake Huron

(3) Lake St. Clair

(4) Lake Erie

(5) Lake Ontario

Results for these five areas were presented in Chapter 7 and take advantage of river discharges and lake turbidity that are natural current tracers. Using all observations with cloud-free data between August 1972 and December 1973 enough observations were available to classify circulation as a function of wind stress.

Five chapters are included that discuss special observations made under this NOAA/NASA effort:

Algal Blooms - Chapter 2

Chemical Precipitation - Chapter 3

Ice - Chapter 4

Sunglint - Chapter 5

Surface Temperature vs. Color - Chapter 6

Chapter 2 ALGAL BLOOMS

Portions of this chapter were first presented at the NASA Symposium on Significant Results obtained from the ERTS-1 (1973) and later amplified in Remote Sensing of Environment (Strong, 1974). An understanding of what was was observed in Lake Erie was provided by an excellent image of a documented algal bloom in Utah Lake observed by ERTS-1 on 12 September 1972.

Introduction

As NOAA aircraft flights were being made over Lake Erie on 15 October 1972, underflying the ERTS-1, a long dark streamer was observed between Kelleys and South Bass islands and the Ohio shoreline. Although it was known that the ERTS-1 multispectral scanner subsystem (MSS) image swath would cover a 100-nautical-mile-wide strip just east of this area (NASA, 1971), the aircraft flight pattern was modified extemporaneously to provide sufficient coverage of this waterborne material. A chart in Figure 2 shows the location of the aircraft and satellite imagery used in this study.

Observations and Results

The NOAA Buffalo DeHavilland aircraft was equipped with a Spectral Data Corporation four-band camera system for spectrally simulating the ERTS MSS. Overlapping photography, through the boresighted camera, viewed a swath 4.6 km wide beneath the aircraft from an altitude of 5.8 km. The purpose of the high resolution photography was to avoid any interpretation difficulties that might arise during examination of the 100-m resolution ERTS-1 imagery.

A Daedalus Dual-Channel Thermal Scanner was also incorporated into the aircraft flight package. The two thermal-infrared channels covered the 3.5-5.0μm and 8-13μm atmospheric "windows". This imagery was centered directly beneath the aircraft and provided an 11-km wide swath from the 5.8-km altitude. The thermal-infrared imagery provided further lake

Figure 2. Chart of Western Lake Erie. The area covered by aircraft thermal scanner is the rectangle marked A/C; the interior elongated box shows the area covered by photography. To the right, the area covered by the ERTS-1 enhancement shown in Fig. 5 is the rectangle marked ERTS.

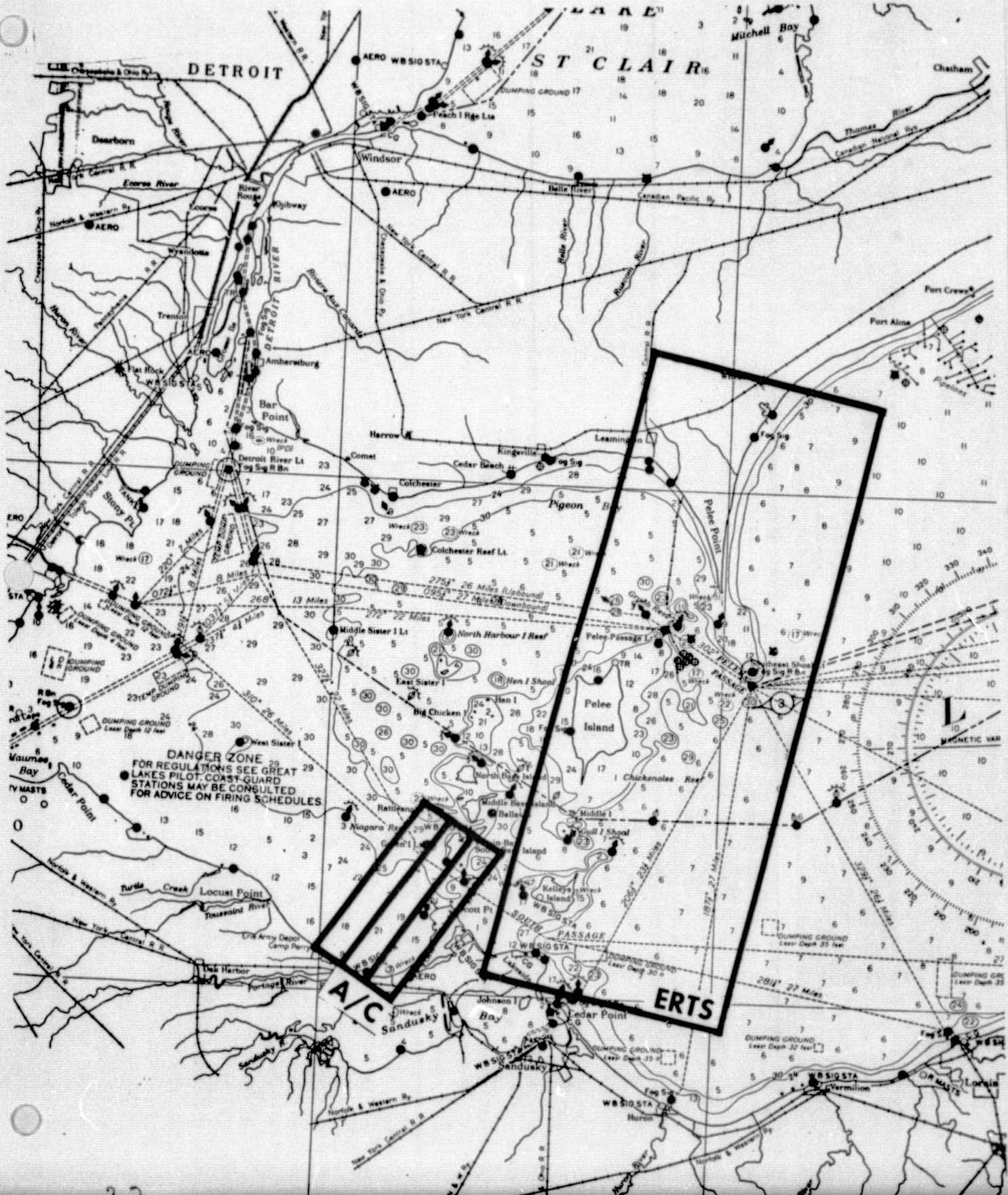
DETROIT
ST CLAIR
Mitchell Bay
Chatham
Thames River
Canadian National Rys
Dearborn
Ecorse River
Ecorse
River Rouge
Ojibway
Windsor
Belle River
Canadian Pacific Ry
Wyandotte
Trenton
Flat Rock
Amherstburg
Bar Point
Detroit River Lt
Fog Sig R Bn
Harrow
Comet
Colchester
Kingsville
Cedar Beach
Leamington
Pigeon Bay
Pelee Point
Port Crewe
Port Alma
Pipelines
Colchester Reef Lt.
Middle Sister I Lt
North Harbour I Reef
East Sister I
Hen I Shoal
Hen I
Big Chicken I
Pelee Island
Pelee Passage Lt
Chickenolee Reef
Middle I
Gull I Shoal
Kelleys Island
SOUTH PASSAGE
West Sister I
Rattlesnake
Niagara Reef
Middle Bass Island
Ballast
Locust Point
Toussaint River
Erie Army Depot Camp Perry
Oak Harbor
Portage River
Sandusky Bay
Johnson I
Cedar Point
Sandusky
Vermilion
Huron
Lorain
Maumee Bay
Cedar Point
Stony Pt
DANGER ZONE
FOR REGULATIONS SEE GREAT LAKES PILOT. COAST GUARD STATIONS MAY BE CONSULTED FOR ADVICE ON FIRING SCHEDULES.
A/C
ERTS
DUMPING GROUND
Least Depth 12 feet
Least Depth 35 feet
Least Depth 32 feet
Least Depth 30 ft
MAGNETIC VAR
Norfolk & Western Ry
New York Central R R
Chesapeake & Ohio Ry
Huron River
Sandusky R
Turtle Creek
Pennsylvania R R
Toledo Shore Line R R
Detroit River
Rouge River
Rivière Aux Canards
Ruscom River
Belle River
Fog Sig
WB SIG STA
AERO
TANK
TEMP DUMPING GROUND
26 Miles (Upbound)
27 Miles (Downbound)
22 Miles
13 Miles
8 Miles
26 Miles
27 Miles
23½ Miles
26½ Miles
28½ Miles

surface information that was related to the color patterns observed by both the aircraft and satellite sensors.

Since our main surface-truth operations were being conducted along the Canadian shore of Lake Erie, no quantitative measurements were obtained for the area off Port Clinton, Ohio. Surface water temperature at Lorain, Ohio (60 km east of Port Clinton) was 14.5°C and is considered representative for much of the southern shore under the prevailing onshore winds.

The multiband aircraft camera observations are presented in Figure 3 as strip mosaics. An abrupt contrast reversal is evident either side of 0.7μm between the ERTS-simulated MSS bands "5" and "6" (0.6-0.7μm and 0.7-0.8μm, respectively). The material that absorbs shortwave energy in the visible wavelengths reflects incident radiation in the near-IR wavelengths. Due to the strong solar absorption in the visible wavelength, it was not surprising to find an associated higher surface temperature in the thermal-IR data (Figure 4) obtained simultaneously. The near-surface nature of this material is made evident by small boat wakes normal to the streamer that interrupt the visible, reflected-IR and thermal-IR features.

A portion of the ERTS-1 MSS digital data was redisplayed on a Digital Muirhead Device (DMD) at the National Environmental Satellite Service. The DMD utilizes a high intensity modulated light source to generate high quality transparencies from a digital input. Use of the DMD makes it possible to enhance the lower radiances characteristic of water. Through the use of the DMD, considerable information frequently can be extracted from MSS data that appear as a uniform black tone in the original unenhanced ERTS imagery. DMD-reprocessed, 14-nautical-mile wide, north-south swaths of the original MSS-5 and MSS-6 imagery are shown in Figure 5. The "chip" begins at Point Pelee on the north shore of Lake Erie and terminates at

Figure 3. 15 October 1972 aircraft multispectral photography obtained at an altitude of 5.8 km. Bandwidths shown simulate the ERTS-1 MSS channels.

AIRCRAFT DATA 5.8KM ALTITUDE 1837 GMT

MULTIBAND CAMERA MOSAICS

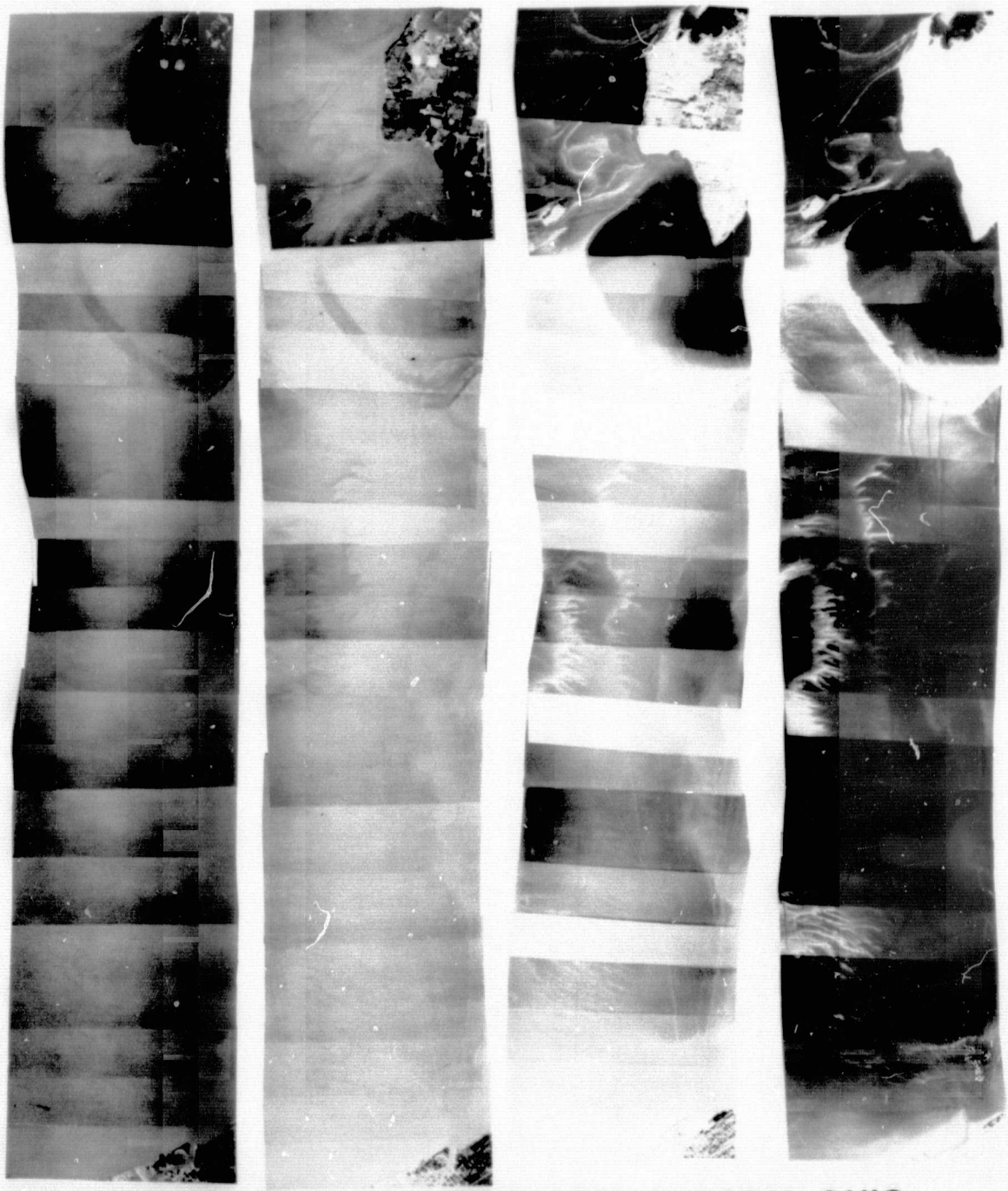

SOUTH BASS ISLAND TO PORT CLINTON, OHIO

(between lower vertical lines on IR imagery)

Figure 4. Thermal scanner image over the area delimited in Fig. 2. Brighter tones indicate higher surface temperature.

PRECEDING PAGE BLANK NOT FILMED

Figure 5. Digitally enhanced ERTS-1 data from 15 October 1972. MSS-5 and MSS-6 (left and right, respectively). Note algal streamer off Kelleys Island and other algal features around and to the east of Pelee Island. The anticyclonic gyre in the vicinity of Point Pelee is a typically observed circulation feature for the location (see Chapter 7).

PRECEDING PAGE BLANK NOT FILMED

Marblehead, Ohio, just north of Sandusky. Although the 15 October ERTS-1 imagery barely covered the phenomenon observed in Figures 2 and 4, the high reflectance of the westernmost portion can be seen in MSS-6 immediately west of Kelleys Island. A large reflective region appears in MSS-6 to the east of Pelee Island. It is suspected this represents lesser algal concentrations, for no similar patterns are observed in MSS-5. It is well known that summer algal blooms make regular appearances in Lake Erie, particularly in the area around the islands (Casper, 1965).

Computer compatible ERTS-1 tapes were processed on General Electric's Multispectral Analyzer - "Image 100" - to see whether a classification training could be established for the algal blooms. A test site was chosen to the west of Kelleys Island where the algal bloom was seen both from the aircraft and ERTS-1. Figure 6 shows the full resolution ERTS data processed on the "Image 100". A fluffy cumulus cloud lies north of (above) the algal streamer that appears as a red line. Table 1 shows the "training" performed for the display in Figure 7. Basically, MSS-7 was used as a water identifier (low values = water) and MSS-6 as the algal bloom detector. Although no surface truth existed to allow us to be more definitive regarding concentrations, Bukata et al. (1974) have demonstrated a correlation of surface biomass with MSS-6. Applying this test site training we were able to produce a "classification" of the entire ERTS-1 scene for 15 October 1972. The resulting image is shown in Figure 8. For this display a 6-line x 6-spot ERTS sampling was used to provide a one-picture overview. Sampling every 6th line ensured that we always display data from the same detector of the six detectors used in ERTS-1, thereby eliminating the troublesome variability in calibration found between detectors. The training display presented in Figure 8 was altered only slightly and appears in Table 2. Although the MSS-6 values are lower in the overview classification there are probably fewer "false alarms" for

Figure 6. "Image 100" false-color enhancement of ERTS-1 MSS-6 data for Kelleys Island test site. Algal streamer lies left of the island. 15 October 1972.

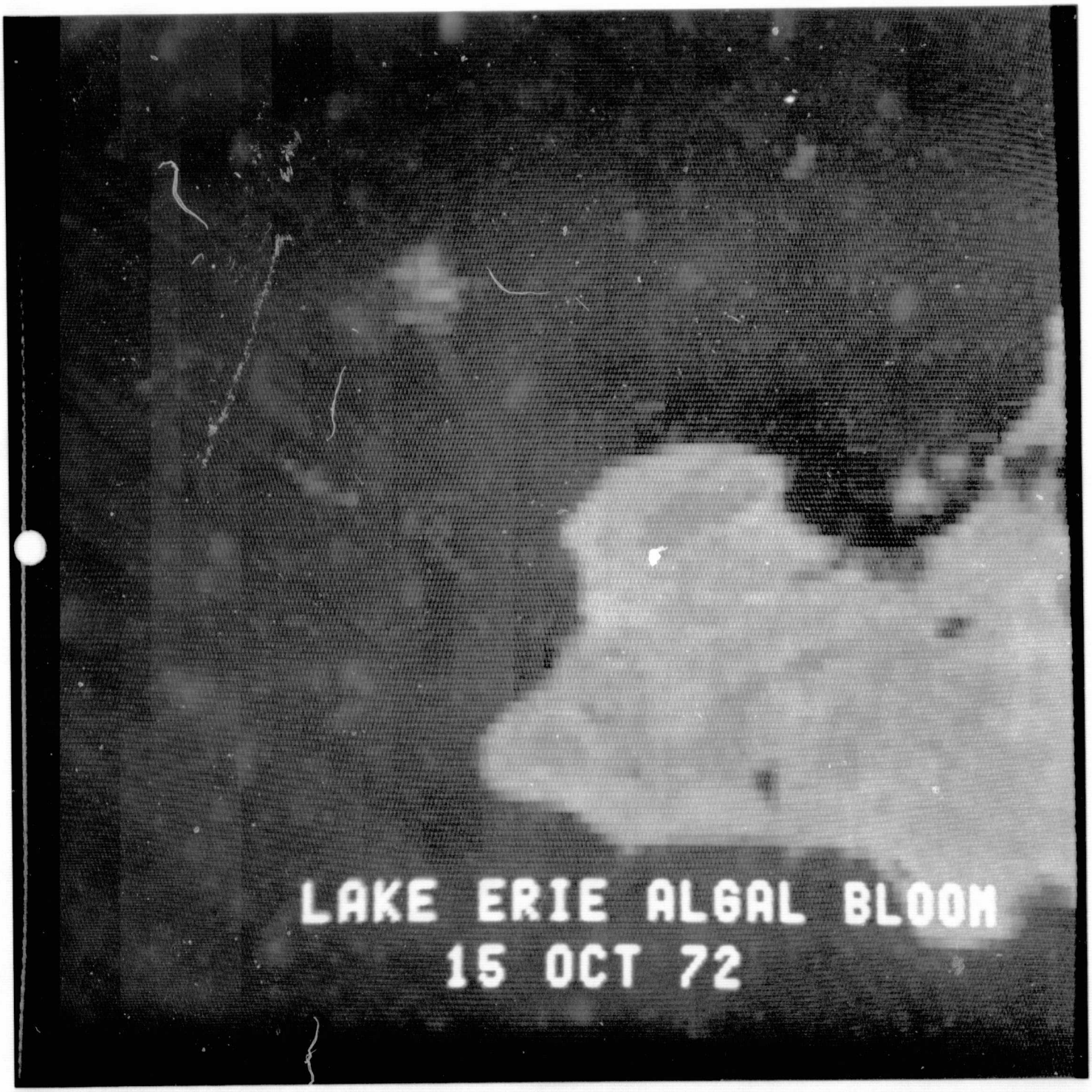
LAKE ERIE ALGAL BLOOM
15 OCT 72

Table 1

Kelleys Island Test Site Training October 15, 1972

MSS Channel	4	5	6	7	Color
Count Range	17-23	9-14	14	3-7	orange
	16-31	8-14	13	3-8	dk. blue
	16-28	8-14	12	2-7	yellow
	16-28	7-14	11	1-5	violet
	15-28	7-13	10	1-5	lt. blue
	16-27	6-13	9	1-5	purple

Figure 7. Kelleys Island 4-channel training on algal bloom. See Table 1 for relationship of theme color to MSS radiance values.

LAKE ERIE ALGAL BL
15 OCT 72

Table 2

Lake Erie Classification October 15, 1972

MSS Channel	4	5	6	7	color
Count Range	14-33	12-25	11	1	orange
	14-33	12-25	10	1	dk. blue
	16-32	13-21	9	1	yellow
	17-33	13-22	8	1	pink
	14-32	12-20	7	1	lt. blue
	14-32	11-18	6	1	purple
	14-28	10-15	5	1	grey
	14-28	10-12	4	1	green

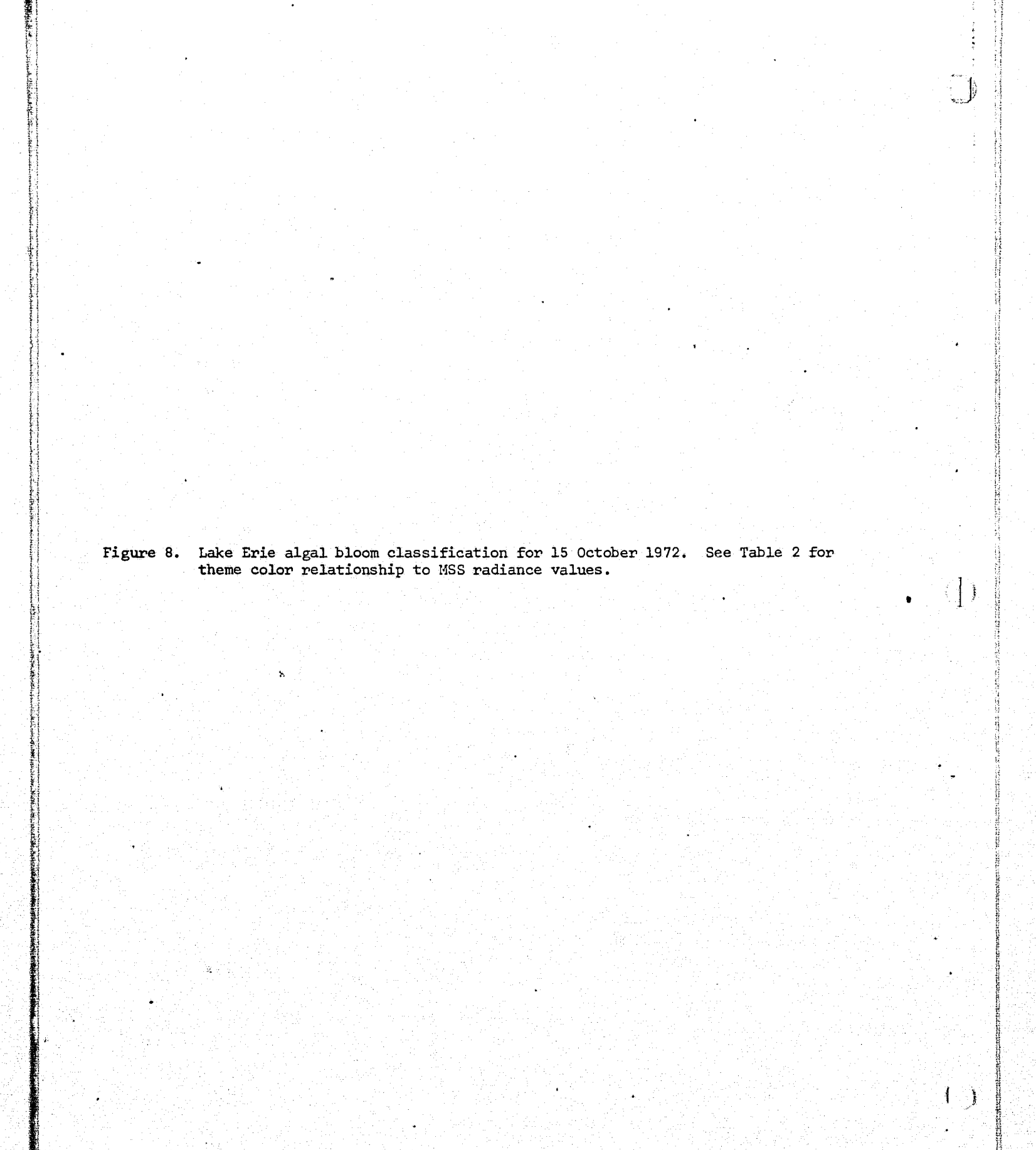

Figure 8. Lake Erie algal bloom classification for 15 October 1972. See Table 2 for theme color relationship to MSS radiance values.

REPRODUCIBILITY OF THE ORIGINAL PAGE IS POOR.

algae as only MSS-7 values of 1 count were permitted. Evidently Sandusky Bay (south of Kelleys Island) and the eastward coastal current along the Ohio shoreline are teeming with algae. Despite considerable cloud cover the classification is not confused by this obscuration. Finally, the eastern portion of Lake St. Clair is classified as a rich source of surface algae along the upper left edge of the ERTS-1 view.

On 9 September 1972, a little more than one month prior to the October observation, ERTS-1 imagery showed another suspected distribution of algal material in Lake Erie. The DMD enhancement of MSS-5 and MSS-6 are shown in Figure 9. This swath is 31-km wide and Point Pelee is at the left side of the strip. The wavelike structure is presumed to be related to the Lake Erie internal seiche and shows the pulse-like nature of the alongshore current moving eastward through the islands and around Point Pelee. The algal streamer appears to originate immediately east of Pelee Island. The streamer extends nearly 46 km and shows widths varying from 0.2 to 2 km. Additional color enhancements are provided of MSS 4, 5 and 6 using "Image 100" in Figures 10, 11, and 12, respectively. Again GE's "Image 100" was utilized to classify the algal bloom in Lake Erie. The training method was similar to the one discussed above. Table 3 indicates what digital information went into each color displayed in Figure 13. This is a 4-channel training on all pixels in the gyre test area off Point Pelee.

The detector banding that appears in Figure 13 is an obvious detraction in the 5 line x 6 spot sampling presented in Figure 14. This demonstrates the need for better calibrations on future space systems. A 6 line x 6 spot sampling (Figure 15) recovers most of the information one would expect from the training above. It is assumed that the higher surface algal concentrations have been mapped by this process.

Figure 9a. Digitally enhanced MSS-5 ERTS-1 data for 9 September 1972.

Figure 9b. Digitally enhanced MSS-6 ERTS-1 data for 9 September 1972.

REPRODUCIBILITY OF THE ORIGINAL PAGE IS POOR.

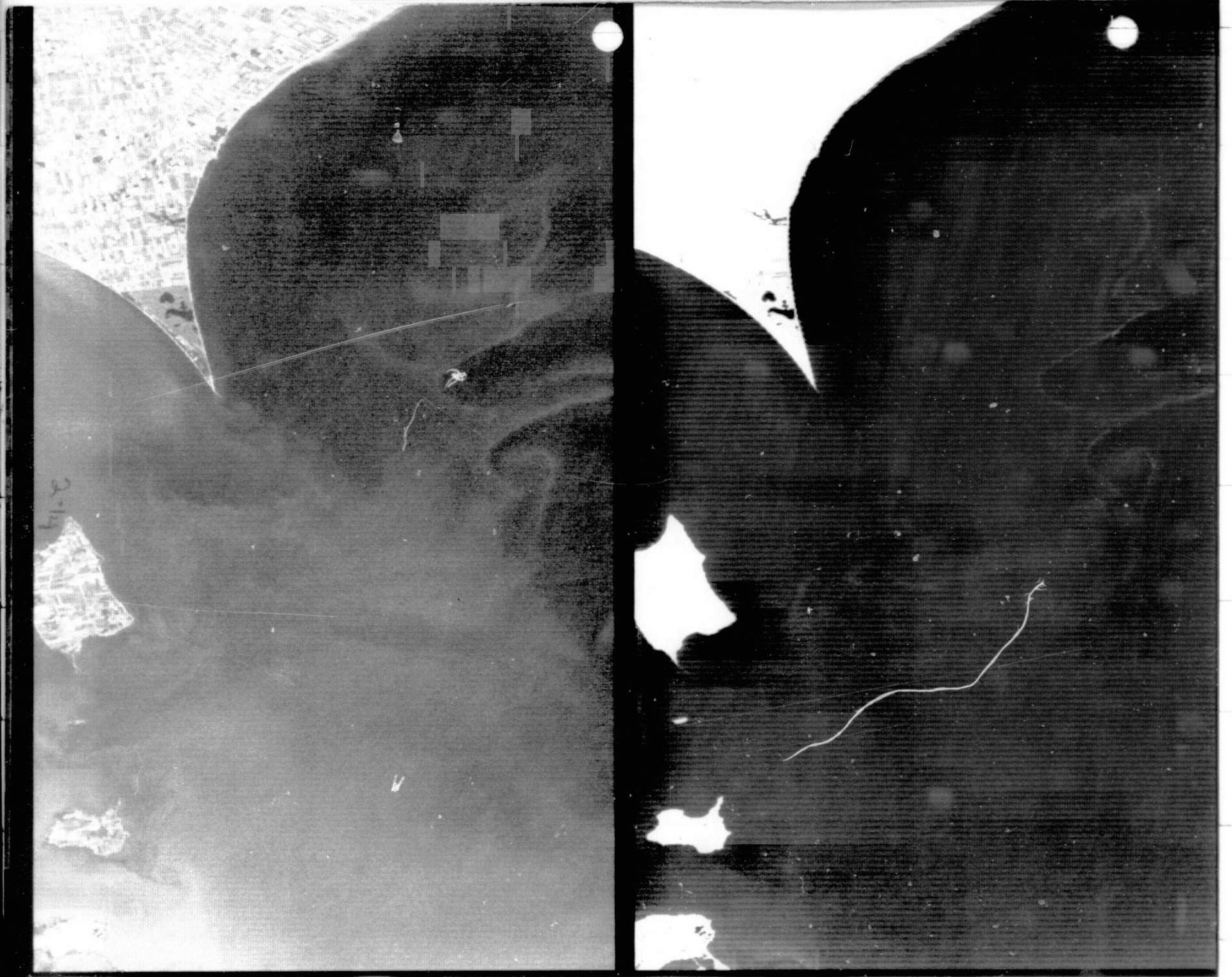

Figure 10. "Image 100" false-color enhancement of 9 September ERTS-1 MSS-4 data for Point Pelee Test Site.

REPRODUCIBILITY OF THE ORIGINAL PAGE IS POOR.

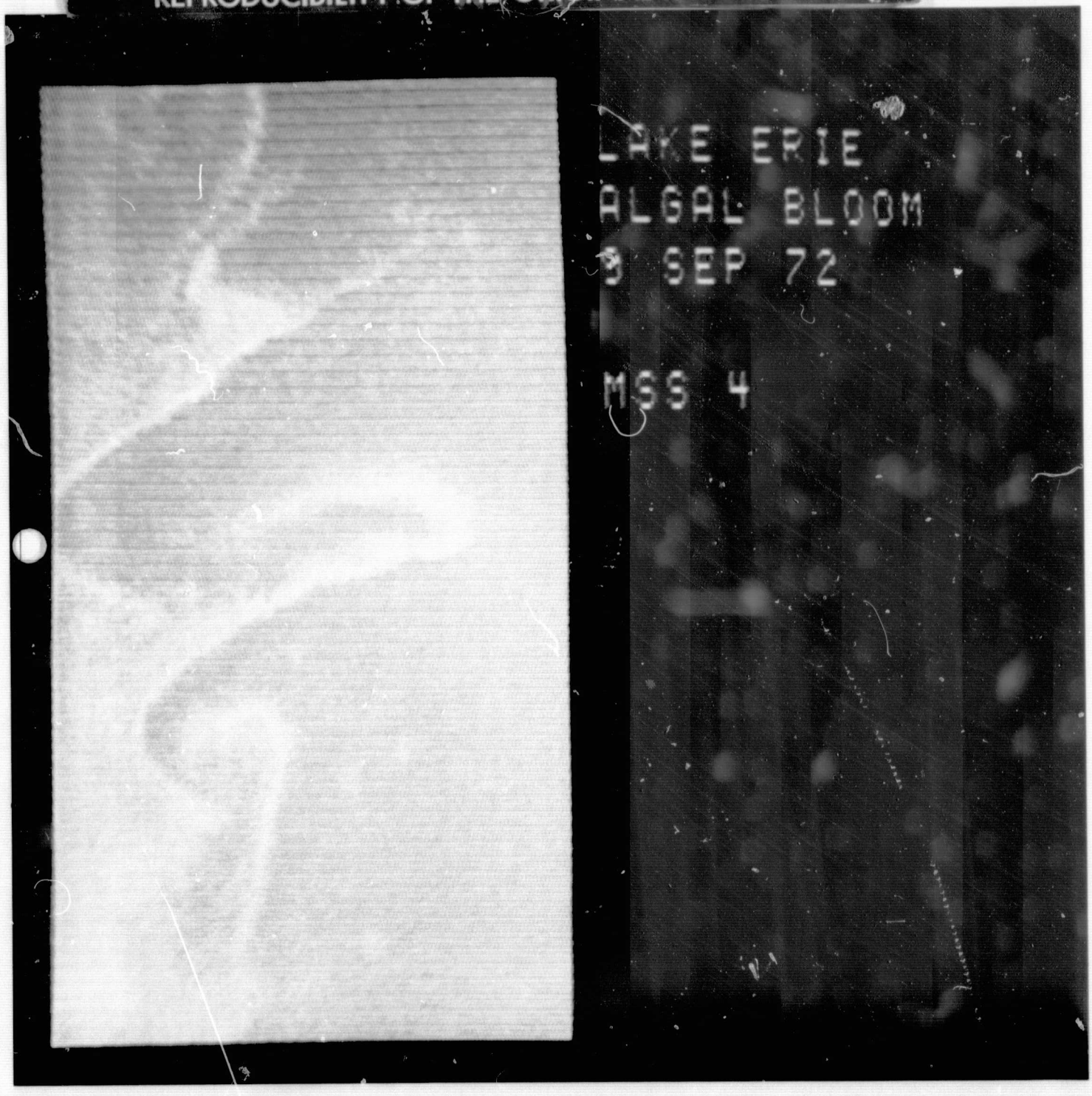

Figure 11. Same as Figure 10--MSS-5.

REPRODUCIBILITY OF THE ORIGINAL PAGE IS POOR.

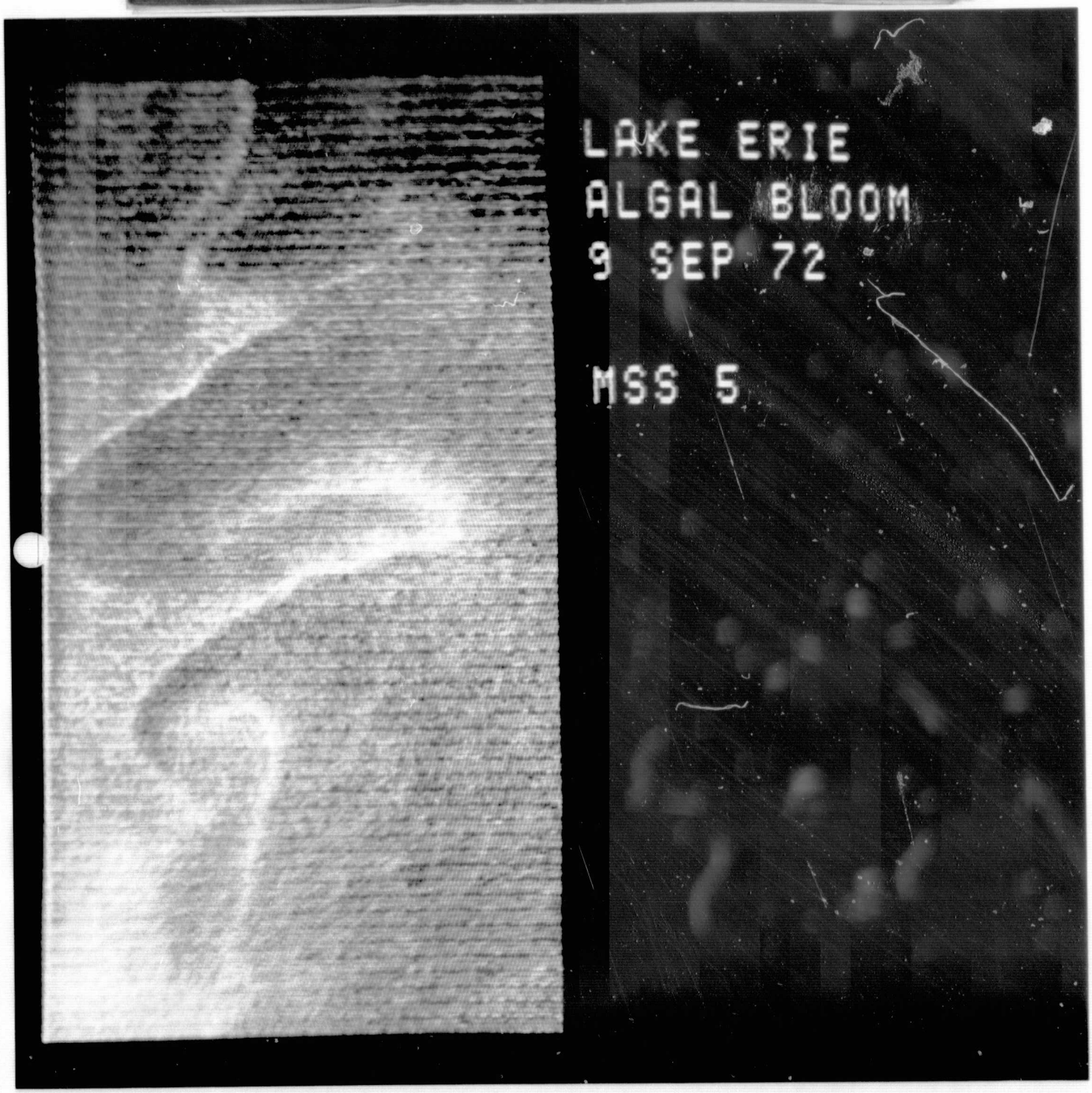

Figure 12. Same as Figure 10--MSS-6.

REPRODUCIBILITY OF THE ORIGINAL PAGE IS POOR.

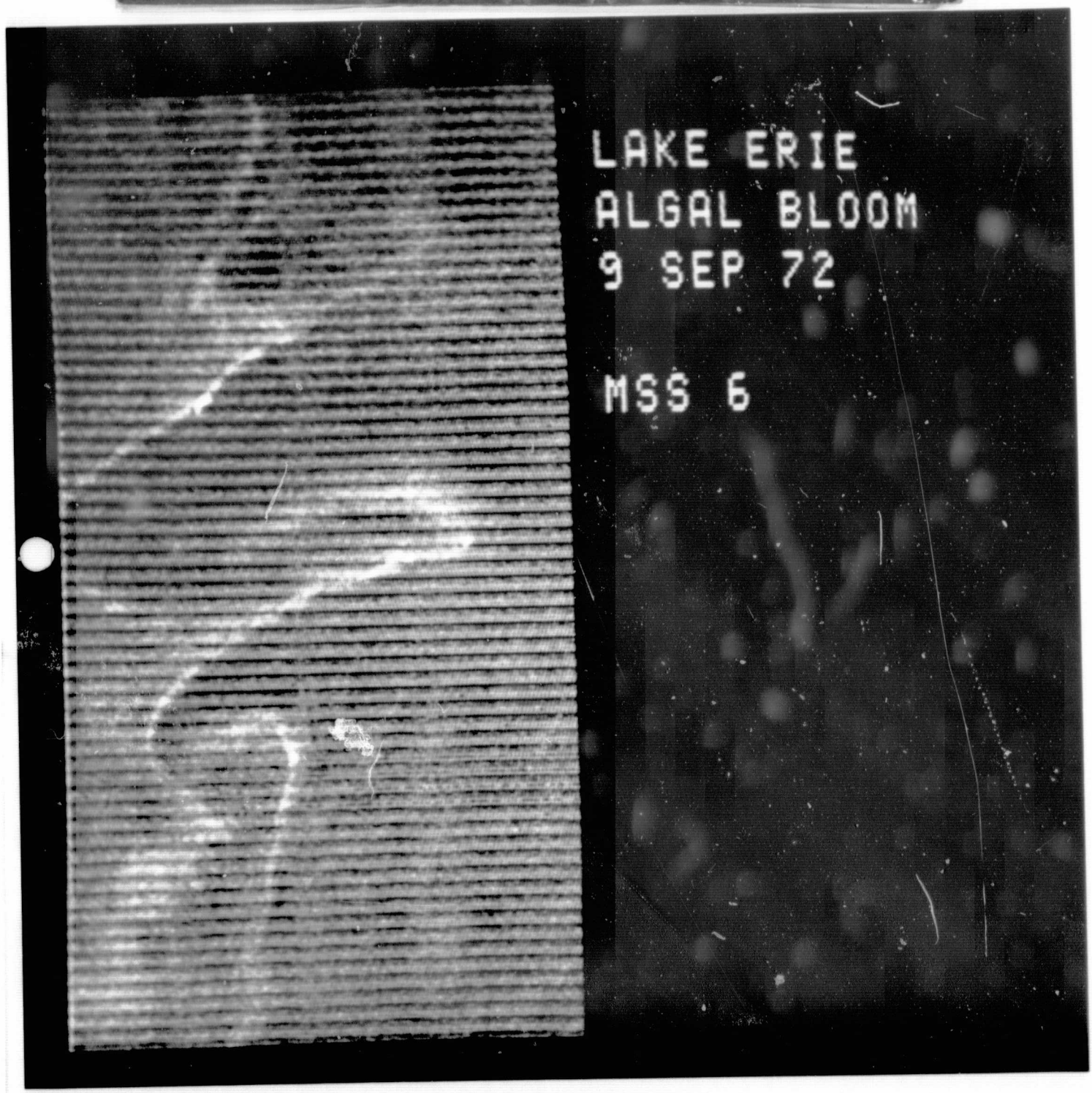

Table 3

Point Pelee Test Site Training — September 9, 1972

MSS Channel	4	5	6	7	Color
Count Range	20-25	11	9	1-2	pink
	19-24	10	8	0-2	orange
	18-24	11	8	0-2	peach
	17-24	10	7	0-2	gold
	16-24	11	7	0-2	purple
	16-24	12	7	0-2	blue

Figure 13. Point Pelee gyre 4-channel training on algal bloom. See Table 3 for relationship of theme color to MSS radiances. Values correspond to normalized MSS-6/MSS-5 ratios.

REPRODUCIBILITY OF THE ORIGINAL PAGE IS POOR.

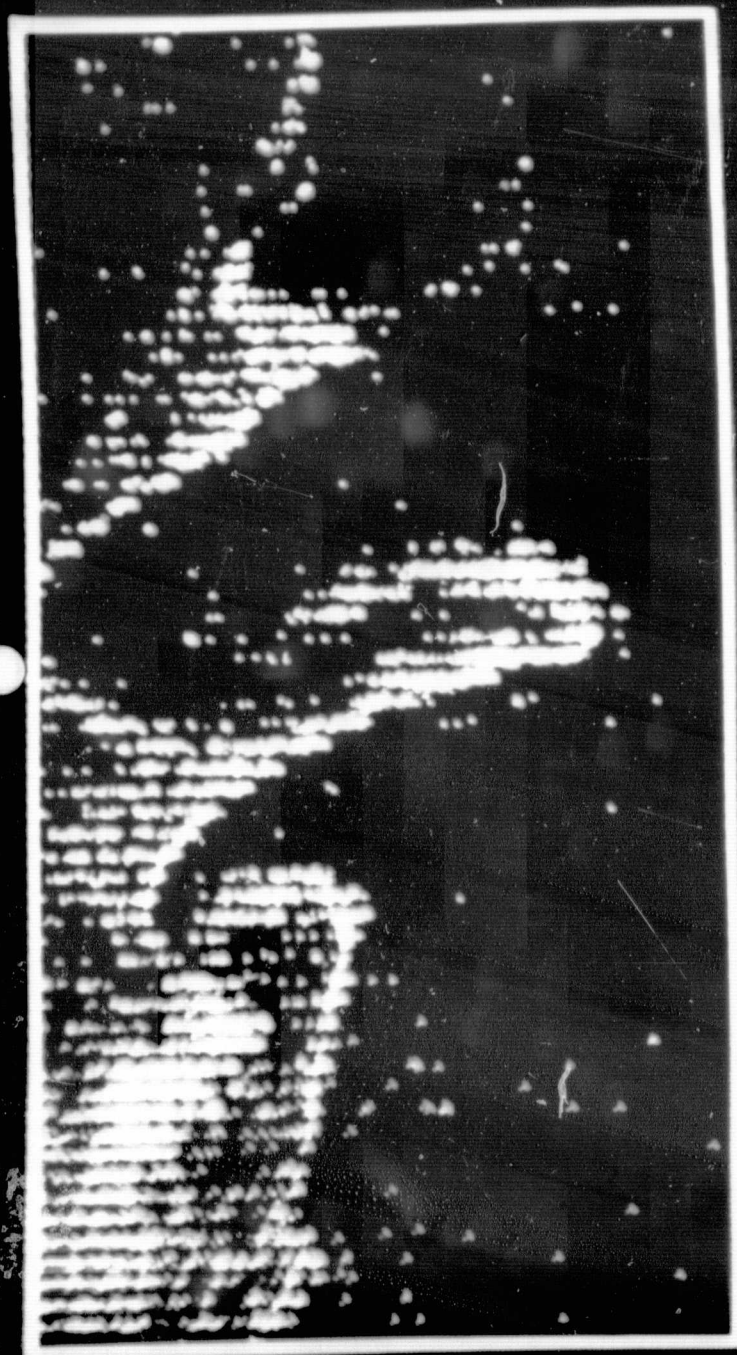

ALGAL BLOOM
9 SEP 72
4 CH TRAINING

26 PINK
25 ORANGE
24 OMIT
23 PEACH
22 GOLD
21 OMIT
20 PURPLE
19 BLUE

Figure 14. Lake Erie algal bloom classification for 9 September 1972 using training established from Figure 13 (see Table 3).

REPRODUCIBILITY OF THE ORIGINAL PAGE IS POOR.

Table 4

Lake Erie Classification September 9, 1972

MSS Channel	4	5	6	7	Color
Count Range	15-25	11	9	1-4	pink
	19-27	10	8	1-3	orange
	19-25	11	8	1-3	peach
	14-29	12	8	1-4	turquoise
	12-29	10	7	1-3	gold
	15-30	11	7	1-3	blue
	13-29	12	7	1-3	green

Figure 15. Unbanded classification of Figure 14 using slightly revised training (see Table 4). 9 September 1972. Banding was eliminated by displaying every 6th line of scanner data.

REPRODUCIBILITY OF THE ORIGINAL PAGE IS POOR.

The gyres off Point Pelee are enhanced. Algal material appears to be flowing out of the western basin of Lake Erie above Kelleys Island and then eastward along the southern shoreline. The surprise from this classification is the apparently low concentrations in the Sandusky Bay area that became extremely high 5 weeks later (Figure 8). Although it is difficult to be quantitative with the MSS data there would appear to be greater surface algal concentrations (higher MSS-6 counts) during the 15 October algal bloom. A second surprise was an inference of a high level of biological activity off Erie, Pennsylvania in the right-hand half of the scene. Although research vessel data were available in this area of Lake Erie, unfortunately no surface chlorophyll or similar data were available.

A much superior ERTS-1 observation of an algal bloom was obtained over Utah Lake on 12 September 1972. Figure 16 shows an anticyclonic gyre in this shallow (about 3-m deep) and highly eutrophic lake ($PO^{=}$ about 0.5 mg/l). The ERTS imagery shows a reversal in contrast for the gyre at 0.7μm. The gyre itself covers a large percentage of the surface of this lake, which has a surface area of about 375 km^2. Utah Lake is known for its high turbidity and summer algal blooms. Within one day of this satellite observation, a limnological cruise on Utah Lake revealed a massive, highly variable bloom of Aphanizomenon flos-aquae (White and Rushforth, 1973).

Discussion

Oceanographers and limnologists have observed that ERTS-1 imagery provides much detail in MSS-4 and -5, yielding information on circulation, biomass, and turbidity distributions (Maul, 1973). Charnell and Maul (1973) have discussed the light penetration expected in pure water for the four ERTS-1 MSS channels. Observed radiances, a function of both absorption and scattering in the water, are noticeably wavelength-dependent. In pure water, 50% light transmission will be observed over a depth of 10 m

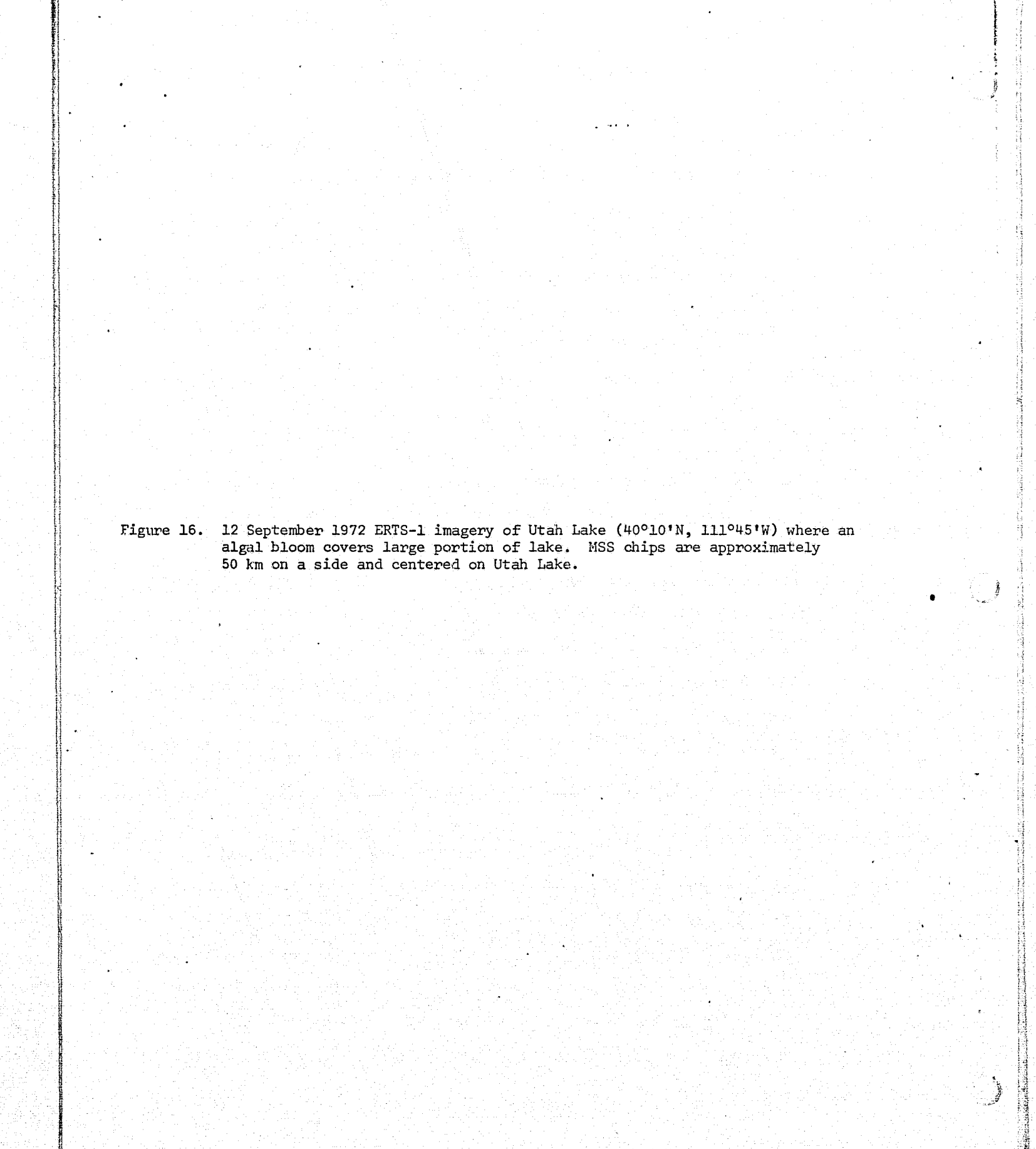

Figure 16. 12 September 1972 ERTS-1 imagery of Utah Lake (40°10'N, 111°45'W) where an algal bloom covers large portion of lake. MSS chips are approximately 50 km on a side and centered on Utah Lake.

REPRODUCIBILITY OF THE ORIGINAL PAGE IS POOR.

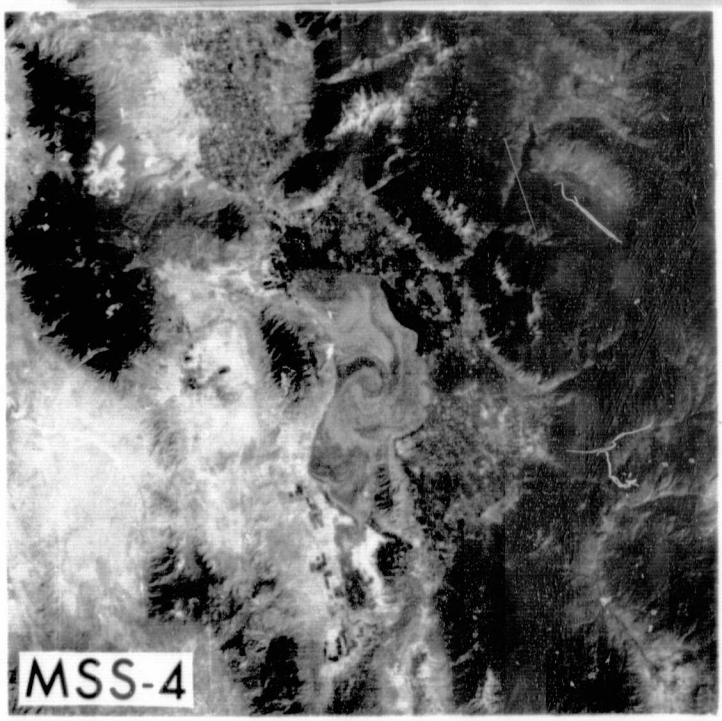

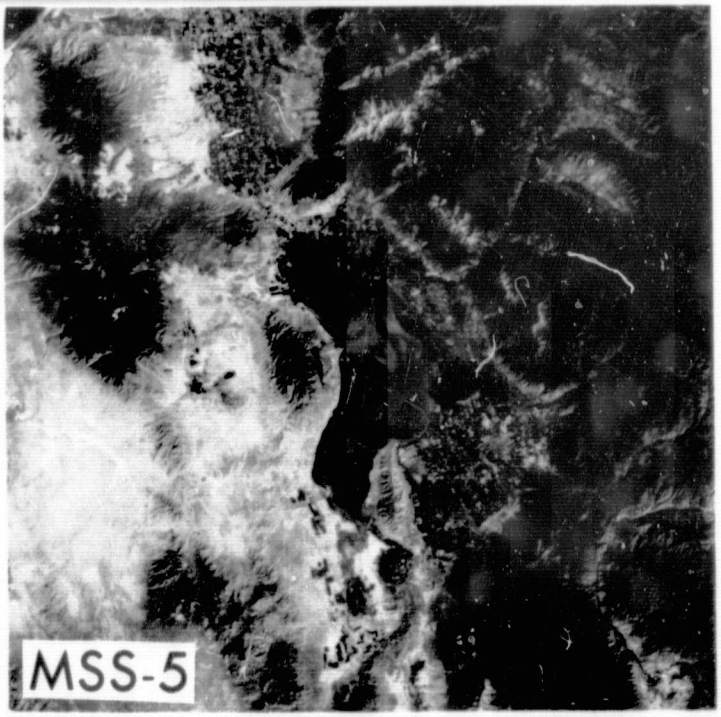

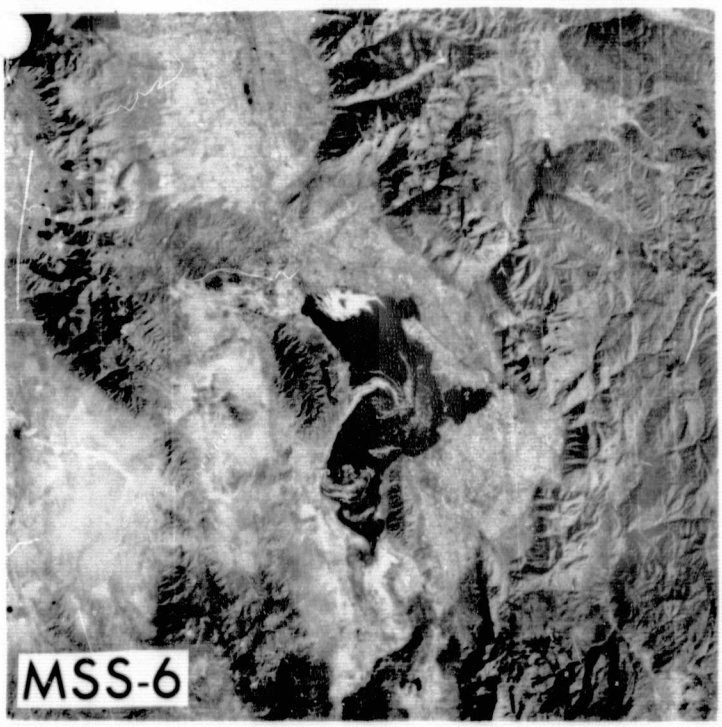

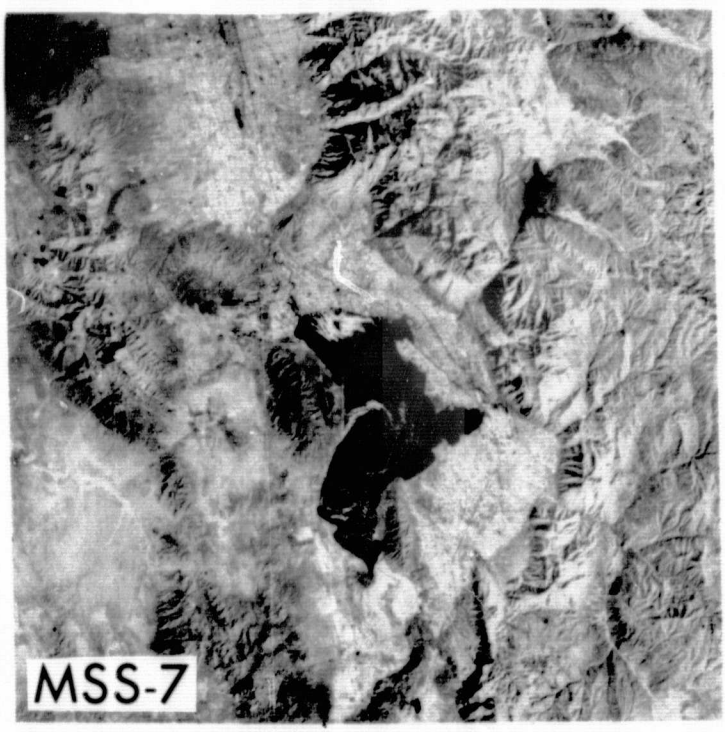

by MSS-4, 2.5 m by MSS-5, 0.5 m by MSS-6, and 0.2 m by MSS-7. In the "real world" of turbid water these depths are noticeably reduced. The strong absorbing characteristic of water for the near-IR wavelengths (greater than 0.7μm) makes it possible to detect substances that are strongly reflective at these wavelengths when they are at or project above the surface of the water. The reflectances of such features diminish in the near-infrared (MSS-6 and MSS-7) whenever they are covered by even a thin layer of water. As an example, a pronounced reduction in reflectance has been observed when a thin layer of melt water covers ice (Strong et al., 1971).

Algal blooms, although not previously documented from space, have been seen and photographed from aircraft. Aero-infrared Ektachrome film has been used successfully to image periphyton in the Great Lakes (Noble et al., 1967). Chlorophyll detection in cropland is extremely useful to the remote sensing agronomist. Using multispectral techniques, he can infer such qualities as crop vigor, stage, moisture stress, and disease. The near-infrared reflectance from living plants increases rapidly between wavelengths of 0.70 and 0.75μm (Bressette and Lear, 1973). Whenever high concentrations of algal materials are found on a water surface they stand out dramatically against an otherwise dark background at these wavelengths. MSS-6 on ERTS-1 is well-suited for surface algae detection. If the algal bloom is thick and provides enough buoyancy to allow the upper surface to dry, the reflectance is sufficiently intense to be observed in MSS-7 imagery as well.

Algal blooms have been noticed during or immediately following calm periods accompanied by abundant insolation. Some blooms are highly toxic (e.g., red tides), whereas others attract fish with beneficial results. They are most notable in eutrophic lakes and in some coastal areas of the

oceans. Unfortunately the evolution of most algal blooms takes place over only a few days. This makes ERTS-1 a poor vehicle from which to monitor these events because of its repeat cycle of 18 days.

Concluding Remarks

Because the ERTS-1 MSS sensing was successful in observing the strong chlorophyll reflectance on Utah Lake, we are reasonably certain that the patterns seen in similar imagery over Lake Erie indicate the existence of an algal bloom there. Although no surface data have yet been found to corroborate this inference, past history indicates that blooms in this area are plentiful. A vigorously growing algal biomass is rich in chlorophyll and strongly reflects radiant energy in the near-IR bands. The dark green or brown color of this biomass is likely to cause the upper algal surface to appear darker at visible wavelengths and its warmth to cause it to appear brighter at thermal-IR wavelengths than the surrounding highly turbid coastal waters. Algal blooms can be expected to occur during periods of low surface winds, warm water conditions, and substantial insolation. These conditions preceded both the Lake Erie and the Utah Lake observations. Although most Great Lake algal blooms can be expected to be on a scale barely resolved by the ERTS-1 system, a careful interpretation and some judicious computer processing and image enhancement should reveal many algal bloom situations that would otherwise go undetected. Additional use of a multispectral analyzer permits rapid interpretation of an entire ERTS-1 scene and classification of several levels of near-surface biological activity. Not all algal blooms should be expected to yield high contrast features. It is for the less distinct growths that the computer is most necessary. Basic training algorithms can quickly be

applied to the entire data array for areal determinations and monitoring of algal concentrations.

Monitoring algal blooms and their distributions not only provides information on the quality of the water that supports them but also provides valuable data on the circulation of the water supporting the rich biomass.

Chapter 3 CHEMICAL PRECIPITATION - $CaCO_3$

WHITINGS

Whitings are defined as areas of milky-white water composed of calcium carbonate crystals (Bathurst, 1971). Portions of this chapter were first presented at the Ninth International Symposium on Remote Sensing of Environment in April 1974 at Ann Arbor, Michigan (Strong et al., 1974). Further findings are incorporated in this chapter. Additional studies are planned during the coming year. A "whiting event" presents truly an interdisciplinary phenomenon as geology, chemistry, biology, meteorology, and physical oceanography are involved.

INTRODUCTION

Satellite limnology received only scant attention until higher resolution sensors became available in 1972 (Strong, 1967; Sabatini, 1971; Strong and Baker, 1971). During that year the ERTS-1 and the NOAA-2 satellites were successfully launched. With the 80-meter multispectral resolutions of ERTS-1 and NOAA-2's Very High Resolution Radiometer (VHRR) 1-kilometer resolution, detailed satellite studies in coastal areas and in the Great Lakes have become possible.

Due to the orbit geometry and the narrow data swath (185 km wide) obtained along each ERTS-1 pass, coverage of the Great Lakes repeats every 18 days, beginning at the eastern end of Lake Ontario. Twelve days later it completes its Great Lakes' coverage over western Lake Superior. The data swath from NOAA-2 is ten times wider, with daily coverage from both visible and IR channels. The IR channel also makes nightly coverage possible. The ERTS-1 satellite transit is approximately 0930 local time, i.e., about 30 minutes after NOAA-2's passage over the same region. Frequently, this separation in coverage from ERTS-1 and NOAA-2

PRECEDING PAGE BLANK NOT FILMED

is considerably less than 30 minutes, greatly facilitating the integration of the ERTS-1 multispectral and NOAA-2 IR data sets.

UPWELLING IN LAKE MICHIGAN

According to local Great Lakes sources, the summer of 1973 was an unusual one for Lake Michigan. Numerous and extensive upwellings occurred on both eastern and western shores. Since upwelling promotes mixing, an immediate consequence during the 1973 summer period was an improvement in water quality.

One of the more intense upwelling periods began on 20 August and continued for nearly a week. Along the eastern shore, from Frankfort, Michigan to Chicago, Illinois, water intake temperatures for all municipalities plunged from typical August levels of 20°C to less than 10°C. Standard meteorological data from nearshore stations indicated offshore winds were generally less than 5 m sec^{-1}, thus failing to forecast any possibility of major upwelling. However, several ship reports from southern Lake Michigan indicated surface wind speeds nearly three times those over land. Recently, additional reports have confirmed these indications of strong winds at the eastern shore (Hicks, 1973; USGS, 1973). Surface pressure ship and land weather observations are shown in Figure 17.

The evolution of the 20 August upwelling episode was monitored on five consecutive occasions by NOAA-2. During the morning transit of NOAA-2 no unusually cold water was in evidence along the entire eastern shoreline. By evening, however, thermal data from NOAA-2 (Figure 18) indicated that upwelling (lighter grey shades) was beginning immediately south and west of the three major points of land south of the Manitou Islands: Point Betsie, Big Sable Point and Little Sable Point. The 21 August morning

Figure 17. Surface weather for 21 August 1973 in the Lake Michigan region. Surface pressure (millibars) is from 1200 GMT observations. The time of ship and selected shoreline observations are indicated above station circle in parenthesis. Parameters included beside station circle are: air temperature (upper) and water temperature (lower) immediately to the left of the station; wind direction and velocity (reported speed, in knots, appears above "feathers"--one "feather" = 10 knots).

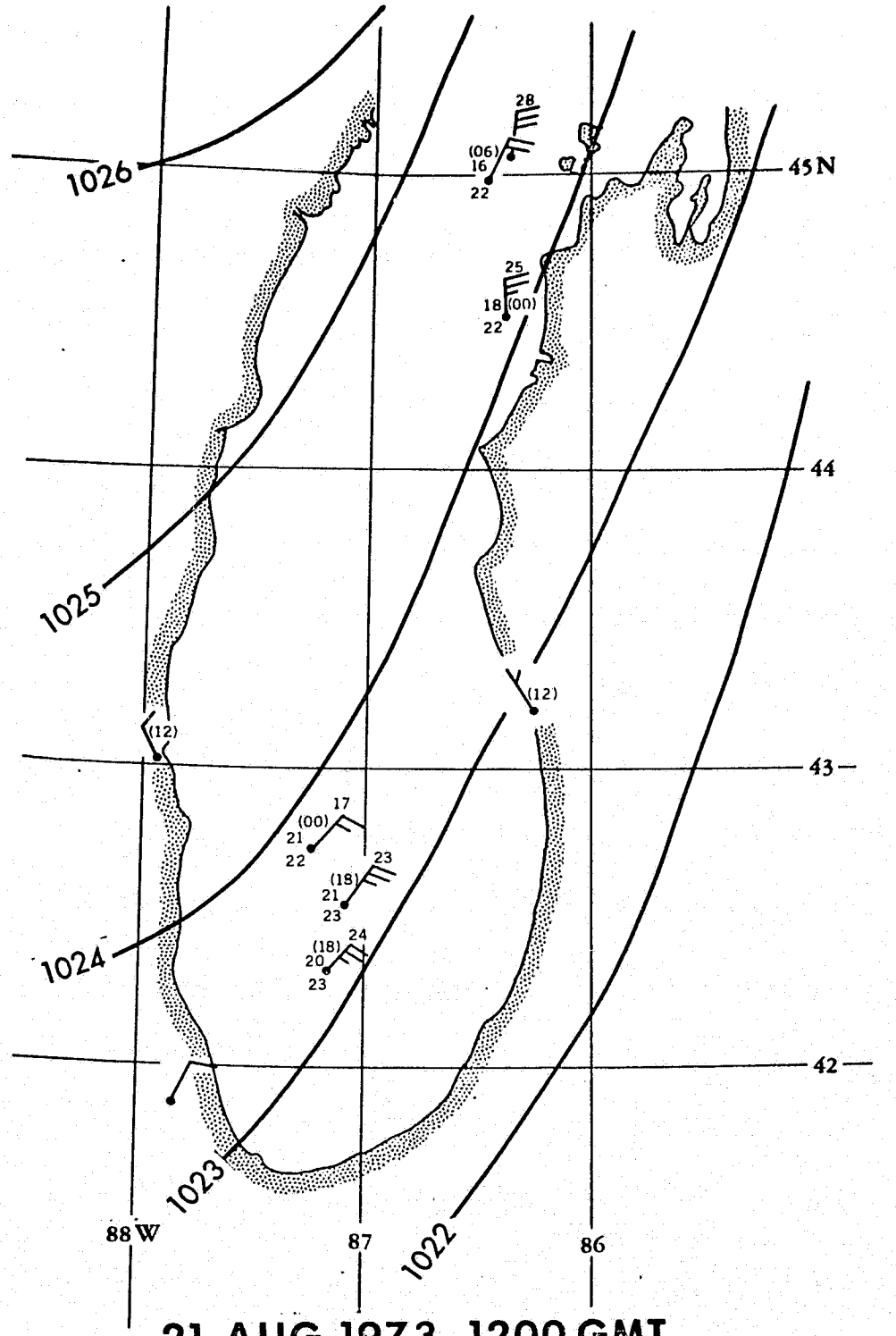

21 AUG 1973, 1200 GMT

Figure 18. 20 August 1973. 2000 EDT (0000 GMT, 21st) NOAA-2 VHRR-IR image. Darker tones represent warmer surfaces viewed by NOAA-2.

REPRODUCIBILITY OF THE ORIGINAL PAGE IS POOR.

imagery from NOAA-2's VHRR-IR channel (Figure 19) shows upwelling that has enveloped the entire Michigan shoreline south of the Manitou Islands. The analysis in Figure 20 shows the resulting surface temperature field obtained from this VHRR data. A spatial averaging of the VHRR data over a 4-km square is necessary to remove a small amount of high frequency noise.

Figure 21 presents the visible (red) channel information from the VHRR on 21 August. Sunglint (see Chap. 5) is evident over Lake Michigan and affects the VHRR-VIS imagery along the eastern (right) sychronization line (white) during summer months when the solar elevation is high. Despite the contamination from sunglint, features evident in the VHRR-VIS over Lake Michigan are also visible in ERTS-1 imagery acquired one hour earlier (Figure 22).

In Figure 22 the MSS-4 channel reveals considerable turbidity in the surface waters of nearly the entire lake; the turbidity is much less obvious in the MSS-5 channel. This effect presumably indicates increased turbidity below the water surface rather than at the surface. This follows from the fact that the radiant energy in the red channel (MSS-5) comes from only the upper few meters of the water and the green channel (MSS-4) is effective for turbidity observations to depths on the order of 10 meters. One area displaying an exception to this is along the shoreline from Muskegon to Benton Harbor; here the turbid water undoubtedly relates to erosion along the high bluffs, which have been threatened by the higher Great Lakes water levels of the last two years.

Displaying CCT data from ERTS-1 for 21 August on the "Image 100" permits a more quantitative understanding. Sampling of the ERTS-1 scene over 6 spots every 6 lines provides a useful overview. Banding is not as

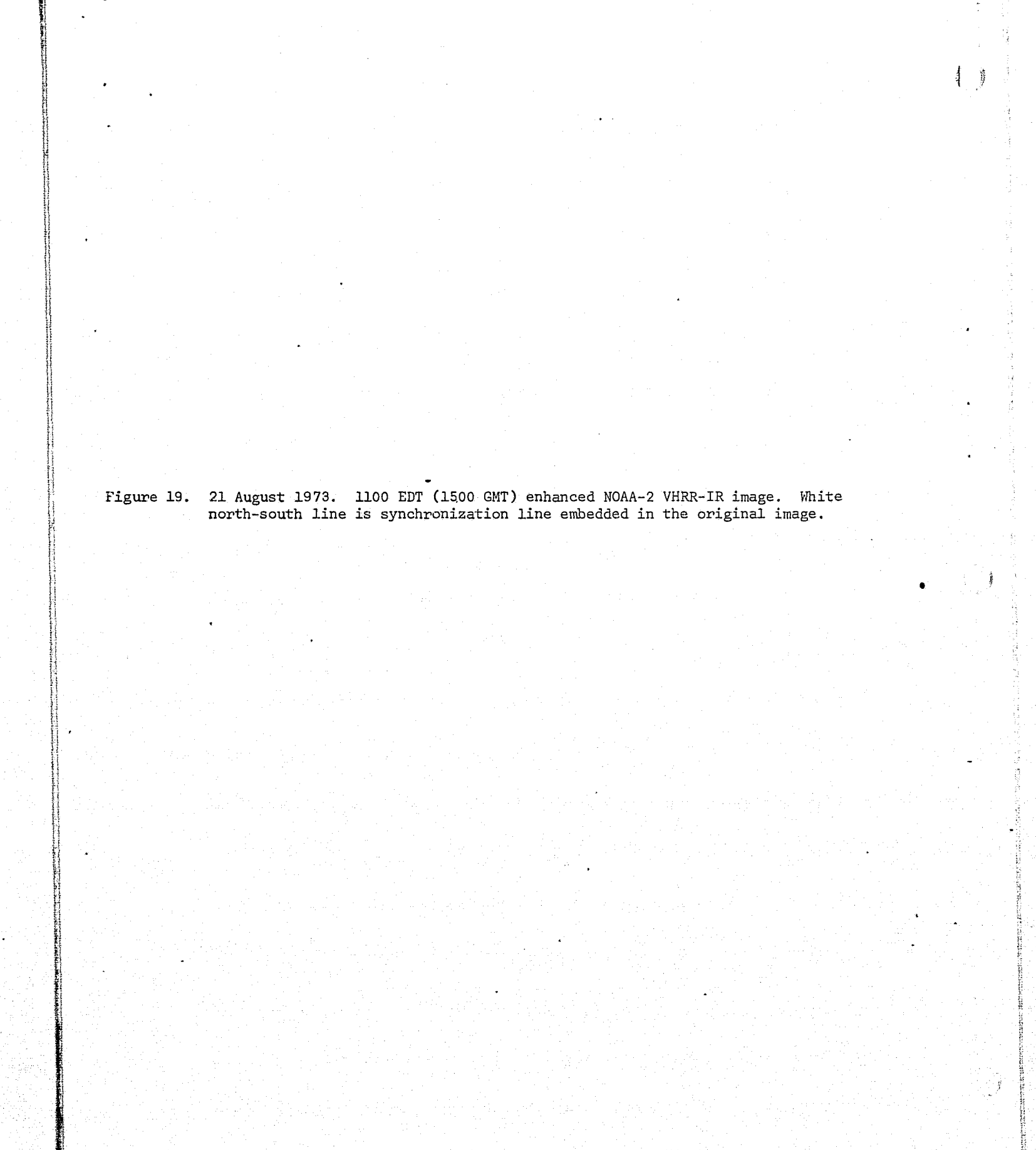

Figure 19. 21 August 1973. 1100 EDT (1500 GMT) enhanced NOAA-2 VHRR-IR image. White north-south line is synchronization line embedded in the original image.

REPRODUCIBILITY OF THE ORIGINAL PAGE IS POOR.

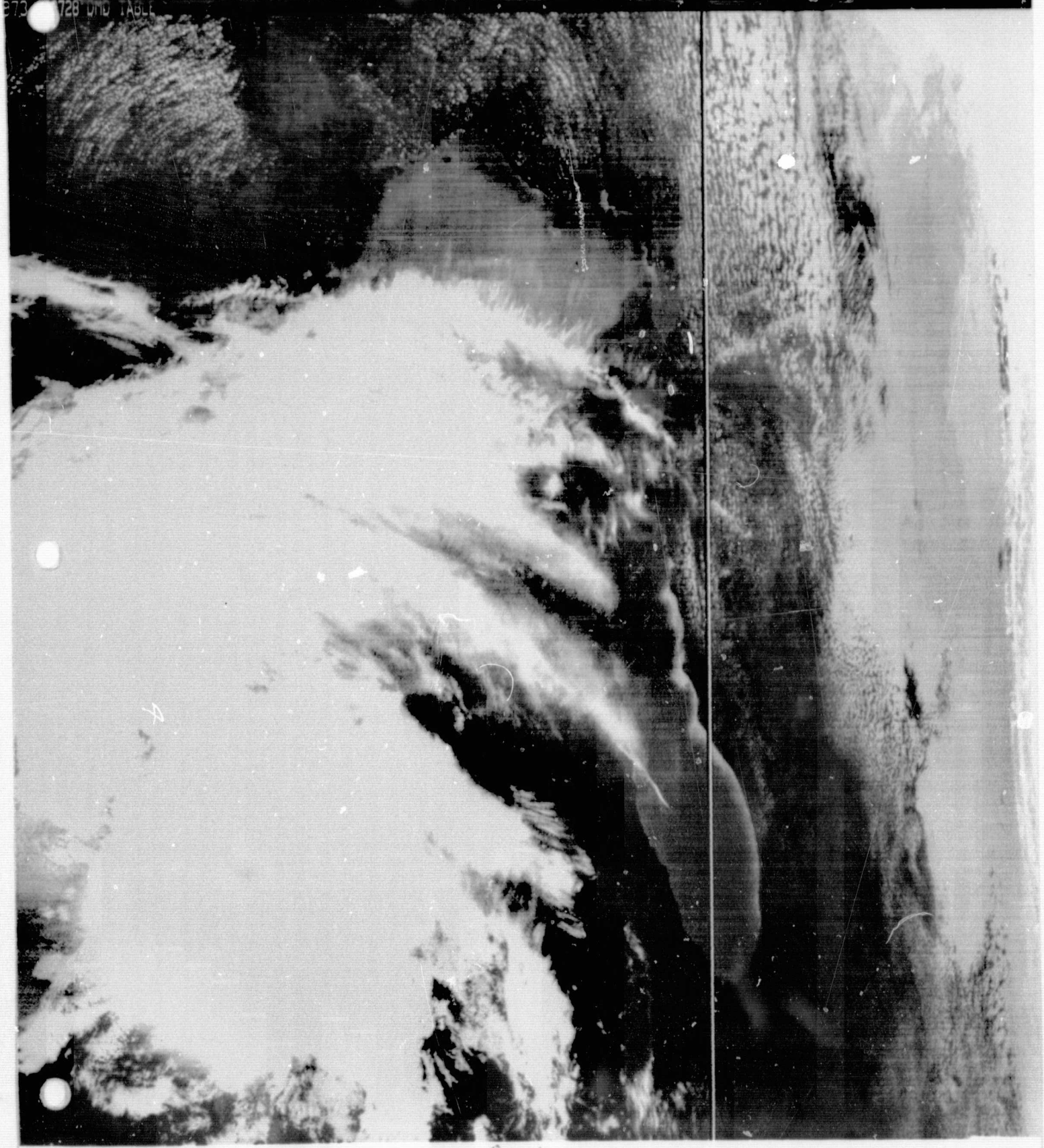

Figure 20. Analysis of Lake Michigan surface temperatures (°C) from Figure 19.

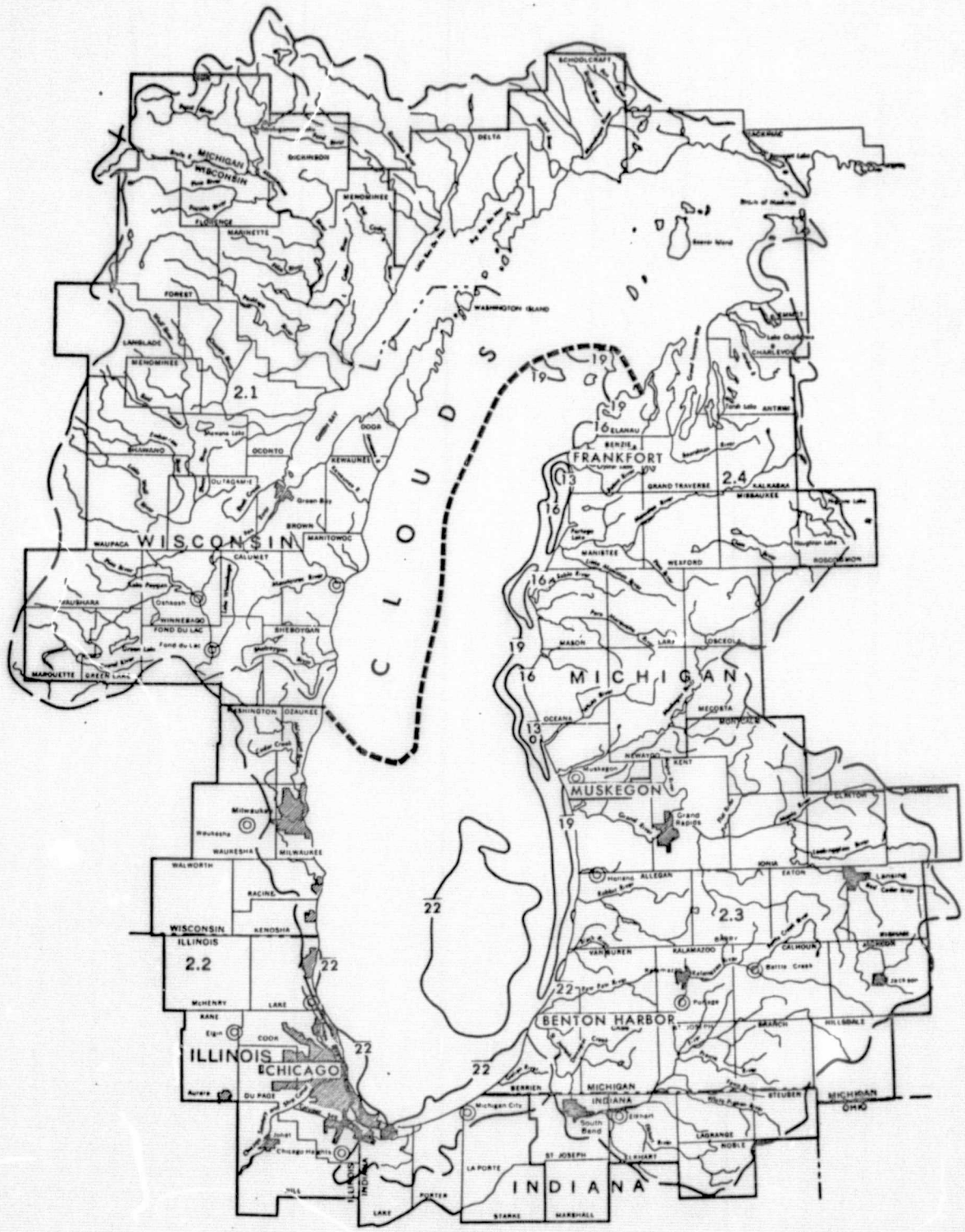
CLOUDS
WISCONSIN
MICHIGAN
ILLINOIS
INDIANA
2.1
2.2
2.3
2.4
FRANKFORT
MUSKEGON
BENTON HARBOR
CHICAGO
MICHIGAN
WISCONSIN
ILLINOIS
INDIANA
MICHIGAN
OHIO

Figure 21. 21 August 1973. 1500 GMT NOAA-2 VHRR-VIS image of Lake Michigan. Coincident image with Figure 19.

REPRODUCIBILITY OF THE ORIGINAL PAGE IS POOR.

Figure 22. 21 August 1973. 1600 GMT ERTS-1 MSS-4 and MSS-5 imagery (left and right, respectively).

REPRODUCIBILITY OF THE ORIGINAL PAGE IS POOR.

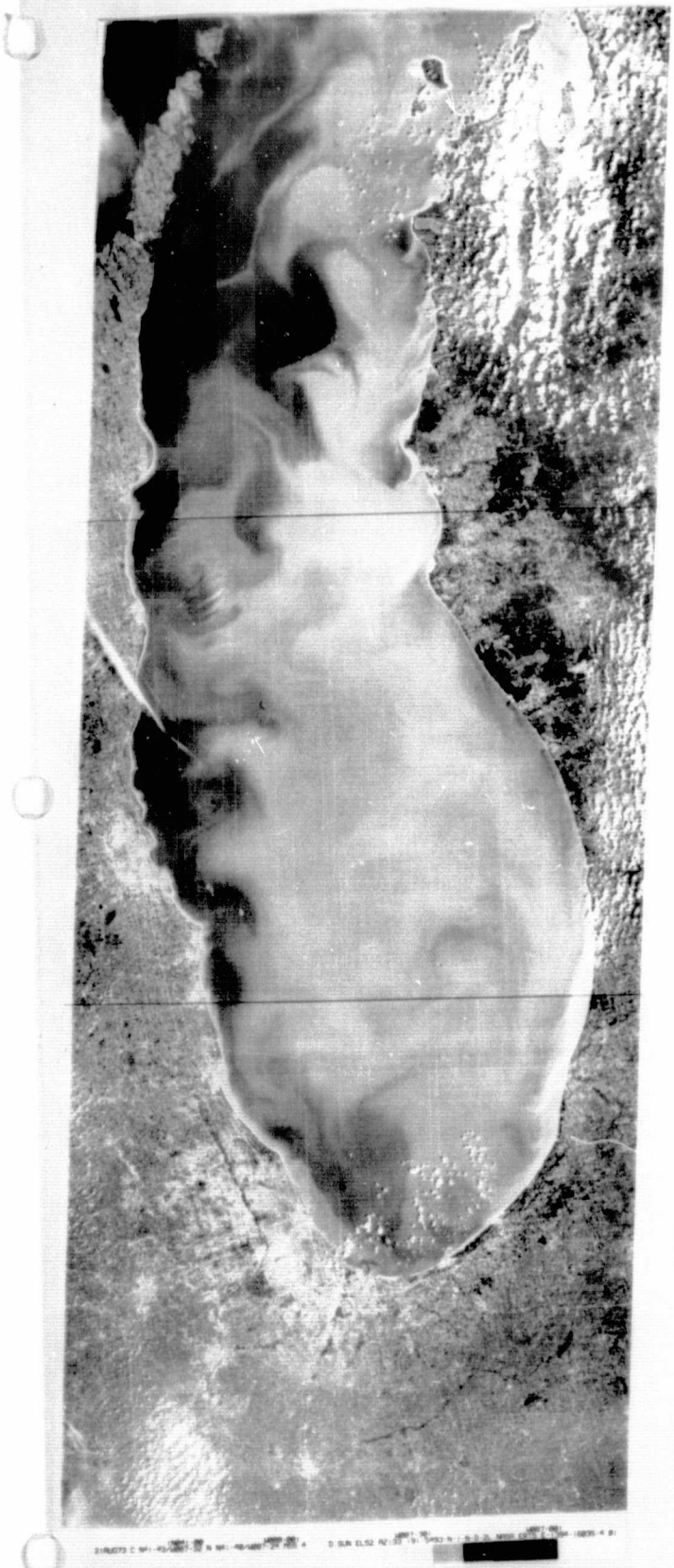

troublesome when observing these very turbid conditions in the visible portion of the spectrum. Banding has been most noticed when trying to use the near-IR data in MSS-6 or -7 (Chap. 2, Figures 14 and 15). Figure 23 is a color image using blue and green light on MSS-4 and red light on MSS-6 data. It is remarkable to see how much of the surface water area is affected. Figure 24 categorizes increasing levels of reflectance in MSS-4 where the other three-dimensional multispectral information for each pixel has a low value of reflectance. Table 5 shows the classification employed. Red is used to designate nearshore turbidity. Higher reflectance levels in MSS-5 are included for this signature and typify the erosion of the bluffs seen near Benton Harbor.

On the following day, 22 August, the VHRR-IR imagery revealed a somewhat enlarged upwelling strip along the coast (Figure 25). The analysis shows lower water temperatures over the central lake and along the shoreline (Figure 26). Ship weather observations revealed winds that were more easterly but continuing strong (around 10 m sec^{-1}).

A similar episode occurred on Lake Michigan beginning on 26 July. This upwelling was observed by ERTS-1 on 3 August, eight days later, when the phenomenon was in its final stages. Considerable turbidity can be seen again (Figure 27), but the MSS-4 levels of reflected radiation in the green band are much lower than observed by ERTS-1 on 21 August. For comparison the VHRR-IR image from NOAA-2 is shown in Figure 28. The same classification scheme used in Figure 24 and Table 5 has been employed in the color image in Figure 29. Only the third CCT for the Chicago scene has been processed on the "Image 100." The strip includes the Gary, Indiana shoreline. Reflectances observed on 3 August appear to be nearly identical to those observed on 21 August, although the latter

Figure 23. "Image 100" false-color enhancement of MSS-4 and -6 for Lake Michigan whiting on 21 August 1973.

REPRODUCIBILITY OF THE ORIGINAL PAGE IS POOR.

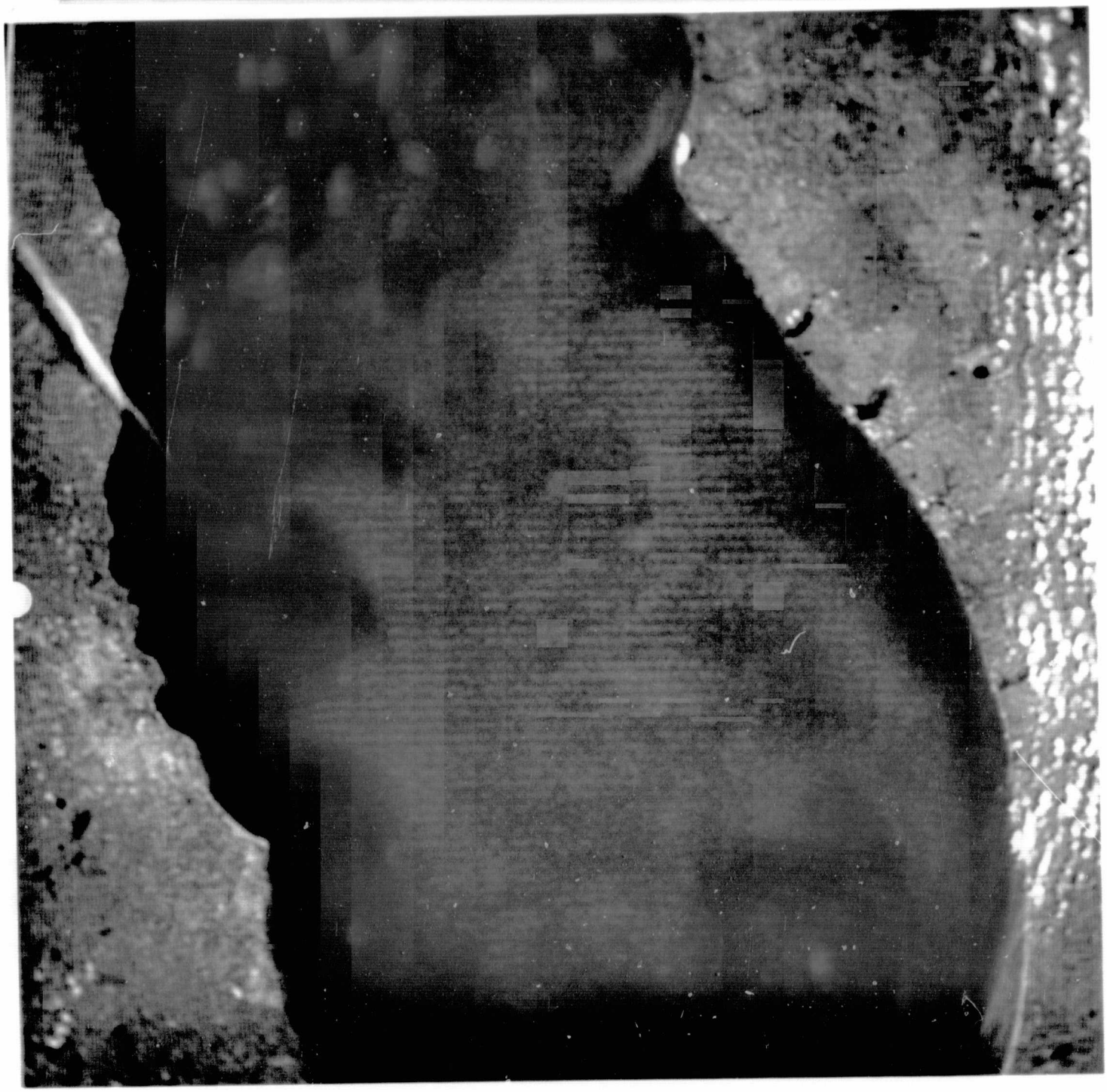

Table 5

Classification: Lake Michigan Whiting

August 3, 1973
August 21, 1973

MSS Channel	4	5	6	7	Color
Count Range	35-40	10-19	3-13	1-8	orange
	32-34	10-19	3-13	1-8	dark blue
	30-31	10-19	3-13	1-8	yellow
	28-29	10-19	3-13	1-8	pink
	26-27	10-19	3-13	1-8	light blue
	24-25	10-19	3-13	1-8	purple
	20-23	10-19	3-13	1-8	grey
	20-40	20-30	3-11	1-8	red

Figure 24a. Whiting classification produced for 21 August 1973 "Milwaukee" ERTS imagery using color classification as defined in Table 5.

REPRODUCIBILITY OF THE ORIGINAL PAGE IS POOR.

combined

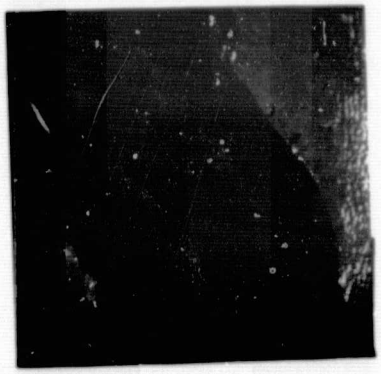

orange

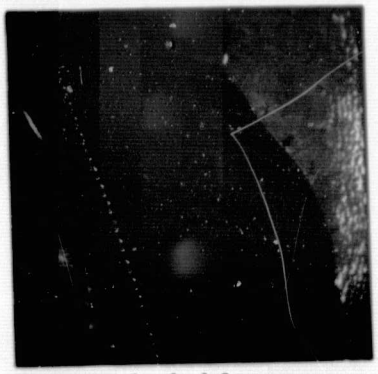

dark blue

yellow

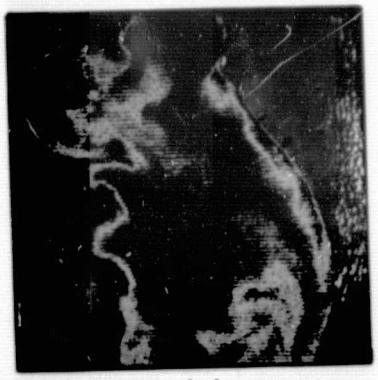

pink

light blue

purple

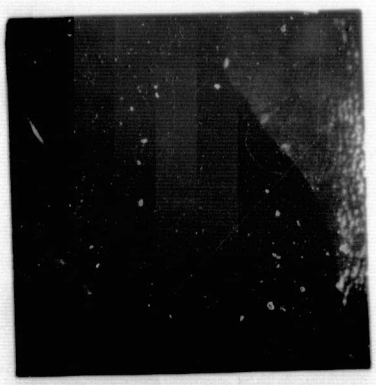

grey

red

Figure 24b. Whiting classification produced for 21 August 1973 "Chicago" ERTS imagery using color classification as defined in Table 5.

REPRODUCIBILITY OF THE ORIGINAL PAGE IS POOR.

combined

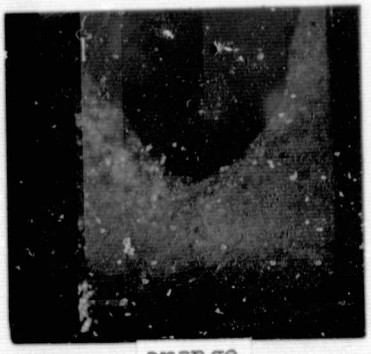
orange

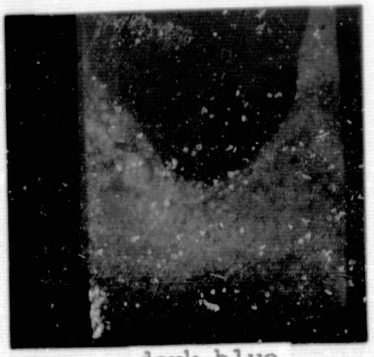
dark blue

yellow

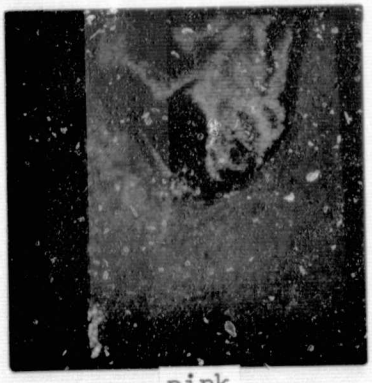
pink

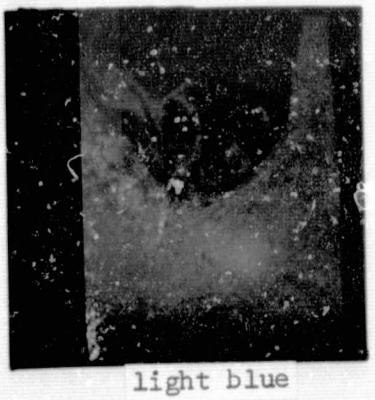
light blue

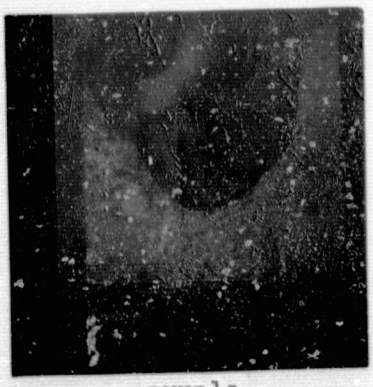
purple

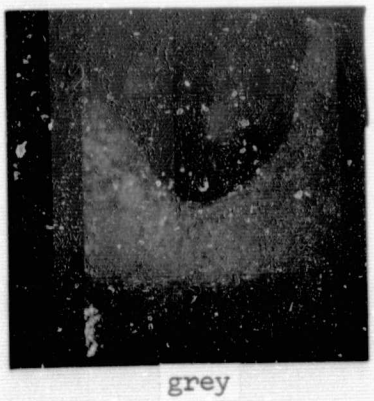
grey

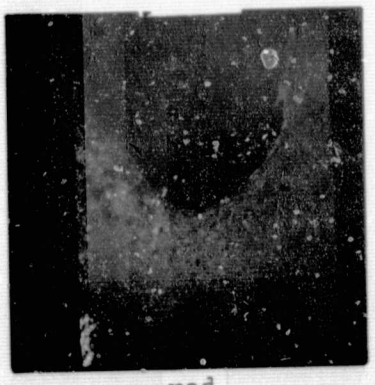
red

Figure 25. 22 August 1973. 1600 GMT NOAA-2 enhanced VHRR-IR image of Lake Michigan.

REPRODUCIBILITY OF THE ORIGINAL PAGE IS POOR.

1973 3870 DMD TABLE

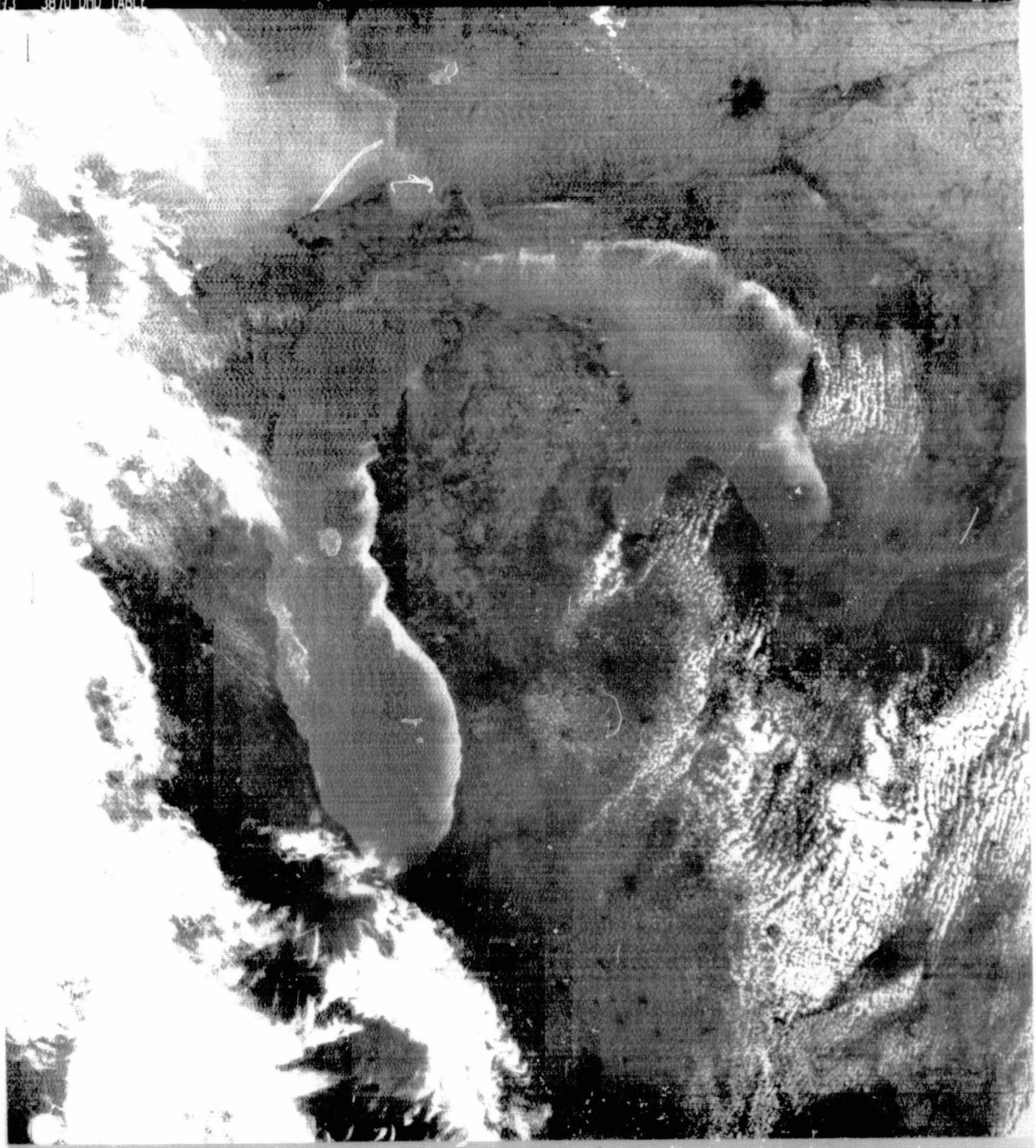

Figure 26. Analysis of Lake Michigan surface temperatures (°C) from Figure 25.

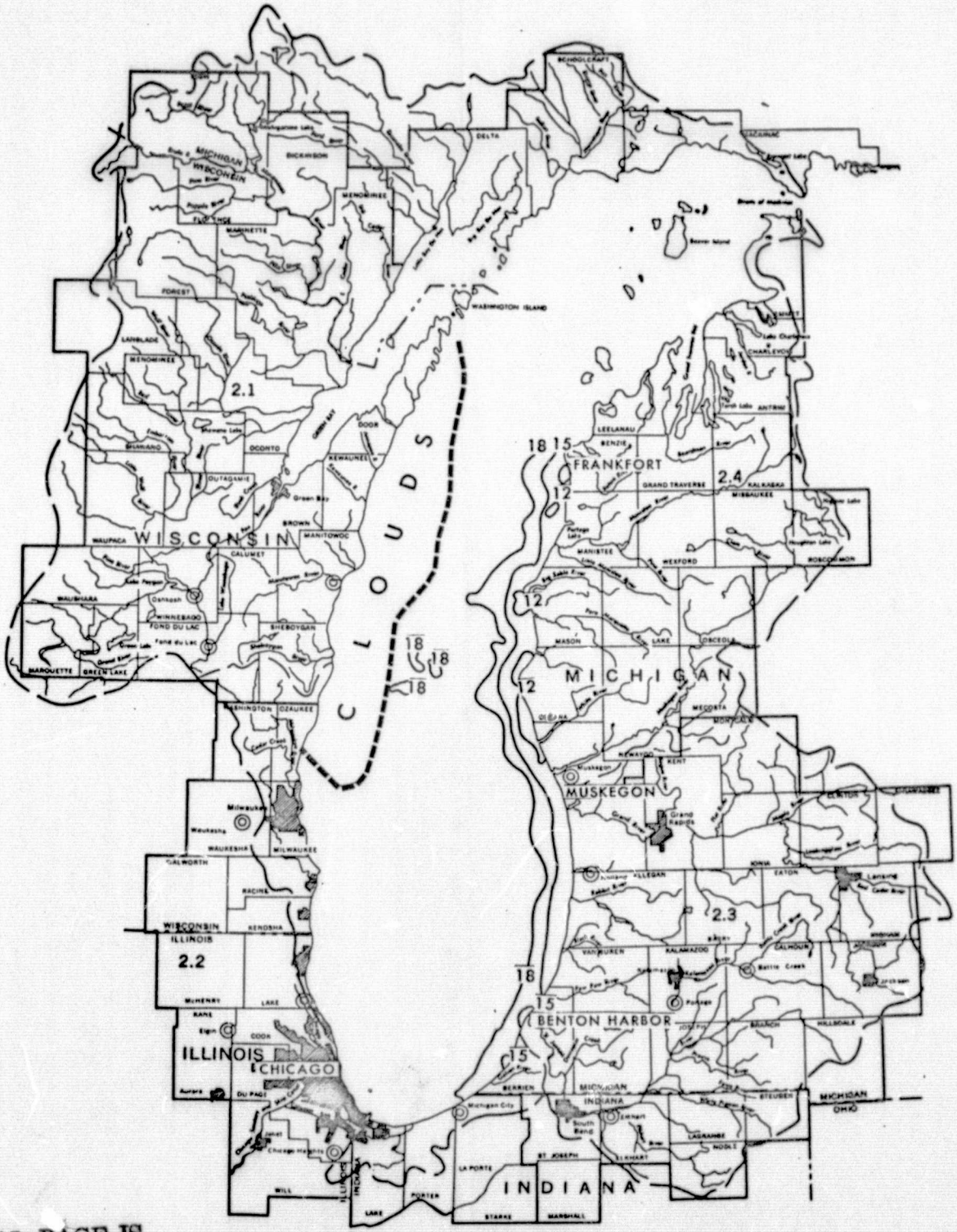

ORIGINAL PAGE IS
OF POOR QUALITY

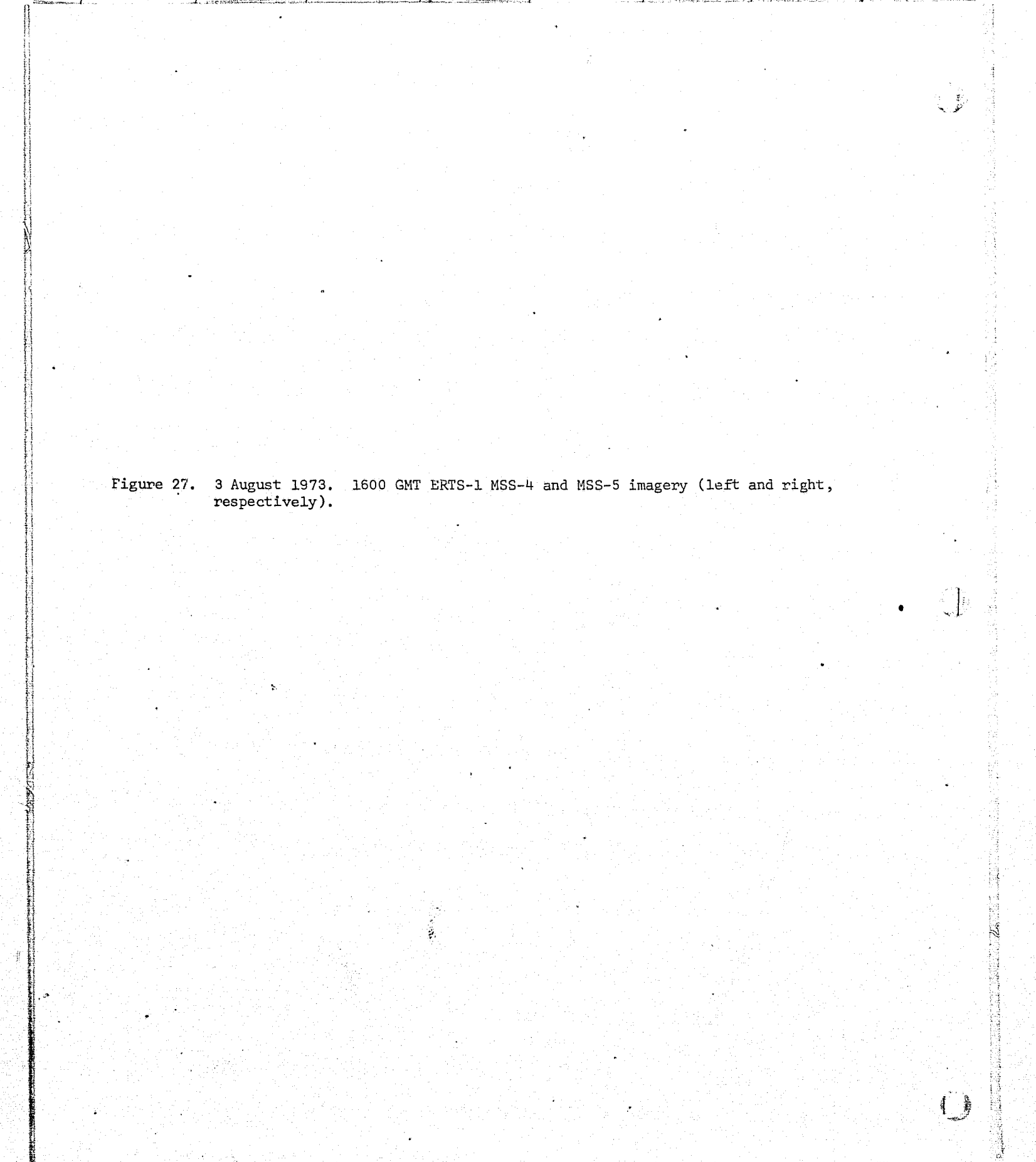

Figure 27. 3 August 1973. 1600 GMT ERTS-1 MSS-4 and MSS-5 imagery (left and right, respectively).

REPRODUCIBILITY OF THE ORIGINAL PAGE IS POOR,

Figure 28. 3 August 1973. 1500 GMT NOAA-2 VHRR-IR image of Lake Michigan.

REPRODUCIBILITY OF THE ORIGINAL PAGE IS POOR.

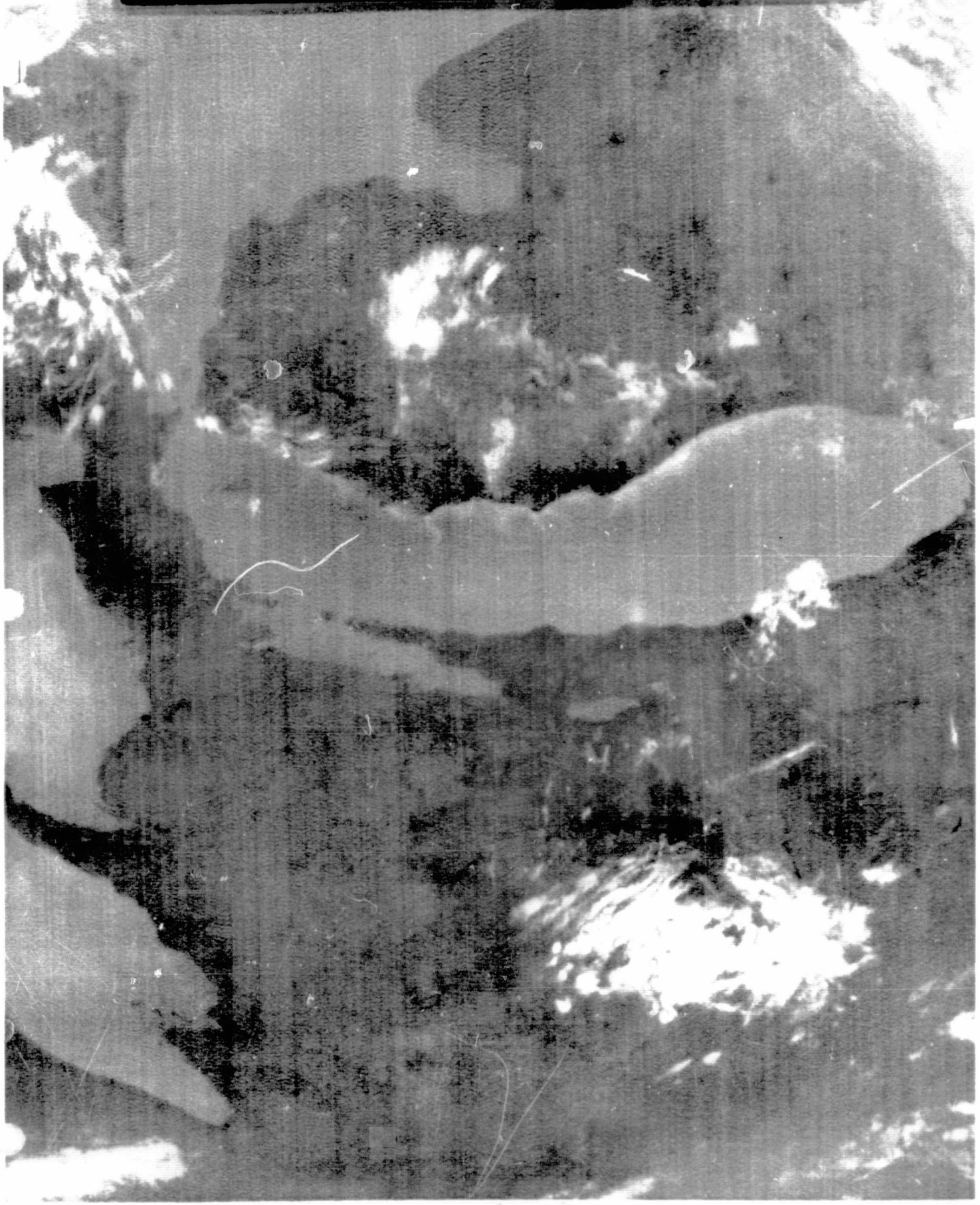

Figure 29. Whiting classification for 3 August 1973 for portions of "Chicago" ERTS imagery using identical "Image 100" color classification as shown in Figure 24 (see Table 5).

REPRODUCIBILITY OF THE ORIGINAL PAGE IS POOR.

combined

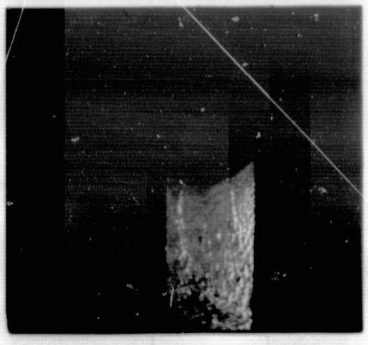

orange

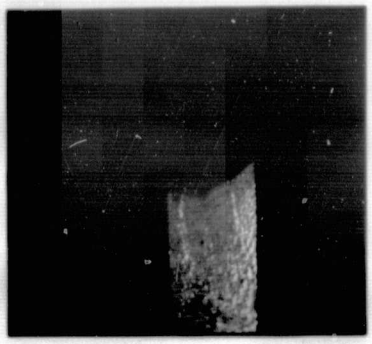

dark blue

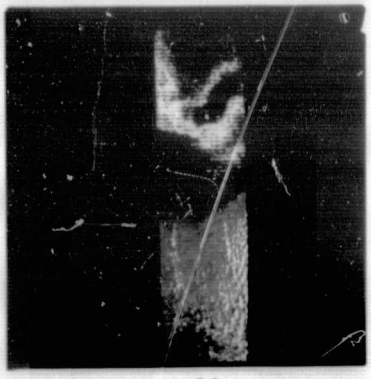

yellow

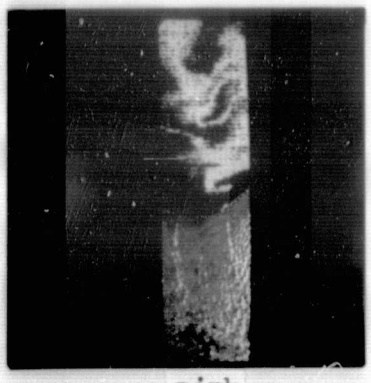

pink

light blue

purple

grey

red

case presents greater contrasts.

In all cases water intake temperatures confirmed the intense upwelling along the eastern shoreline. Several locations reported temperatures below 10°C during the maximum upwelling. Standard chemical analyses performed on the raw water from these intakes (Muskegon, Grand Rapids, South Haven, Benton Harbor, St. Joseph, and Chicago) indicated no abnormalities. Values of pH dropped from typical epilimnetic readings of 8.0 to 8.5 to slightly below 8.0 as cold and slightly more acidic hypolimnetic waters were drawn from deep in the lake's interior. Turbidity levels were not in excess of those expected, peaking while the wind blew onshore during the 20th, and dropping when the winds blew offshore on the 21st. The lowest surface temperature found was that observed during the night of the 21st by the University of Michigan research vessel MYSIS, viz. 9°C just off Benton Harbor.

DISCUSSION AND CONCLUSIONS

Combination of ERTS-1 and VHRR-IR data allow one to make numerous interpretations of surface current under this extreme upwelling condition. Among such features are river plumes entering Lake Michigan in the upwelling area seen in Figures 22 and 27 that appear dark in contrast to the "whiting" effect of the lake water. After these plumes enter the lake they veer abruptly to the left (south) parallel to the shoreline. Secondly, darker areas in the ERTS-1 image are presumed to be regions of sinking or downwelling. For the most part these vertical circulations are found on the downwind shore across the lake. A rather large area of less milky water is seen off Chicago. This region would be expected to receive maximum water elevations (pile up) from the southwestward wind stress. In this

area, sinking water is depressing the main thermocline of the lake. Thirdly, eddy circulations may be seen in the lee of headlands along the eastern shore, where some of the coldest surface waters are found. Finally, an eddy in the middle of the southern Lake Michigan basin is characterized by the warmest surface water observed on 21 August (Figure 20). Circulation of this large-scale feature is clockwise. Sinking would also be expected to accompany this unexpected circulation and may partially explain why some of this water is darker in the ERTS-1 imagery (Figure 22).

From the "Image 100" results (Figs. 24 and 29) a careful breakdown of the whiting is revealed. Similar structure and signature is observed for the 3 August and 21 August observations. The multispectral classification is both concentration and depth dependent and therefore not complete, as additional data are needed to separate these parameters. If all of the chemical precipitation is found to occur at a single level the classification becomes one of concentration (or vice versa).

From the 1973 observations it is our hypothesis that upwelling initiated the milky water phenomenon of August 1973. Cold upwelling waters and considerable mixing of the upper epilimnetic waters would trigger extensive phytoplankton development. Divers in Grand Traverse Bay noticed an abundant phytoplankton population at this time (L. Somers, 1974). These processes result in the removal of CO_2 from the surface waters and force a precipitation of carbonate ($CO_3^=$) with an appropriate anion, most probably calcium (Ca^{++}).

Ayers et al. (1967) have reported several instances of widespread milky water in Lake Michigan. In August 1966 observations conducted by the University of Michigan indicated Secchi disc readings reduced from

6-14 m, which are typical of mid-lake, to 2-4 m. No conclusive results came from their study, but they strongly suspected the milky conditions were the result of the precipitation of calcium carbonate from the surface waters.

The resulting late-summer die-off of deep-water shrimp, Mysis relicta, observed by Ayers et al. (1967) was presumed to be related to the presence of the milky water. A reoccurrence of this kill has not been reported in 1973.

Chapter 4 ICE

The 1972-73 ice season on the Great Lakes was unusually short due to mild winter temperatures. A siege of cold Arctic air during mid-February succeeded in producing a short period of nearly complete ice coverage on Lake Erie; however, this thin cover deteriorated rapidly later in the month, leaving the surface nearly ice-free during the remainder of the winter.

Whenever cloud cover permitted, the operational NOAA environmental satellite, NOAA-2, was able to record valuable information on the surface temperature of the lakes and, when ice was present, the areas and amount of coverage. It was observed that even during light winds, a change in the direction of this wind can drastically and rapidly alter the ice distribution and concentration.

Special attempts have been made to assure the acquisition of VHRR data at the National Environmental Satellite Service whenever the Earth Resources Technology Satellite (ERTS-1) overflies the region every 18 days.

USING SATELLITE IMAGERY TO MONITOR ICE COVER

Several VHRR illustrations are provided that show ice conditions, primarily in Lake Erie, during (1) freeze-up, (2) total ice cover, and (3) thaw. Nearly all imagery is derived from visible channel data because the thermal data have not been specially displayed for the small range of temperatures encountered. Several ERTS-1 images are presented for comparative purposes.

Freeze-up

ORIGINAL PAGE IS OF POOR QUALITY

On 29 January 1973 an exceptional VHRR-VIS view of Lake Erie was obtained; a portion of this image is shown in Figure 30. A typical winter scene prevails. On this cold morning (-10°C at Cleveland) the instability

PRECEDING PAGE BLANK NOT FILMED

C-2

Figure 30. 29 January 1973. 0900 EST NOAA-2 VHRR-VIS image of Great Lakes at initiation of freeze-up on Lake Erie. Note lake-effect cloudiness extending downwind from lake moisture sources.

REPRODUCIBILITY OF THE ORIGINAL PAGE IS POOR.

of cold air over warmer waters is made evident by "lake effect" lines of stratocumulus carried downwind from the lakes. One line, initiated by Lake Huron to the north, is especially prominent over Lake Erie and extends from Cleveland to Wheeling, West Virginia and the Appalachian Mountains. Numerous snow showers were observed to be embedded in this line of convective cloudiness. The ice that had first been detected on 13 January in both ERTS-1 and NOAA-2 imagery had melted, so all that is seen on 29 January is a small floe between Pointe aux Pins and Long Point just off the Canadian shoreline. Cloud cover prohibits any detection of ice in the island area off Sandusky, Ohio, although it is likely that some ice remains there.

Cold Arctic air again moved into the Great Lakes region in early February. Ice growth was dramatic, especially around 14 February. Figure 31 shows the VHRR-VIS imagery on this day and affords a nearly cloud-free view of all of the Great Lakes except Lake Superior. New ice in central Lake Erie is not nearly as reflective as that in Whitefish Bay, Georgian Bay, or Saginaw Bay where thickness and snow cover enhance surface reflectance (McClain, 1973). A windrow of ice can be seen near the center of southern Lake Huron.

Total Ice Cover

By 17 February, three days later, sustained "subzero" (°F, -18°C) weather produced nearly total ice coverage on Lake Erie. The VHRR-IR imagery is shown in Figure 32 (no VHRR-VIS is available). Air temperatures along the shoreline of near -20°C provide large thermal contrasts over the ice for interpreting thickness. Ice acts as an insulator, so that as its thickness increases, its upper surface temperature more closely approaches the much lower air temperatures immediately over the air-ice interface.

Figure 31. 14 February 1973. 0900 EST NOAA-2 VHRR-VIS image of Great Lakes just prior to total ice cover in Lake Erie.

REPRODUCIBILITY OF THE ORIGINAL PAGE IS POOR.

Figure 32. 17 February 1973. 0900 EST NOAA-2 VHRR-VIR enhanced imagery of Great Lakes at time of near-100% ice cover on Lake Erie.

REPRODUCIBILITY OF THE ORIGINAL PAGE IS POOR.

Figure 33. 18 February 1973. 1000 EST NOAA-2 VHRR-VIS image of Great Lakes area. Lake Erie lies distorted to the right of the right-hand north-south synchronization line. Ice is observed to be breaking up.

REPRODUCIBILITY OF THE ORIGINAL PAGE IS POOR.

Figure 34. (right) 17 February 1973. 1000 EST ERTS-1 MSS-5 of Lake Ontario and eastern half of Lake Erie.

Figure 35. (left) 18 February 1973. 1000 EST ERTS-1 MSS-5 of middle portion of Lake Erie. Overlap portion is delimited by black line.

REPRODUCIBILITY OF THE ORIGINAL PAGE IS POOR.

18 FEB. 1973

17 FEB. 1973

Breakup and Thaw

On the following day (18 February) 10-kt southwesterly winds drastically altered the ice pattern. In Figure 33, VHRR-VIS imagery shows large cracks, often approaching 5- to 10-km wide, that have developed in the ice cover.

ERTS-1 imagery was acquired over Lake Erie on both 17 and 18 February. ERTS-1 obtains four-channel, 100-meter resolution visible imagery of a given Earth location every 18 days. This makes it possible, at times, to compare the 0.6-0.7μm imagery of NOAA satellites and ERTS. The ERTS-1 images in Figures 34 and 35 should be compared with the NOAA images in Figures 32 and 33, respectively. Ice-movement vectors were obtained by locating ice features seen in the overlap area of the consecutive-day ERTS-1 observations. This analysis is presented in Figure 36. Many of these features, of course, are unresolvable in VHRR imagery, but the large ice features will permit the production of ice motion charts for cloud-free periods.

Break-up and thaw proceeded at a rapid rate during March. By 27 March no ice of any consequence remained. The VHRR-VIS image shown in Figure 37 attests to this condition. The lake is extremely turbid following recent rains and high winds. A VHRR-IR image coincident with Figure 37 is presented in Figure 38. At this time of year all water surfaces in the Great Lakes are very uniform in thermal expression (the water temperatures are within two degrees of 2°C).

CONCLUSIONS

It has been demonstrated that NOAA-2 VHRR imagery can permit an accurate ice cover chart to be made of the Great Lakes, provided cloud cover is not persistent. Resolutions of 1 km appear adequate not only for assessing ice coverage and condition but also, when available on a day-to-day basis, charting ice motions that result from changing wind and current conditions. Snow cover enhances the ice cover as seen from space, and may

Figure 36. Ice motions from overlap area of Figures 34 and 35. Station weather observations (times are "Z" or GMT) include air temperature (°F), cloud cover, present weather, and wind direction and speed.

4-9

REPRODUCIBILITY OF THE ORIGINAL PAGE IS POOR

Figure 37. 27 March 1973. 0900 EST NOAA-2 VHRR-VIS image of Great Lakes. Note extensive sediment in Lake Erie surface waters.

REPRODUCIBILITY OF THE ORIGINAL PAGE IS POOR.

Figure 38. 27 March 1973. 0900 EST NOAA-2 VHRR-IR enhanced image coincident with Figure 37. Lakes are nearly isothermal at surface.

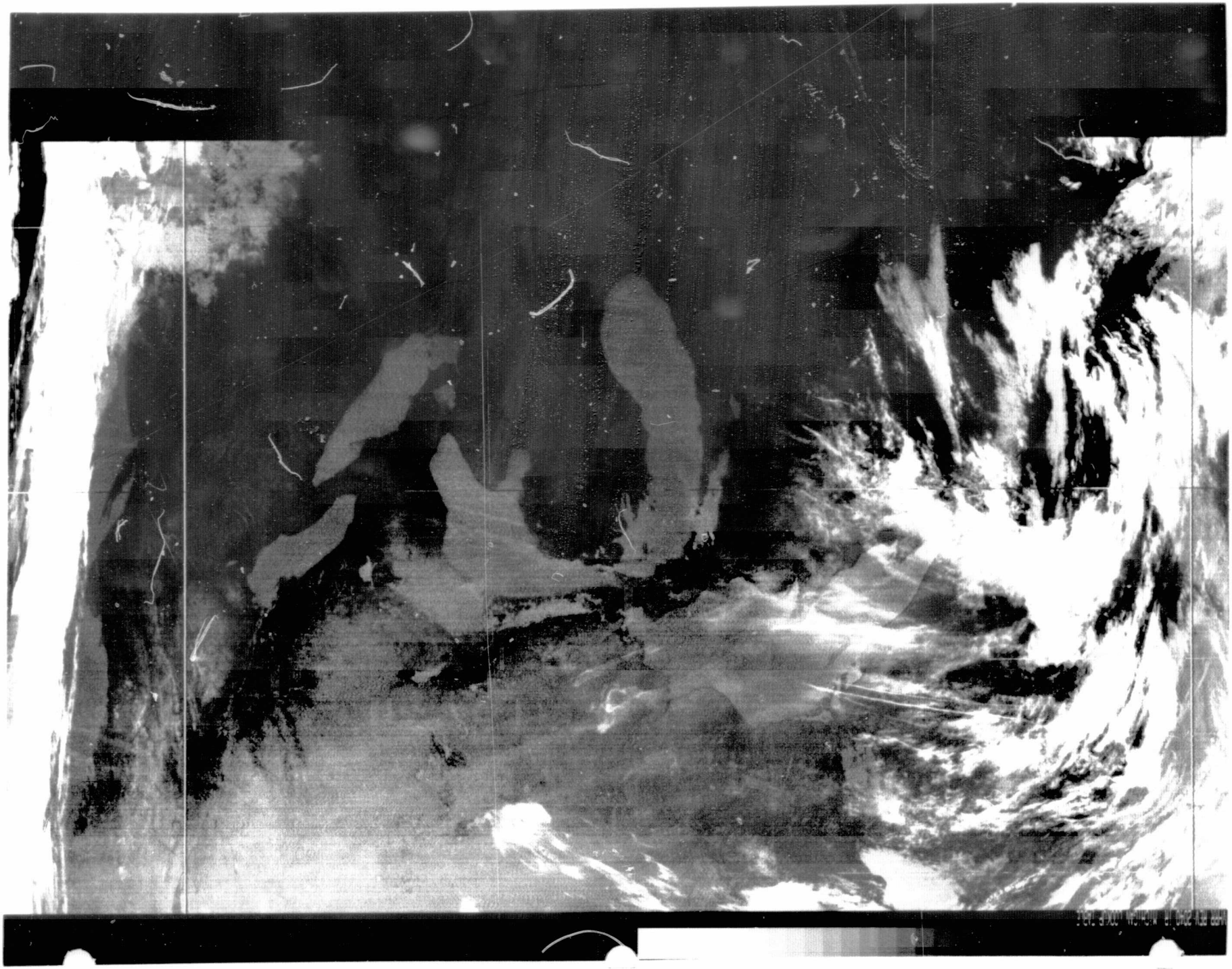

allow further judgments to be made on the age and thickness of the ice. Use of the IR data permits nighttime observations to augment the daytime observations. Furthermore, the availability of calibrated information will provide valuable surface temperature information. During cold periods this thermal measurement could be useful for relating to thickness and condition of the ice.

Although the 1972-73 ice year on the Great Lakes was a rather brief event, use of VHRR data for monitoring Great Lakes ice conditions will continue, and we expect it will increase substantially during succeeding winters. Those with shipping and coastal interests should expect to benefit from the new perspective on our environment. Use of ERTS-1 imagery is warranted in specialized circumstances where higher resolutions are required. However, daily coverage is the most critical weapon for ice monitoring in the Lakes. Further ERTS-1 ice and snow studies are available in another ERTS-1 Final Report from NOAA (Wiesnet, McGinnis and McMillan, 1975).

ERTS-1 imagery can be useful, as demonstrated, for monitoring ice motions in cloud-free areas where day-to-day sidelap is obtained. Although two successive clear days in the Great Lakes region are rare during winter, they become more probable if the Lakes become completely ice-covered in February. During late winter and spring ice-breakup, satellite observations are less frequented by cloudy conditions and may be extremely valuable to early shipping interests in the Great Lakes, provided imagery can be made available.

Chapter 5 SUNGLINT*

It was reported to NASA/GSFC in July and August 1973 that sunglint effects on surface waters could be expected in ERTS-1 imagery whenever solar elevations are in excess of 55°. These effects have been particularly evident under light variable wind conditions and make oceanographic/limnologic ERTS-1 work much more difficult, especially since clear sky (needed for satellite observation) and light winds tend to occur simultaneously. Furthermore, it was suggested at that time that several perplexing scenes, some of which had been discussed at recent conferences, could easily be explained using Cox and Munk (1954) data that had been modeled by NOAA for a satellite's perspective (Strong, 1972; Strong and Ruff, 1970; and McClain and Strong, 1969).

Although the true horizontal specular point (center of the sunglint) lies well outside the ERTS-1 imagery, the wind-roughened surface produces wave facets that are able to direct glint onto the MSS detectors. As the wind speed increases, this condition becomes more probable and the ocean surface appears brighter at greater and greater distances from the specular point. As discussed by Levanon (1971), this surface reflectance is best observed at red and reflected (near) IR wavelengths. The effects are best observed in MSS-6 and -7 (if properly enhanced) because sub-surface color differences are not apparent at these near-IR wavelengths.

Figure 39 shows an ERTS-1 image of Lake Michigan on 16 July 1973. MSS-5 and -6 are shown to illustrate the need for multispectral data in water color research, especially when solar elevations are high. Dark areas along the shoreline are particularly apparent in MSS-6 (right).

*The authors are indebted to Mr. I. Ruff for much of the modeling work.

PRECEDING PAGE BLANK NOT FILMED

Figure 39a. 16 July 1973. 1600 GMT ERTS-1 MSS-5 image of Lake Michigan (Milwaukee 1/3 distance up western shore). Note variable reflectance patterns especially along eastern shoreline. This is sunglint-induced.

REPRODUCIBILITY OF THE ORIGINAL PAGE IS POOR.

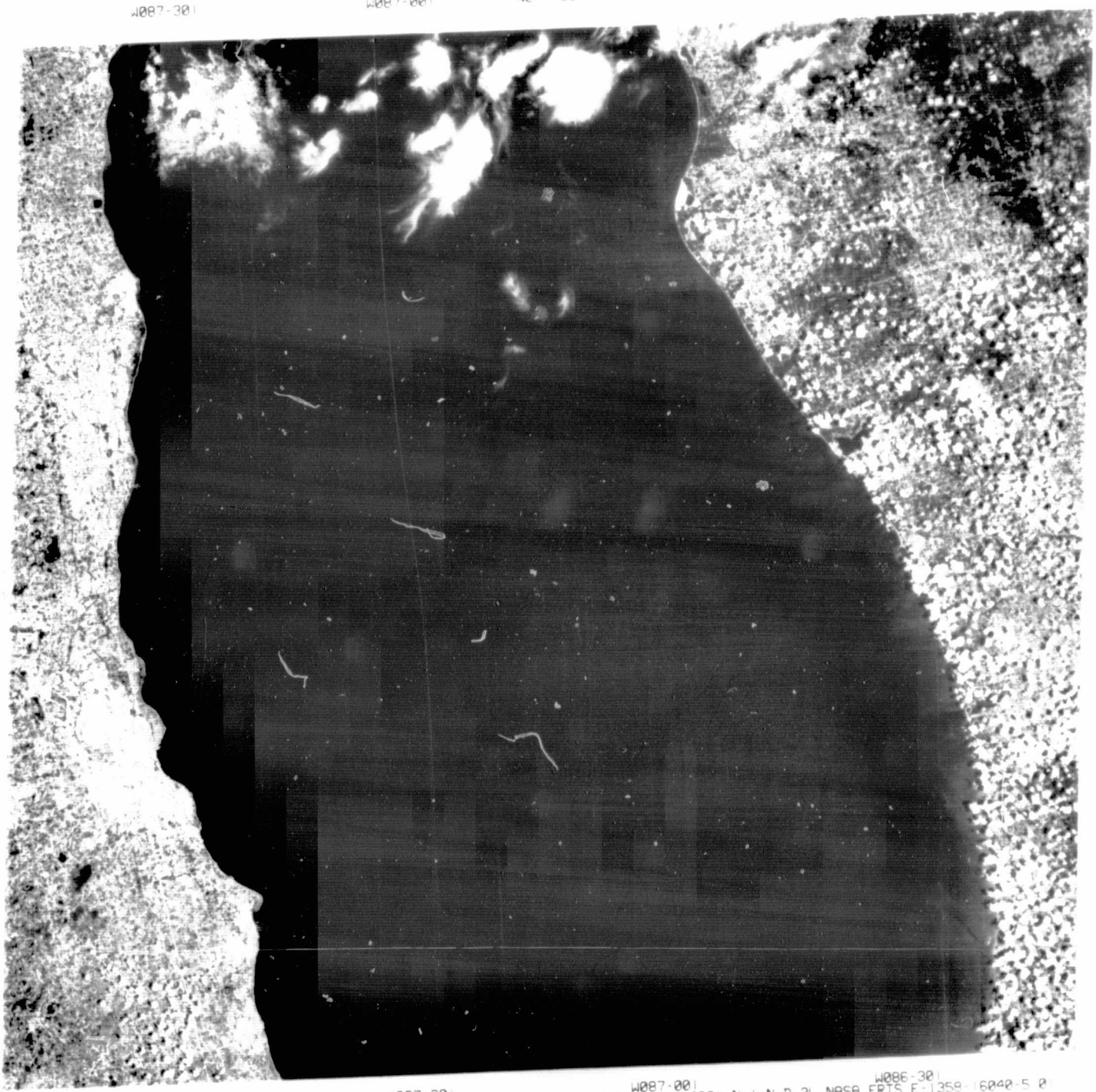

Figure 39b. 16 July 1973. 1600 GMT ERTS-1 MSS-6 image of Lake Michigan. Sunglint only is revealed in MSS-6 as waterborne sediment features are suppressed.

REPRODUCIBILITY OF THE ORIGINAL PAGE IS POOR.

W087-30| W087-00| N044-00| |W086-30 W086-00|

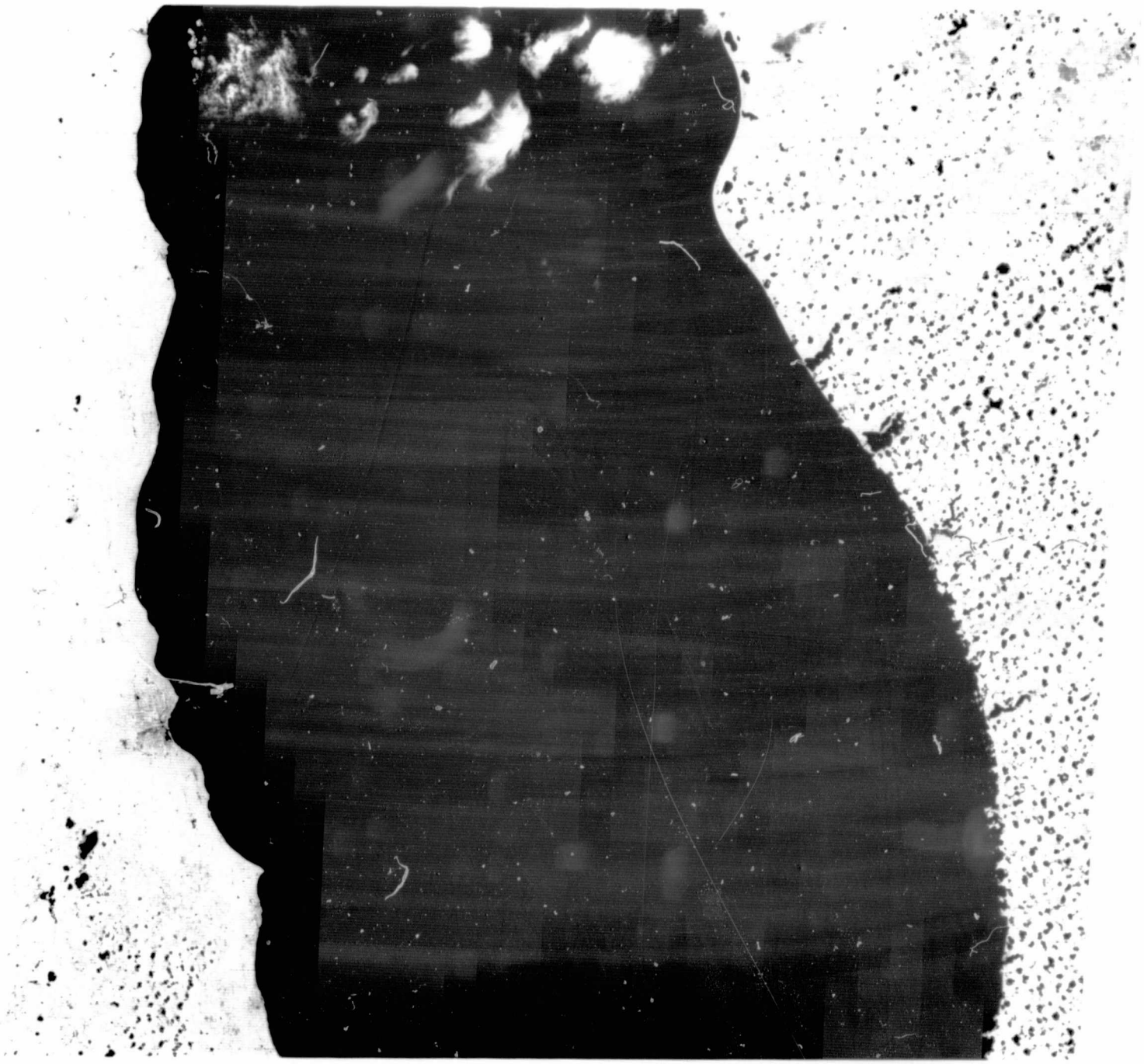

|W088-00 W087-30| W087-00| W086-30|
16JUL73 C N43-12/W087-02 N N43-08/W086-53 MSS 6 D SUN EL58 AZ125 19|-499|-N-|-N-D-2L NASA ERTS E-1358-16040-6 01

W088-00| W087-30| W087-00| |N042-30

Winds for this period were northeasterly, thus putting the nearshore waters in a wind shadow. Reported wind speeds ranged from calm to 5 m sec^{-1}. The NOAA-2 VHRR-VIS image, Figure 40, acquired soon after the ERTS-1 observation, provides an expanded perspective with the horizontal specular point nearly coincident with the Lake Michigan shoreline. In Figure 40, we observe that the southern area of this wind-shadowed darker water seen by ERTS-1 (Figure 39) reverts to a more brilliant near-specular reflection. Based on the Strong and Ruff (1970) model and similar work using time-lapse pictures from ATS (McClain and Strong, 1969), a case is easily made that the dark water in Figure 39 and the coincident bright water areas in Figure 40 are free of capillary waves. Simply stated, the surface is smooth because no wind stress reaches the interface.

The sunglint model adapted to satellite use (Strong and Ruff, 1970) has been further refined to provide definitive reflectances to overlay ERTS-1 imagery. Reflectance values are calculated as percentages of the incoming solar radiation under specified wind speeds without including any intervening atmosphere. The 16 July NOAA-2 VHRR-VIS image in Figure 40 has been overlain with an expected brightness distribution for calm winds and 5 m sec^{-1} winds in Figures 41 and 42, respectively. A latitude/longitude grid is also included. The observed reflectances in Figure 40 agree qualitatively with the predicted calm water results (Figure 41) near the eastern shoreline of Lake Michigan and the rough water results (Figure 42) away from shore.

A similar overlay series has been constructed for the ERTS-1 scene of Lake Michigan (Figure 39). Here we present brightness isolines calculated for windspeeds of 0, 2, 5, and 10 m sec^{-1} in Figure 43, 44, 45, and 46, respectively. It should be mentioned that no whitecap brightnesses

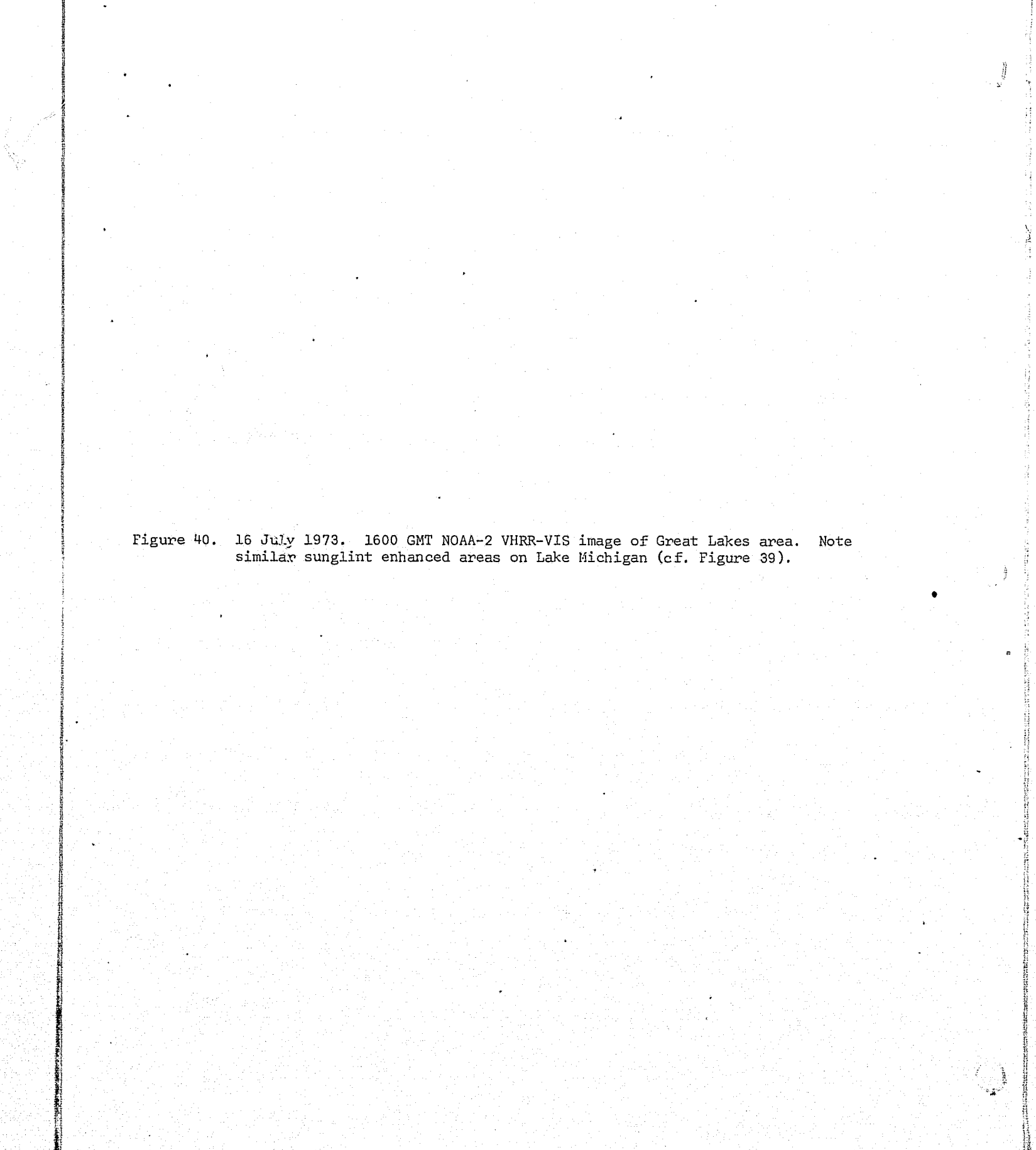

Figure 40. 16 July 1973. 1600 GMT NOAA-2 VHRR-VIS image of Great Lakes area. Note similar sunglint enhanced areas on Lake Michigan (cf. Figure 39).

REPRODUCIBILITY OF THE ORIGINAL PAGE IS POOR

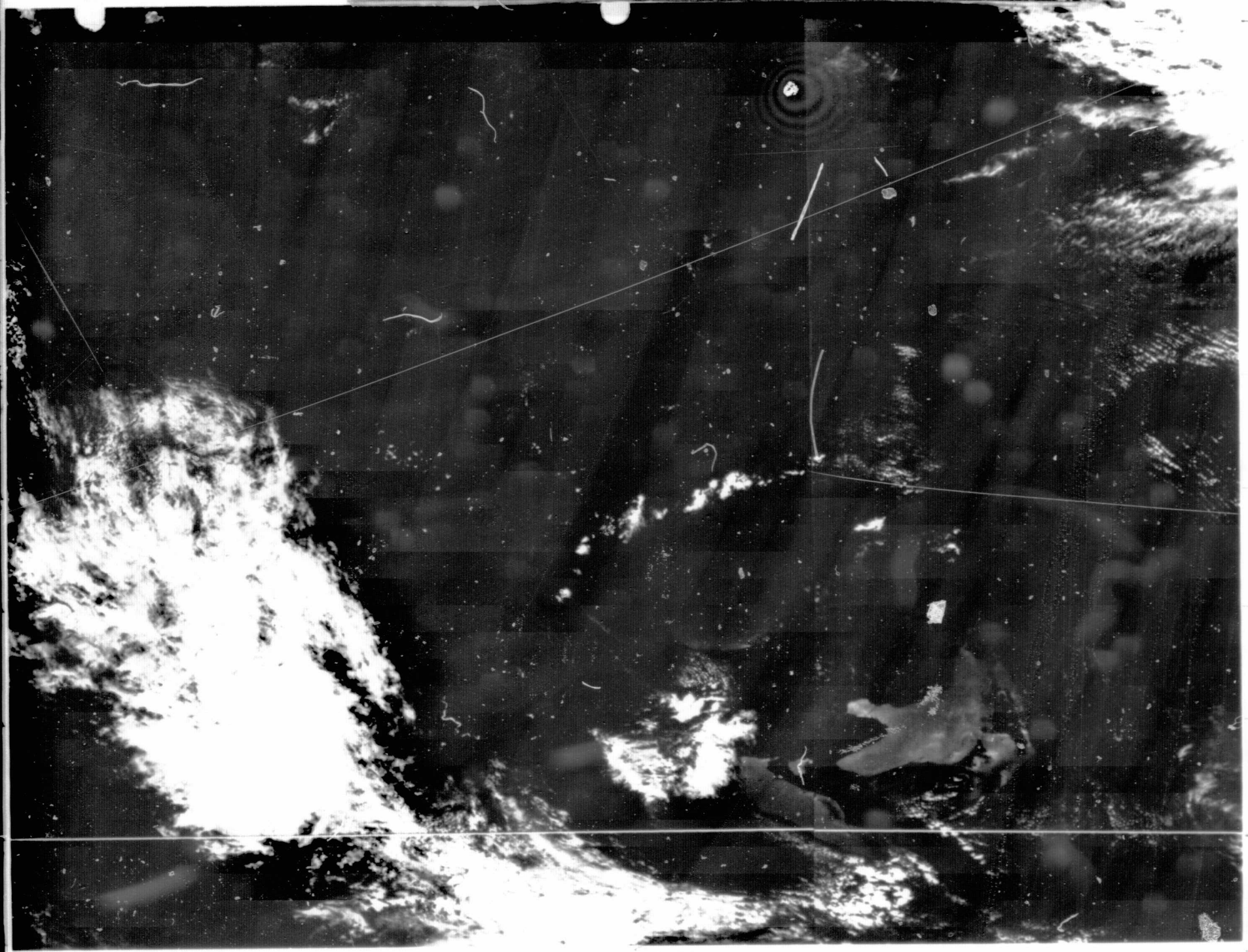

Figure 41. Sunglint modelled NOAA-2 brightness patterns for 0 m sec^{-1} wind speed. Patterns superimposed with lat/long grid on Figure 40. Reflectances are in percent of incoming flux.

REPRODUCIBILITY OF THE ORIGINAL PAGE IS POOR

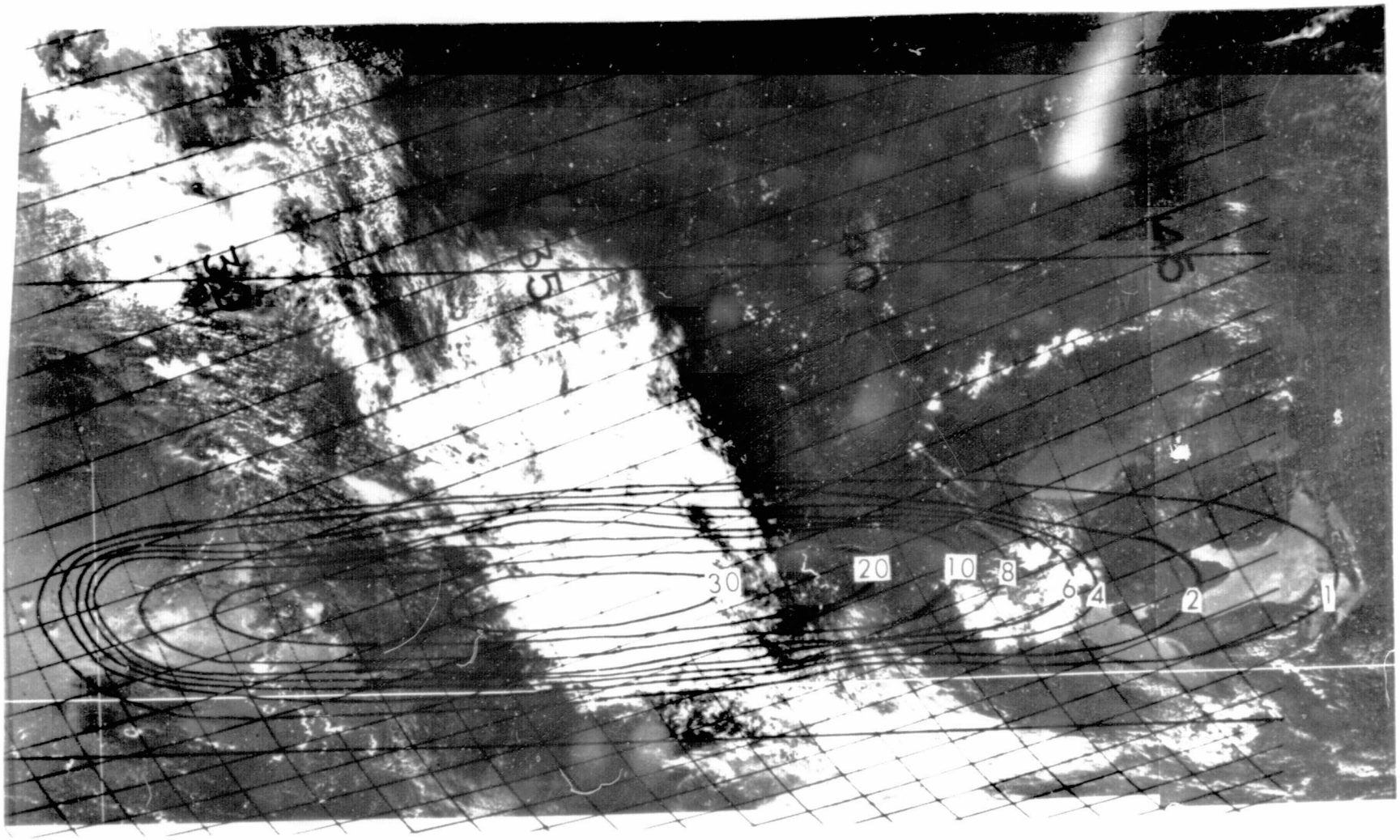

Figure 42. Sunglint modelled NOAA-2 brightness patterns for 5 m sec^{-1} wind speed. Patterns superimposed with lat/long grid on Figure 40. Reflectances are in percent of incoming flux.

REPRODUCIBILITY OF THE ORIGINAL PAGE IS POOR.

Figure 43. Sunglint modelled ERTS-1 brightness patterns for 0 m sec^{-1} wind speed. Reflectances, in percent of incoming flux, are superimposed on Figure 39a.

REPRODUCIBILITY OF THE ORIGINAL PAGE IS POOR.

Figure 44. Same as Figure 43 for 2 m sec^{-1} wind speed.

REPRODUCIBILITY OF THE ORIGINAL PAGE IS POOR.

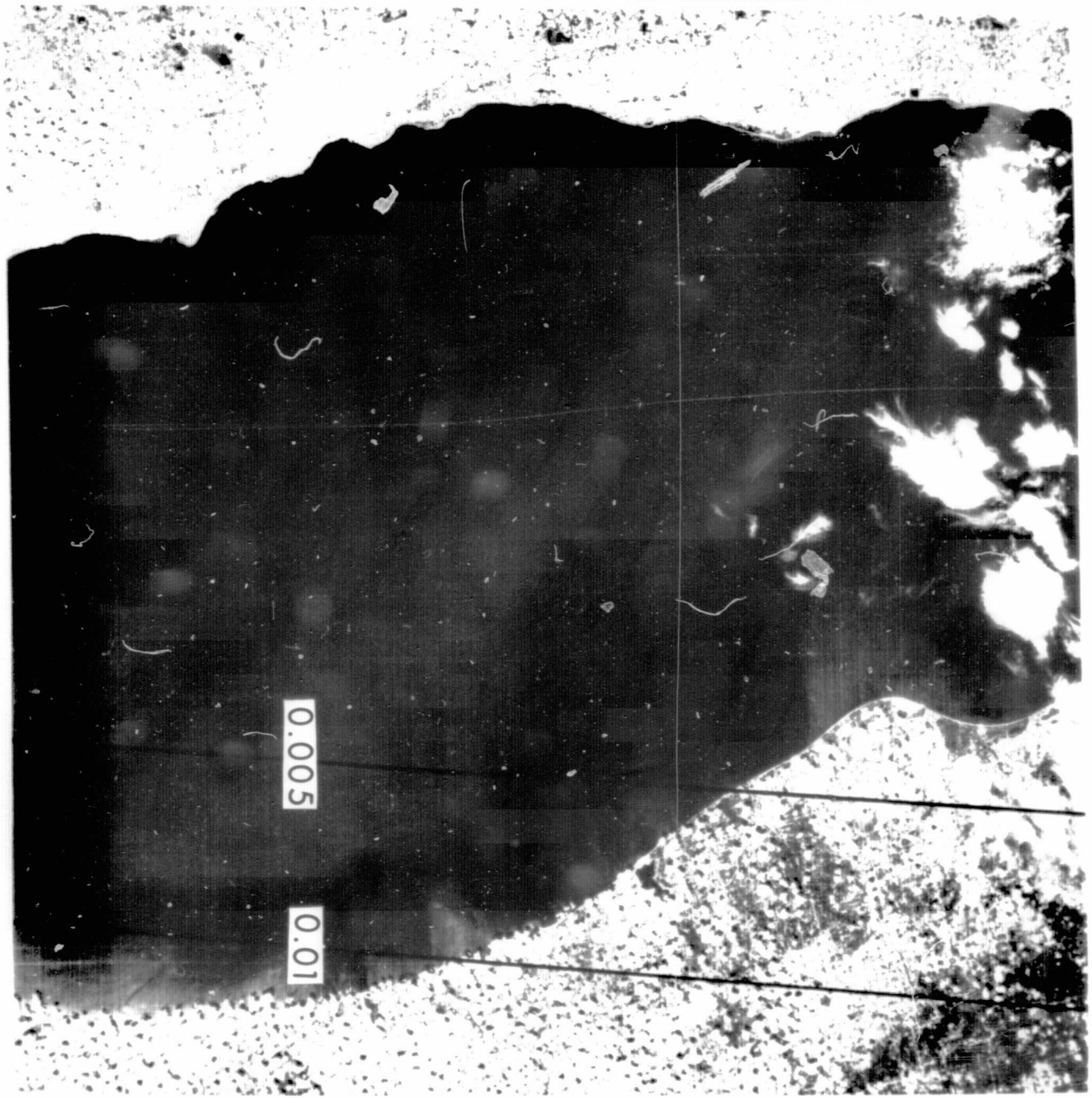

Figure 45. Same as Figure 43 for 5 m sec^{-1} wind speed.

REPRODUCIBILITY OF THE ORIGINAL PAGE IS POOR

Figure 46. Same as Figure 43 for 10 m sec^{-1} wind speed.

REPRODUCIBILITY OF THE ORIGINAL PAGE IS POOR.

have been incorporated into this sunglint model. Above 5 m sec^{-1} some allowance should be made for additional reflectance from whitecaps.

It can be readily demonstrated that nothing is sacred regarding a threshold solar elevation below which no sunglint effects are possible. An extremely strong offshore wind can undoubtedly impose lee effects on the roughness generated in the small-scale wave field permitting the observation of variable sunglint features when solar elevations lie well below 50° on ERTS-1 images. It appears that solar elevations greater than 50° to 55° are sufficient to cause considerable brightness anomalies when wind speeds and associated roughnesses approach the calm-rough surface transition.

Sunglint wind-generated features are evident in the following ERTS-1 scenes that are chosen as representative samples:

28 July 1972	Rhode Island Sound
14 October 1972	Lee of the Antilles
28 July 1972	Monterey Bay
7 July 1973	Off Delaware Bay

It should be obvious that sunglint and its contaminating effects on water color observations from space must be recognized. Any dedicated satellite water-color mission must utilize a pointing sensor that is capable of looking away from the sunglint. Despite the more brilliant sunglint observed during a noon orbit it is possible to look away from the sunglint and observe ocean waters under high solar elevations without any sunglint contamination (Strong, 1972). Thus it would appear that a near-noon orbit would be optimum for ocean color and sunglint (wind speed/roughness) observations if provision can be made to avoid the glitter area.

Chapter 6 WATER COLOR vs. WATER TEMPERATURE

During spring and fall months a good relationship is frequently observed between Great Lakes' surface water color and temperature. This relationship is probably best developed late in the spring when the lakes are warming rapidly and contributions from surface runoff are high (Wiesnet et al., 1975). NOAA-2 satellite VHRR data are presented in selected cases where ERTS-1 imagery is coincident with the thermal-IR from VHRR.

Although little surface temperature structure was evident on 27 March 1973 (Figure 47) in the NOAA-2 VHRR analysis, water color was abundant (Figure 48). The NOAA-2 VHRR data have been averaged over a 4-km grid to remove some high spatial frequency noise in the system (Strong, 1974). The resulting reduced resolution makes color/temperature correlations difficult under these nearly isothermal conditions. The VHRR temperature resolution is slightly better than 1°C.

One can detect a warmer turbid Detroit River effluent. VHRR data show surface temperatures in excess of 3°C. This is also true for the nearshore areas in Lake St. Clair. Only a slight indication of warmer (2-3°C) water is found along the southern Canadian shoreline of Lake Huron where waters were extremely turbid also (Figure 48).

By late April the lakes have progressed well into their warming cycle and reveal significant temperature patterns, particularly in nearshore surface waters. On 29 April 1973 ERTS-1 acquired imagery along its Buffalo swath. This nearly cloud-free Great Lakes pass provides turbidity information for Lakes Erie and Ontario as seen in Figure 49. The VHRR image showed warmer water emanating from the Niagara River and elsewhere along the southern shore of Lake Ontario. These areas are the turbid regions in the ERTS-1 imagery. A VHRR temperature analysis overlay in Figure 50

PRECEDING PAGE BLANK NOT FILMED

Figure 47. 27 March 1973. 1600 GMT ERTS-1 MSS-5 turbidity patterns in Lakes Huron, St. Clair and Erie.

REPRODUCIBILITY OF THE ORIGINAL PAGE IS POOR.

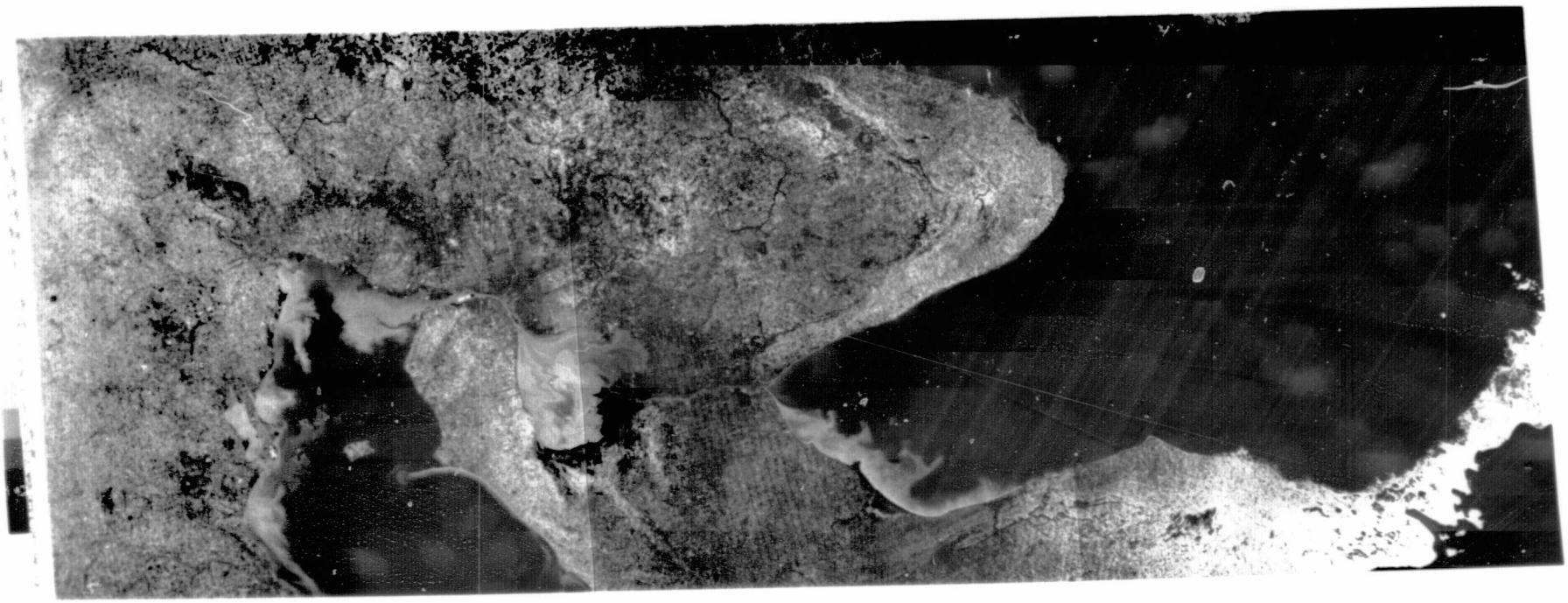

Figure 48. 27 March 1973. 1500 GMT NOAA-2 temperature analysis from VHRR-IR at 1°C interval (see Figure 38 for enhanced image).

REPRODUCIBILITY OF THE ORIGINAL PAGE IS POOR.

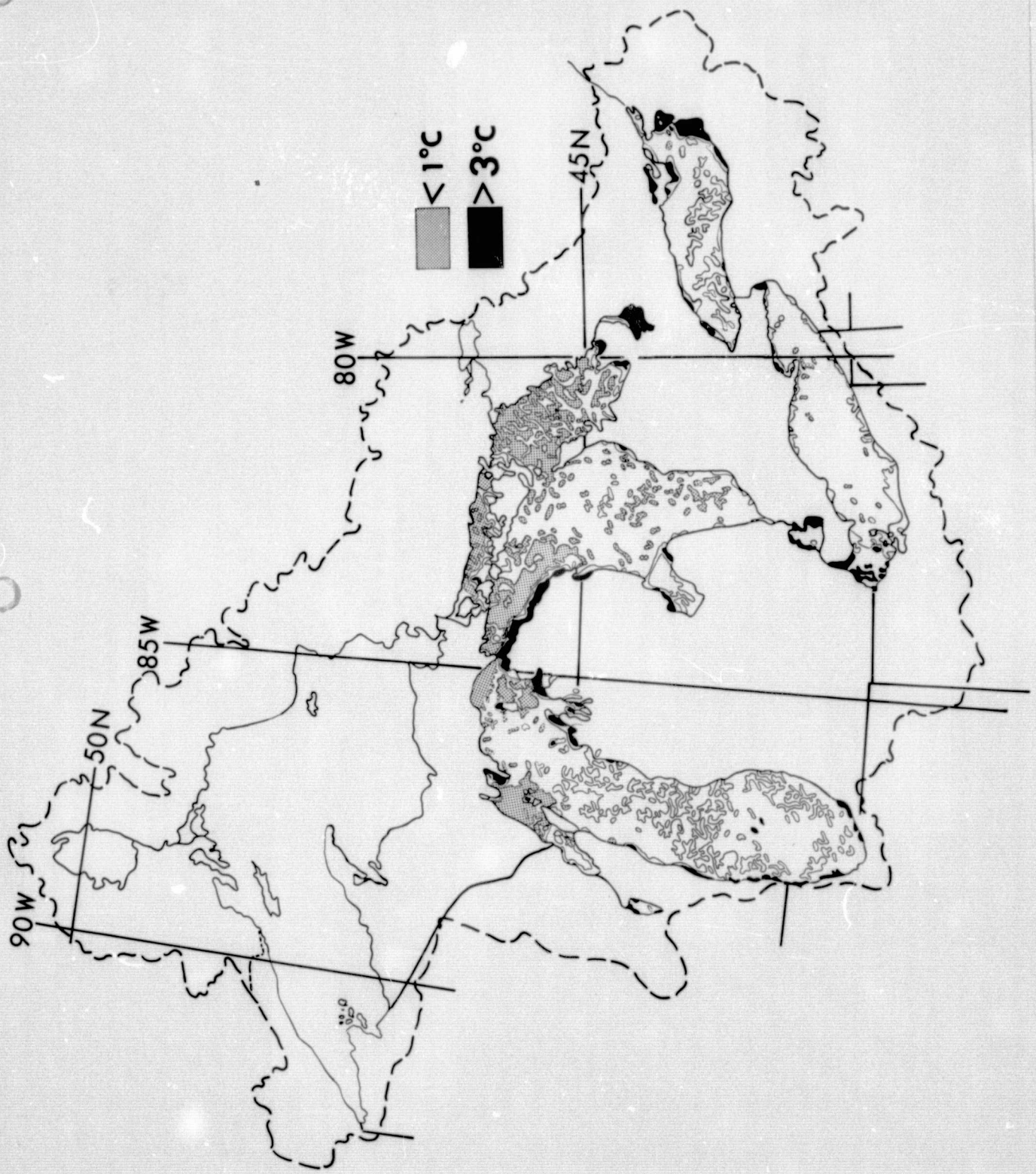

Figure 49. 29 April 1973. 1500 GMT ERTS-1 MSS-4. Lake Ontario and eastern Lake Erie.

REPRODUCIBILITY OF THE ORIGINAL PAGE IS POOR.

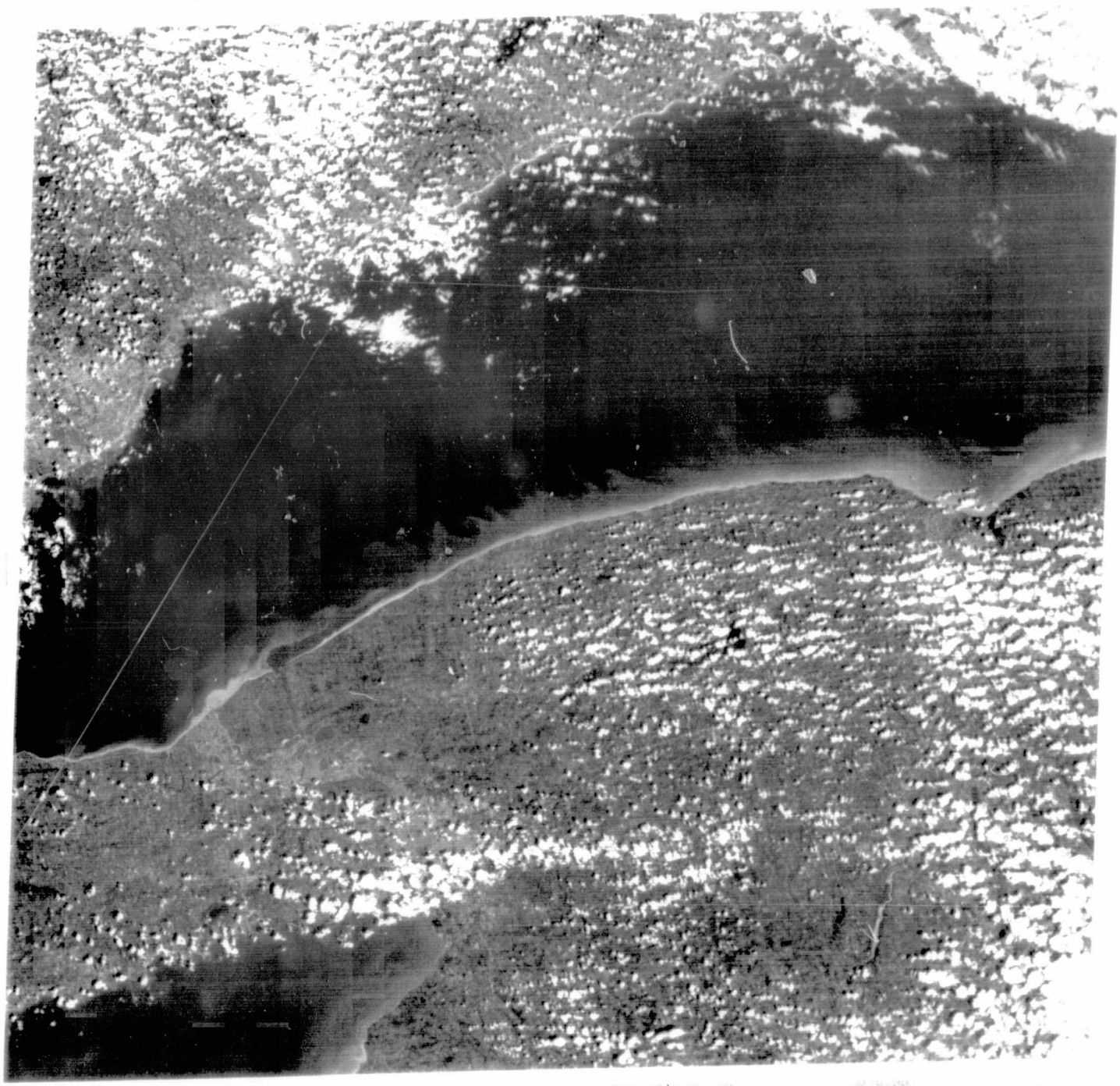

Figure 50. 29 April 1973. 1500 GMT NOAA-2 temperature analysis from VHRR-IR at a 2°C interval. Cloudiness along Canadian shoreline of Lake Ontario prevented an extension of the analysis to those waters.

REPRODUCIBILITY OF THE ORIGINAL PAGE IS POOR.

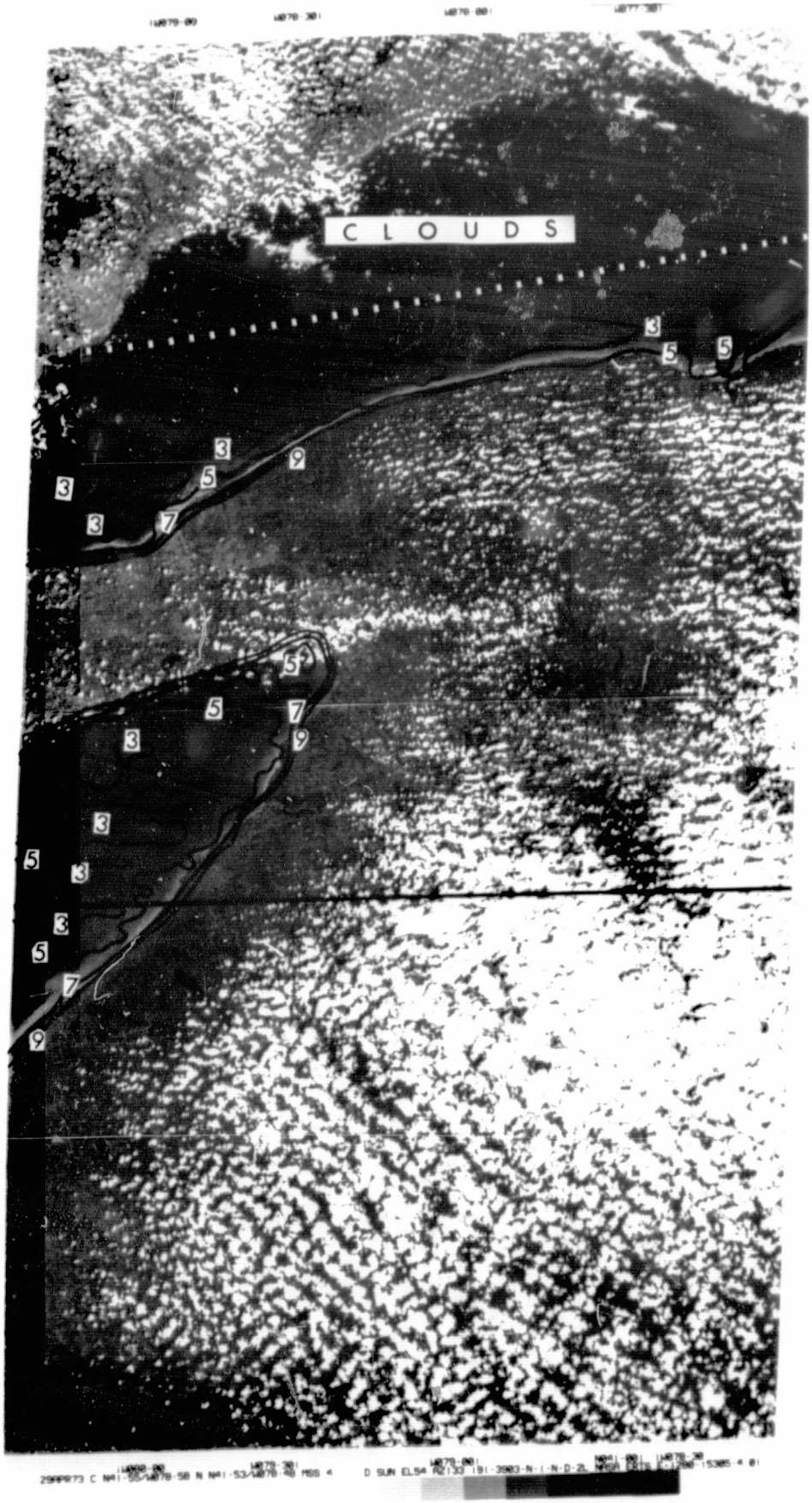

demonstrates this good correlation and the obvious need for ERTS thermal-IR data on future satellites. The same correlation may be observed between thermal and turbidity data in Lake Huron on 20 May 1973 (Figures 51, 52, and 53).

A summer upwelling in Lake Michigan discussed in Chapter 3 reveals a more complicated relationship between thermal and turbidity data. The warmer mid-lake waters (ca. 20°C), away from the upwelling, support the green milky waters that are believed rich in phytoplankton and calcium carbonate. This temperature/color relationship parallels the observed spring color/temperature relationship. However, along the Michigan shore in the southern portion of the lake, surface turbidity at a very high level can be observed where waters are quite cold (ca. 10°C). This reverse relationship is expected during fall and early winter, but it was difficult to observe by ERTS-1 and NOAA-2 because of persistent cloud cover.

Figure 51. 20 May 1973. 1600 GMT ERTS-1 MSS-5. Lake Huron (south).

REPRODUCIBILITY OF THE ORIGINAL PAGE IS POOR.

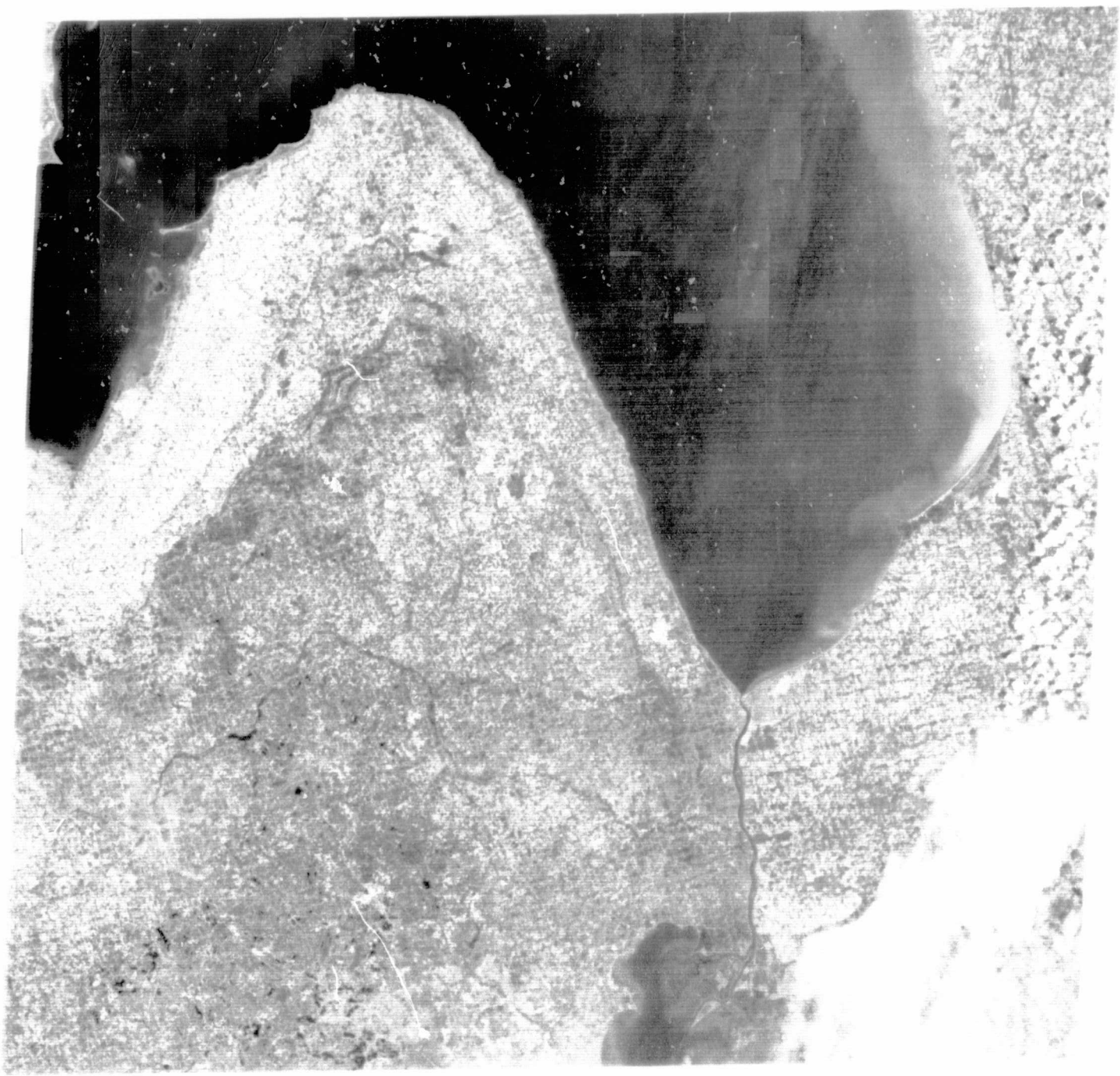

Figure 51. 20 May 1973. 1600 GMT ERTS-1 MSS-5. Lake Huron (north).

REPRODUCIBILITY OF THE ORIGINAL PAGE IS POOR.

Figure 25. 22 August 1973. 1600 GMT NOAA-2 enhanced VHRR-IR image of Lake Michigan.

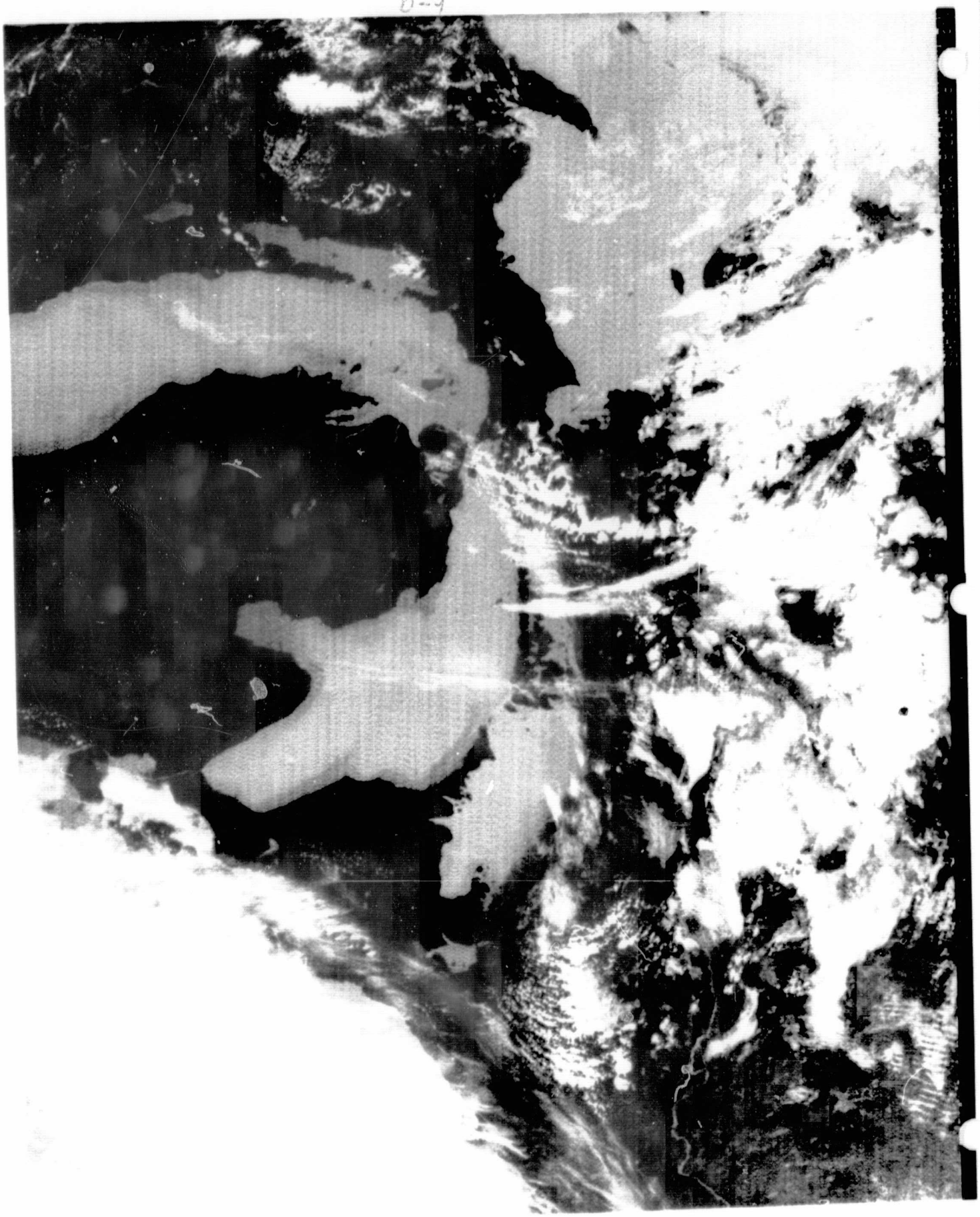

Figure 53. Temperature analysis from VHRR-IR data in Figure 52 analyzed on ERTS-1 Figure 51 image.

REPRODUCIBILITY OF THE ORIGINAL PAGE IS POOR.

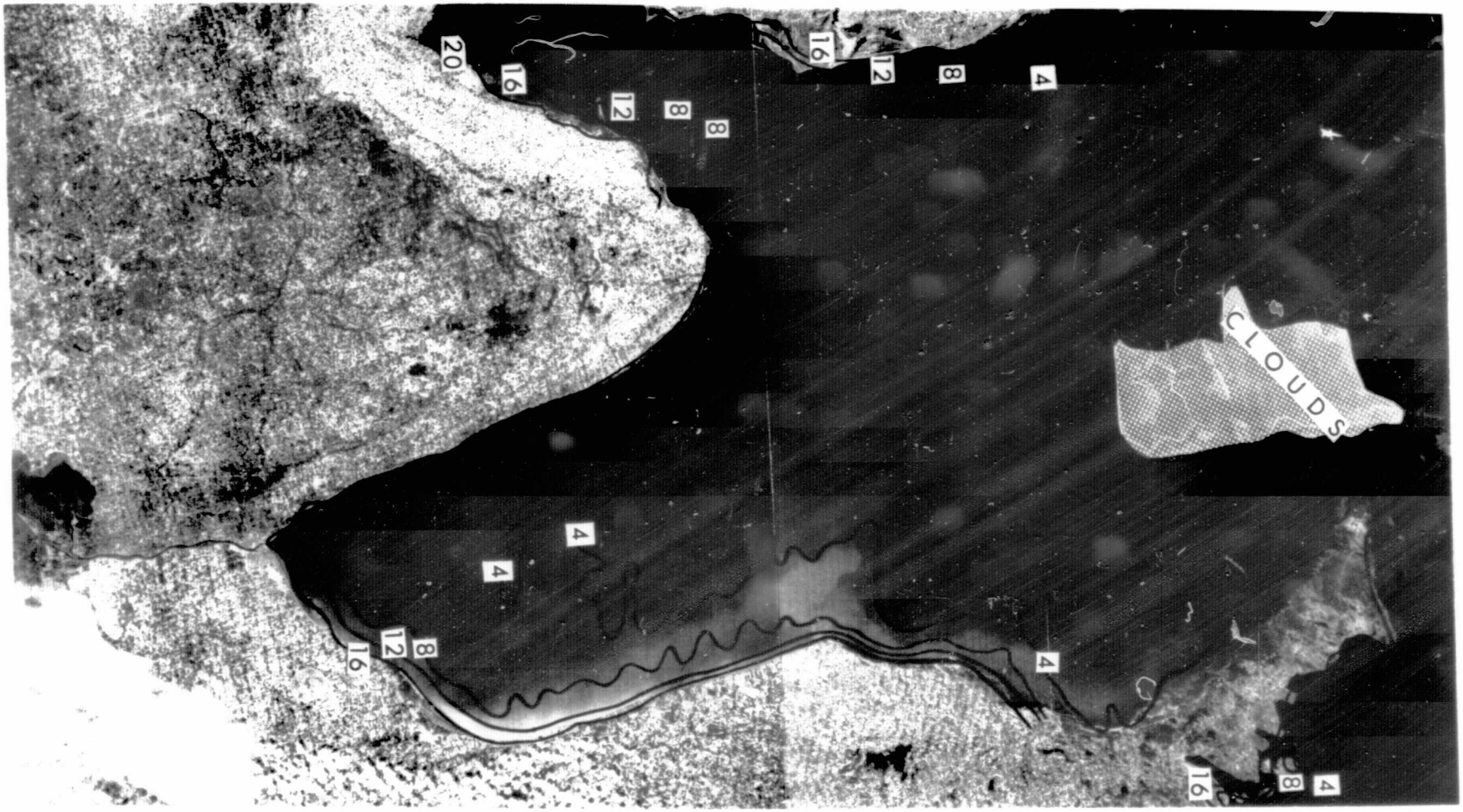

Chapter 7 WIND vs. CIRCULATION

Case Studies

The ERTS-1 system has added a new dimension to physical oceanography. Conditions permitting, one is now able to chart circulation patterns using natural tracing material borne in the surface waters. These colorants are chiefly turbidities from riverine effluents consisting of sediments, pollutants, algae or natural dyes. Occasionally chemical precipitations are noted (see Chapter 3); these too are employed in this chapter as circulation tracers. Synoptic oceanographic or limnologic studies have always been difficult if not impossible from shipboard. Circulation patterns are constantly being altered by changing meteorological influences. Observing tracer features from space, a nearly instantaneous "snap shot" provides circulation information that should relate to the present and near-past meteorological forces.

Ayers (1959) has developed an empirical relationship that takes into account the large time lag between the onset of a given wind condition and the response of the water circulation to this wind. A complete response of current to the wind takes many hours, or even several days. The resultant effective wind stress relationship developed reduces the forcing influence of the previous day by one-half that of the given day. In this report we have chosen to utilize three days of wind data prior to each ERTS-1 scene. In addition, to better emphasize the 24-hour period immediately prior to the ERTS-1 data, we have represented the 6-hourly winds in a weighted resultant stress vector as follows:

$$\vec{w}_{(\text{day 1})} = \frac{\vec{w}_{(-24)} + 2\vec{w}_{(-18)} + 3\vec{w}_{(-12)} + 4\vec{w}_{(-6)}}{10}$$

PRECEDING PAGE BLANK NOT FILMED

The subscript after each vector wind observation denotes observation time (hours) before noon of the day of the ERTS-1 observation.

A final vector resultant wind for the three-day period was obtained using the following formula:

$$\vec{W} = \frac{\vec{w}_{(\text{day } 3)} + 2\vec{w}_{(\text{day } 2)} + 4\vec{w}_{(\text{day } 1)}}{7}$$

For a more rigorous relationship one needs to take into account additional parameters such as atmospheric stability over the water, wave condition, current locations as a function of the distance to shore, etc. (see Jones and Bellaire, 1962). Much of this fine tuning, however, is not too realistic with the present paucity of wind data. In this study, we have chosen, wherever possible, to use the U.S. Coast Guard weather observations from shore installations rather than inland sites. Although these winds may suffer some due to local anomalies in the wind field (e.g. lake breeze circulations) they are felt to be the most representative of true lake winds.

Circulation vectors have been extracted from each ERTS-1 scene using all natural or man-made tracers in the surface waters available to the analyst. As an illustrative example, the interested reader should compare the circulation derived for Lake Michigan under a resultant northerly wind (Figure 55a) with the whiting image in Chapter 3 (Figure 22). Although complex much of the analysis is straightforward when a trained interpreter is used.

Wherever possible the circulations inferred from the ERTS-1 data have been compared with past studies, empirical or theoretical, of surface circulation patterns in the Great Lakes. The five areas selected for intensive current depiction as a function of effective wind stress are:

Southern Lake Michigan

Southern Lake Huron

Lake St. Clair

Lake Erie

Lake Ontario

These areas were selected because they regularly display the high turbidities that are necessary to observe circulation from ERTS-1.

Charts were prepared for all cardinal and subcardinal resultant wind directions (i.e., N, NE...NW). Some ERTS-1 observations of currents under a few wind directions were not available during the study period (August 1972 to December 1973). Whenever more than one ERTS-1 observation was used in a given area, the currents presented are composites. Although most current charts are based on only one ERTS scene, if two scenes were available for a given resultant wind direction the observation under the stronger wind stress was generally used. It should be mentioned that circulation variations should be expected under weaker or stronger resultant wind stress from the same direction. It was chosen to concentrate primarily on the direction of the wind vector rather than vector magnitude in this report. Figure 1 shows the areas covered by any given ERTS-1 pass. The reader should be aware of the sunglint difficulty whenever the solar elevation exceeds 55° (see Chapter 5). Current interpretations are subject to errors under these conditions. Future studies should utilize a sunglint removal technique (e.g. MSS-6 minus MSS-5, Watanabe, 1974) for more credible results.

Southern Lake Michigan

The location of wind information used in preparation of the southern Lake Michigan current charts is shown in Figure 54. All locations referenced in the text are also identified on this base chart. Only incomplete wind data were available from the Milwaukee and Muskegon Coast Guard facilities. Table 6 presents a summary of ERTS-1 scenes utilized in

Figure 54. Wind station used for southern Lake Michigan (Dunne Crib - Chicago).

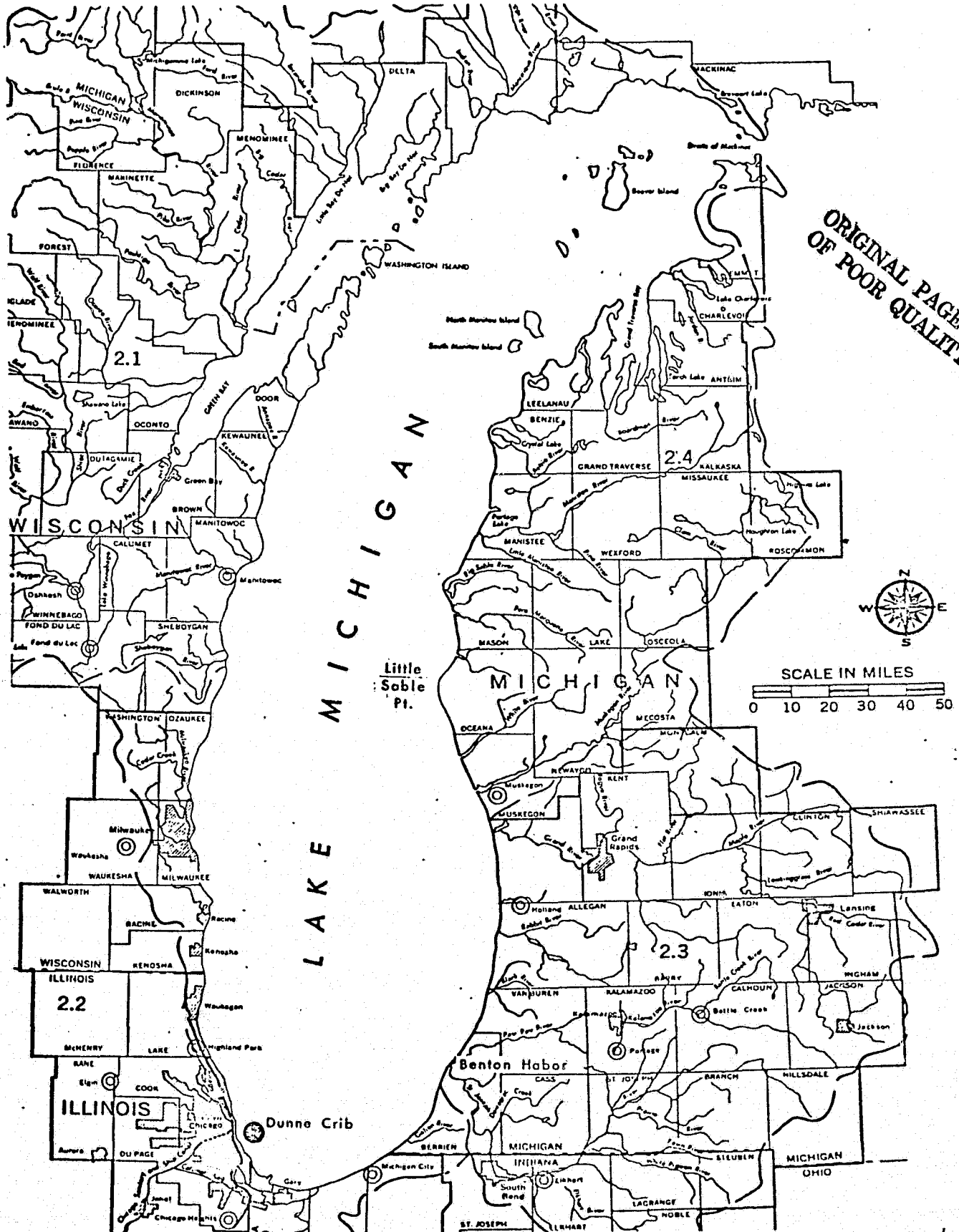

ORIGINAL PAGE IS OF POOR QUALITY

TABLE 6

LAKE MICHIGAN - ERTS-1 frames used for surface circulation charts

Resultant Wind Direction	Orbit #	Date	ID #	Sun Elevation
N	4991	16 Jul 73	1358-16040	58*
			1358-16042	58*
	5493	21 Aug 73	1394-16030	50
			1394-16033	51
			1394-16035	52
NE	5005	17 Jul 73	1359-16094	58*
E	3220	11 Mar 73	1231-15591	36
			1231-15593	37
SE	----------NONE----------			
S	----------NONE----------			
SW	4489	10 Jun 73	1322-16042	60*
			1322-16045	61*
	6246	14 Oct 73	1448-16021	34
			1448-16023	35
W	1728	24 Nov 72	1124-16043	23
			1124-16050	24
	1993	13 Dec 72	1143-16102	20
	3973	4 May 73	1285-15590	55*
			1258-15592	56*
NW	5242	3 Aug 73	1376-16034	55*
			1376-16041	55*

* - Solar elevation equal to or greater than 55°. (Possible sunglint contamination and confusion with sediment features used for circulation charting. See Chapter 5.)

addition to resultant wind direction calculated from the above formula. Additional coverage data are available in the Appendix (Table A2).

Northerly Winds - Figure 55a

The figure indicates the general surface circulation established by predominantly northerly light/moderate winds as derived from two cloud-free ERTS-1 passes (16 July 1973 and 21 August 1973). The latter pass was particularly useful because that date marked the occurrence of an extensive $CaCO_3$ precipitation that was especially evident in MSS-4 (see Chapter 3). The major features established by this wind regime are several large gyres and distinct alongshore currents. An east shore southward current extends from Little Sable Point to Michigan City, where it becomes deflected to the northwest to become part of the eastern boundary of a large counter-clockwise eddy off Chicago, first described by Ayers et al. (1958) and confirmed by Bellaire (1964). In this case, the eddy extends as far north as Waukegan. From Little Sable Point a branch of the east shore current flows southwestward and becomes incorporated in a second mid-lake counter-clockwise gyre. This corresponds to the eddy noted by Bellaire (1964) above the mid-lake sill between Milwaukee and Muskegon. A third eddy has a clockwise circulation and lies off Benton Harbor, Michigan, in the eastern part of the lake. This eddy has been previously observed (Ayers et al., 1958 and Bellaire, 1964), but here it is much smaller than reported previously. Along the Wisconsin shore at Milwaukee there may be a small nearshore clockwise eddy; it has been previously documented (Ayers et al., 1958), but the evidence in the ERTS-1 images indicates only that there is a southward current some distance offshore.

Northeasterly Winds - Figure 55b

Only one ERTS-1 pass was available for northeasterly wind conditions (17 July 1973), and only the Milwaukee area was sufficiently cloud-free

to allow mapping of the sediment distribution patterns. The outflow current begins along the Wisconsin shore at Sheboygan and flows southward. After several days of northeasterly winds, water is transported onto the west shore from Milwaukee to Gary and is piled up there; on the slope of this wind set-up, the water flows southward and northeastward (Ayers, 1959).

Easterly Winds - Figure 55c

On 11 March 1973, ERTS-1 passed over the southeast portion of Lake Michigan. It was evident from the sediment patterns observed that the east shore current flowed southward from Holland to Michigan City and then westward to Chicago. Off Michigan City is an apparent small flattened counterclockwise eddy, previously described by Ayers et al. (1958) under a similar easterly wind regime. North of Benton Harbor a branch from the east shore current flows southwestward toward the middle of the lake, presumably to become part of the large clockwise gyre located along the shore between Holland and Benton Harbor. This is the same clockwise gyre discussed under Northerly Winds and documented by Ayers et al. (1958) and Bellaire (1964).

Southwesterly Winds - Figure 55d

The current diagram is a composite analysis of two ERTS-1 passes (10 June 1973 and 14 October 1973). The major feature evident in the figure has already been discussed--the large clockwise gyre along the east shore between Benton Harbor and Holland. The southward current along the east shore is very narrow under these southwesterly winds and it was not observed to extend south beyond Benton Harbor, where it turns westward to become incorporated into the eddy. According to the sediment distribution patterns, water is flowing northeasterly directly offshore from Chicago to the center of the lake. This apparent major upwelling has not been previously documented; Ayers et al. (1958) and Bellaire (1964) have described fully-developed gyres at this location. Offshore currents are indicated all along

Figure 55a-f. Surface current analyses for southern Lake Michigan as determined from turbidity patterns in ERTS-1 scenes. Weighted wind directions from Table A2 are indicated in upper right-hand corners.

ORIGINAL PAGE IS
OF POOR QUALITY

Na

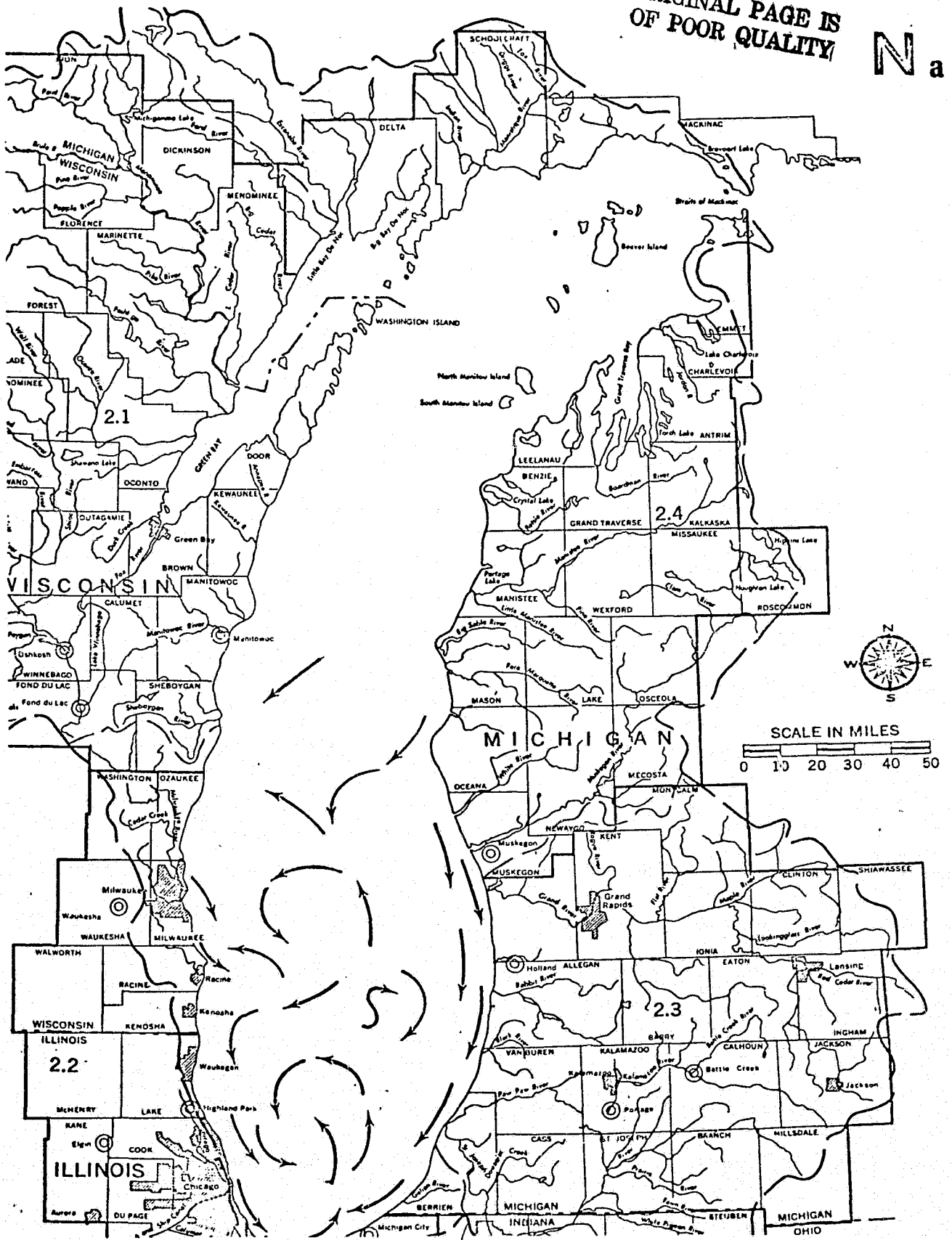

NE b

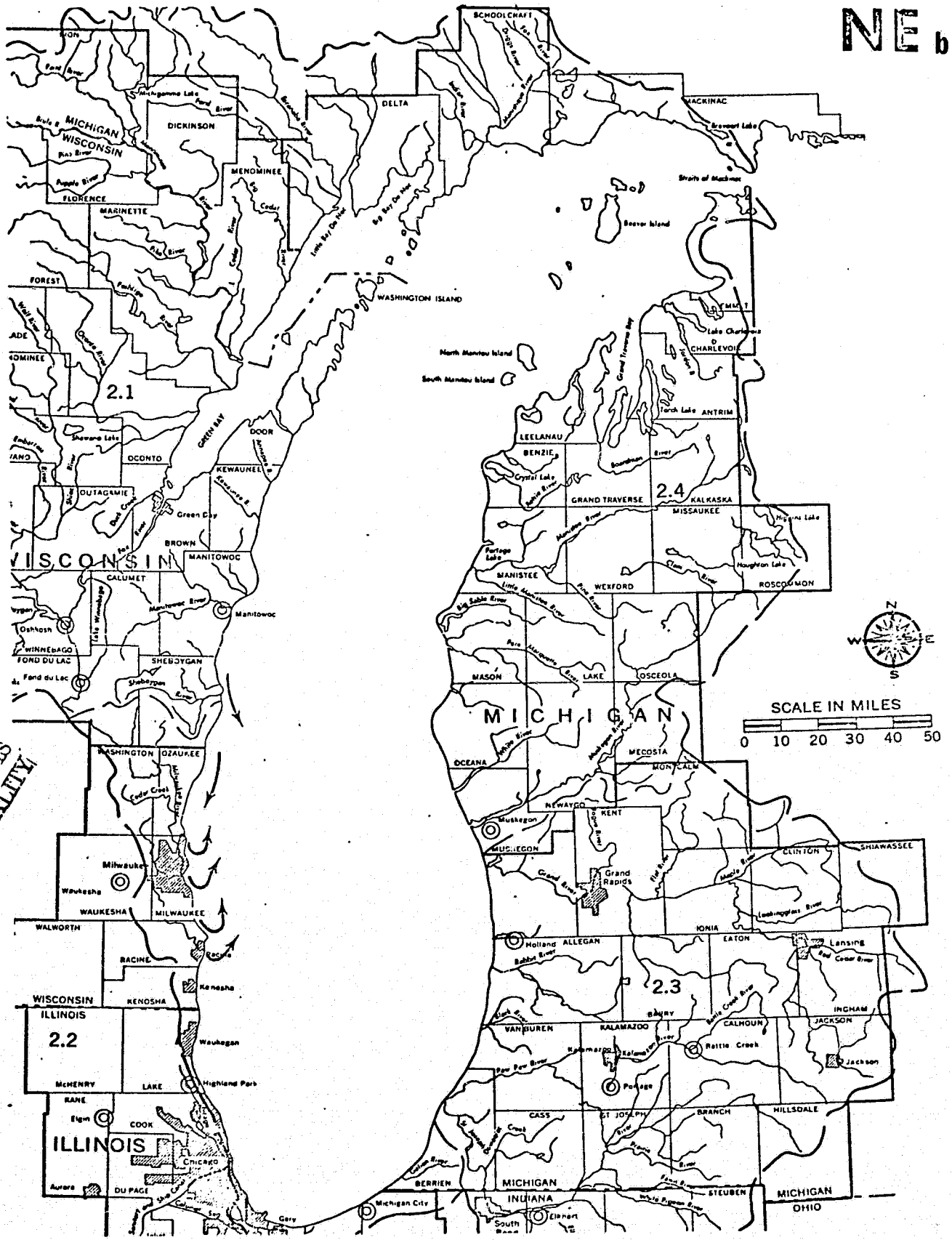

ORIGINAL PAGE IS OF POOR QUALITY

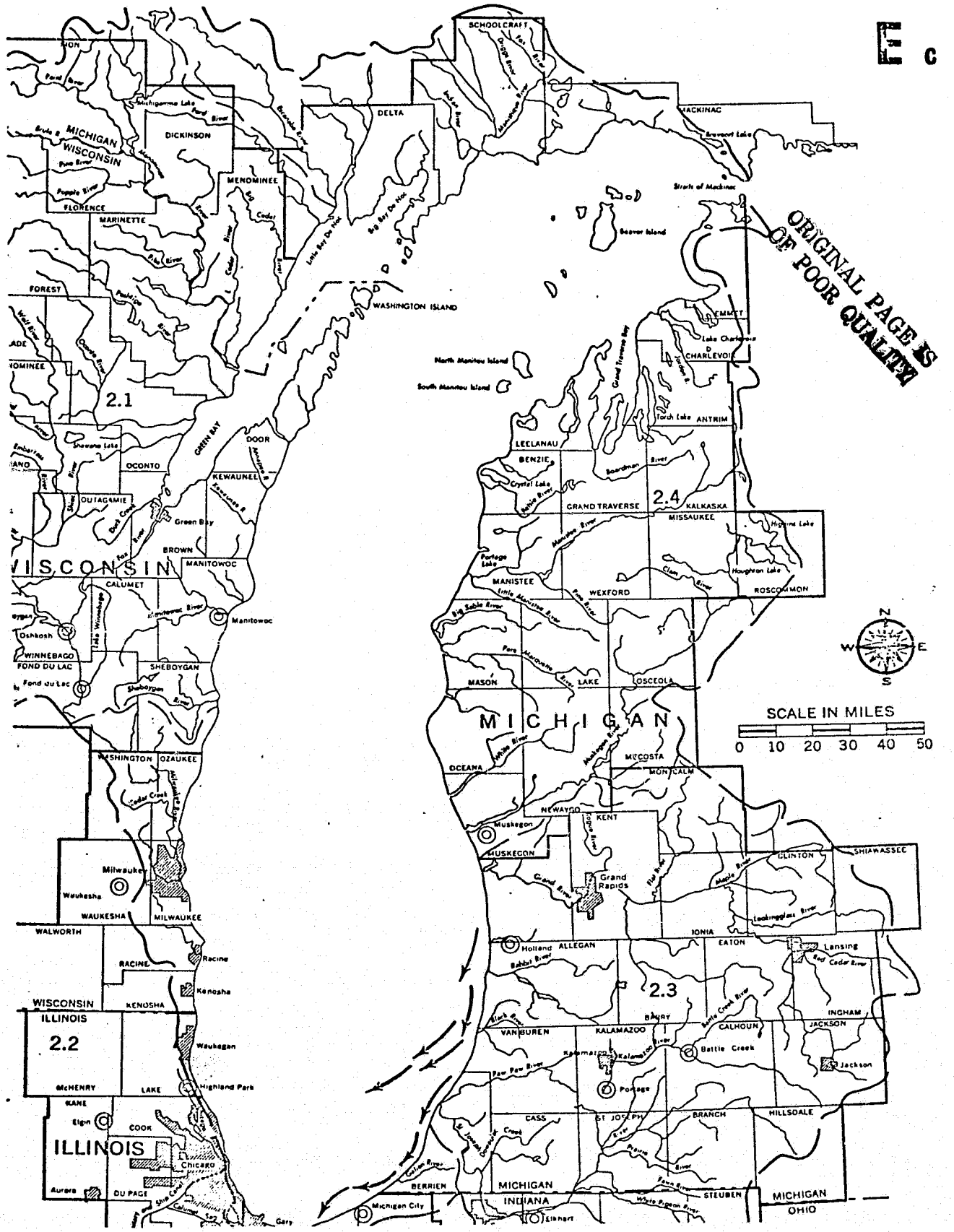
ORIGINAL PAGE IS OF POOR QUALITY
MICHIGAN
WISCONSIN
ILLINOIS
INDIANA
OHIO
2.1
2.2
2.3
2.4
SCALE IN MILES
0 10 20 30 40 50
N
S
E
W
Green Bay
Manitowoc
Milwaukee
Racine
Kenosha
Waukegan
Chicago
Gary
Grand Rapids
Muskegon
Holland
Lansing
Battle Creek
Jackson
Portage
Kalamazoo
Michigan City
Elkhart
Mackinac
Straits of Mackinac
Beaver Island
Washington Island
North Manitou Island
South Manitou Island
Traverse City
Charlevoix
Petoskey
Escanaba
Menominee
Marinette
Sturgeon Bay
Door
Oconto
Kewaunee
Brown
Manitowoc
Calumet
Sheboygan
Fond du Lac
Winnebago
Oshkosh
Outagamie
Waupaca
Shawano
Forest
Florence
Dickinson
Delta
Schoolcraft
Alger
Luce
Chippewa
Mason
Lake
Oceana
Newaygo
Kent
Ottawa
Allegan
Van Buren
Berrien
Cass
St. Joseph
Branch
Hillsdale
Steuben
Lenawee
Monroe
Wayne
Washtenaw
Livingston
Oakland
Macomb
St. Clair
Lapeer
Genesee
Shiawassee
Clinton
Eaton
Ingham
Jackson
Calhoun
Barry
Ionia
Montcalm
Mecosta
Osceola
Lake
Wexford
Missaukee
Roscommon
Ogemaw
Iosco
Arenac
Bay
Midland
Gladwin
Clare
Isabella
Gratiot
Saginaw
Tuscola
Huron
Sanilac
Grand Traverse
Kalkaska
Antrim
Leelanau
Benzie
Manistee
Emmet
Cheboygan
Presque Isle
Montmorency
Alpena
Alcona
Oscoda
Crawford
Otsego
Charlevoix
Lake Michigan
Green Bay
Lake Huron
Lake Erie
Lake Superior
Lake Winnebago
Lake St. Clair
Saginaw Bay
Grand Traverse Bay
Little Bay De Noc
Big Bay De Noc
Menominee River
Brule River
Pine River
Peshtigo River
Oconto River
Fox River
Wolf River
Embarrass River
Shioc River
Duck Creek
Green Bay
Sheboygan River
Milwaukee River
Cedar Creek
Menominee River
Pere Marquette River
Big Sable River
Little Manistee River
Manistee River
Muskegon River
White River
Grand River
Flat River
Maple River
Looking Glass River
Thornapple River
Kalamazoo River
Black River
Battle Creek River
Portage River
Paw Paw River
Dowagiac Creek
St. Joseph River
Fawn River
Coldwater River
Tiffin River
Raisin River
Huron River
Rouge River
Clinton River
Shiawassee River
Flint River
Cass River
Tittabawassee River
Pine River
Chippewa River
Muskegon
Grand Rapids
Holland
Lansing
Battle Creek
Jackson
Portage
Kalamazoo
Michigan City
Elkhart
Chicago
Gary
Aurora
Elgin
Waukegan
Highland Park
Racine
Kenosha
Milwaukee
Waukesha
Manitowoc
Green Bay
Oshkosh
Fond du Lac
Sheboygan
Escanaba
Menominee
Marinette
Sturgeon Bay
Petoskey
Traverse City
Charlevoix
Mackinac
Straits of Mackinac
Beaver Island
Washington Island
North Manitou Island
South Manitou Island
Saginaw
Bay City
Midland
Alpena
Cheboygan
Presque Isle
Gaylord
Grayling
Houghton Lake
Higgins Lake
Torch Lake
Lake Charlevoix
Crystal Lake
Portage Lake
Clam River
Manistee River
Boardman River
Betsie River
Platte River
Crystal River
Grand Traverse Bay
Little Bay De Noc
Big Bay De Noc
Menominee River
Brule River
Pine River
Peshtigo River
Oconto River
Fox River
Wolf River
Embarrass River
Shioc River
Duck Creek
Green Bay
Sheboygan River
Milwaukee River
Cedar Creek
Menominee River
Pere Marquette River
Big Sable River
Little Manistee River
Manistee River
Muskegon River
White River
Grand River
Flat River
Maple River
Looking Glass River
Thornapple River
Kalamazoo River
Black River
Battle Creek River
Portage River
Paw Paw River
Dowagiac Creek
St. Joseph River
Fawn River
Coldwater River
Tiffin River
Raisin River
Huron River
Rouge River
Clinton River
Shiawassee River
Flint River
Cass River
Tittabawassee River
Pine River
Chippewa River

SW d

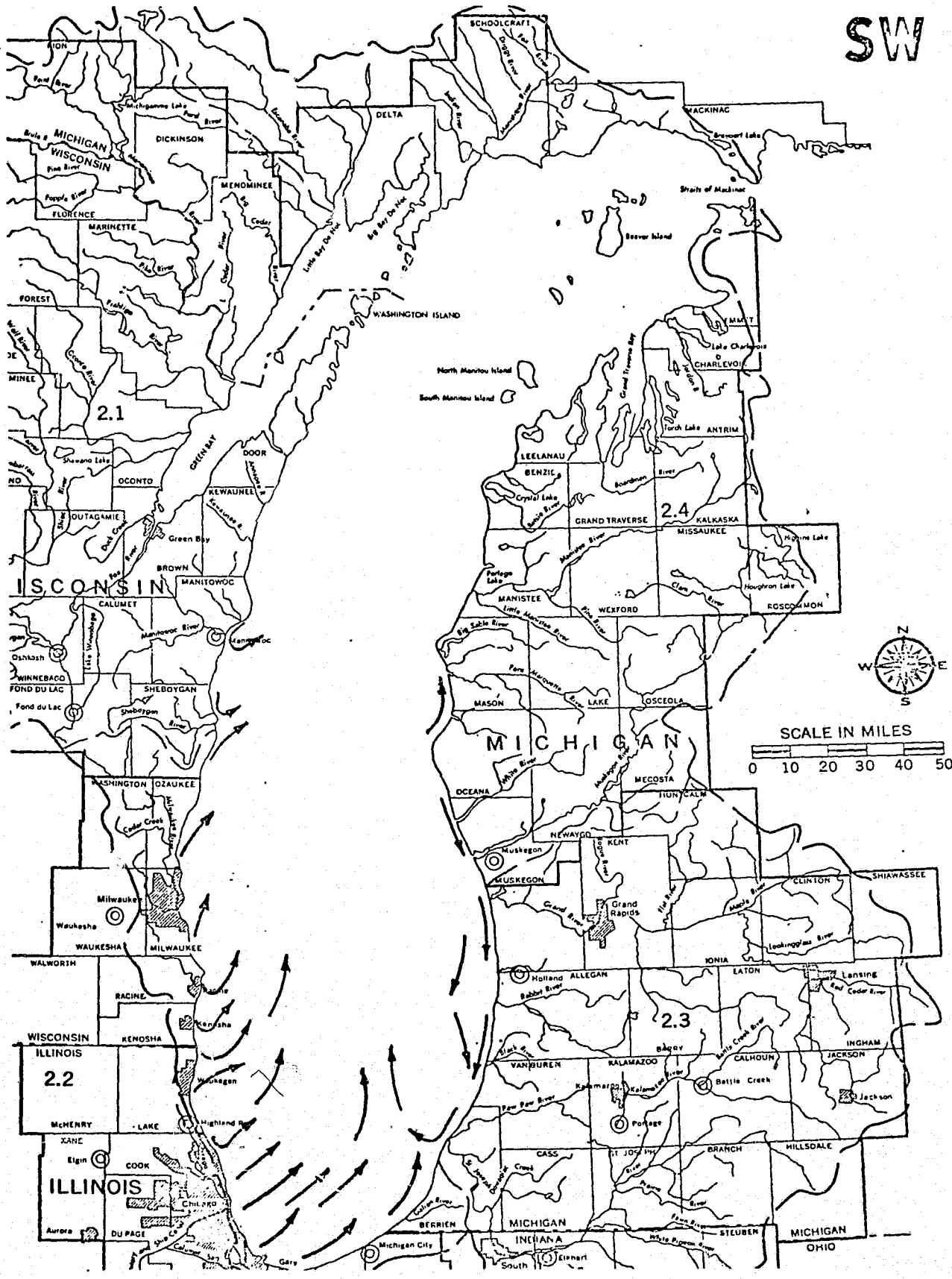

ORIGINAL PAGE IS OF POOR QUALITY

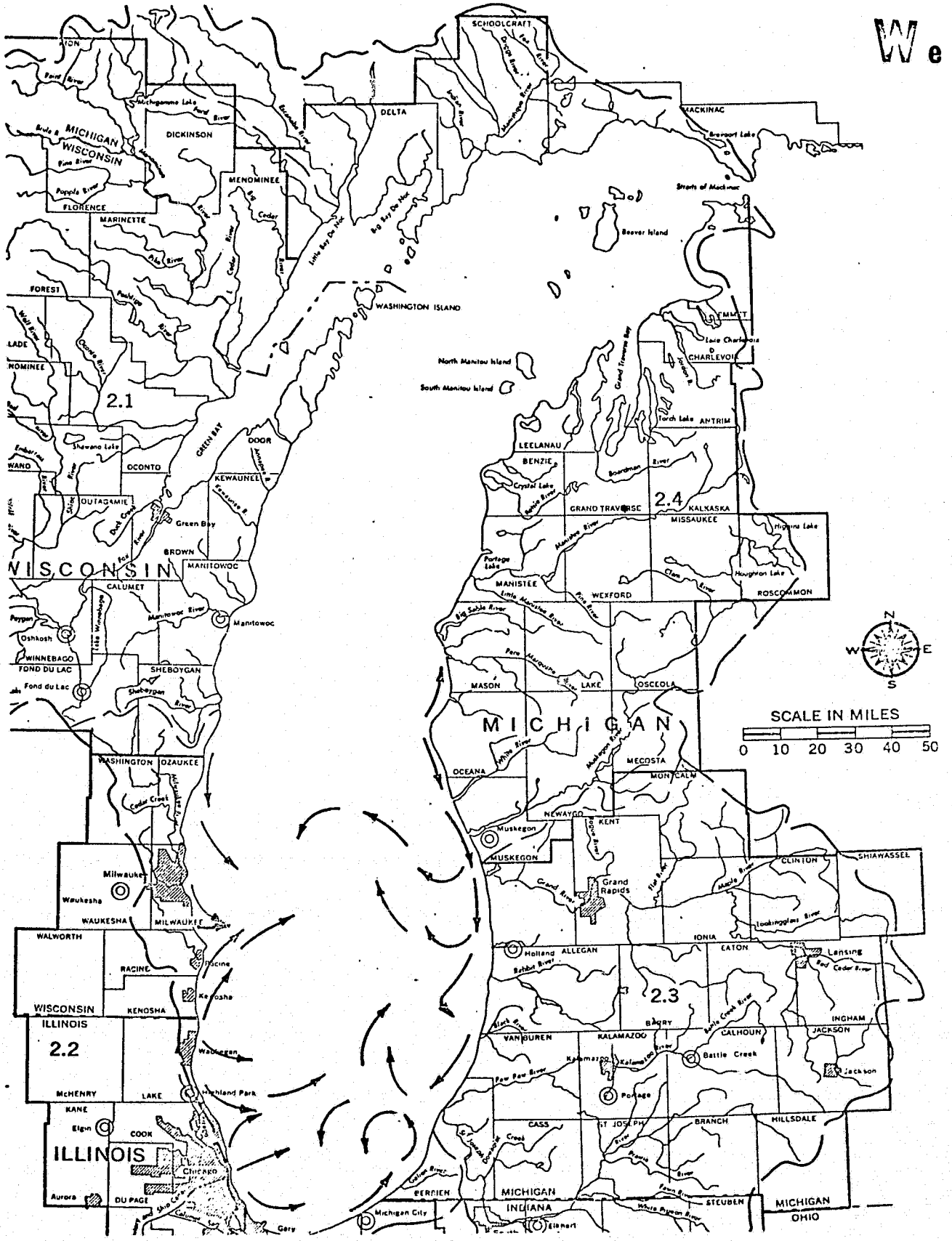

ORIGINAL PAGE IS
OF POOR QUALITY

NW f

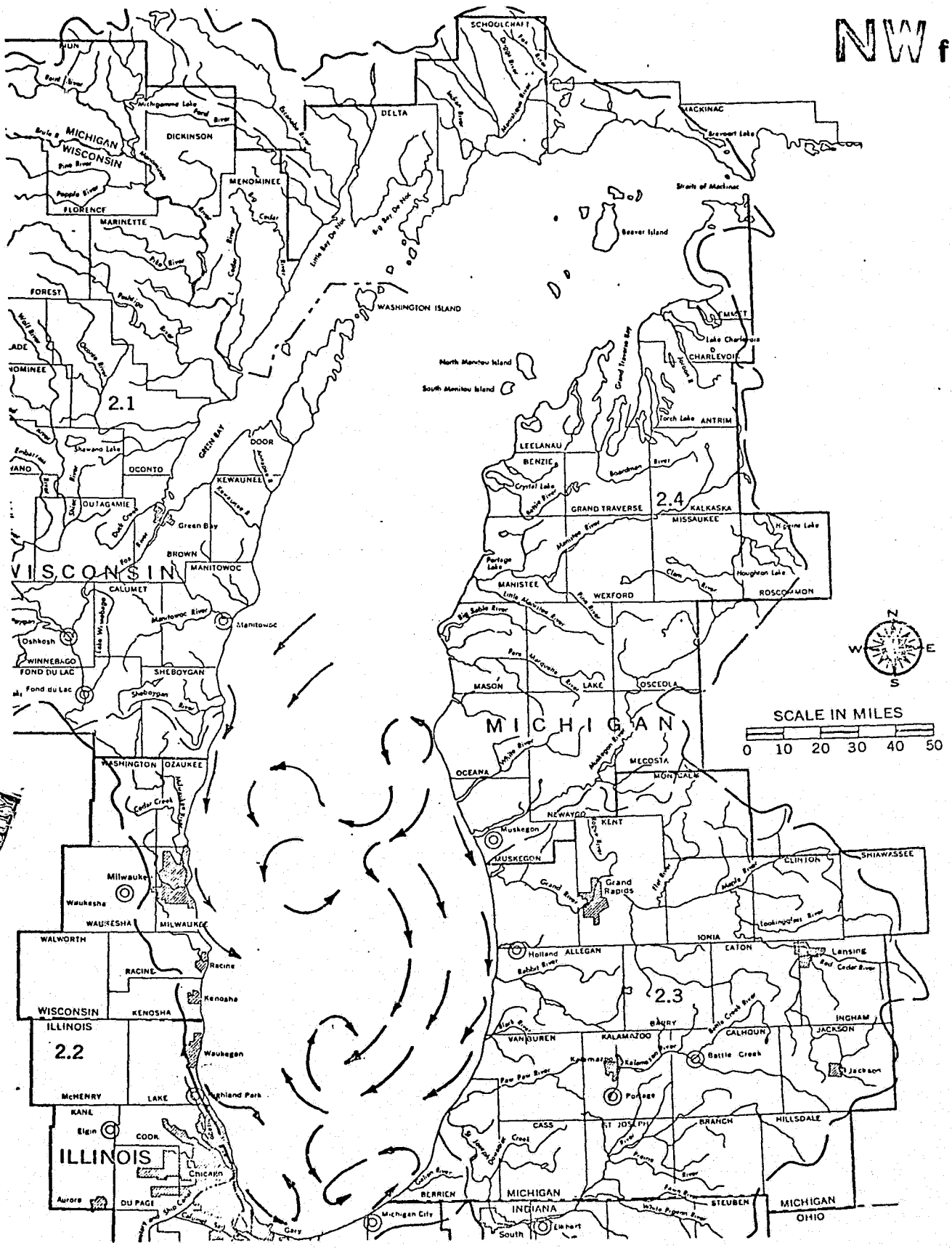
MICHIGAN
WISCONSIN
ILLINOIS
2.1
2.2
2.3
2.4
WASHINGTON ISLAND
Beaver Island
North Manitou Island
South Manitou Island
Green Bay
Lake Michigan
Chicago
Milwaukee
Manitowoc
Grand Rapids
Lansing
Battle Creek
Jackson
Kalamazoo
Muskegon
Holland
Benton Harbor
Michigan City
Gary
Elkhart
South Bend
Aurora
Waukegan
Racine
Kenosha
Oshkosh
Fond du Lac
Sheboygan
Escanaba
Menominee
Marinette
Iron Mountain
Ironwood
Houghton Lake
Roscommon
Mackinac
Straits of Mackinac
Petoskey
Charlevoix
Traverse City
Manistee
Ludington
Big Rapids
Mount Pleasant
Alma
Ionia
Owosso
Flint
Saginaw
Bay City
Midland
Port Huron
Detroit
Toledo
Ann Arbor
Monroe
Adrian
Coldwater
Three Rivers
Sturgis
Hillsdale
Niles
Dowagiac
Paw Paw
Portage
Allegan
Holland
Zeeland
Grand Haven
Muskegon
Newaygo
Big Rapids
Reed City
Cadillac
Baldwin
Scottville
Manistee
Wexford
Missaukee
Roscommon
Gladwin
Clare
Mount Pleasant
Isabella
Gratiot
Clinton
Shiawassee
Genesee
Lapeer
St. Clair
Macomb
Oakland
Wayne
Monroe
Lenawee
Hillsdale
Branch
St. Joseph
Cass
Berrien
Van Buren
Kalamazoo
Calhoun
Jackson
Ingham
Eaton
Ionia
Montcalm
Mecosta
Osceola
Lake
Mason
Oceana
Newaygo
Kent
Ottawa
Muskegon
Oceana
Wexford
Grand Traverse
Leelanau
Benzie
Antrim
Charlevoix
Emmet
Cheboygan
Presque Isle
Alpena
Montmorency
Otsego
Crawford
Roscommon
Ogemaw
Iosco
Arenac
Bay
Saginaw
Midland
Gladwin
Clare
Isabella
Gratiot
Shiawassee
Clinton
Eaton
Ingham
Livingston
Washtenaw
Jackson
Calhoun
Kalamazoo
Van Buren
Cass
St. Joseph
Branch
Hillsdale
Lenawee
Monroe
Wayne
Oakland
Macomb
St. Clair
Lapeer
Genesee
Tuscola
Huron
Sanilac
Lake Huron
Lake Erie
Lake Michigan
Lake Superior
Lake Michigan

the west shore from Chicago to Sheboygan, suggesting that extensive upwelling was occurring. There may be a small clockwise gyre along the west shore at Waukegan, as suggested by Ayers et al. (1958), but the satellite data are inconclusive.

Westerly Winds - Figure 55e

Three cloud-free ERTS-1 passes (24 November 1972, 13 December 1972, and 4 May 1973) were composited to obtain the current diagram. The clockwise eddy along the east shore discussed above and previously (Ayers et al., 1958 and Bellaire, 1964) apparently has enlarged considerably from its size under other wind regimes. It now extends from Benton Harbor north to Muskegon with a rather elongated shape. Between Gary and Michigan City lies a large counterclockwise gyre, which was discussed under Northerly Winds. In this case, however, the gyre has been displaced to the southeast as compared with other observations. Sediment distribution patterns suggest also the presence of a counterclockwise eddy above the mid-lake sill between Milwaukee and Muskegon; apparently a northwestward-flowing branch of the east shore southward current provides the driving force for this gyre. This was discussed under Northerly Winds. Alongshore currents converge in the Milwaukee - Racine area and then flow offshore, creating upwelling there and contributing to the circulation of the mid-lake eddy. A similar current convergence exists immediately north of Chicago in the Highland Park area; this offshore flow joins the east shore eddy system in the middle of the southern basin.

Northwesterly Winds - Figure 55f

The diagram for northwesterly wind-generated currents is based solely on one ERTS-1 pass (3 August 1973), which coincided with an extensive episode of calcium carbonate precipitation that turned the entire southern basin "milky" in MSS-4 (see Chapter 3). The east shore southward current is very

narrow alongshore. Lakeward of that current is a long narrow band of upwelling from Benton Harbor to Muskegon; this was evident from the sunglint pattern on all four MSS bands (Strong, 1973). In the center of the lake is an elongate clockwise eddy that was discussed above and by Ayers et al. (1958) and Bellaire (1964); this wind regime has apparently displaced this gyre from the east shore toward the lake center. It extends from as far north as Milwaukee south to Benton Harbor. Between Milwaukee and Muskegon lies the mid-lake counterclockwise gyre discussed above; again it is driven by a westward branch of the east shore southward current that forms the northern boundary of the eddy. As discussed above, there is a flattened counterclockwise gyre from Gary to Benton Harbor driven by a branch current of the large central eddy and by the east shore southward current. Sediment patterns indicate a southward-flowing alongshore current at Chicago and suggest that a counterclockwise eddy exists there (Ayers et al., 1958 and Bellaire, 1964). Alongshore currents from Sheboygan to Highland Park are narrow and southward; at Racine and Highland Park they turn offshore (eastward), indicating upwelling at these locations.

Summary

The prevailing wind direction on Lake Michigan is southwesterly, although during winter northwesterly stresses are common. Along the western shore the current favors a northward direction, beginning with northeasterly to easterly winds, and probably (no ERTS-1 observations for easterly, southeasterly or southerly winds along this shore) continuing through southwesterly winds. Along the eastern shore a southward current appears dominant for all winds observed. South of Benton Harbor this flow reverses under southwesterly, westerly and northwesterly winds. The nearshore area between Michigan City, Indiana and Waukegan, Illinois contains an extremely complex circulation. Gyres in the central lake basin have been witnessed under southwesterly,

Figure 56. Wind station used for southern Lake Huron (Port Huron).

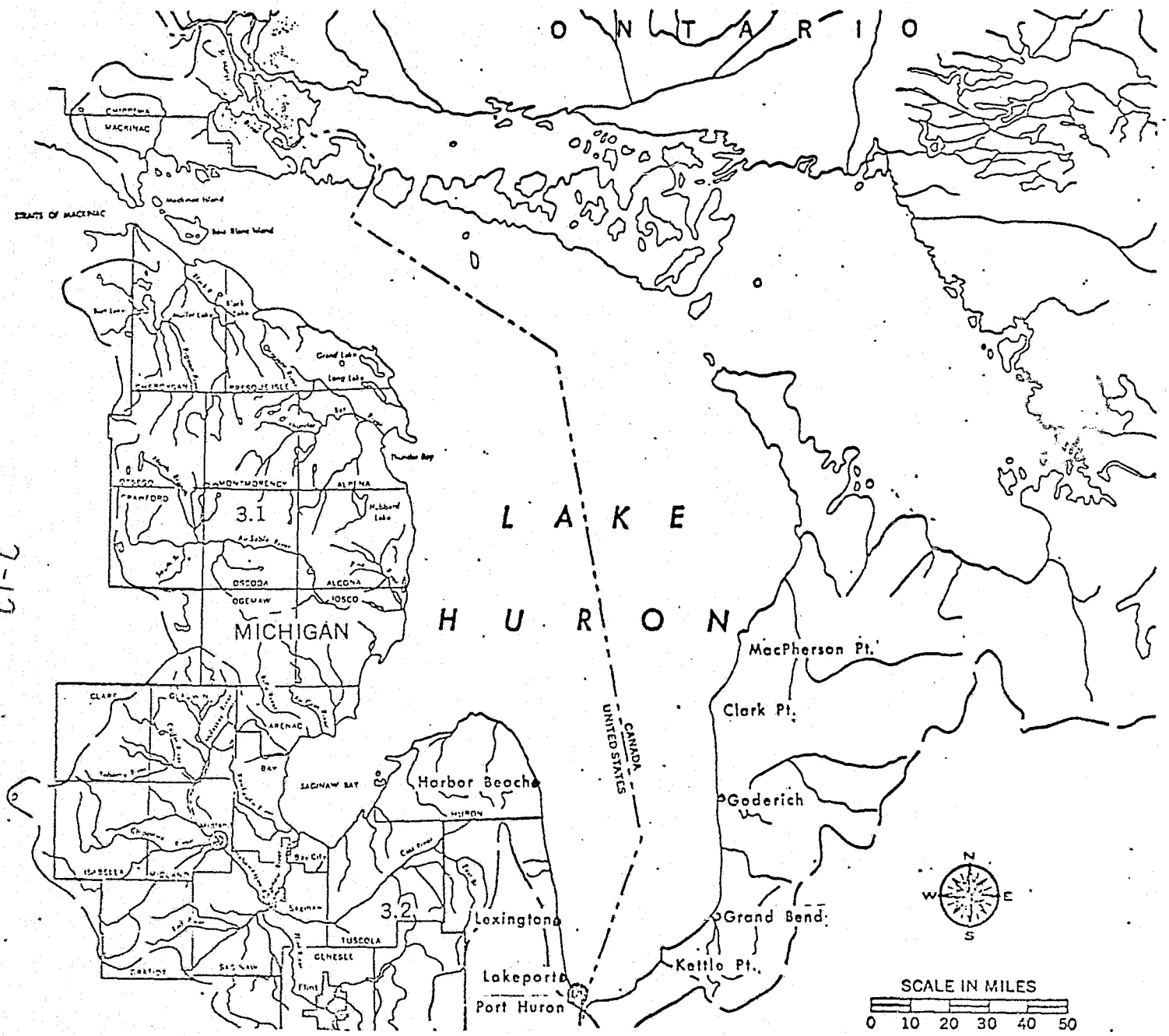
ONTARIO
LAKE HURON
MICHIGAN
CANADA
UNITED STATES
MACKINAC
STRAITS OF MACKINAC
CHEBOYGAN
PRESQUE ISLE
OTSEGO
CRAWFORD
MONTMORENCY
ALPENA
OSCODA
ALCONA
OGEMAW
IOSCO
CLARE
GLADWIN
ARENAC
BAY
SAGINAW BAY
HURON
ISABELLA
MIDLAND
TUSCOLA
GENESEE
GRATIOT
SAGINAW
Bay City
Saginaw
Flint
Thunder Bay
Hubbard Lake
Grand Lake
Long Lake
Harbor Beach
Lexington
Lakeport
Port Huron
MacPherson Pt.
Clark Pt.
Goderich
Grand Bend
Kettle Pt.
3.1
3.2
N
S
E
W
SCALE IN MILES
0 10 20 30 40 50

7-17

TABLE 7

LAKE HURON - ERTS-1 frames used for surface circulation charts

Resultant Wind Direction	Orbit #	Date	ID #	Sun Elevation
N	3443	27 Mar 73	1247-15472	42
			1247-15474	42
NE	3429	26 Mar 73	1246-15420	42
	5451	18 Aug 73	1391-15462	52
E	1672	20 Nov 72	1120-15413	23
SE	933	28 Sep 72	1067-15460	38
			1067-15463	40
S	4182	19 May 73	1300-15414	58*
	4447	7 Jun 73	1319-15471	60*
SW	----------NONE----------			
W	3694	14 Apr 73	1265-15471	48
			1265-15474	49
NW	3680	13 Apr 73	1264-15413	48
			1264-15420	49

* - Solar elevation $\geq 55°$ (see Chapter 5).

westerly, northwesterly and northerly resultant wind regimes. Comparison with previously-observed, specific, localized circulations shows good agreement.

Southern Lake Huron

The location of the wind station used in preparation of Southern Lake Huron currents is shown in Figure 56. Also identified in the figure are all locations referred to in the text. Table 7 presents a summary of ERTS-1 scenes utilized in addition to resultant wind direction calculations. Table A3 in the Appendix provides further specifics on southern Lake Huron ERTS-1 views.

Northerly Winds - Figure 57a

The current diagram is based on a single ERTS-1 pass on 27 March 1973. The flow-through current flows southward along the west shore of the lower lake directly into the St. Clair River; there is no apparent southeastward component as Ayers (1959) described. Southwest of Kettle Point appears to be a counterclockwise eddy defined by the flow-through current and the projection of Kettle Point. At Kettle Point upwelling occurs as the currents flow offshore. This opposes the circulation described by Ayers (1959) for northerly wind conditions. From Grand Bend to Goderich lies a large nearshore counterclockwise gyre that apparently exists as a semipermanent feature regardless of wind regime (Ayers et al., 1956). A small weak counterclockwise eddy exists just off MacPherson Point; a similar circulation was described by Ayers et al. (1956) and Ayers (1959) for northerly winds. The current that extends northward from the large counterclockwise eddy leaves the east shore near Clark Point and the winds transport the water across the lake to the southwest, perhaps to join the flow-through current. This original northward current may be a remnant of a previous wind regime or may simply be part of the flow-through current complex as discussed by Ayers (1959) for the Synoptic II cruise under winds from the northern quadrants.

Northeasterly Winds - Figure 57b

ERTS-1 passes on 26 March 1973 and 18 August 1973 were composited for this

analysis. The major features are identical to those that were observed under northerly wind regimes. The general circulation is counterclockwise throughout the southern part of the lake. The flow-through current flows directly to the St. Clair River along the west shore. Southwest of Kettle Point is a nearshore counterclockwise eddy which is apparently created in part by the topographic barrier of Kettle Point. Again between Grand Bend and Goderich along the east shore is a large counterclockwise eddy. The winds transport the mid-lake water to the south and southwest, augmenting the flow-through current. At Lakeport on the west shore a branch current flows abruptly offshore to the northeast, which is inconsistent with all other current indicators.

Easterly Winds - Figure 57c

For easterly wind regimes, only one partly cloudy ERTS-1 pass (20 November 1972) was available for analysis. The only currents that could be determined flowed directly offshore from Goderich to Grand Bend along the east shore, indicating that a band of upwelling existed alongshore.

Southeasterly Winds - Figure 57d

The current diagram was derived from one ERTS-1 pass on 28 September 1972. As discussed above under northerly wind regimes, the general circulation in the southern part of the lake is counterclockwise across the lake and southward into the St. Clair River. At the head of the St. Clair River is a small counterclockwise gyre that was established under northerly winds but not found by Ayers et al. (1956) under any conditions. A larger counterclockwise eddy is located along the curved shoreline between Kettle Point and Grand Bend. The position is somewhat closer to shore than the eddy shown by Ayers et al. (1956) for southerly winds. Along the east shore from Grand Bend to Clark Point upwelling occurs as the currents flow offshore to the northwest. The sediment patterns are inconclusive, but it appears that there is a large counter-clockwise gyre in the middle of the area; the southeasterly winds have

displaced this eddy westward from the more nearshore location shown by Ayers et al. (1956) for a wind regime more southerly than normal. Off MacPherson Point a long sediment plume appears to have a counterclockwise component in the same area as under northerly winds; otherwise, the alongshore currents north of Clark Point flow southwesterly to join the overall counterclockwise circulation.

Southerly Winds - Figure 57e

Two relatively cloud-free ERTS-1 passes (19 May 1973 and 7 June 1973) were available to derive the current analysis in Figure 57e. Off the Lakeport-Lexington area is a small clockwise eddy first described by Ayers et al. (1956). From Lexington to Harbor Beach, northeast currents flow offshore creating upwelling and displacing the flow-through current, which is normally alongshore, toward the center of the Lake as described by Ayers et al. (1956). Counterclockwise gyres exist, as discussed above, between Kettle Point and the St. Clair River, northeast of Kettle Point, and southwest of Clark Point. The western portions of each of these individual circulations are incorporated into the southward-flowing mid-lake flow-through current as depicted in the diagram of the selected cruise results (Ayers et al., 1956 and Ayers, 1959). The flow-through current does not appear as a distinct current at the head of the St. Clair River; however, since this flow would draw from relatively clean comparatively sediment-free upwelled water it should be in this area.

Southwesterly Winds

No resultant wind stress was observed from this direction during the period of investigation.

Westerly Winds - Figure 57f

ERTS-1 passed over this area on 14 April 1973 when a westerly wind regime existed. The flow-through current lies along the west shore

where it flows southward, then southeastward and finally southwestward to the St. Clair River. A small clockwise eddy, which is apparently driven by the flow-through current, lies off Lakeport. This was also found by Ayers et al. (1956). A very large elongated counterclockwise gyre exists between Kettle Point and Clark Point, but it is somewhat larger and farther offshore than indicated by Ayers et al. (1956) and Ayers (1959). The current flowing southwestward from Clark Point appears to help drive this large gyre. There is also a large but weak counterclockwise circulation off MacPherson Point.

Northwesterly Winds - Figure 57g

The ERTS-1 pass for 13 April 1973 was used to derive the current diagram in Figure 57g. The flow-through current flows southward along the west shore. At Lexington, it flows southeastward and forms a small clockwise eddy off Lakeport as it returns to the southwest corner of the Lake. This is the "typical" pattern described by Ayers et al. (1956). The sediment patterns in the eastern part of the lake do not define with any certainty the presence of a large counterclockwise gyre, but a counterclockwise circulation is suggested northwest of Clark Point in the middle of the Lake. The situation is very similar to 14 April 1973 (westerly winds), and a gyre was indicated at that time. Off MacPherson Point there exists again a large but weak counterclockwise circulation, augmented by alongshore currents flowing northeast from Clark Point, as Ayers et al. (1956) indicated.

Summary

ERTS-1 observations indicate that the southward-flowing current along the Michigan shoreline of the "Thumb" is only reversed by southerly (and probably southwesterly) resultant wind stress. Along the Canadian shoreline a northward current was observed north of Kettle Point for all winds

Figure 57a-g. Surface current analyses for southern Lake Huron as determined from turbidity patterns in ERTS-1 scenes. Weighted wind directions from Table A3 are indicated in upper right-hand corners.

ORIGINAL PAGE IS
OF POOR QUALITY

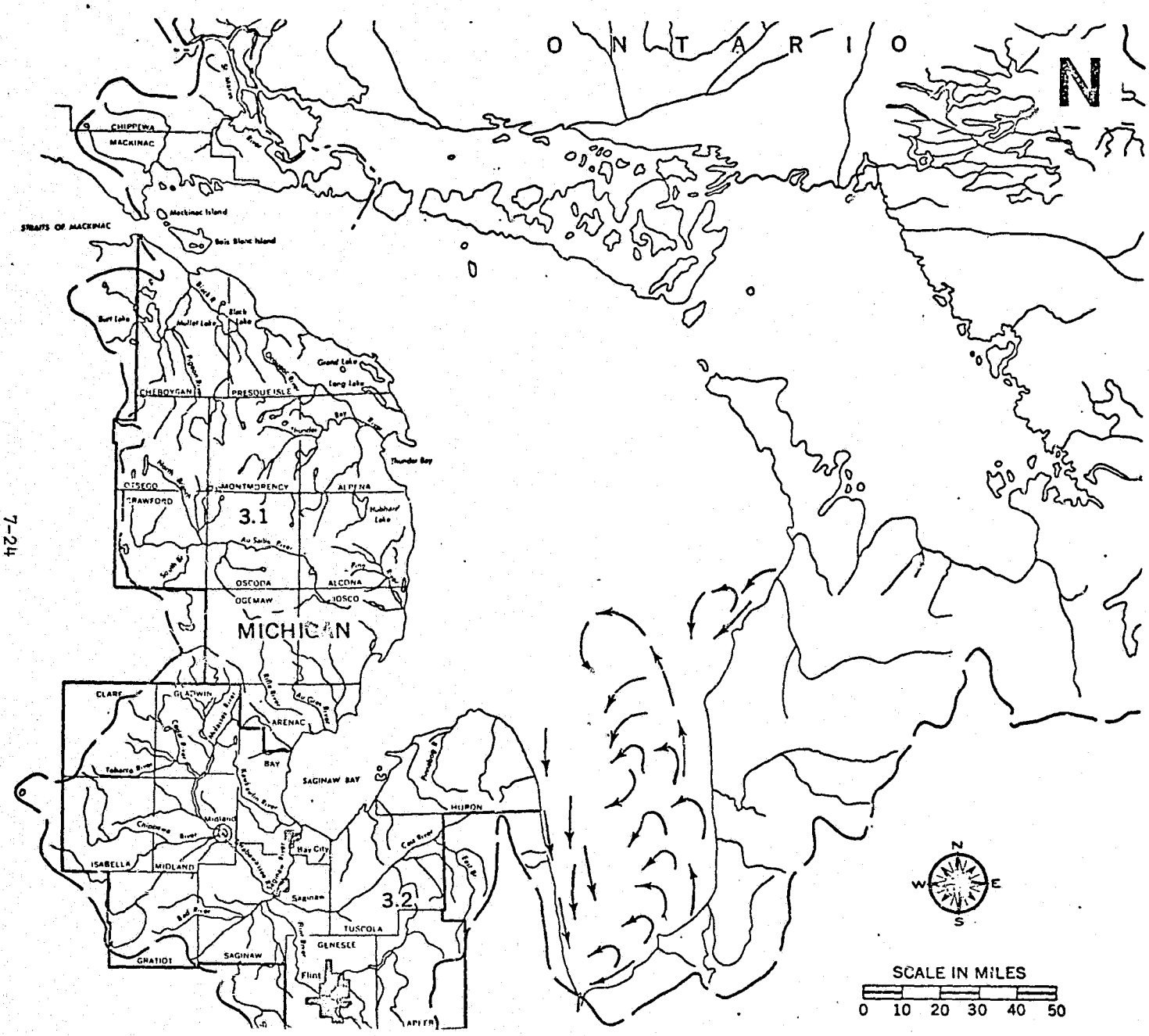

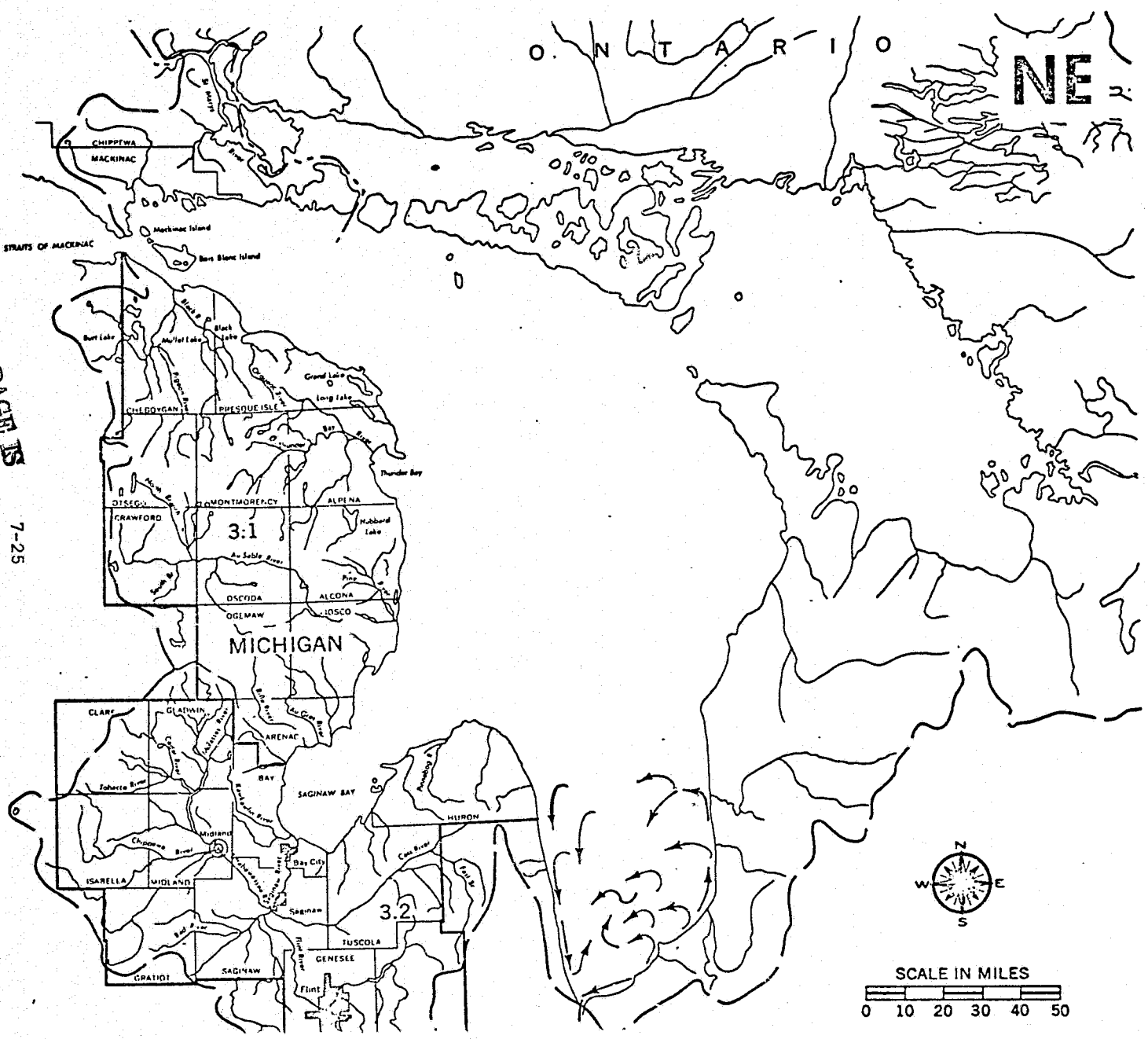

b

ORIGINAL PAGE IS
OF POOR QUALITY

7-25

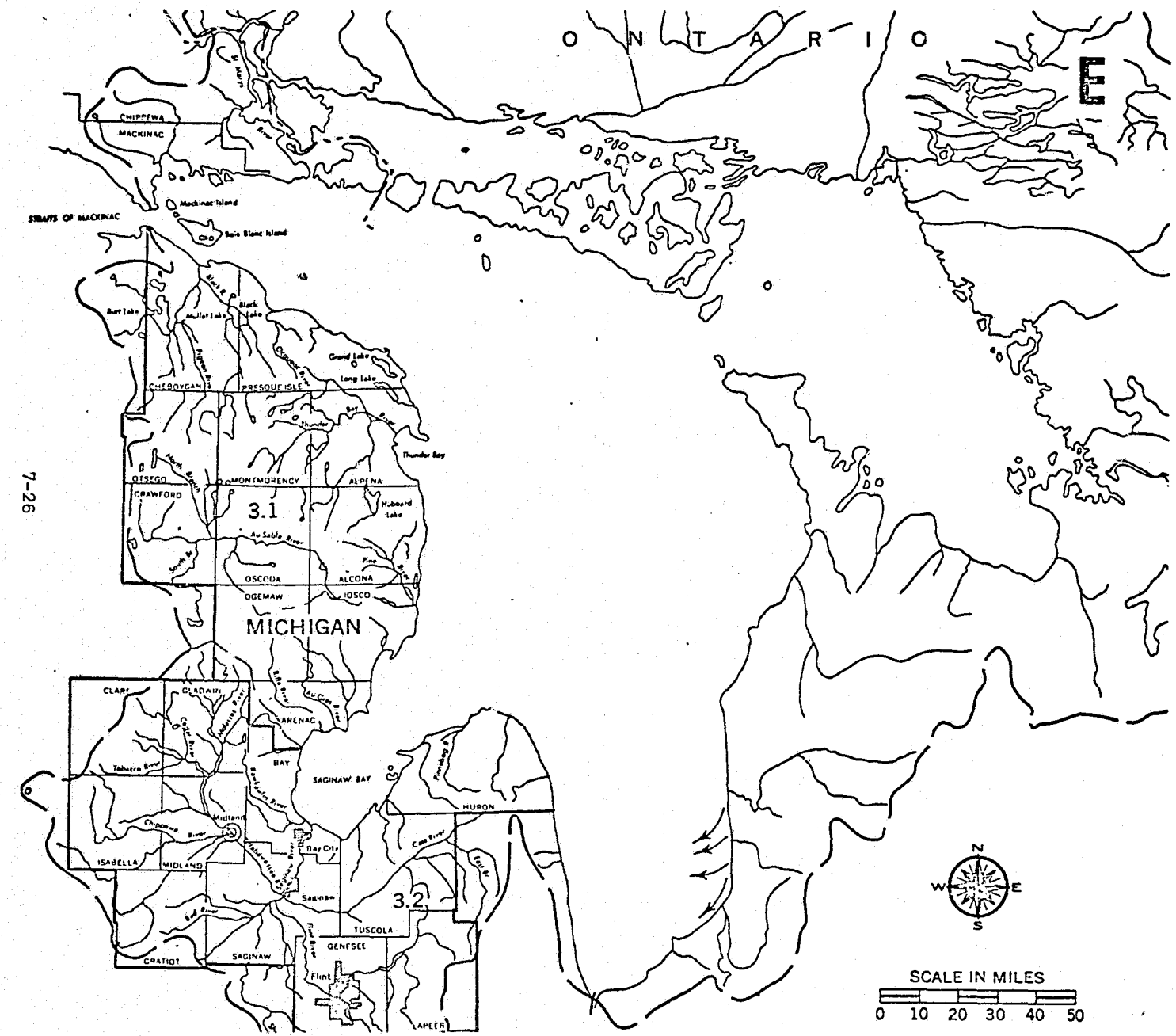
ONTARIO
E
C
CHIPPEWA
MACKINAC
Mackinac Island
STRAITS OF MACKINAC
Bois Blanc Island
Burt Lake
Mullet Lake
Black Lake
Grand Lake
Long Lake
CHEBOYGAN
PRESQUE ISLE
Thunder Bay
OTSEGO
MONTMORENCY
ALPENA
CRAWFORD
3.1
Hubbard Lake
Au Sable River
OSCODA
ALCONA
OGEMAW
IOSCO
MICHIGAN
CLARE
GLADWIN
ARENAC
BAY
SAGINAW BAY
HURON
Midland
ISABELLA
MIDLAND
Bay City
Saginaw
3.2
TUSCOLA
GENESEE
GRATIOT
SAGINAW
Flint
LAPEER
N
W
E
S
SCALE IN MILES
0 10 20 30 40 50

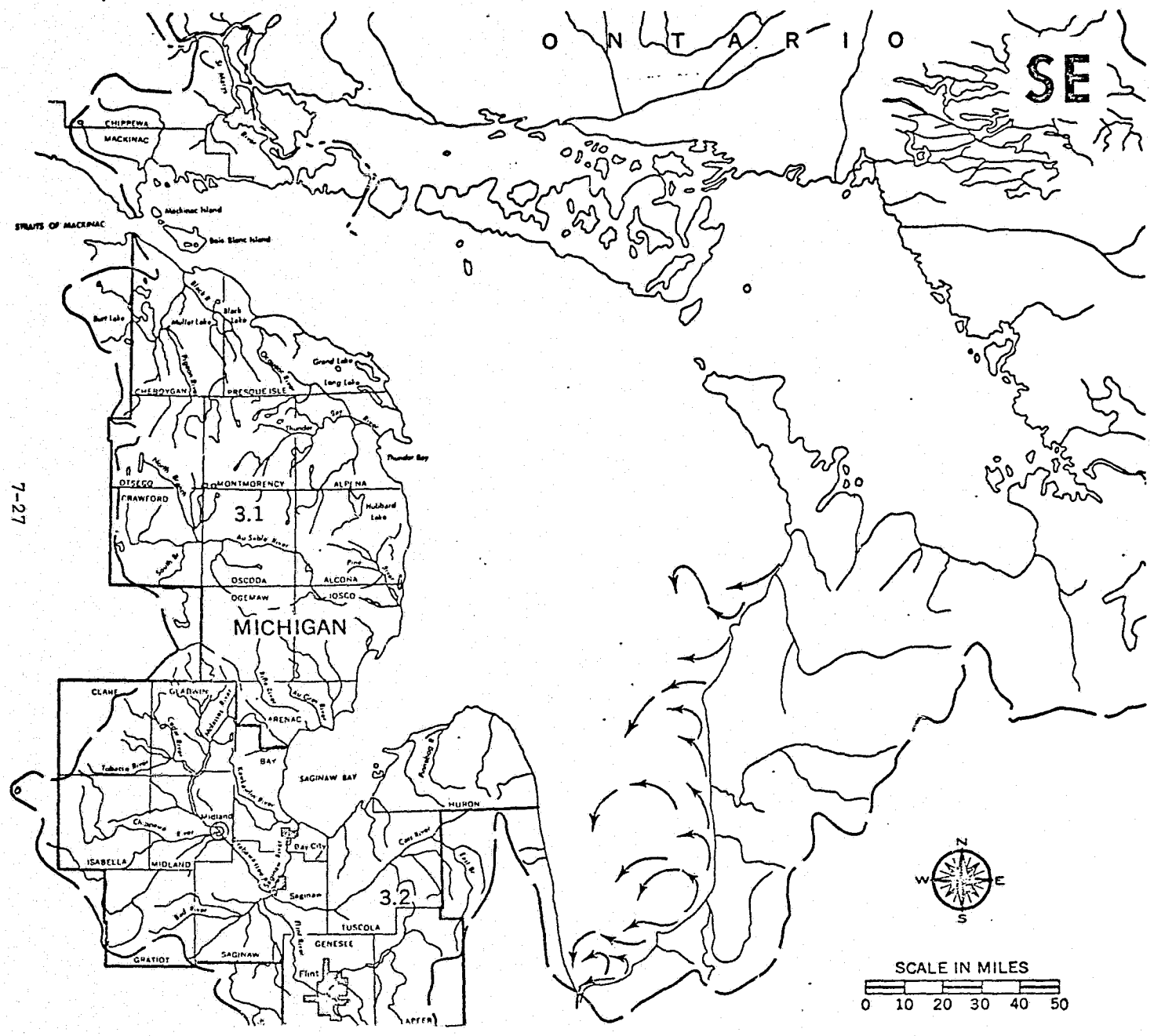
O N T A R I O
SE
d
CHIPPEWA
MACKINAC
Mackinac Island
STRAITS OF MACKINAC
Bois Blanc Island
Burt Lake
Mullet Lake
Black Lake
Grand Lake
Long Lake
CHEBOYGAN
PRESQUE ISLE
Thunder Bay
OTSEGO
CRAWFORD
MONTMORENCY
ALPENA
Hubbard Lake
3.1
Au Sable River
OSCODA
ALCONA
OGEMAW
IOSCO
MICHIGAN
CLARE
GLADWIN
ARENAC
BAY
SAGINAW BAY
HURON
Midland
Bay City
ISABELLA
MIDLAND
Saginaw
3.2
TUSCOLA
GENESEE
GRATIOT
SAGINAW
Flint
N
W
E
S
SCALE IN MILES
0 10 20 30 40 50

ORIGINAL PAGE IS
OF POOR QUALITY

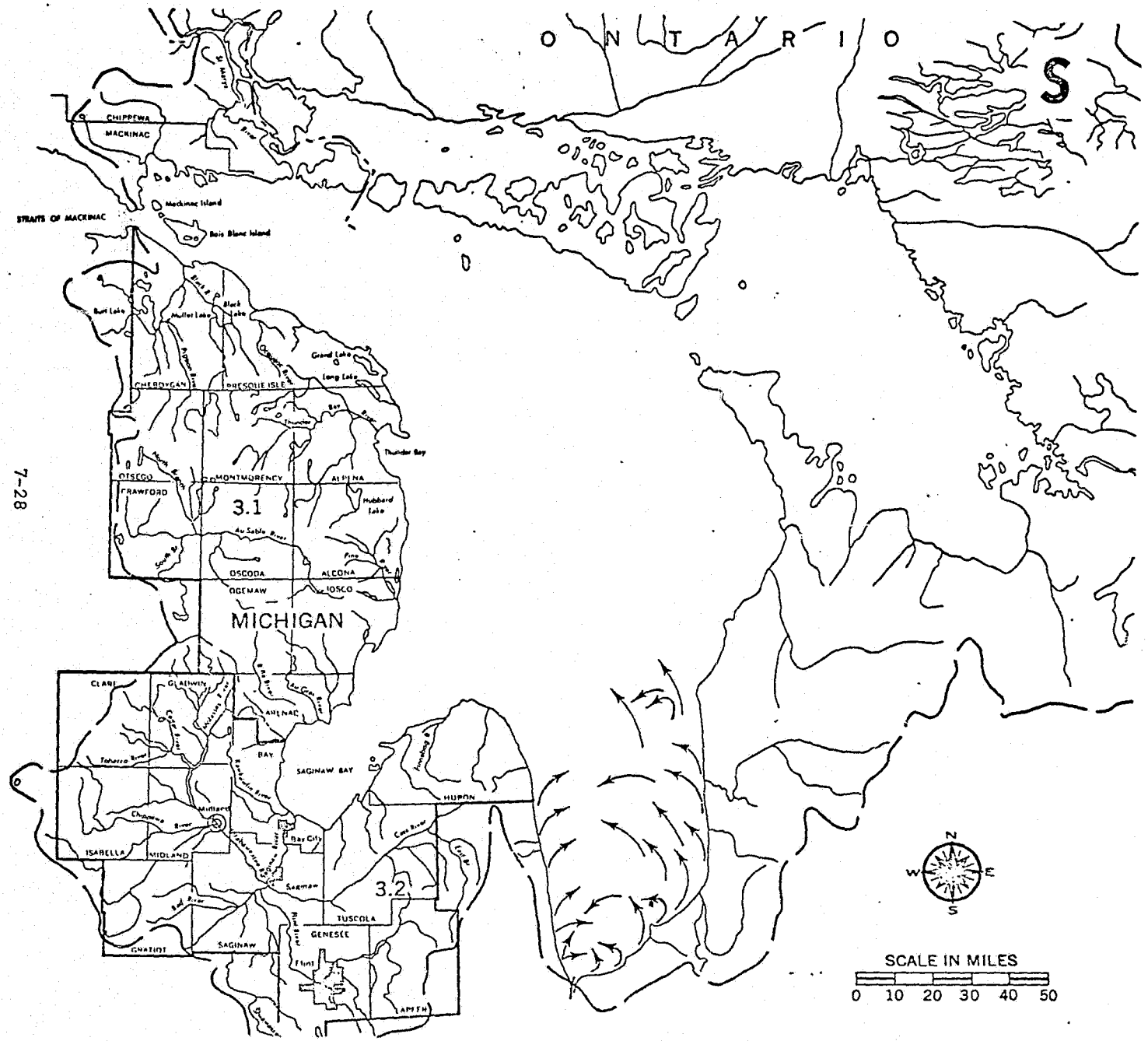

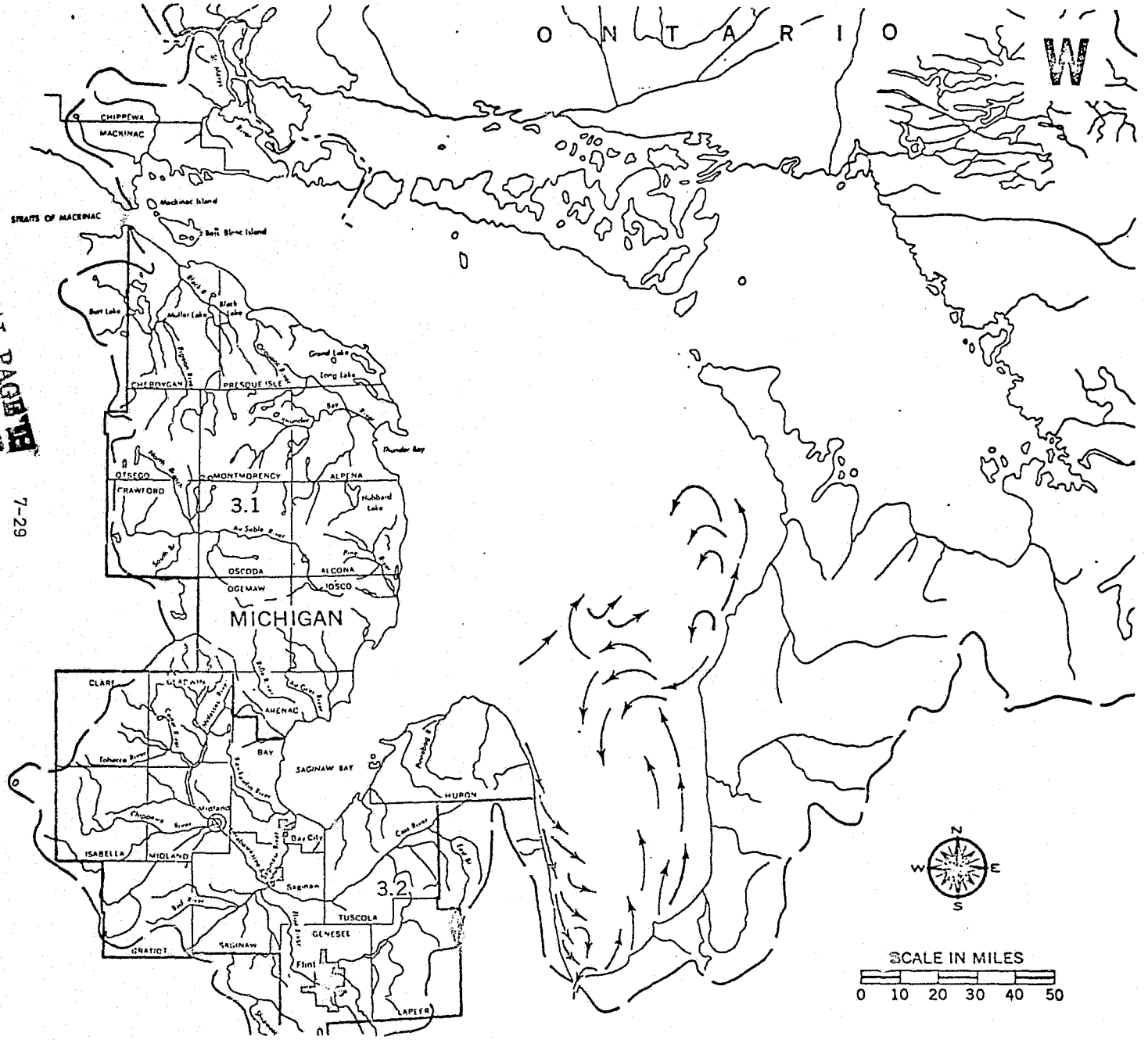

ORIGINAL PAGE IS
OF POOR QUALITY

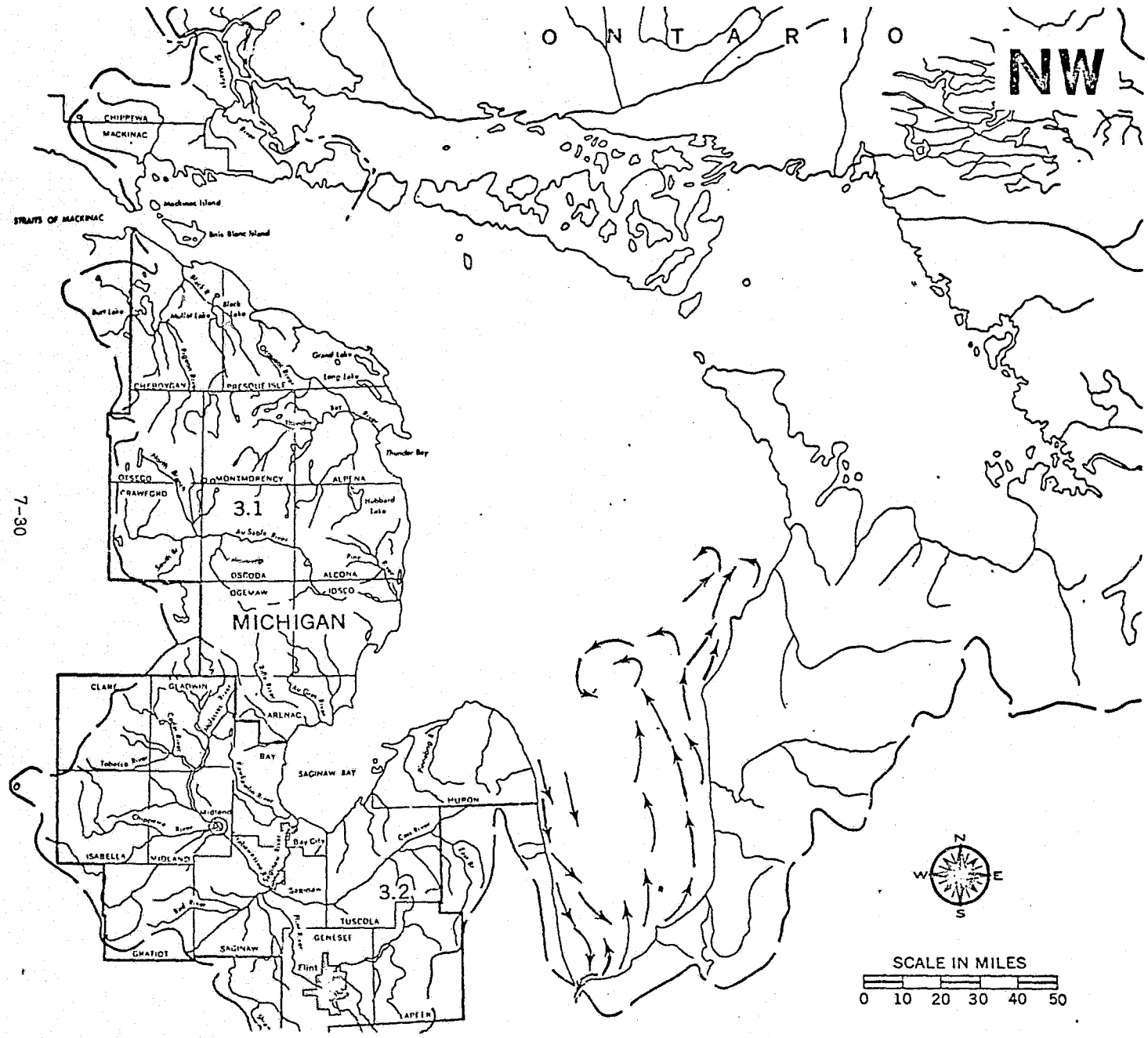
ONTARIO
NW
CHIPPEWA
MACKINAC
STRAITS OF MACKINAC
Mackinac Island
Bois Blanc Island
CHEBOYGAN
PRESQUE ISLE
Thunder Bay
OTSEGO
MONTMORENCY
ALPENA
CRAWFORD
3.1
Hubbard Lake
Au Sable River
OSCODA
ALCONA
OGEMAW
IOSCO
MICHIGAN
CLARE
GLADWIN
ARENAC
BAY
SAGINAW BAY
HURON
Tobacco River
Midland
Chippewa River
Bay City
ISABELLA
MIDLAND
Saginaw
3.2
TUSCOLA
GENESEE
GRATIOT
SAGINAW
Flint
LAPEER
N
W
E
S
SCALE IN MILES
0 10 20 30 40 50

with the exception of easterly--when the flow was offshore. An offshore current component was incorporated in this dominant northward flow whenever wind stress accumulated from the easterly or southerly directions. Also typical for all observed wind directions was a gyre located offshore in the vicinity of Clark Point. Alongshore currents have a tendency to converge in this area. Although the circulation in the central part of the Lake is complex, a decided counterclockwise flow usually prevails.

Lake St. Clair

Since there are no regularly maintained meteorological records along Lake St. Clair, three sites are shown in Figure 58. The observations from Selfridge AFB (near Mt. Clemens, Michigan), when available, were accepted as primary input to the resultant wind determinations. Table 8 presents the key ERTS-1 scenes employed for the Lake St. Clair analyses. More complete coverage information is available in Appendix Table A4.

Northerly Winds - Figure 59a

The ERTS-1 pass for 14 April 1973 indicated that, as usual, the water in Lake St. Clair is very turbid, although less so in the surface layers. The currents in Anchor Bay flow westward and southwestward to the outflow of the Clinton River, where the combined currents flow southward along the Detroit shore. A model study by Ayers (1964) has shown Anchor Bay to have an independent clockwise circulation. This view is not supported by this investigation, which indicates that the surface currents in Anchor Bay respond more fully to the wind regime. North of Detroit a branch current flows eastward to the center of the lake. The major component of outflow to the head of the Detroit River appears to come from Chenal Ecarte and Johnston Channels, similar to the situation described by Ayers (1964). Part of this source current flows directly across the

Figure 58. Wind stations used for Lake St. Clair (Port Huron, Selfridge AFB, Detroit River Light).

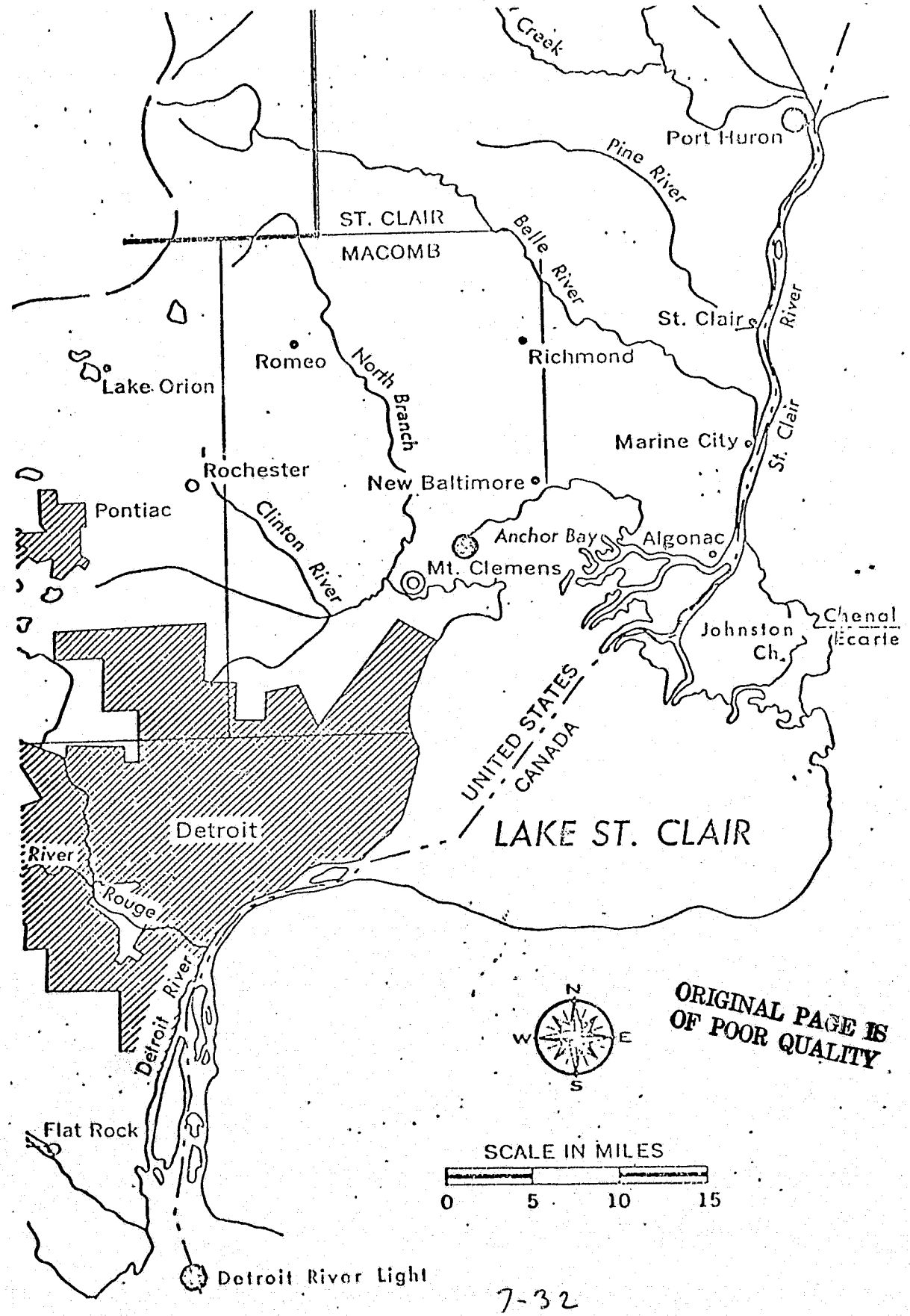

ORIGINAL PAGE IS
OF POOR QUALITY

TABLE 8

LAKE ST. CLAIR - ERTS-1 frames used for surface circulation charts

Resultant Wind Direction	Orbit #	Date	ID #	Sun Elevation
N	3694	14 Apr 73	1265-15474	49
			1265-15480	50
NE	3443	27 Mar 73	1247-15474	42
			1247-15481	43
E	4196	20 May 73	1301-15472	58*
			1301-15475	59*
SE	----------NONE----------			
S	----------NONE----------			
SW	3178	8 Mar 73	1228-15422	36
W	4698	25 Jun 73	1337-15470	60*
			1337-15472	61*
NW	3680	13 Apr 73	1264-15422	50

** - Solar elevation $\geq$ 55° (see Chapter 5).

lake southwestward to the Detroit River, and part flows southward along the east shore then westward somewhat offshore. Eastward-flowing alongshore currents are well-defined along the south shore for this wind regime. There is an apparently small weak counterclockwise gyre in the eastern part of the lake; this corresponds to the "water left by previous wind", shown by Ayers (1964), although here it is smaller and less well-defined.

Northeasterly Winds - Figure 59b

The ERTS-1 pass on 27 March 1973 indicated a strong outflow to the head of the Detroit River over the entire lake in response to a northeasterly wind regime. The large counterclockwise gyre that Ayers (1964) found for the southeast portion of the lake was not observed under these conditions. The surface currents in this portion respond to the wind and flow southward from Chenal Ecarte and Johnston Channels, then westward to the Detroit River. Again, there is no evidence to support Ayers' (1964) contention that an independent clockwise gyre exists in Anchor Bay; the sediment patterns strongly indicate that the currents in Anchor Bay flow southward alongshore.

Easterly Winds - Figure 59c

The current diagram shown in Figure 59c was based on the 20 May 1973 ERTS-1 pass; the eastern portion of the lake was partially obscured by clouds. Again, there is no evidence to suggest that the southeastern half of the lake is the site of a large counterclockwise gyre or that Anchor Bay has a clockwise circulation independent of the wind regime (Ayers, 1964). The sediment patterns strongly indicate that there is a rather distinct and straightforward flow-through from the mouth of the St. Clair River to the head of the Detroit River.

Southeasterly Winds
Southerly Winds

These conditions were not observed by ERTS-1 during the study period.

Southwesterly Winds - Figure 59d

The surface current analysis in Figure 59d is based on a single ERTS-1 pass on 8 March 1973. The northwest portion of the lake, from the south channel of the St. Clair River to Detroit, was ice-covered and analysis could not be made. The plumes from the St. Clair River and Chenal Ecarte and Johnston Channel are extremely turbid, and remain near the channel mouths because their outflow is directly opposed by the southwesterly stress. There is also a large, vaguely-defined, apparently weak, clockwise circulation in the east part of the lake that developed in response to the wind; this is contradictory to Ayers' (1964) model for this case. The alongshore currents flow eastward along the south shore and partly contribute to the clockwise circulation. The general southwestward outflow current is located only in the central portion of the lake; and under these wind and ice condition, it is relatively narrow. The major source for this current is the outflow from Chenal Ecarte and Johnston Channel. Ayers (1964) indicated another clockwise gyre northwest of the cross-lake outflow current, and a counterclockwise circulation in Anchor Bay; neither of these could be confirmed because of ice cover.

Westerly Winds - Figure 59e

The ERTS-1 pass for 25 June 1973 was employed to derive the surface current diagram. A full counterclockwise gyre was evident in Anchor Bay, as Ayers (1964) indicated. The northwest half of the lake is characterized by southward currents originating from the upper channels of the St. Clair River that turn southwestward somewhat offshore from Detroit. There does not appear to be a significant clockwise circulation north of Detroit as indicated by Ayers (1964). The outflow from the Southeast Bend Cutoff and Chenal Ecarte and Johnston Channel responds to the wind and flows southeastward and along the east shore, driving a weak clockwise gyre. This

circulation is somewhat larger than the one described in Ayers' (1964) model for this wind condition. West of this clockwise gyre lies a smaller weak counterclockwise eddy that may be driven by the outflow current and a branch from the clockwise gyre. Alongshore currents flow eastward along the south shore, separated from both eddies by a vague westward-flowing outflow.

Northwesterly Winds - Figure 59f

The surface current analysis for northwesterly resultant winds was derived from a single ERTS-1 overpass on 13 April 1973. Here there was very little agreement with Ayers' (1964) model for a northwesterly wind regime. The outflow from the upper channels of the St. Clair River flows southward and southwestward directly to the Detroit River. The outflow from Chenal Ecarte and Johnston Channel is first transported southeastward then southwestward across the lake to join the general outflow, in the process driving a small counterclockwise gyre in the east portion of the lake. This eddy apparently is much less significant than Ayers (1964) believed. The cross-lake current flows southwestward, not southeastward as Ayers (1964) illustrated. Alongshore currents flow eastward along the south shore.

Summary

The ERTS-1 observations reveal that a preferred southward-flowing current is found along the Detroit shoreline. It is presumed, as indicated by the Ayers (1964) model, that only a southwesterly resultant wind stress reverses this southward flow. No ERTS-1 data were available for charting this condition along the Detroit shoreline because of ice cover at the time of the only sufficiently cloud-free overpass to coincide with a southwesterly wind regime. Currents along the southern shoreline (Canada) flow

Figure 59a-f. Surface current analyses for Lake St. Clair as determined from turbidity patterns in ERTS-1 scenes. Weighted wind directions from Table A4 are indicated in upper right-hand corners.

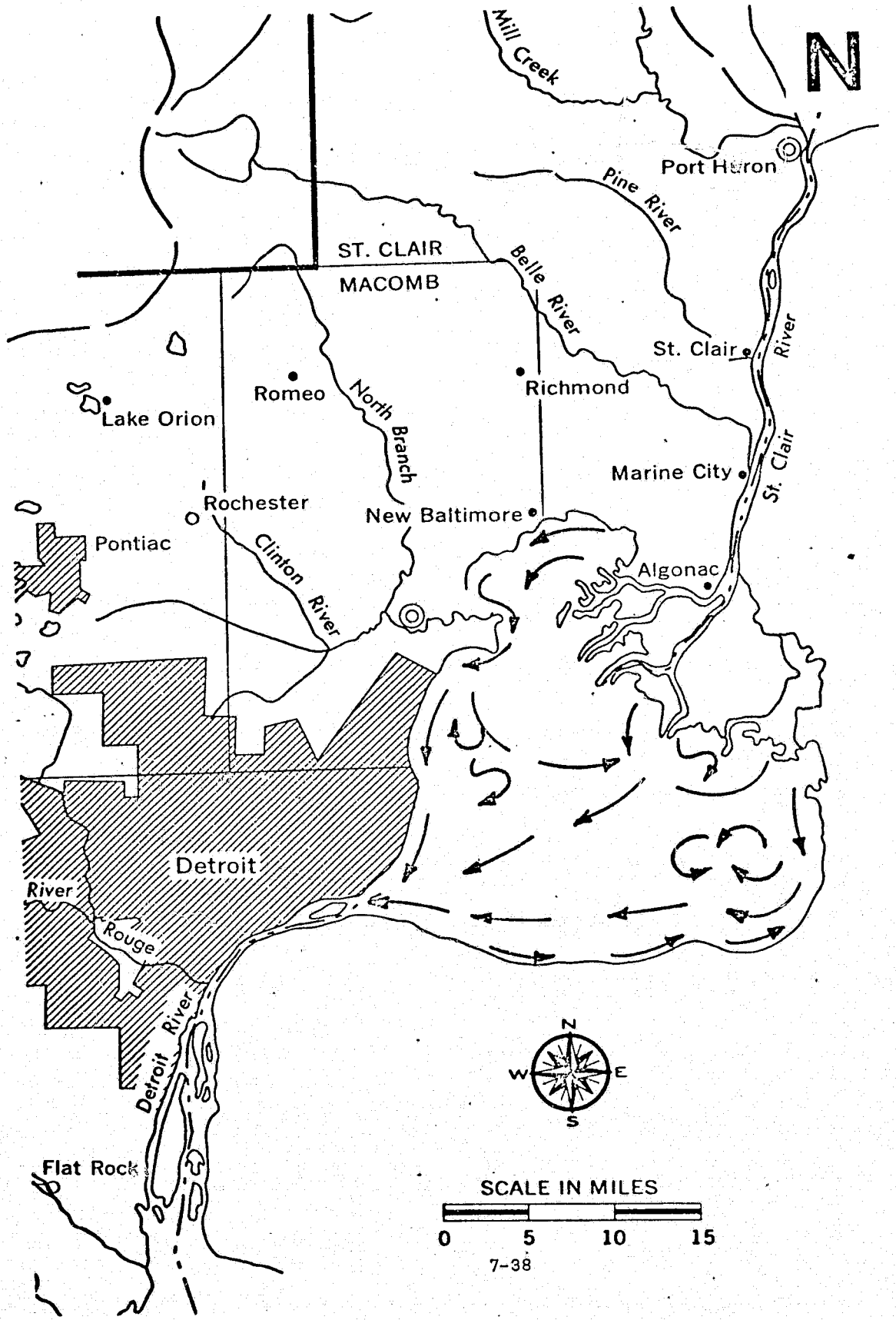
N
Mill Creek
Port Huron
Pine River
ST. CLAIR
MACOMB
Belle River
St. Clair River
Romeo
North Branch
Richmond
Lake Orion
Marine City
St. Clair
Rochester
New Baltimore
Pontiac
Clinton River
Algonac
Detroit
River
Rouge
Detroit River
Flat Rock
N
W
E
S
SCALE IN MILES
0
5
10
15

7-38

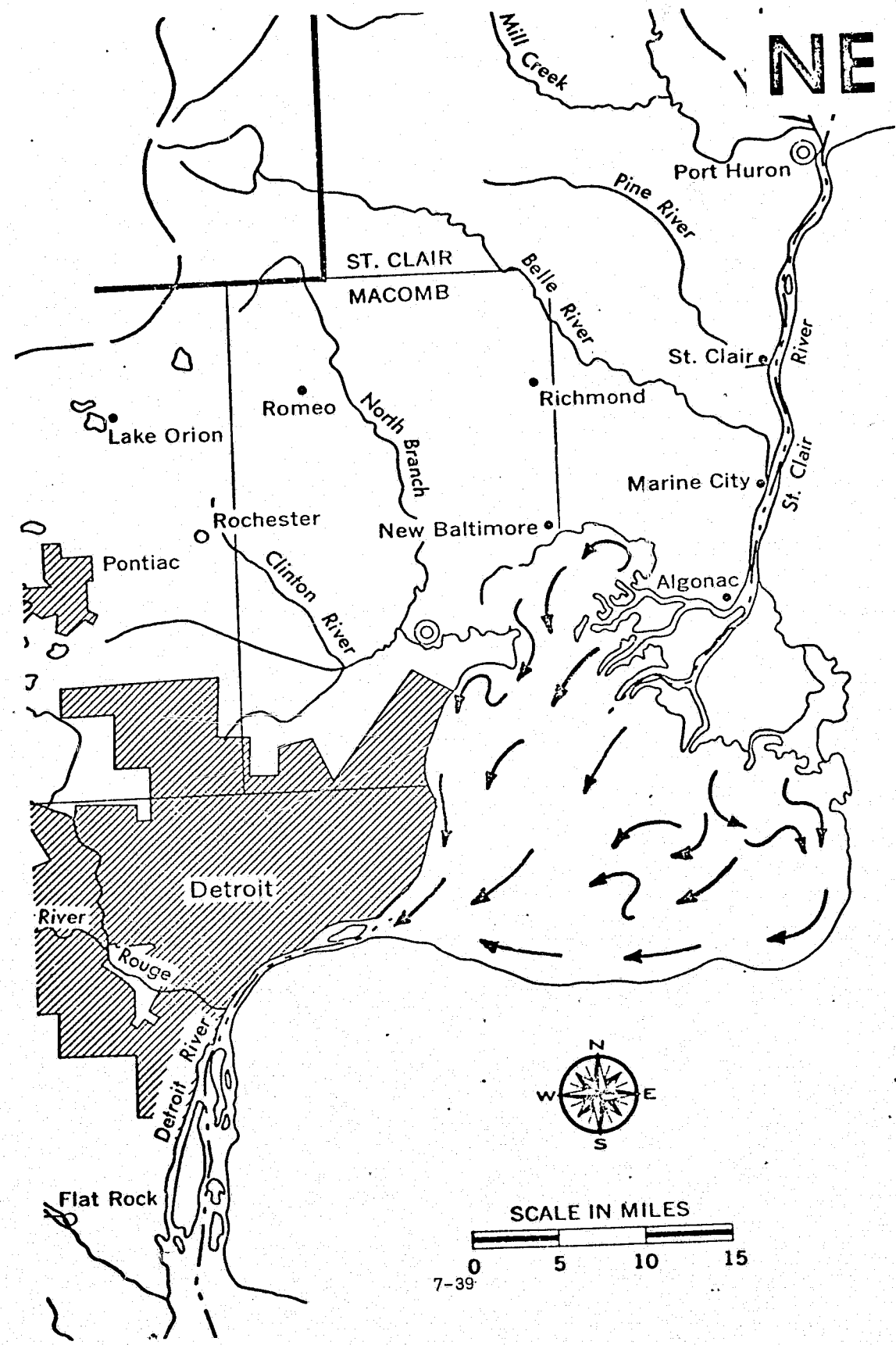
NE
b
Mill Creek
Port Huron
Pine River
ST. CLAIR
MACOMB
Belle River
St. Clair River
St. Clair
Richmond
Romeo
North Branch
Lake Orion
Marine City
St. Clair
Rochester
New Baltimore
Pontiac
Clinton River
Algonac
Detroit
River
Rouge
Detroit River
Flat Rock
N
W
E
S
SCALE IN MILES
0
5
10
15

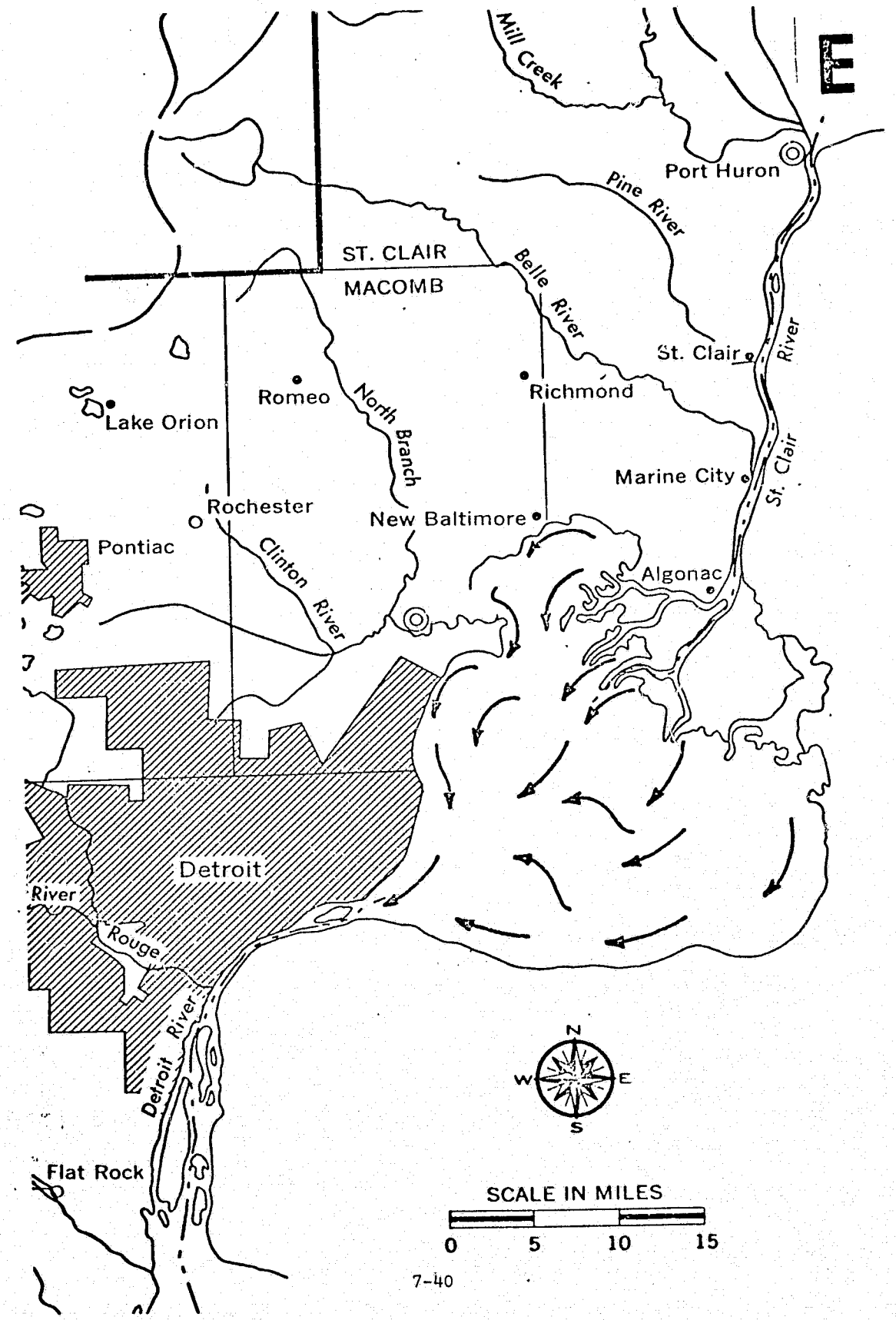
Mill Creek
Port Huron
Pine River
ST. CLAIR
MACOMB
Belle River
St. Clair
River
Romeo
North Branch
Richmond
Lake Orion
Marine City
St. Clair
Rochester
New Baltimore
Pontiac
Clinton River
Algonac
Detroit
River
Rouge
Detroit River
Flat Rock
N
W
E
S
SCALE IN MILES
0
5
10
15

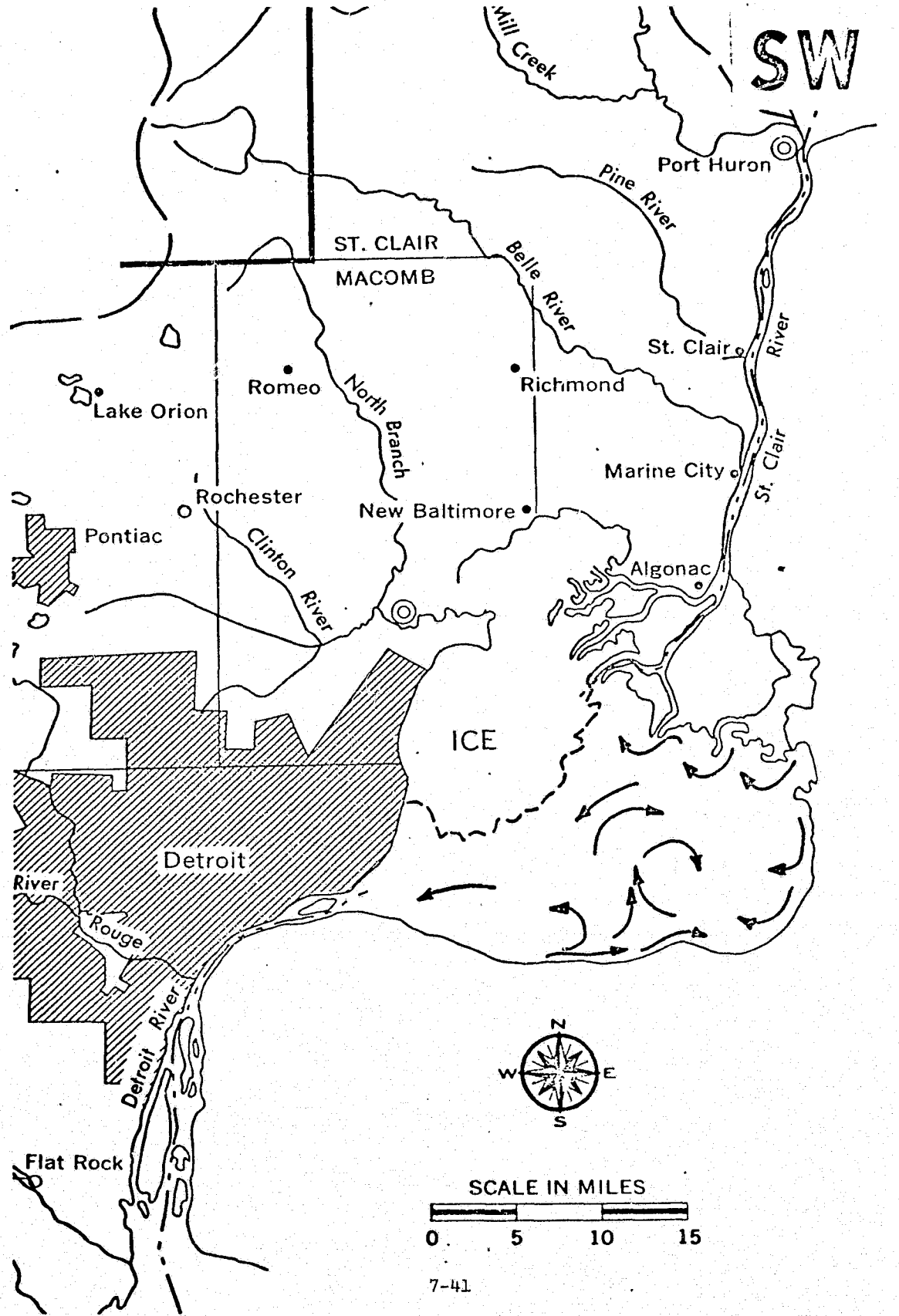
SW
Mill Creek
Port Huron
Pine River
ST. CLAIR
MACOMB
Belle River
St. Clair
River
Romeo
North Branch
Richmond
Lake Orion
Marine City
St. Clair
Rochester
New Baltimore
Pontiac
Clinton River
Algonac
ICE
Detroit
River
Rouge
Detroit River
Flat Rock
N
W
E
S
SCALE IN MILES
0
5
10
15

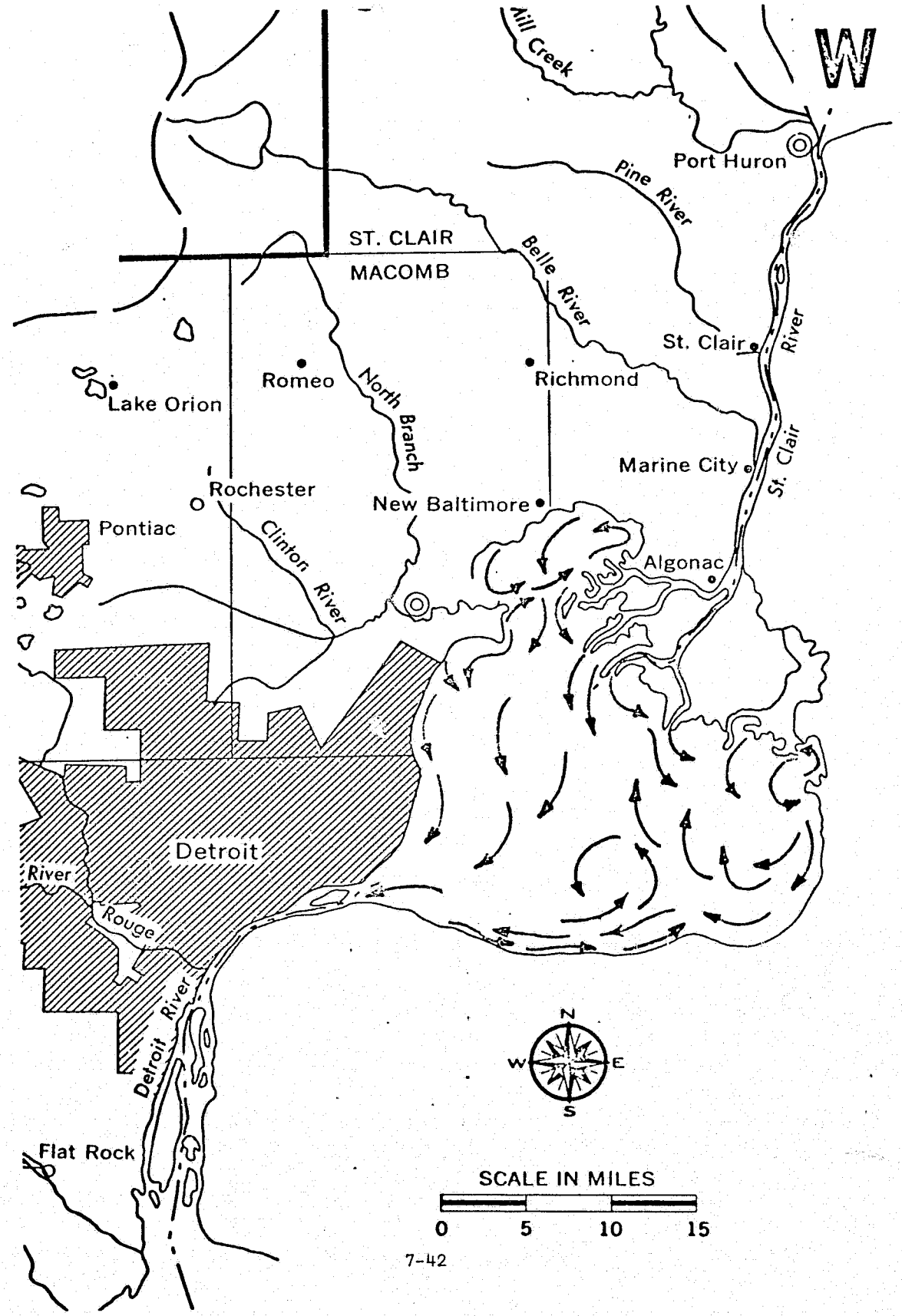
Aill Creek
W
e
Port Huron
Pine River
ST. CLAIR
MACOMB
Belle River
St. Clair
River
Romeo
North Branch
Richmond
Lake Orion
Marine City
St. Clair
Rochester
New Baltimore
Pontiac
Clinton River
Algonac
Detroit
River
Rouge
Detroit River
N
W
E
S
Flat Rock
SCALE IN MILES
0
5
10
15

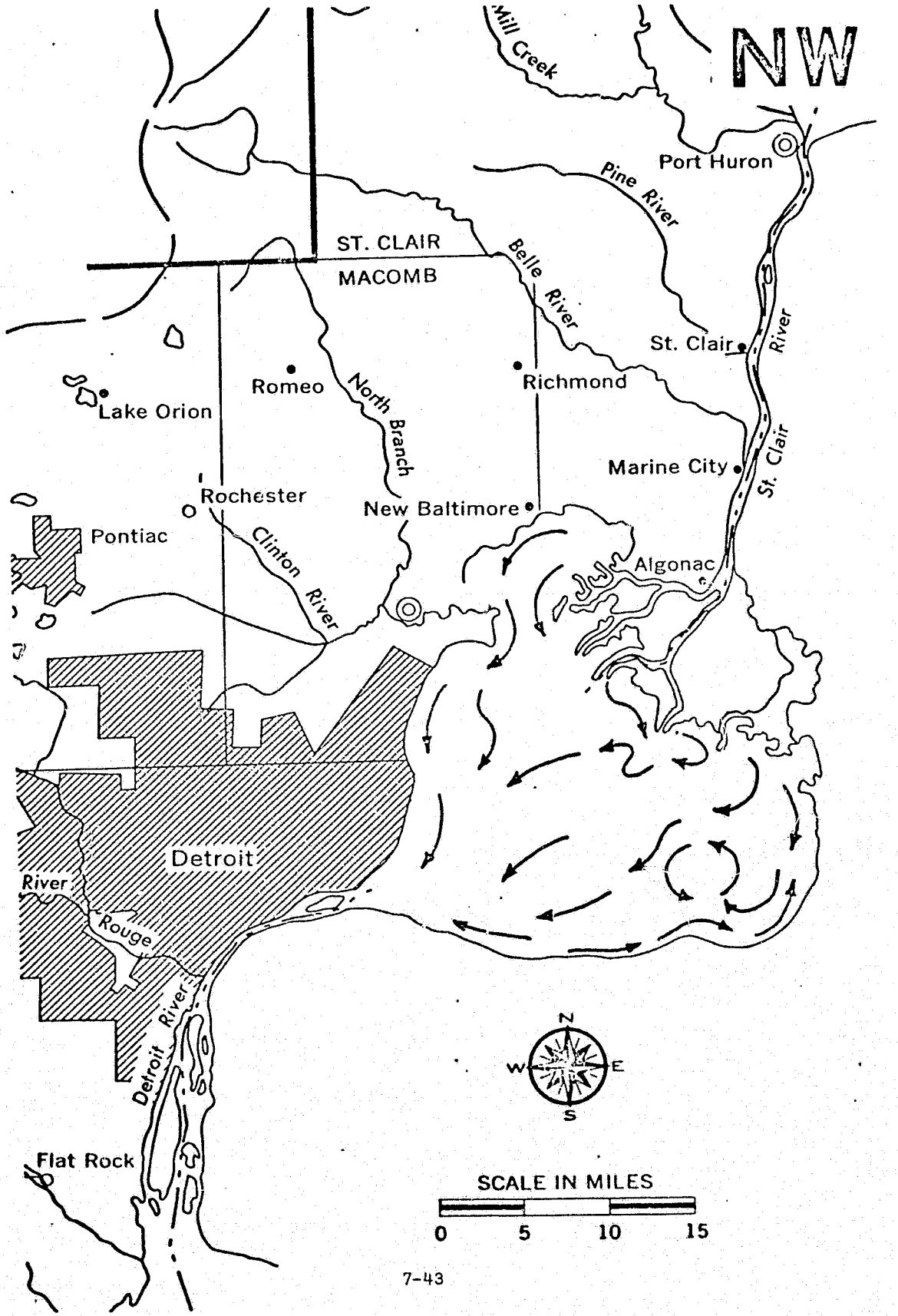
NW
Mill Creek
Port Huron
Pine River
ST. CLAIR
MACOMB
Belle River
St. Clair
River
Romeo
North Branch
Richmond
Lake Orion
Marine City
St. Clair
Rochester
New Baltimore
Pontiac
Clinton River
Algonac
Detroit
River
Rouge
Detroit River
Flat Rock
N
W
E
S
SCALE IN MILES
0
5
10
15

eastward away from the headwaters of the Detroit River for all wind conditions observed except northeasterly and easterly. At times, however, this eastward flow is opposed offshore by westward flow.

Mid-lake circulations are complex under most winds, with several gyres present. Easterly wind stress produces the most straightforward circulation--the one most expected for a shallow flow-through lake. The prevailing wind (westerly) shows the Canadian portion of the lake benefiting most from the clean, clear waters of the St. Clair River and Lake Huron.

Lake Erie

The location chart for the Lake Erie analyses (Figure 60) shows six stations that were used for resultant wind vectors. These U.S. Coast Guard observations were considered to be representative for the immediate area of Lake Erie surrounding the respective locations. Table 9 provides a listing of all ERTS-1 scenes used in producing the surface current charts. The resulting charts are derived from several ERTS-1 scenes in the form of composite analyses. A more complete listing of all ERTS-1 passes over Lake Erie can be found in Appendix Table A5.

Northerly Winds - Figure 61a

This current diagram was based on two ERTS-1 passes (14 and 29 April 1973) and is obviously incomplete, the major gap being the central basin. Outflow from the Detroit and Maumee rivers flows southeastward and eastward, filling the west basin with highly turbid water. This flow continues eastward beyond Cleveland along the south shore. Local deflection of currents occurs around Pelee Island but a general eastward transport is maintained. There is a small clockwise circulation west of Point Pelee along the north shore; upwelling may be occurring in this area as well as south of Point Pelee where the alongshore currents converge and are no longer influenced

Figure 60. Wind stations used for Lake Erie (Detroit River Light, Lorain, Cleveland Ashtabula, Erie, Buffalo).

ORIGINAL PAGE IS
OF POOR QUALITY

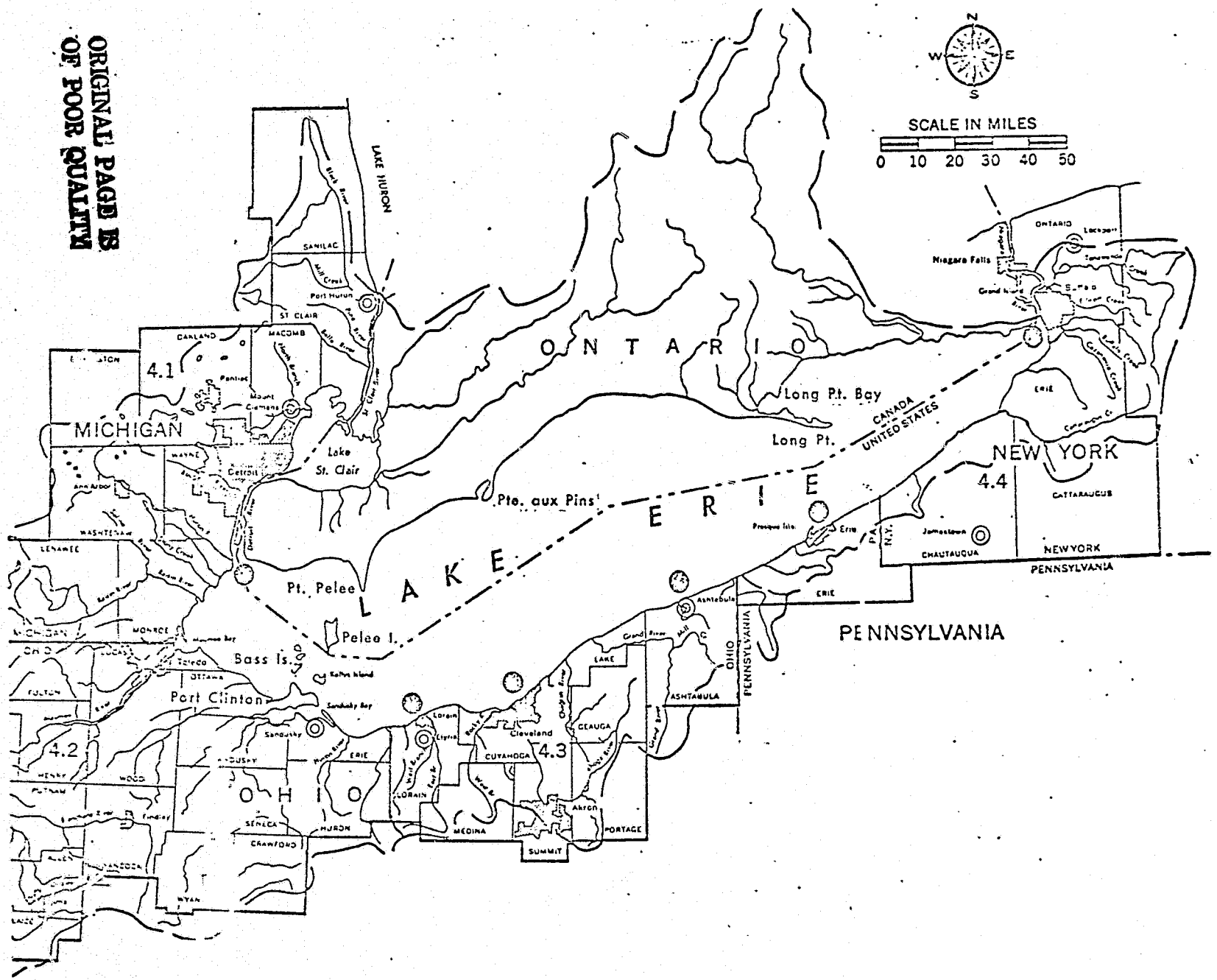

7-45

TABLE 9

LAKE ERIE - ERTS-1 frames used for surface circulation charts

Resultant Wind Direction	Orbit #	Date	ID #	Sun Elevation
N	3694	14 Apr 73	1265-15480	50
	3903	29 Apr 73	1280-15302	54
			1280-15305	54
NE	1672	20 Nov 72	1120-15413	23
			1120-15420	25
	3429	26 Mar 73	1246-15420	42
	3443	27 Mar 73	1247-15481	43
E	933	28 Sep 72	1067-15465	41
	3429	26 Mar 73	1246-15420	42
SE	4698	25 Jun 73	1337-15472	61*
	5688	4 Sep 73	1408-15401	47
			1408-15404	48
S	3178	8 Mar 73	1228-15422	36
	4447	7 Jun 73	1319-15474	61*
	6943	3 Dec 73	1498-15384	21
			1498-15391	22
SW	4684	24 Jun 73	1336-15414	61*
W	4168	18 May 73	1299-15362	59*
NW	668	9 Sep 72	1048-15411	46
	3680	13 Apr 73	1264-15420	49
			1264-15422	50
	3947	30 Apr 73	1281-15363	55*

* - Solar elevation $\geq 55°$ (see Chapter 5).

by the boundary geometry. There a series of small counterclockwise circulations is established, perhaps as a result of wind or river outflow pulses. As Harrington (1895) and Hough (1958) showed, there appears to be a large counterclockwise eddy alongshore between Point Pelee and Pte. aux Pins. Although the analysis is incomplete, alongshore currents would appear to converge in the vicinity of Erie, Pennsylvania.

Northeasterly Winds - Figure 61b

Northeasterly winds prevailed during the ERTS-1 overpasses on 20 November 1972, and 26-27 March 1973. Figure 59b indicates a counterclockwise flow of surface currents in Long Point Bay, and apparently two minor clockwise gyres south and west of Long Point along the shore; these may be parts of a larger clockwise gyre in the central basin (Gedney and Lick, 1972). Midway between Long Point and Pte. aux Pins, the alongshore currents change direction and flow southwestward to Point Pelee, indicating that upwelling may be occurring extensively along the north shore. South of Pte. aux Pins there appears to be a small nearshore counterclockwise gyre. At Point Pelee the alongshore currents converge and there is a hint of incipient counterclockwise circulation from the sediment patterns. The outflow from the Detroit River is transported southward into the west basin and eastward alongshore to Point Pelee. The outflow of the Maumee River is directly opposed by the northeasterly wind; the result is a complex convergence of the two river outflows in the west basin. North of Port Clinton, Ohio is a small counterclockwise eddy. A current flows northward between Kelleys Island and Bass Islands. East of Sandusky Bay, the alongshore currents flow eastward. No additional sufficiently cloud-free observations were available for the remainder of the Lake Erie circulation pattern under northeasterly resultant wind.

Easterly Winds - Figure 61c

The incomplete analysis in Figure 61c was derived from the only two cloud-free ERTS-1 passes (28 September 1972 and 26 March 1973) that coincided with easterly winds. A large clockwise circulation in the central basin is indicated by the sediment patterns southwest of Long Point; the alongshore currents initially flow eastward, then branch southward and southwestward in response to the wind. A similar extensive gyre was described by Gedney and Lick (1972). The extreme western part of the lake was the only other area adequately covered by ERTS-1 under these conditions. The outflow currents from the Detroit and Maumee Rivers are forced to remain nearshore by the easterly wind. The Detroit River outflow flows directly southward, while the Maumee discharge flows northward to converge with the Detroit River plume and thence southeastward alongshore to Port Clinton.

Southeasterly Winds - Figure 61d

Southeasterly winds prevailed during the ERTS-1 overpasses on 25 June 1973 and 4 September 1973; the resulting surface current analysis is relatively complete. As mentioned above the large clockwise gyre in the central basin appears to be a semipermanent feature; the alongshore currents flow eastward to Long Point, then turn lakeward (Gedney and Lick, 1972). Near Pte. aux Pins the alongshore currents flow eastward then southward the center of the lake, suggesting upwelling at Pte. aux Pins. At Point Pelee the alongshore currents converge and appear to radiate eastward toward the currents from Pte. aux Pins, southward to the current leaving the west basin, and westward to form a clockwise gyre west of Point Pelee. The outflow from the Detroit River meanders southeastward through the west basin and exits at mid-lake. The Maumee River plume forms a clockwise

gyre northeast of Toledo, but flows mainly eastward to Port Clinton. The Huron River discharge flows northward and eastward, then northwestward to meet the currents coming south from Point Pelee, and then exits from the west basin. Alongshore currents flow in a wide diffuse band, generally eastward along the south shore from Lorain to Buffalo, as Harrington (1895) indicated. There is a northeastward component to this flow due to the prevailing winds; river discharges extend lakeward farther than usual along the south shore.

Southerly Winds - Figure 61e

A full analysis was made of the surface currents for the western half of Lake Erie based on the ERTS-1 overpasses of 8 March 1973, 7 June 1973, and 3 December 1973, under southerly wind regimes. The western basin is marked by a general outflow to the east. The Maumee River outflow initially flows northward, then eastward in a vaguely clockwise circulation. The southerly winds produce a distinct outflow from Sandusky Bay. There is a series of small counterclockwise eddies south of Point Pelee as the eastward and southward alongshore currents leave the restricting influence of lake boundary. Alongshore currents converge at Pte. aux Pins and turn eastward and southward, suggesting that upwelling may be occurring at Pte. aux Pins. There appears to be an elongate counterclockwise gyre along the south shore from Lorain to Ashtabula. Gedney and Lick (1972) substantiate this feature. Within this area, local currents flow directly offshore at Cleveland, indicating that upwelling may be occurring there.

Southwesterly Winds - Figure 61f

Southwesterly winds prevailed during the ERTS-1 overpass on 24 June 1973. In the west basin, the alongshore current flows eastward to Point Pelee, then southward and westward back into the basin north of Pelee Island. The

winds again force water out of Sandusky Bay alongshore to Lorain. At Cleveland and Ashtabula there appear to be two distinct counterclockwise gyres. These may be part of a larger elongate near-shore circulation as discussed above under Southerly Winds. Alongshore currents converge at Pte. aux Pins, forming a vaguely-defined clockwise circulation south of that promontory. A branch of the current that flows through the west basin from Point Pelee flows eastward as part of the general flow-through current in the Lake Erie basin.

Westerly Winds - Figure 61g

Only one ERTS-1 pass (18 May 1973) was clear enough for a preliminary analysis of the surface currents under prevailing westerly winds. The only feature of note is a general easterly flow over the entire lake surface in the central basin. North of Ashtabula there is a northeasterly component of transport that may indicate some upwelling alongshore between Ashtabula and Erie. The alongshore current west of Long Point appears very narrow as defined by the sediment distribution patterns.

Northwesterly Winds - Figure 61h

Northwesterly resultant winds prevailed during the ERTS-1 passes for 9 September 1972, 13 April 1973, and 30 April 1973; the surface current analysis for the west and central basins is given in Figure 61h. The combined outflow from the Detroit and Maumee Rivers flows southeastward through the west basin. There is a general clockwise circulation around the Bass Islands and west of Sandusky Bay. Alongshore currents converge at Point Pelee, and small counterclockwise eddies are generated; under other wind regimes these eddies were directly south of Point Pelee, but here they have been displaced eastward by the westerly component of the wind. The eastward-flowing alongshore currents that turn lakeward at

Pte. aux Pins may be part of a clockwise gyre there; the sediment patterns are not conclusive in this region. There is a distinct nearshore counterclockwise gyre at Cleveland. This may be the western edge of the above-mentioned larger counterclockwise circulation that lies near the south shore from Cleveland to Erie (Gedney and Lick, 1972). A number of currents flow directly northward along the south shore, suggesting that extensive upwelling was occurring there during the satellite overpasses. Surface currents in mid-lake flow generally eastward. No coverage was available for the eastern basin under this wind condition.

Summary

Eastward flow of surface water from the shallow western basin of Lake Erie into the middle basin is most obvious during northwesterly and northerly (and probably westerly) wind stresses. The reverse wind directions, especially east and southeasterly, appear to hold the effluents from the Detroit and Maumee Rivers in the western basin as would be expected.

East of Sandusky, Ohio, along the southern (U.S.) shoreline the favored current is eastward. Under southeasterly, southerly, and southwesterly winds, alongshore eddies and return circulations are occasionally noted. Perhaps the most complex condition along the southern shore was noted under northwesterly wind stress; then much of the observed surface current was directed offshore.

Currents show a tendency to form gyres off the three points along the Canadian shore--Point Pelee being a producer of the most dramatic lake boundary effects. A clockwise gyre between Long Point and Pte. aux Pins is well developed under easterly and southeasterly wind stresses. West-to-east flow in the middle basin is best developed during southwesterly and westerly

Figure 61a-h. Surface current analyses for Lake Erie as determined from turbidity patterns in ERTS-1 scenes. Weighted wind directions from Table A5 are indicated in upper right-hand corners.

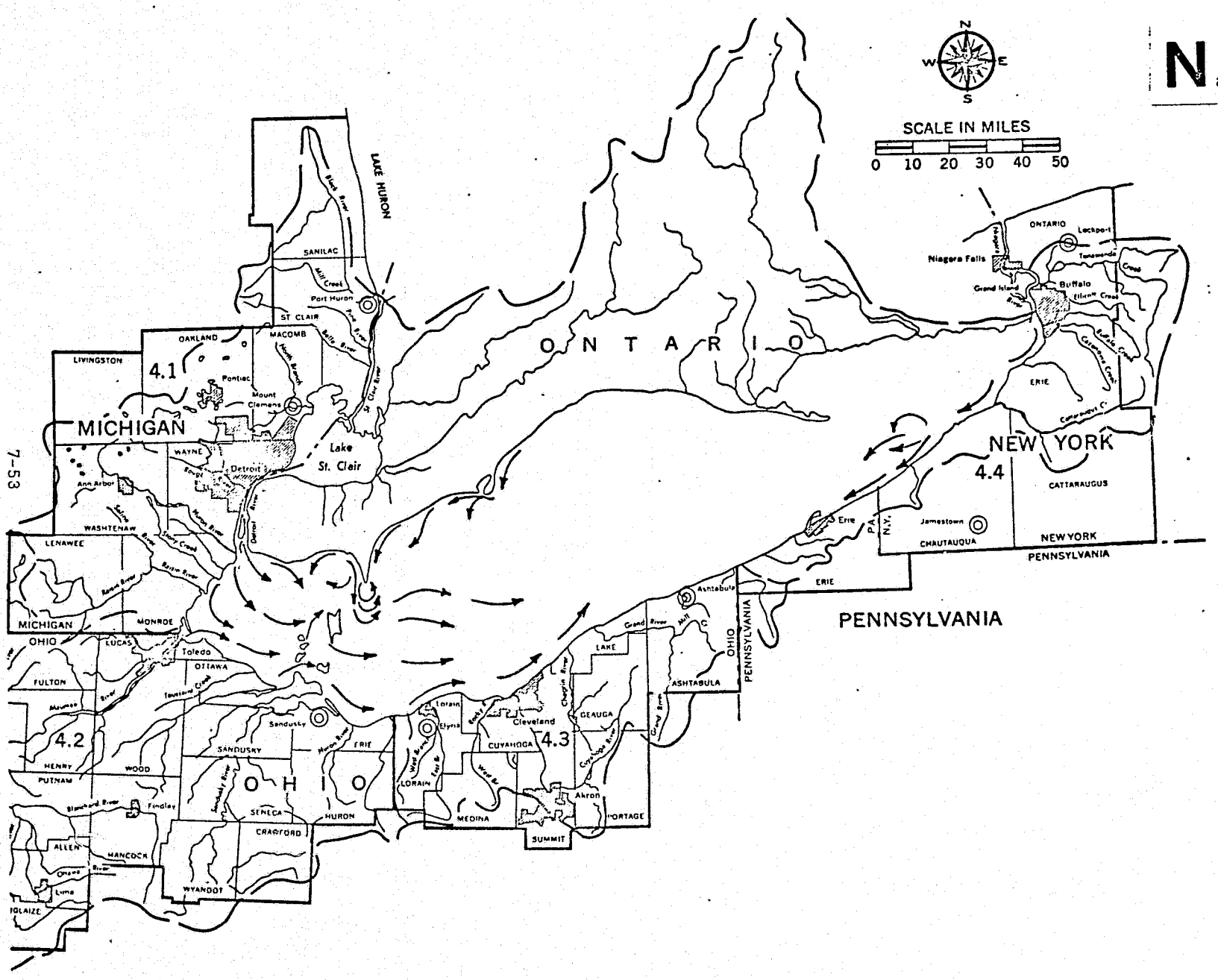
N
W
E
S
SCALE IN MILES
0 10 20 30 40 50
LAKE HURON
SANILAC
Port Huron
ST CLAIR
OAKLAND
MACOMB
LIVINGSTON
4.1
Pontiac
Mount Clemens
MICHIGAN
WAYNE
Detroit
Lake St. Clair
Ann Arbor
WASHTENAW
LENAWEE
MONROE
MICHIGAN
OHIO
LUCAS
Toledo
OTTAWA
FULTON
4.2
HENRY
WOOD
PUTNAM
Findlay
ALLEN
HANCOCK
Lima
WYANDOT
SANDUSKY
Sandusky
ERIE
SENECA
HURON
CRAWFORD
O H I O
O N T A R I O
Lorain
Elyria
LORAIN
MEDINA
Cleveland
CUYAHOGA
4.3
SUMMIT
Akron
PORTAGE
LAKE
GEAUGA
ASHTABULA
Ashtabula
OHIO
PENNSYLVANIA
ERIE
PENNSYLVANIA
Erie
PA
N.Y.
Jamestown
CHAUTAUQUA
NEW YORK
PENNSYLVANIA
NEW YORK
4.4
CATTARAUGUS
ERIE
Buffalo
Grand Island
Niagara Falls
ONTARIO
Lockport

Na

ORIGINAL PAGE IS
OF POOR QUALITY

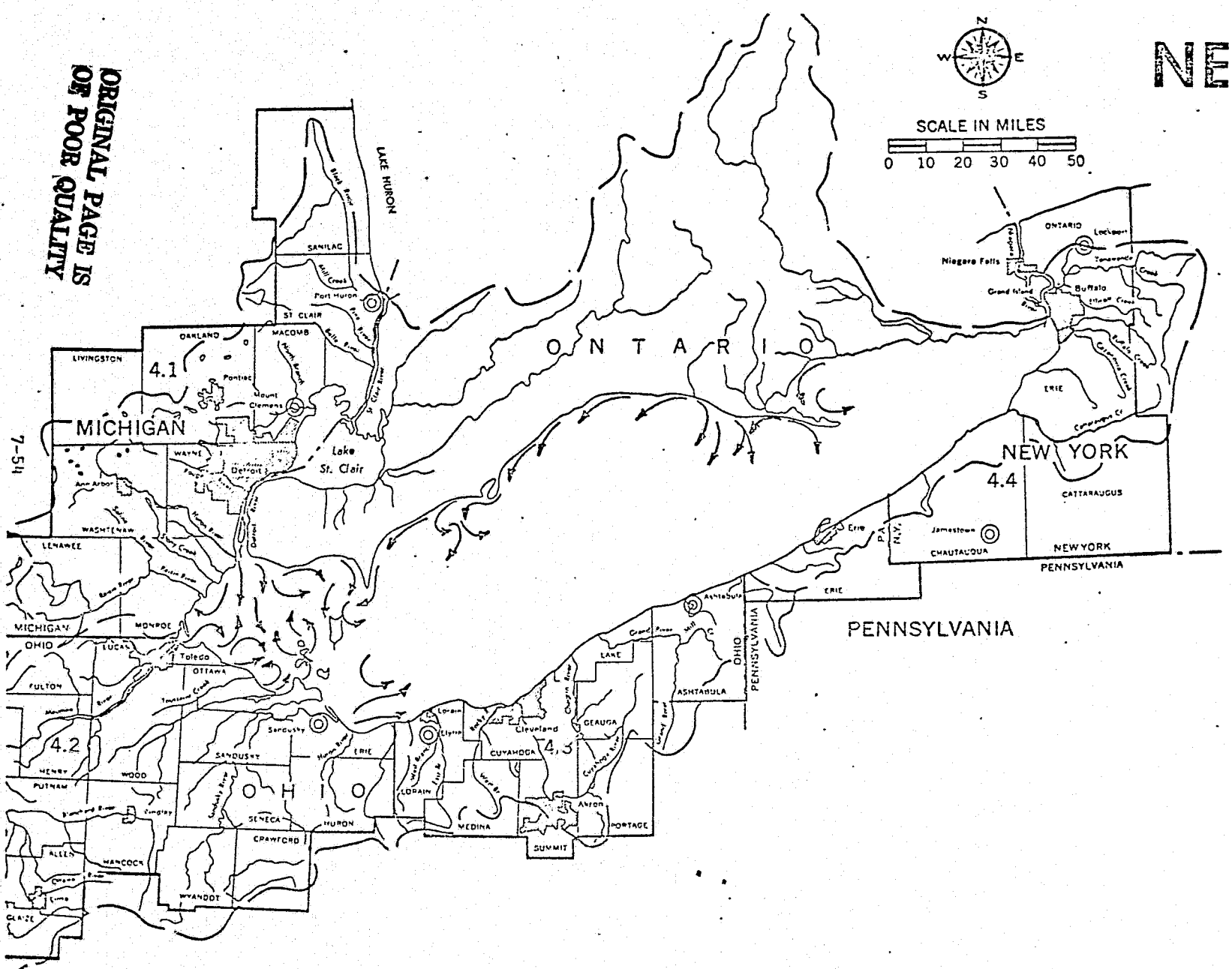

ORIGINAL PAGE IS
OF POOR QUALITY

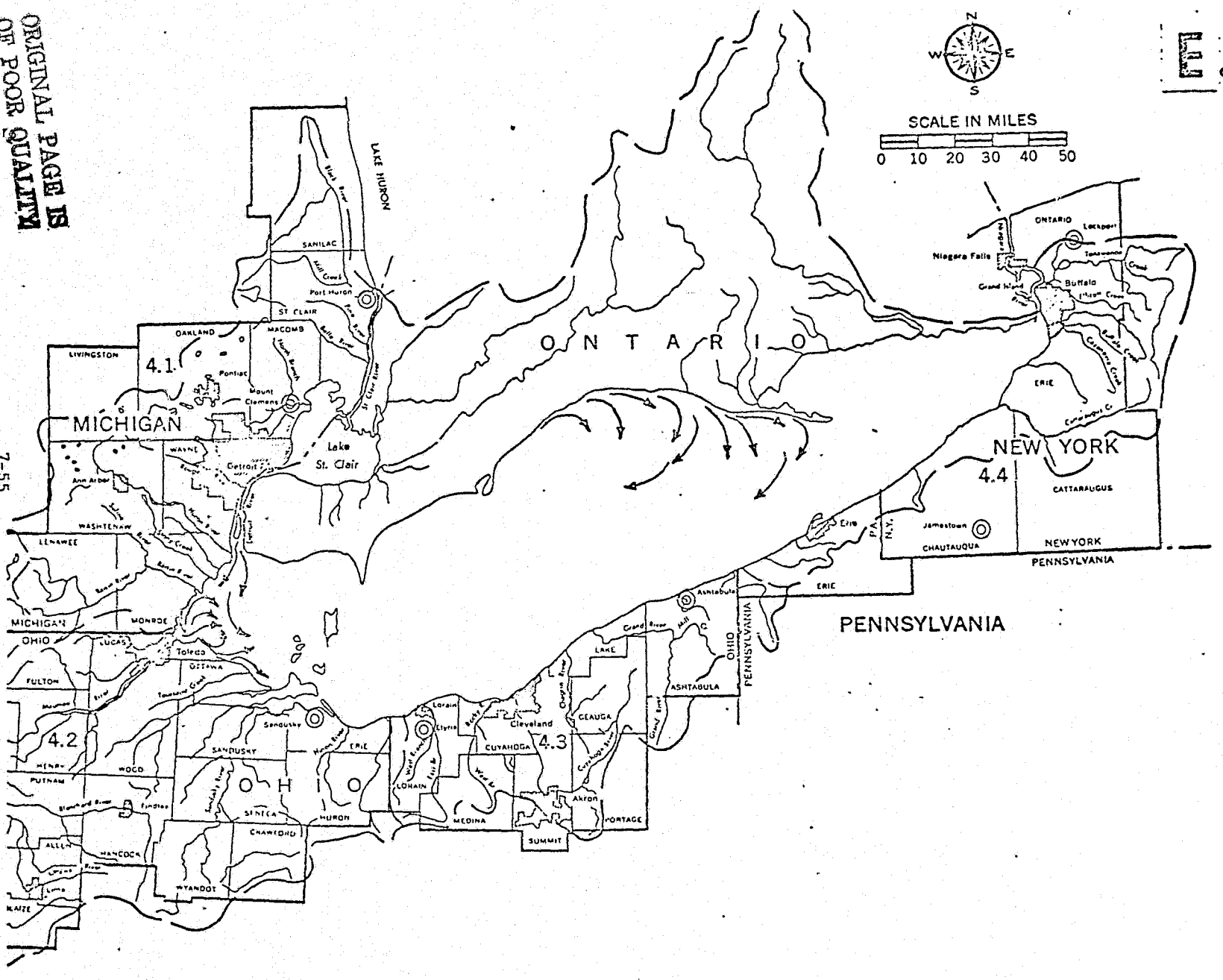

ORIGINAL PAGE IS
OF POOR QUALITY

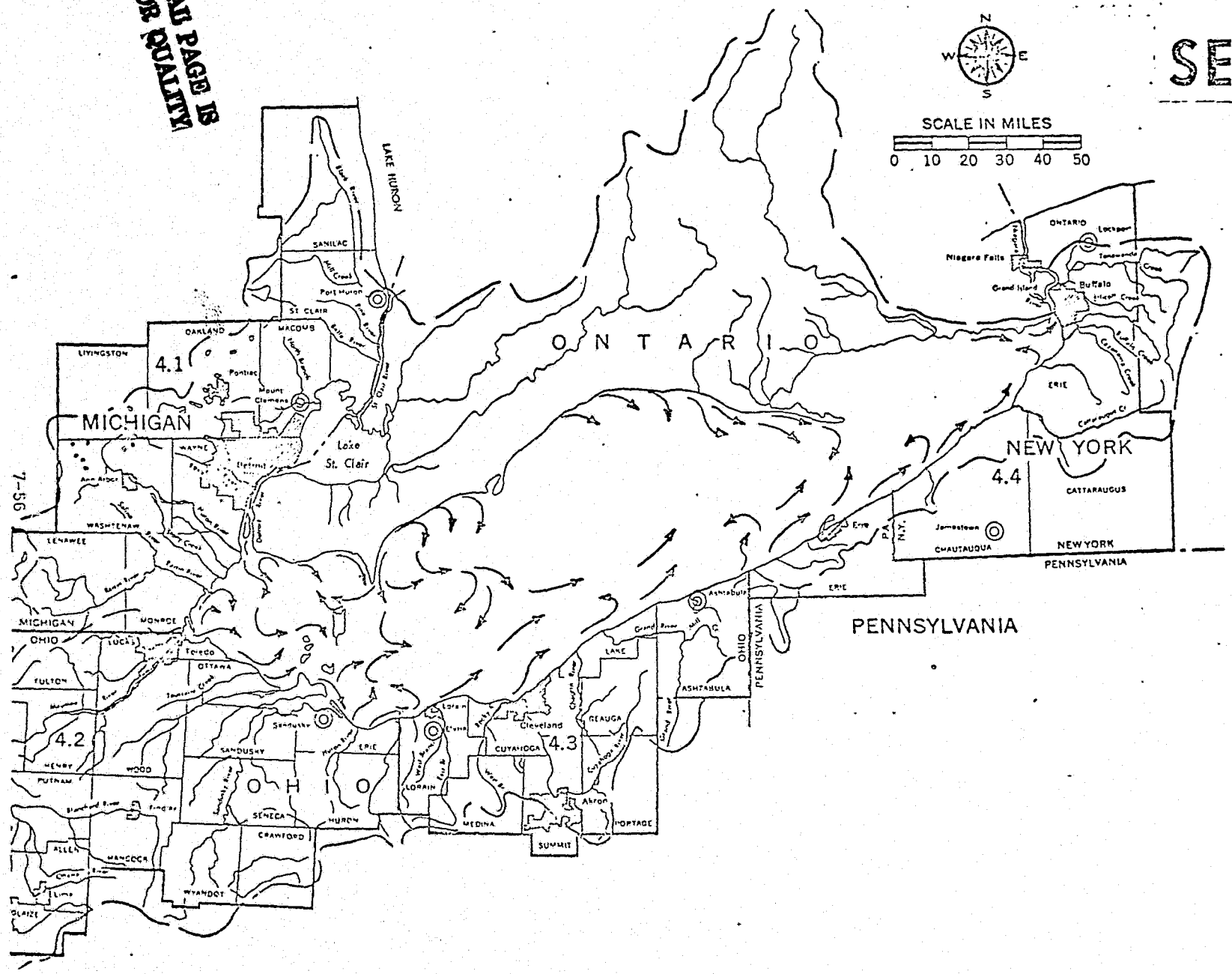

ORIGINAL PAGE IS
OF POOR QUALITY

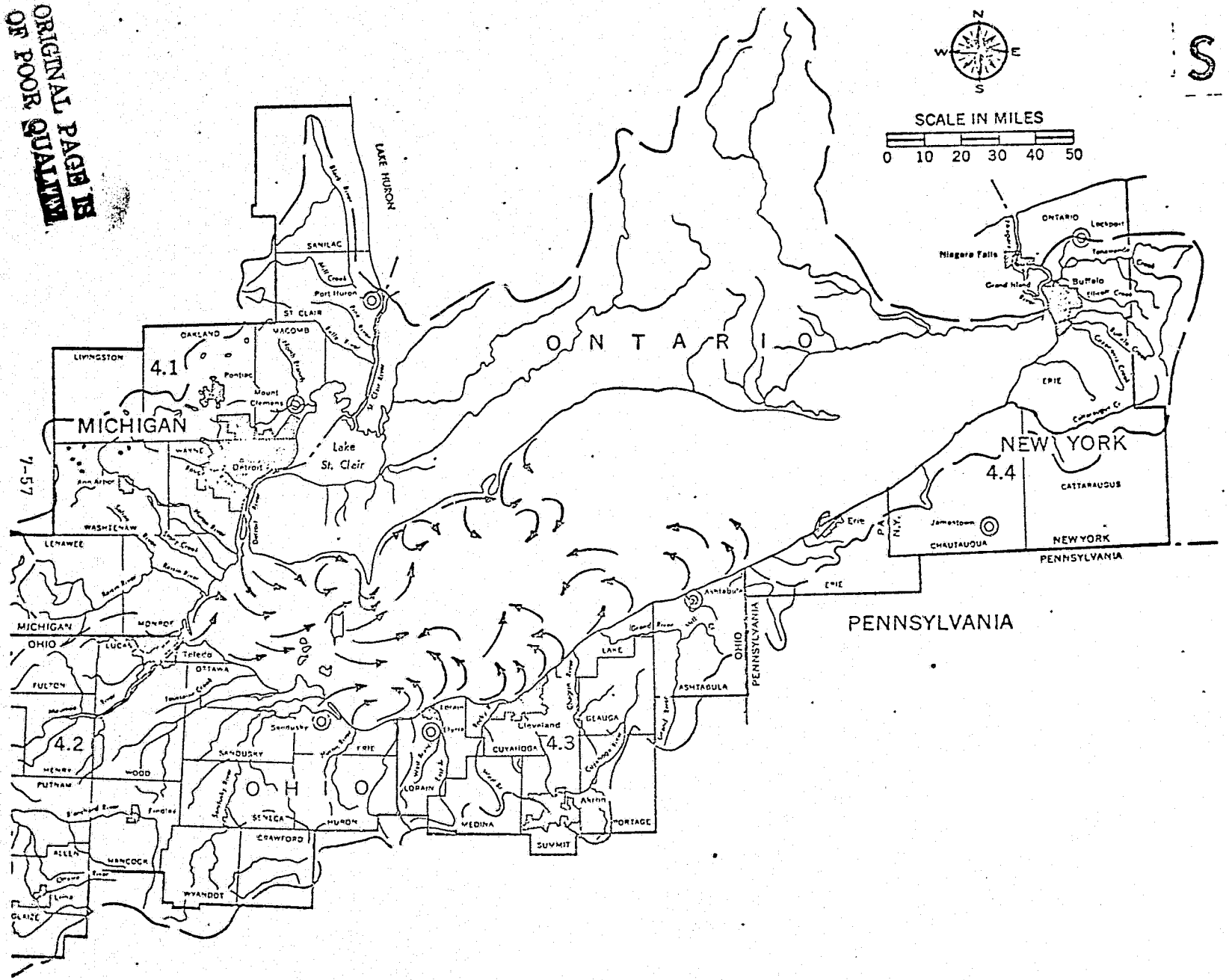

ORIGINAL PAGE IS
OF POOR QUALITY

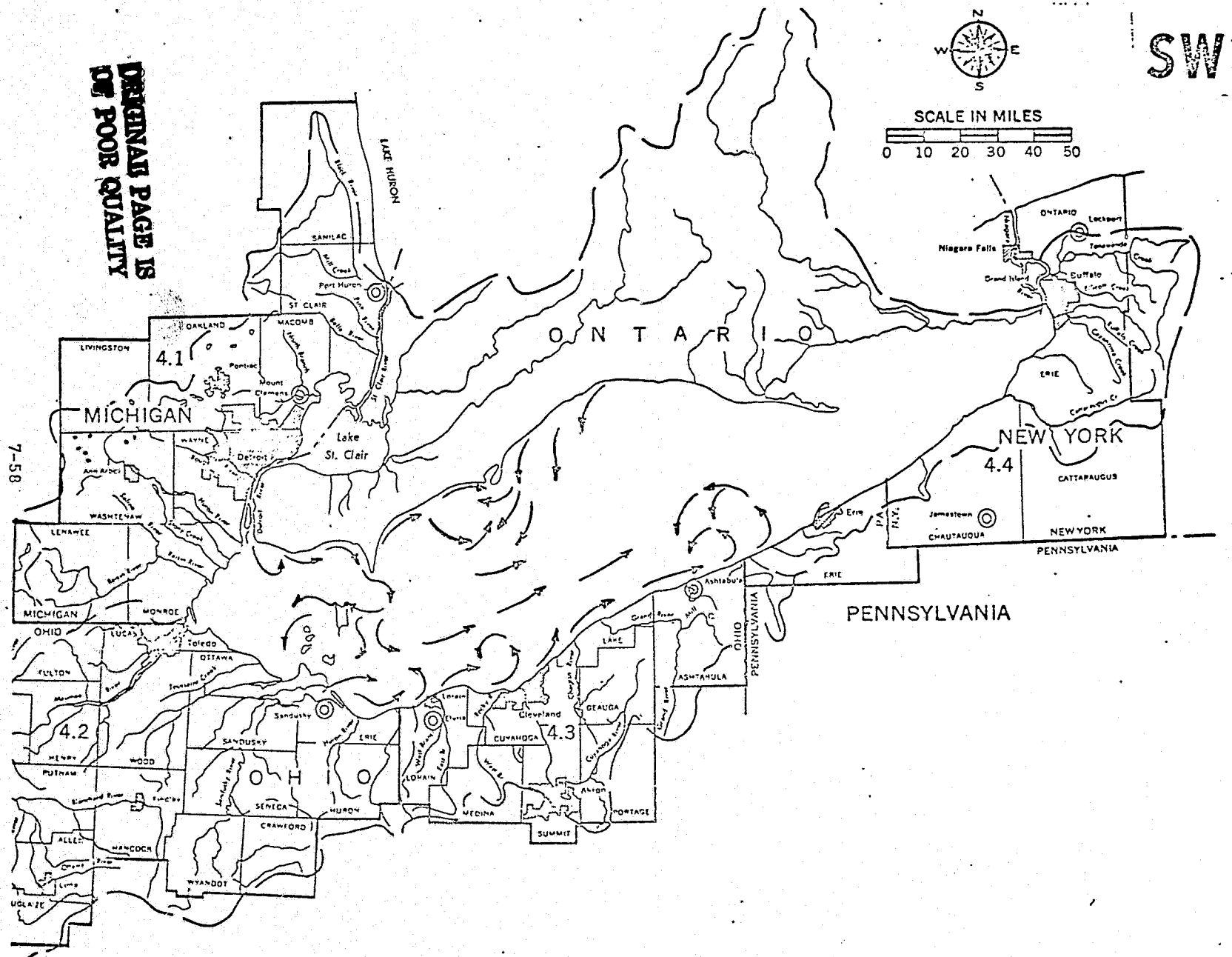

7-58

ORIGINAL PAGE IS
OF POOR QUALITY

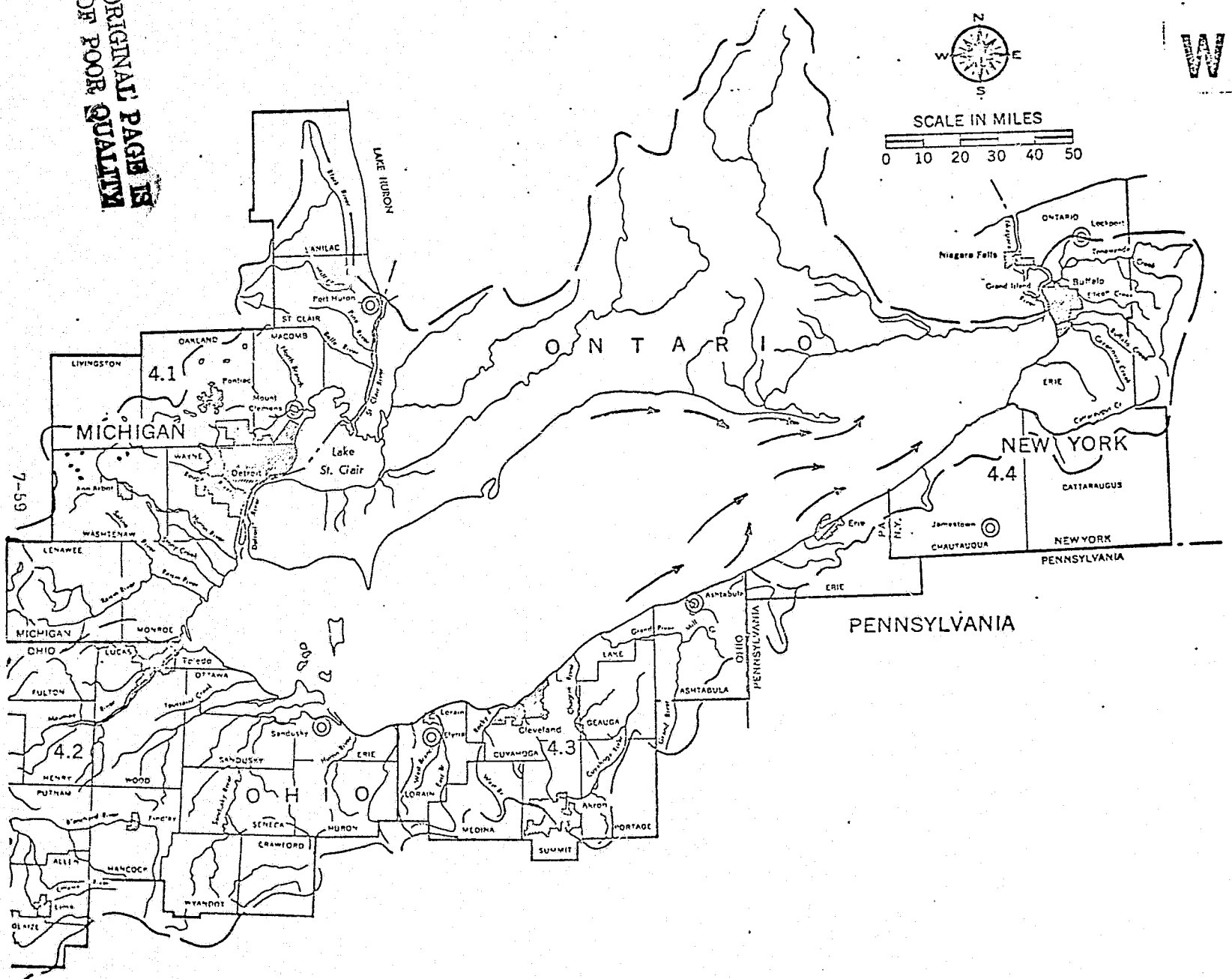

ORIGINAL PAGE IS
OF POOR QUALITY

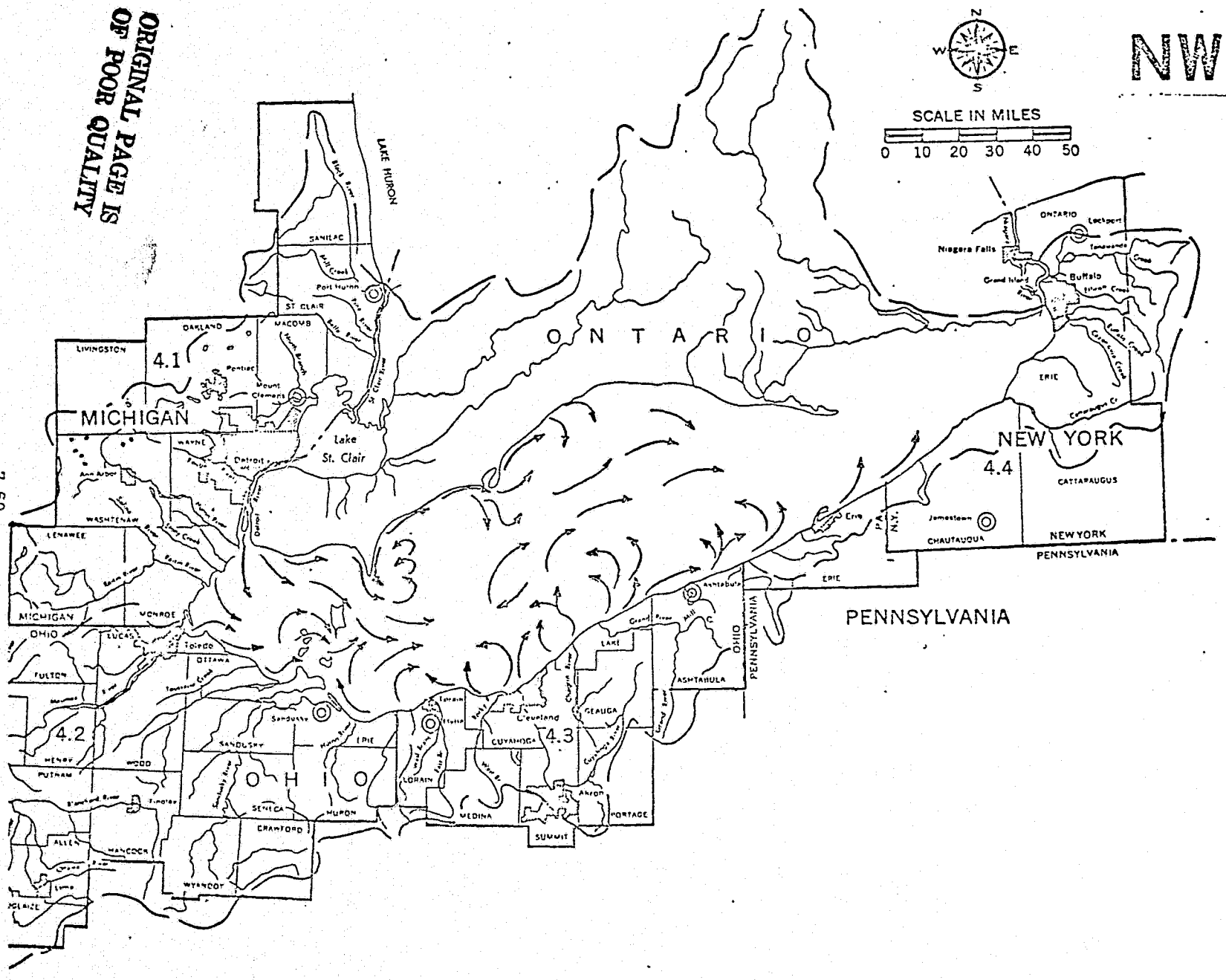

stresses. Between Erie, Pennsylvania and Ashtabula, Ohio, a brief reverse circulation is occasionally observed.

The only westward currents observed in the eastern basin of Lake Erie occurred under northerly wind stress. It is believed that a similar current should be observed under northeasterly and easterly resultant winds.

Lake Ontario

Figure 62 locates the three wind record sites utilized in the Lake Ontario current charts. Table 10 lists all ERTS-1 scenes utilized in producing the following surface current charts. These charts are composited from several ERTS-1 scenes as it takes three days to cover the entire lake. See the Appendix (Table A6) for a more complete listing of ERTS-1 imagery available during the study period.

Northerly Winds - Figure 63a

The ERTS-1 pass for 29 January 1973, although partially obscured by clouds, was used to derive the current diagram for northerly winds shown in Figure 63a. Upwelling apparently occurred extensively along the north shore as the currents were driven southwesterly in response to the prevailing winds. In the west end of the lake, a counterclockwise gyre began at Toronto, driven by the winds and modified by the lake boundary. This circulation was first described by Harrington (1895) and later substantiated by Simons and Jordon (1972). Its eastern extent is limited by the Niagara River plume which flows offshore and is divided by the wind into eastward- and westward-flowing branches. The sediment pattern is not fully developed, but a small nearshore clockwise eddy may be established by the eastward-flowing branch. The easternmost currents flowing offshore from the Canadian shore turn southward and southeastward at mid-lake suggesting that a large counterclockwise circulation has been established in the

Figure 62. Wind stations used for Lake Ontario (Fort Niagara, Rochester, Oswego).

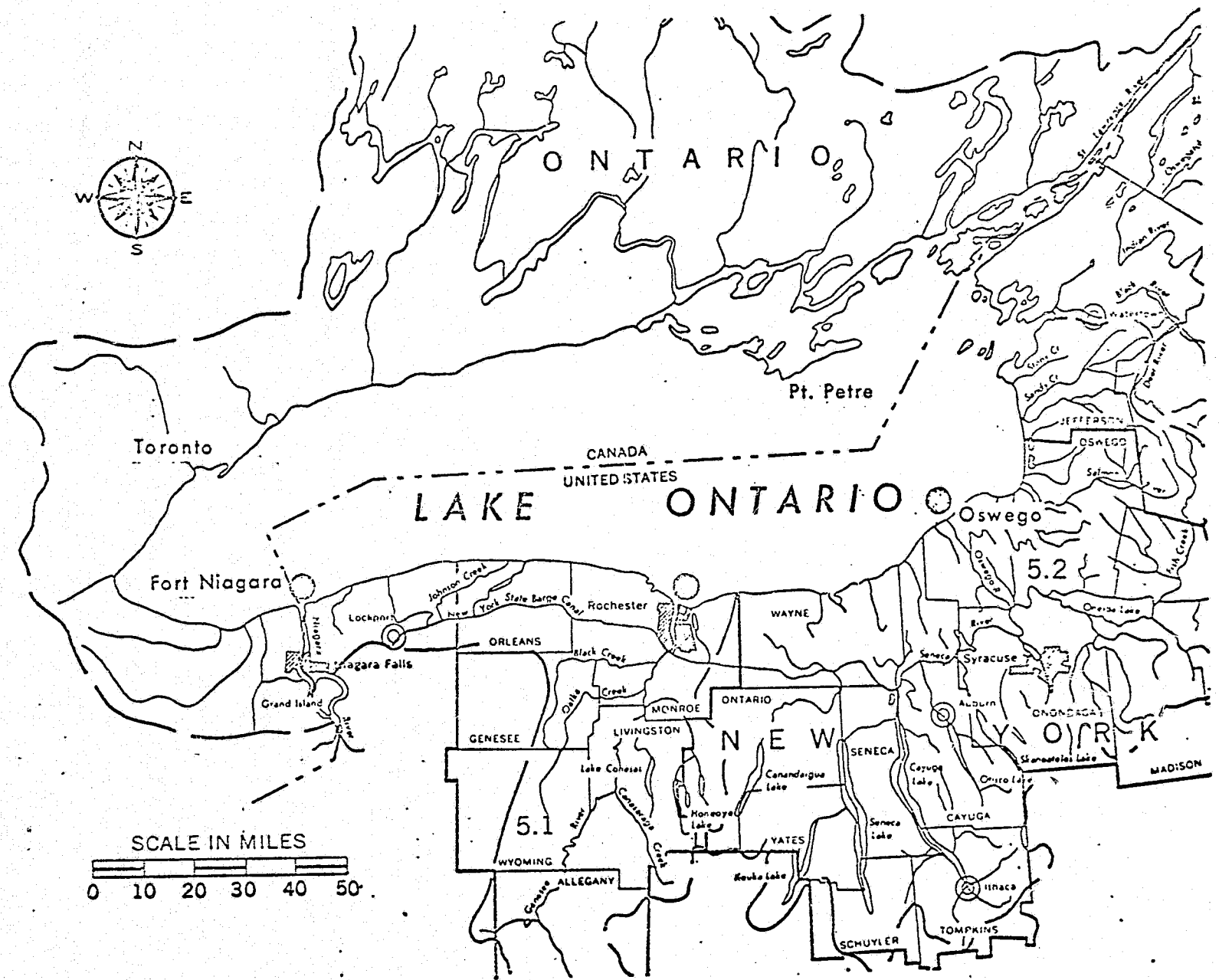

N
W
E
S
ONTARIO
Pt. Petre
Toronto
CANADA
UNITED STATES
LAKE ONTARIO
Oswego
Fort Niagara
Lockport
Niagara Falls
Grand Island
Rochester
ORLEANS
GENESEE
WYOMING
ALLEGANY
LIVINGSTON
MONROE
ONTARIO
WAYNE
YATES
SENECA
SCHUYLER
TOMPKINS
CAYUGA
Syracuse
Auburn
ONONDAGA
MADISON
JEFFERSON
OSWEGO
NEW YORK
5.1
5.2
Lake Conesus
Honeoye Lake
Canandaigua Lake
Keuka Lake
Seneca Lake
Cayuga Lake
Otisco Lake
Skaneateles Lake
Oneida Lake
Watertown
Indian River
Black River
Dear River
Sandy Cr
Salmon River
Fish Creek
Oswego R
Seneca River
Canaseraga Creek
Genesee River
Oatka Creek
Black Creek
Johnson Creek
New York State Barge Canal
Niagara River
SCALE IN MILES
0 10 20 30 40 50

7-62

TABLE 10

LAKE ONTARIO - ERTS-1 frames used for surface circulation charts

Resultant Wind Direction	Orbit #	Date	ID #	Sun Elevation
N	2648	29 Jan 73	1190-15300	23
				40
NE	3401	24 Mar 73	1244-15300	40
			1244-15303	41
E	----------NONE----------			
SE	----------NONE----------			
S	5674	3 Sep 73	1407-15343	47
	6399	25 Oct 73	1459-15214	31
SW	375	19 Aug 72	1027-15231	50
			1027-15233	51
	626	6 Sep 72	1045-15234	46
	5897	19 Sep 73	1423-15222	41
			1423-15224	42
W	4140	16 May 73	1297-15240	57*
			1297-15243	58*
	4670	23 Jun 73	1335-15353	60*
	4893	9 Jul 73	1351-15233	58*
			1351-15235	59*
	5172	29 Jul 73	1371-15350	56*
NW	389	20 Aug 72	1028-15290	51
	3666	12 Apr 73	1263-15361	48
	3903	29 Apr 73	1280-15302	54
	4377	2 Jun 73	1314-15183	60*
	4921	11 Jul 73	1353-15352	59*

* - Solar elevation $\geq 55°$ (see Chapter 5).

eastern basin, with the currents perhaps turning eastward at the south shore and finally northeastward out through the St. Lawrence River.

Northeasterly Winds - Figure 63b

The surface current analysis shown was derived from the ERTS-1 pass for 24 March 1973 for northeasterly winds. The currents along the Canadian shore have a more westerly component than the alongshore currents for northerly winds, as is to be expected. The counterclockwise eddy off Toronto evidently is much smaller than it was under northerly winds, extending only to mid-lake. The Niagara River plume is forced to the northwest by the winds, as are other visible remnant pulses of the discharge. Apparently at mid-lake there exists an eastward return flow which is fed by both the southwestward and northwestward-flowing currents from opposite shores. The alongshore currents flow eastward between the Niagara River mouth and Rochester, where they are interrupted by the outflow from the Rochester embayment and the Genesee River that perturbs the general eastward flow to the St. Lawrence River. The data in the eastern region are incomplete, but there may exist a large counterclockwise cell in the central and eastern basins as suggested by Simons and Jordon (1972) for winds with an easterly resultant component.

Easterly

No adequate imagery available for analysis.

Southeasterly

No observable sediment features were detected in imagery available under this resultant wind direction.

Southerly Winds - Figure 63c

The ERTS-1 overpasses for 3 September 1973 and 25 October 1973 were used to construct the surface current diagram for southerly winds. The entire western half of the Lake is occupied by a large clockwise gyre

centered at mid-lake north of the Niagara River mouth. In the center of the Lake the alongshore and mid-lake currents flow eastward; northwest of Rochester there appears to be a small nearshore counterclockwise eddy driven by the Genesee River discharge. Northeast of Rochester there is a large counterclockwise gyre that is driven by the prevailing winds (transport to right of wind) and which may be confined to the southern half of the lake; the outflow current flows eastward north of this gyre. This general circulation, a clockwise gyre in the west and a counterclockwise gyre in the east, corresponds to the transport pattern presented by Simons (1971 and 1972).

Southwesterly Winds - Figure 63d

The surface current analysis shown was based on the sediment distribution pattern on ERTS-1 images obtained 19 August 1972, 6 September 1972, and 19 September 1973 during prevailing southwesterly wind regimes. As discussed above for southerly winds and by Simons (1972), there exists a counterclockwise gyre in the southeast part of the lake. The central area is occupied by general eastward-flowing currents from the Canadian shore to the U.S. shore. Under southerly wind conditions, a small eddy was observed alongshore northwest of Rochester; under southwesterly winds, these currents at that point flow clearly offshore, inducing a small area of upwelling alongshore. There may also be a small counterclockwise eddy along the Ontario shore at Point Petre, in an area where the eastward-flowing current approaches the St. Lawrence River exit. No imagery was available for the western portion of the lake under this wind condition. The general circulation cell in the eastern basin as shown in Figure 63d is unsupported by the findings of Simons and Jordon (1972). They described a clockwise gyre under generally westerly wind regimes as a result of their

numerical model.

Westerly Winds - Figure 63e

The unusually complete analysis shown here was based on the four ERTS-1 overpasses for 16 May 1973, 23 June 1973, 9 and 29 July 1973. As discussed above under northerly winds, there is a large counterclockwise gyre located in the west end of the lake beginning at Toronto on the north shore, the eastward extent of the gyre is indeterminate. All alongshore currents flow generally eastward, as do the currents at mid-lake. Beginning east of Toronto there is a cross-lake current that flows southeastward to join the outflow current at mid-lake. Alongshore northwest of Rochester there may be a small counterclockwise eddy identical to that found for southerly winds. Northeast of Rochester is the large semipermanent counterclockwise gyre similar to that existing for other wind regimes; in this case it appears to occupy the entire surface of the lake east of Rochester. Confined to the far northeast portion at the head of the St. Lawrence River is another, smaller, counterclockwise feature. The general circulations in the western and eastern basins shown in Figure 63e are in direct conflict with the computed surface current analyses indicated by Simons and Jordon (1972); however their computation was based on a one-day wind stress.

Northwesterly Winds - Figure 63f

Five clear ERTS-1 overpasses (20 August 1972, 12 April 1973, 29 April 1973, 2 June 1973, 11 July 1973) were used to develop the surface current diagram for northwesterly winds. There is a broadly-defined counterclockwise circulation in the western half of the lake. The Niagara River plume is split by the wind into a radial pattern and may represent the eastern limit of the gyre. Along the south shore a sharply-defined nearshore current is periodically interrupted by equally-strong offshore currents,

suggesting that perhaps there exists a series of small cells between the Niagara River and Rochester; upwelling is certainly occurring where the currents flow offshore. In the center of the lake, currents flow southeastward from the Canadian shore to merge with the currents flowing eastward alongshore from Rochester. A counterclockwise gyre exists again in the eastern end, but it is smaller and displaced northward from its location under southerly to westerly wind regimes (Simons, 1972). An extensive analysis for northwesterly winds is presented by Simons and Jordon (1972); they described a counterclockwise eddy in the western basin and a large well-defined clockwise circulation over the entire central portion of the lake. The data used to construct Figure 63f are inconclusive over the central lake, but it is likely that the large clockwise gyre has been established, judging from the directions of the currents along the north and south shores. The counterclockwise gyre in the east basin shown in Figure 63f corresponds to the circulation described by Simons and Jordon (1972) as a strong counterclockwise gyre located in the southeast portion.

Summary

Across-lake winds from the north and south induce eddy-like circulation in surface waters of Lake Ontario. Counterclockwise alongshore flow persists in the western basin under most wind conditions. This circulation reverses direction (clockwise) under southerly (and probably southeasterly and southwesterly) wind stress. Along the southern (New York) shoreline of Lake Ontario an eastward flow is typical, as is the case in Lake Erie. As was also observed in Lake Erie, the northwesterly wind stress produces considerable offshore flow along the southern shore. Under southerly and probably southeasterly wind stress conditions the effluent of the Niagara River is carried northward out into the center of the Lake. Northeast (and

probably easterly) wind stress also favors this condition. East of Rochester eastward flow was observed exclusively.

Along the Canadian shoreline east of Toronto, eastward currents prevail. Under northwesterly stresses, however, a divergent flow begins mid-way between Toronto and Point Petre. Complete reversal to a westward flow occurs for northerly and northeasterly wind stresses (also probable under easterly winds).

Westerly and southwesterly winds route the surface currents most straightforwardly through the lake from west to east whereas the opposite resultant winds introduce complexities to the circulation pattern.

Figure 63a-f. Surface current analyses for Lake Ontario as determined from turbidity patterns in ERTS-1 scenes. Weighted wind directions from Table A6 are indicated in upper right-hand corners.

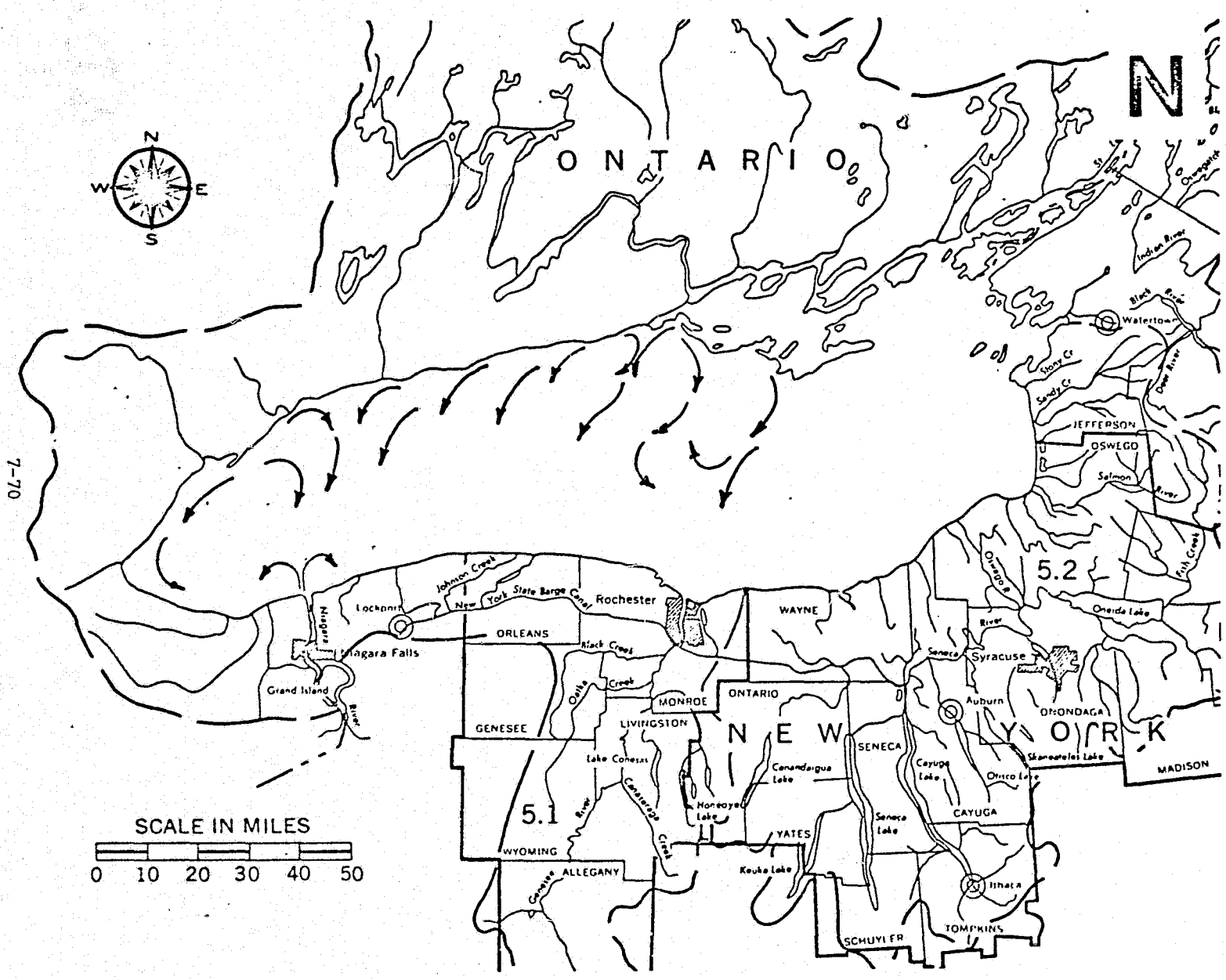
N
W
E
S
ONTARIO
N
a
Indian River
Black River
Watertown
Stony Cr
Sandy Cr
Deer River
JEFFERSON
OSWEGO
Salmon River
Oswego River
Fish Creek
5.2
Oneida Lake
Oneida River
Seneca River
Syracuse
Auburn
ONONDAGA
MADISON
Skaneateles Lake
Onondaga Lake
Cayuga Lake
SENECA
CAYUGA
Seneca Lake
Canandaigua Lake
Honeoye Lake
YATES
Keuka Lake
Ithaca
TOMPKINS
SCHUYLER
WAYNE
ONTARIO
MONROE
LIVINGSTON
GENESEE
Lake Conesus
Conesus Creek
Genesee River
5.1
WYOMING
ALLEGANY
ORLEANS
Black Creek
Oatka Creek
Rochester
New York State Barge Canal
Johnson Creek
Lockport
Niagara River
Niagara Falls
Grand Island
SCALE IN MILES
0 10 20 30 40 50

7-70

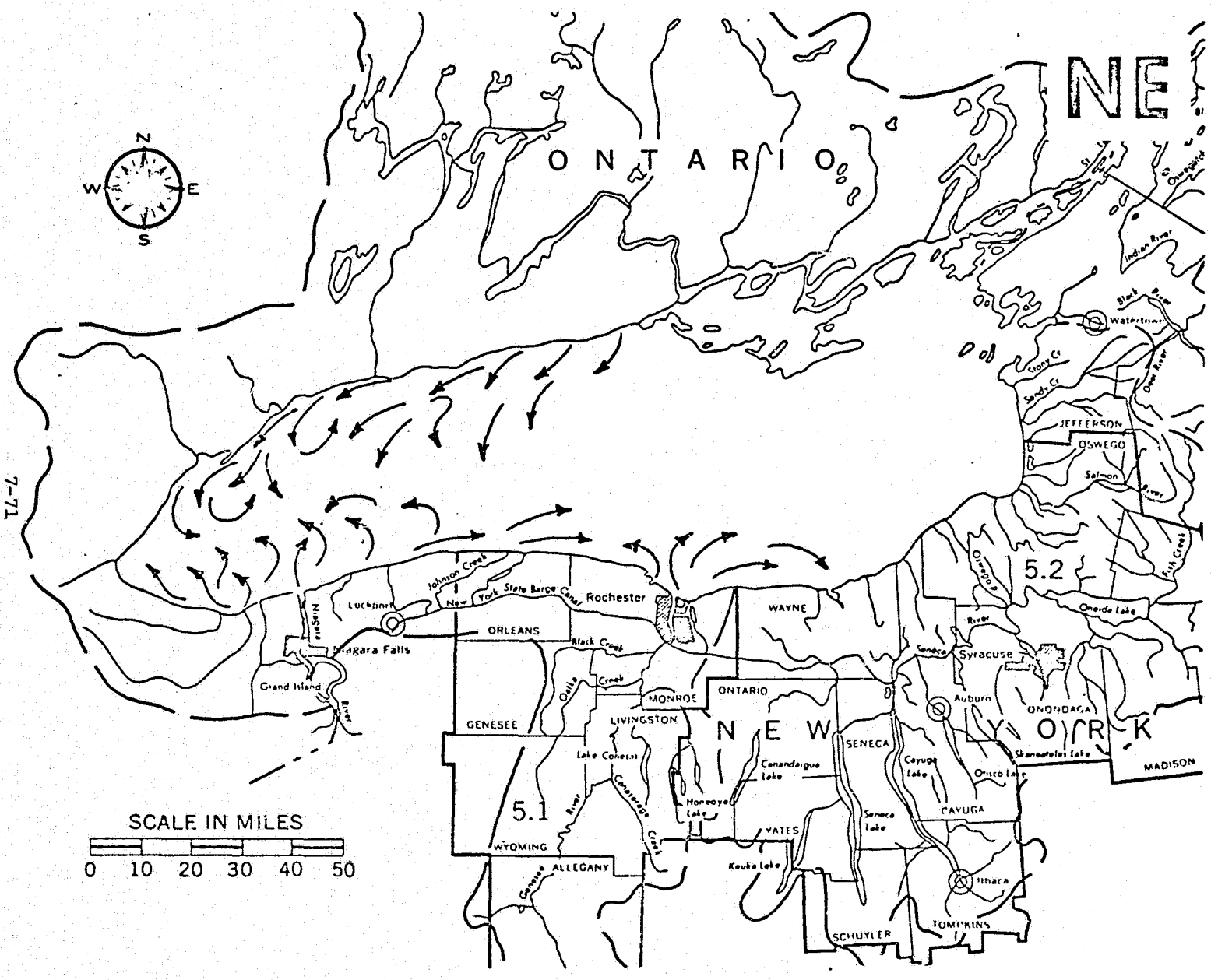

NE
b
ONTARIO
N
W
E
S
Indian River
Black River
Watertown
Stony Cr
Sandy Cr
Deer River
JEFFERSON
OSWEGO
Salmon River
Fish Creek
Oswego R
5.2
Oneida Lake
Johnson Creek
New York State Barge Canal
Rochester
Lockport
Niagara
Niagara Falls
ORLEANS
Black Creek
WAYNE
Seneca River
Syracuse
Grand Island
River
Oatka Creek
MONROE
ONTARIO
Auburn
ONONDAGA
GENESEE
LIVINGSTON
NEW YORK
SENECA
Skaneateles Lake
MADISON
Lake Conesus
Canandaigua Lake
Cayuga Lake
Otisco Lake
Honeoye Lake
Seneca Lake
CAYUGA
5.1
Canaseraga Creek
YATES
WYOMING
ALLEGANY
Keuka Lake
Ithaca
SCHUYLER
TOMPKINS
SCALE IN MILES
0 10 20 30 40 50

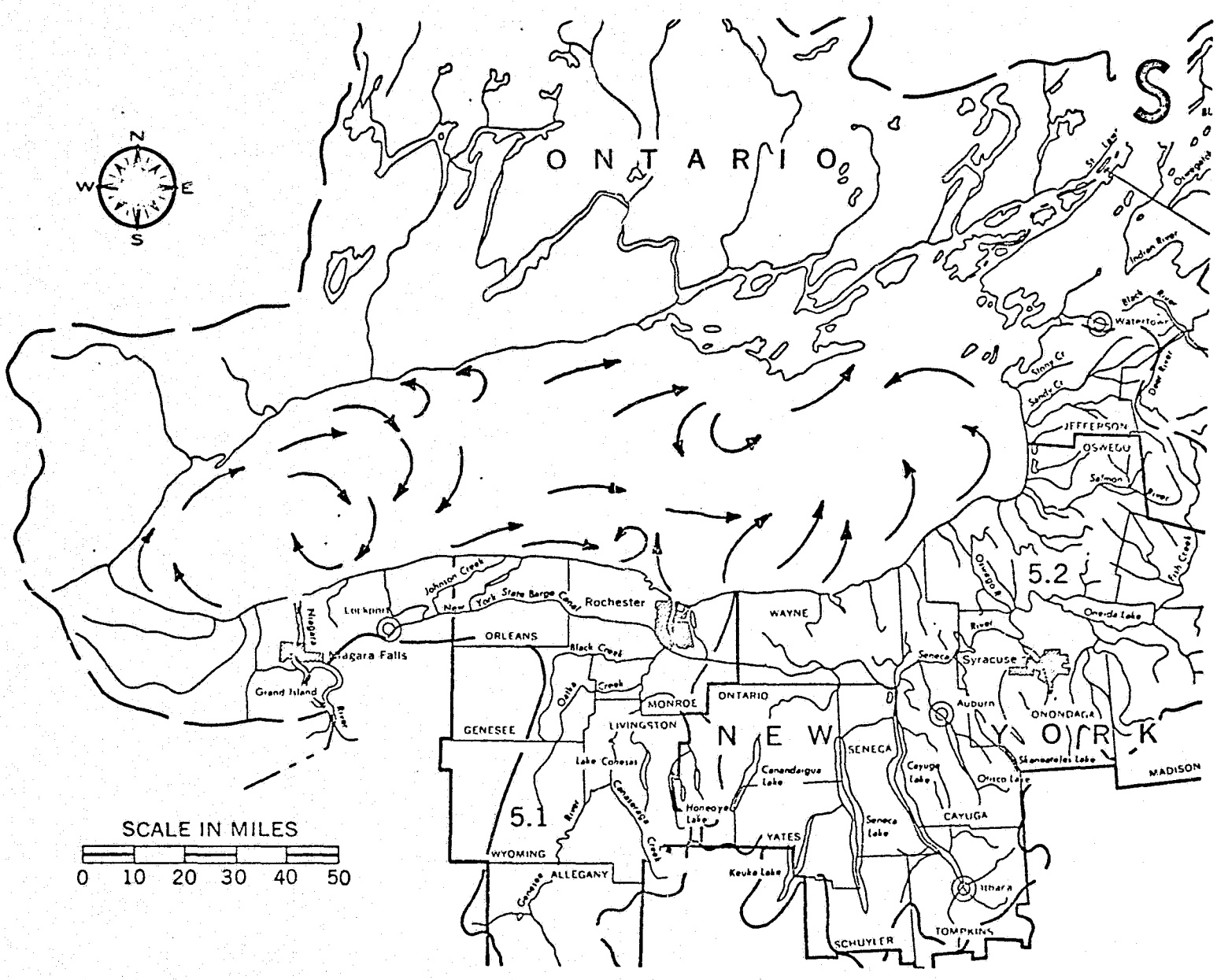

ONTARIO
NEW YORK
N
S
E
W
Rochester
Lockport
Niagara Falls
Grand Island
Niagara River
Johnson Creek
New York State Barge Canal
ORLEANS
Black Creek
Oatka Creek
MONROE
ONTARIO
WAYNE
GENESEE
LIVINGSTON
Lake Conesus
Canaseraga Creek
Honeoye Lake
Canandaigua Lake
SENECA
Cayuga Lake
Seneca Lake
CAYUGA
YATES
Keuka Lake
WYOMING
ALLEGANY
Genesee River
SCHUYLER
TOMPKINS
Ithaca
Auburn
Syracuse
Seneca River
Oswego R.
Oneida Lake
Fish Creek
ONONDAGA
Skaneateles Lake
Otisco Lake
MADISON
JEFFERSON
OSWEGO
Salmon River
Deer River
Stony Cr
Sandy Cr
Watertown
Black River
Indian River
St. Lawr
Oswegatch
5.1
5.2
SCALE IN MILES
0 10 20 30 40 50

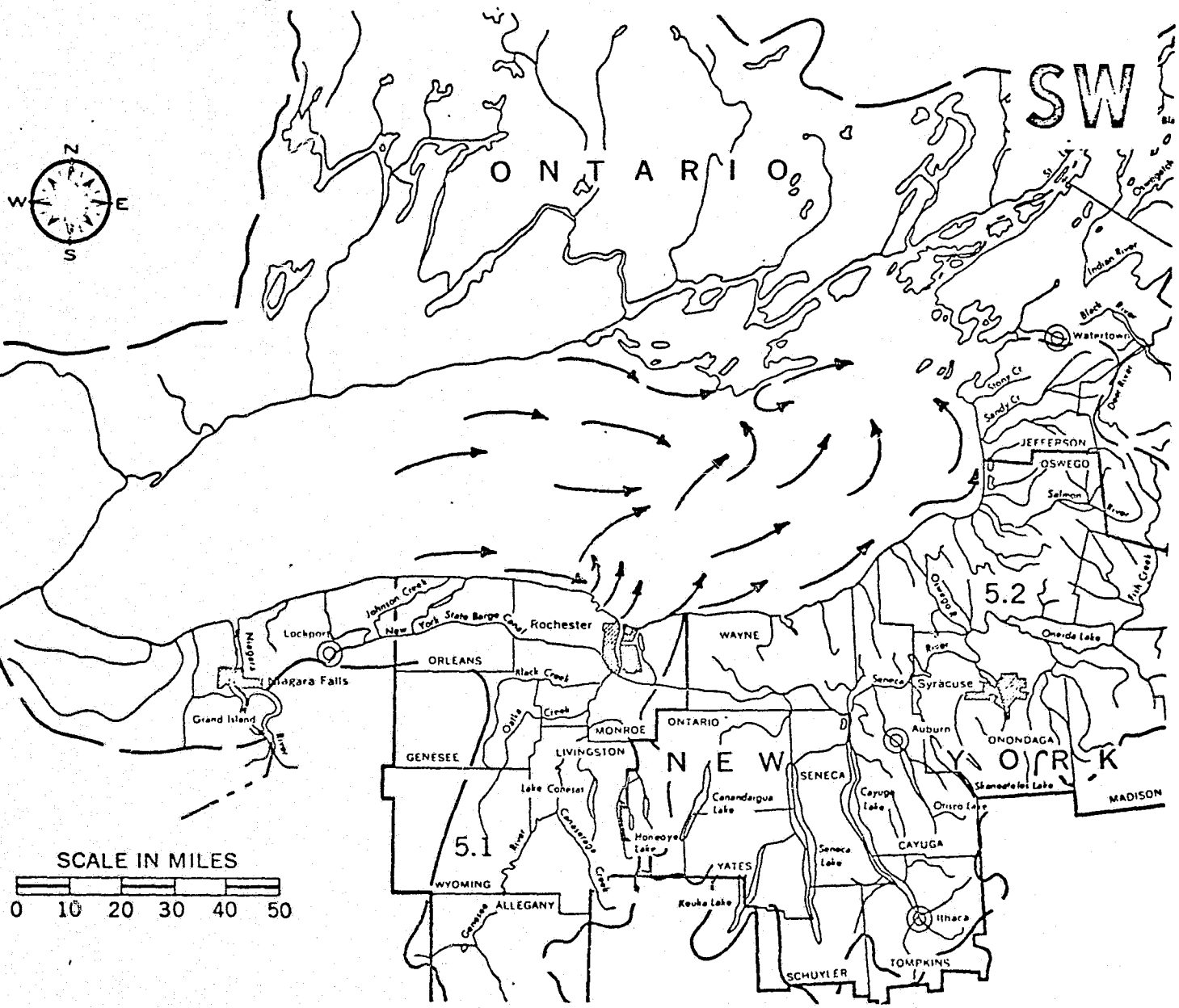

N
W
E
S
ONTARIO
SW
NEW YORK
Watertown
Indian River
Black River
Stony Cr
Sandy Cr
Deer River
JEFFERSON
OSWEGO
Salmon River
Fish Creek
Oswego R
5.2
Oneida Lake
Syracuse
Seneca River
Auburn
ONONDAGA
Skaneateles Lake
MADISON
Otisco Lake
Cayuga Lake
CAYUGA
Seneca Lake
Ithaca
TOMPKINS
SCHUYLER
Keuka Lake
YATES
Canandaigua Lake
Honeoye Lake
Canaseraga Creek
Lake Conesus
LIVINGSTON
MONROE
ONTARIO
WAYNE
SENECA
Oatka Creek
Black Creek
Rochester
Johnson Creek
New York State Barge Canal
ORLEANS
Lockport
Niagara Falls
Niagara River
Grand Island
GENESEE
5.1
WYOMING
ALLEGANY
Genesee River
SCALE IN MILES
0 10 20 30 40 50

d

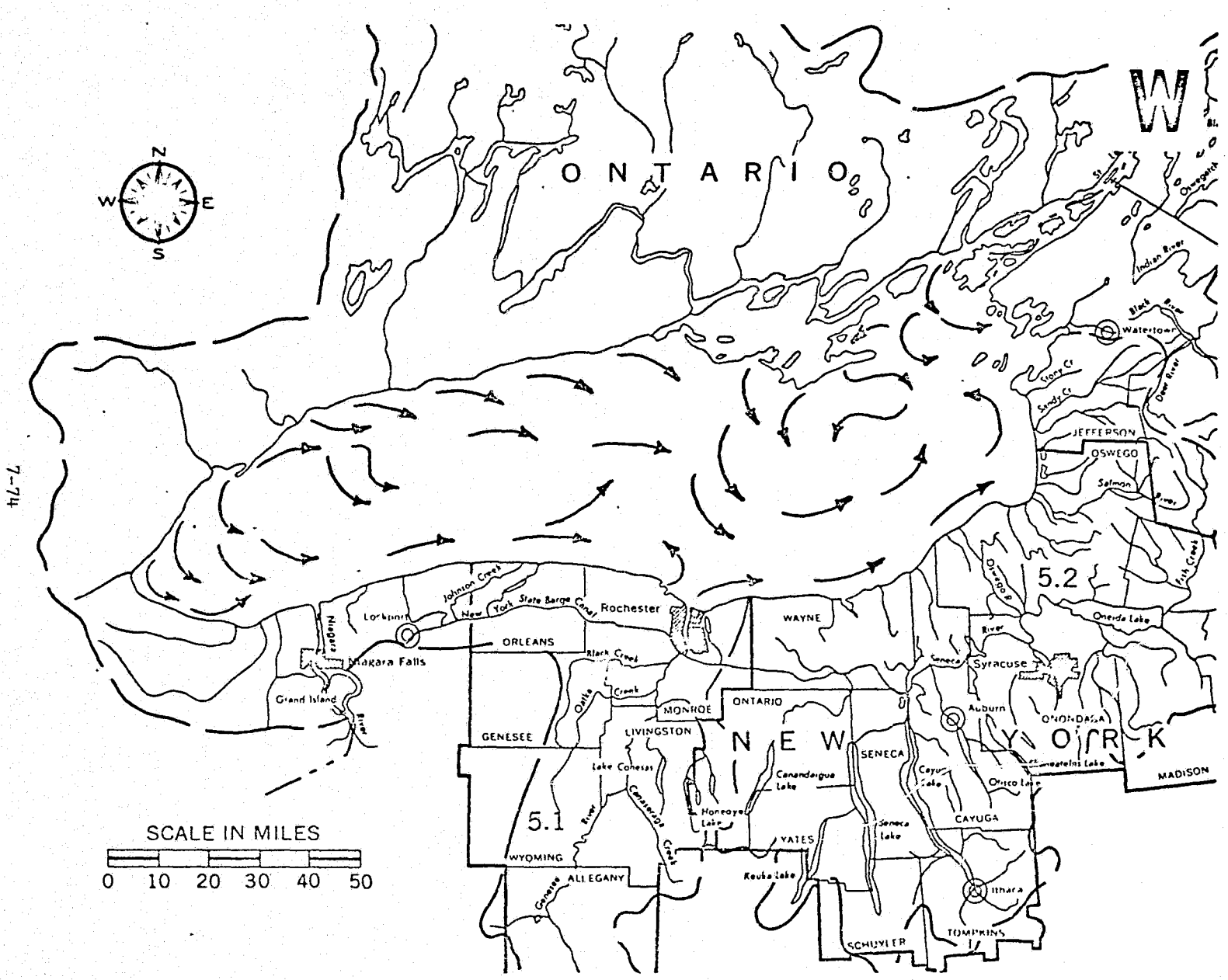
N
W
E
S
ONTARIO
W
e
Indian River
Black River
Watertown
Stony Cr
Sandy Cr
Deer River
JEFFERSON
OSWEGO
Salmon
Oneida R
Fish Creek
5.2
Oneida Lake
River
Seneca
Syracuse
Johnson Creek
New York State Barge Canal
Rochester
Lockport
Niagara
Niagara Falls
ORLEANS
Black Creek
WAYNE
Grand Island
River
Oatka Creek
MONROE
ONTARIO
Auburn
ONONDAGA
GENESEE
LIVINGSTON
N E W
Y O R K
SENECA
Lake Conesus
Canandaigua Lake
Cayuga Lake
Otisco Lake
Honeoye Lake
Seneca Lake
CAYUGA
MADISON
5.1
Genesee River
Conesus Creek
YATES
WYOMING
Keuka Lake
ALLEGANY
Genesee
Ithaca
TOMPKINS
SCHUYLER
SCALE IN MILES
0 10 20 30 40 50

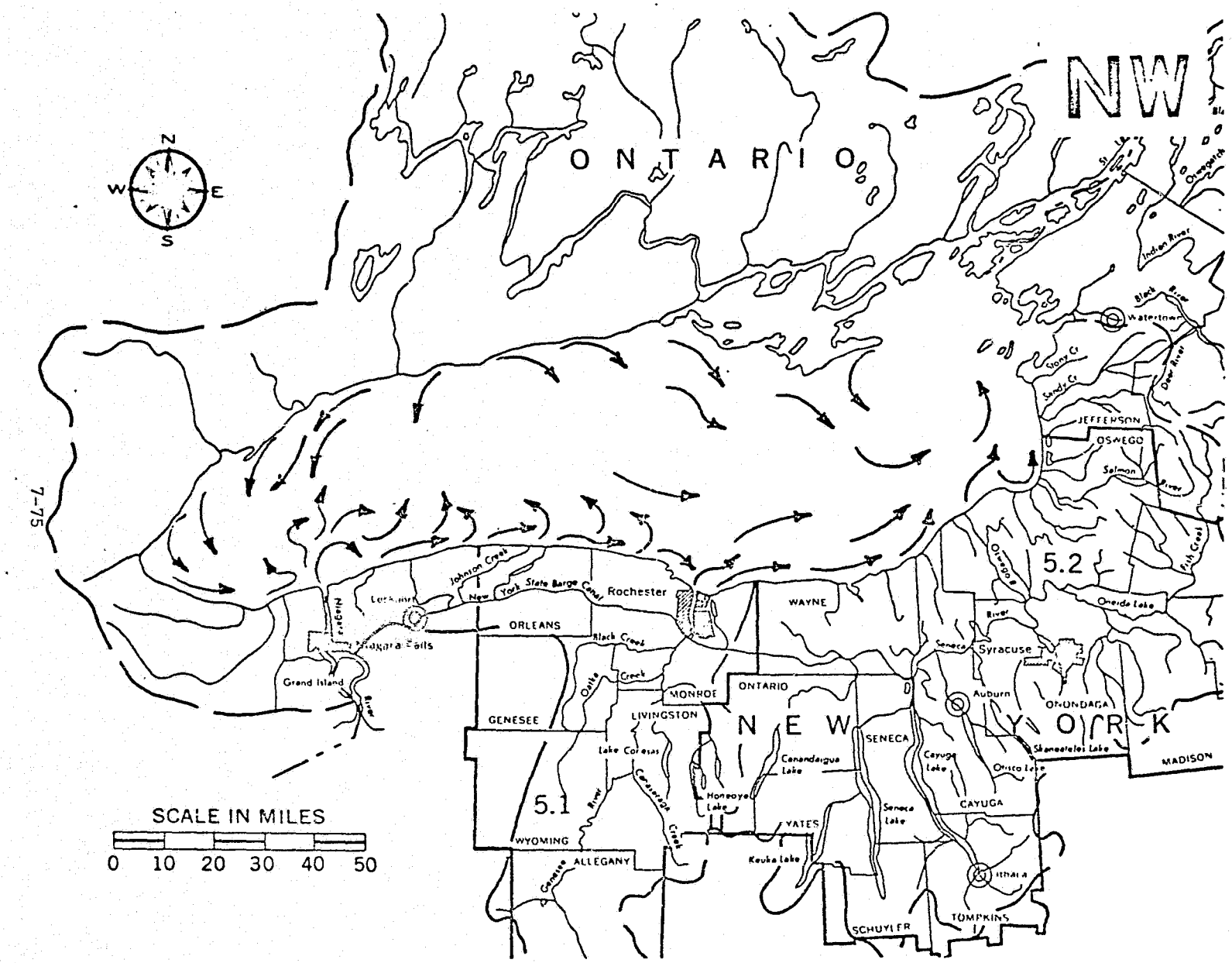
NW
ONTARIO
N
S
E
W
Watertown
Indian River
Black River
Stony Cr
Sandy Cr
Deer River
JEFFERSON
OSWEGO
Salmon River
Fish Creek
Oswego R
5.2
Oneida Lake
Johnson Creek
New York State Barge Canal
Rochester
WAYNE
ORLEANS
Black Creek
Niagara Falls
Grand Island
Oatka Creek
MONROE
ONTARIO
Seneca River
Syracuse
Auburn
ONONDAGA
GENESEE
LIVINGSTON
NEW YORK
SENECA
Skaneateles Lake
MADISON
Lake Conesus
Canandaigua Lake
Cayuga Lake
Otisco Lake
Honeoye Lake
Canaseraga Creek
5.1
Seneca Lake
CAYUGA
YATES
WYOMING
Keuka Lake
ALLEGANY
Genesee River
Ithaca
SCHUYLER
TOMPKINS
SCALE IN MILES
0 10 20 30 40 50

Chapter 1

REFERENCE

Strong, A.E. (1972). Detection of circulation features in the Great Lakes. In proc. ERTS-1 Symp., 29 September 1972, NASA/GSFC, Greenbelt, Md., pp. 133-134.

PRECEDING PAGE BLANK NOT FILMED

Chapter 2

REFERENCES

Bressette, W.E. and D.E. Lear (1973), The use of near-infrared photography for biodegradable pollution monitoring of tidal rivers, presented at Symposium on Remote Sensing in Oceanography, Orlando, Florida (American Society of Photogrammetry), October 2-5.

Bukata, R.P., Harris, G.P. and J.E. Bruton (1974). The Detection of Suspended Solids and Chlorophyll a Utilizing Digital Multispectral ERTS-1 Data. Preprint. Canada Centre for Inland Waters, Burlington, Ontario, 13 pp.

Casper, V.L. (1965), A phytoplankton bloom in western Lake Erie, in Proc. 8th Conf. on Great Lakes Res., Great Lakes Res. Div., Univ. of Mich., pp. 29-35.

Charnell and G.A. Maul (1973), Oceanic observations of New York Bight by ERTS-1, Nature 242, 451-452.

Maul, G.A. (1973), Applications of ERTS data to oceanography and the marine environment, in Proc. of May 1973 COSPAR Meeting, Konstanz, F.R.G. (in press).

National Aeronautics and Space Administration (1971), ERTS Data Users Handbook, GE Document #71SD4249, Goddard Space Flight Center.

National Aeronautics and Space Administration (1972), Earth Resources Technology Satellite-1, September 1972 Symp. Proceedings, Goddard Space Flight Center, Greenbelt, Maryland, 165 pp.

Noble, V.E., et al. (1967), Lake Michigan NAVOCEANO flight, Special Rept. #31, Great Lakes Res. Div., Univ. of Mich., 52 pp.

Strong, A.E., McClain, E.P., and D.F. McGinnis (1971), Detection of thawing snow and ice packs through combined use of visible and near-infrared measurements from earth satellites, Monthly Weather

Rev. 99 (11), 828-830.

Strong, A.E. (1974). Remote Sensing of Algal Blooms by Aircraft and Satellite in Lake Erie and Utah Lake, Remote Sensing of Environment, 3:99=107.

White, D. and S. Rushforth (1973), Brigham Young University, personal communication.

Chapter 3

REFERENCES

Ayers, J.C., Stoermer, E.F. and P. McWilliam (1967), "Recently Noted Changes in the Biology-Chemistry of Lake Michigan," in "Studies on the Environment on Eutrophication of Lake Michigan," Special Report #30, Grt. Lakes Res. Div., U. of Mich., pp. 95-111.

Bathurst, Robin G.C. (1971), "Carbonate Sediments and Their Diagenesis," Developments in Sedimentology 12, Elsevier Publ. Co., N.Y., N.Y.

Hicks, S. (1973), personal communication.

Sabatini, R.R. (1971), "The Feasibility of using Nimbus HRIR and their Measurements for Obtaining Surface Temperatures of Lake Michigan," Proc. 14th Conf. on Grt. Lakes Res., Int'l. Assoc. Grt. Lakes Res., pp. 487-494.

Somers, L.H. (1974), personal communication.

Strong, A.E. (1967), "The Over-water Development of a Lake Breeze in an Offshore Gradient Flow," Proc. 10th Conf. on Grt. Lakes Res., Int'l. Assoc. Grt. Lakes Res., pp. 240-250.

Strong, A.E., and D.R. Baker (1971), "Mapping Surface Temperatures on the Great Lakes from Satellite Infrared Data," Abstract of paper presented at 14th Conf. on Grt. Lakes Res., Toronto, Canada.

Strong, A.E., Stumpf, H.G., Hart, J.L. and J.A. Pritchard (1974), "Extensive Summer Upwelling on Lake Michigan during 1973 observed by NOAA-2 and ERTS-1 Satellites," In Proc. 9th Int'l. Symp. on Remote Sensing of Environ., pp. 923-932

United States Coast Guard (1973), Frankfort Lifeboat Station, personal communication.

Chapter 4

REFERENCES

McClain, E.P. (1973). Qualitative Use of Satellite Vidicon Data for Delimiting Sea Ice Conditions. Arctic, Vol. 26, No. 1, pp. 44-57.

Wiesnet, D.R., McGinnis, D.F. and M.C. McMillan (1975). Evaluation of ERTS-1 data for certain hydrological uses. Final Report NASA/GSFC, Greenbelt, Md.

Chapter 5

REFERENCES

Cox, C. and W. Munk (1954). Measurement of the roughness of the sea surface from photographs of sun's glitter. J. Opt. Soc. Am. 44: 838-850.

Levanon, N. (1971). Determination of the sea surface slope distribution and wind velocity using sun glitter viewed from a synchronous satellite. J. Phys. Oc. 1(3):214-220.

McClain, E.P. and Strong, A.E. (1969). On anomalous dark patches in satellite-viewed areas. Mon. Wea. Rev. 97(12):875-884.

Strong, A.E. and I.S. Ruff (1970). Utilizing satellite-observed solar reflections from the sea surface as an indicator of surface wind speeds. Rem. Sens. of Environ. 1(3):181-185.

Strong, A.E. (1972). The constraint of sunglint on visible data gathered by Earth satellites. In proc. 4th Annual Earth Resources Program Review, NASA/MSC, Houston, Tex. pp.86-1 to 86-13.

Chapter 6

REFERENCES

Strong, A.E. (1974). Great Lakes Temperature Maps by Satellite. Proc. 17th Conf. on Great Lakes Research, Internat. Assoc. Grt. Lakes Res., pp. 321-333.

Wiesnet, D.R., McGinnis, D.F. and M.C. McMillan (1975). Evaluation of ERTS-1 data for certain hydrological uses. Final Report. NASA/GSFC, Greenbelt, Md.

Chapter 7

REFERENCES

Ayers, J.C. (1959). The Currents of Lakes Michigan and Huron, Great Lakes Res. Inst., U. of Michigan, 51 pp.

Ayers, J.C. (1959), "Great Lakes waters, their circulation and physical and chemical characteristics." Paper presented to the Great Lakes Basin Symp., 29 December 1959, Chicago, Ill.

Ayers, J.C. (1964). Currents and Related Problems at Metropolitan Beach, Lake St. Clair, Great Lakes Res. Div., U. of Michigan, 55 pp.

Ayers, J.C., D.V. Anderson, D.C. Chandler, and G.H. Lauff (1956). Currents and Water Masses of Lake Huron, Treat Lakes Res. Inst., U. of Michigan, 101 pp.

Ayers, J.C., D.C. Chandler, G.H. Lauff, C.F. Powers, and E.B. Henson (1958). Currents and Water Masses of Lake Michigan, Great Lakes Res. Inst., U. of Michigan, 169 pp.

Bellaire, F.R. (1964). A comparison of methods of current determinations, Proc. 7th Conf. on Great Lakes Res., Great Lakes Res. Div., U. of Michigan, pp. 171-178.

Gedney, R.T. and W. Lick (1972). Wind-driven currents in Lake Erie, J. Geophys. Res., 77:2714-2723.

Harrington, M.W. (1895). The Surface Currents of the Great Lakes, U.S. Weather Bureau Bulletin B.

Hough, J.L. (1958), Geology of the Great Lakes, University of Illinois Press, Urbana, 313 pp.

Jones, D.L. and Bellaire, F.R. (1962), "A Numerical Procedure for computing wind-driven currents on the Great Lakes." Proc. 5th Conf. on Great Lakes Res., Public. #9, Great Lakes Res. Div., Univ. of Ann Arbor, pp. 93-102.

Simons, T.J. (1971). Development of numerical models of Lake Ontario, Proc. 14th Conf. on Great Lakes Res., Internat. Assoc. Great Lakes Res., pp. 654-669.

Simons, T.J. (1972). Development of numerical models of Lake Ontario: Part 2, Proc. 15th Conf. on Great Lakes Res., Internat. Assoc. Great Lakes Res., pp. 655-672.

Simons, T.J. and D.E. Jordan (1972). Computation of Water Circulation of Lake Ontario for Observed Winds, 20 April - 14 May 1971, Canada Centre for Inland Waters, Paper No. 9, 43 pp.

Strong, A.E. (1973), NASA ERSP Weekly Abstracts, NTIS (E73-70747), U.S. Dept. of Commerce, p. 119-120.

Watanabe, K. (1974). Detection of several sea states around Japan from multispectral scanner imageries by ERTS-1. In Proc. 9th Internat. Symp. on Rem. Sens. of Environ., Environ. Res. Inst. of Mich., Ann Arbor (in press).

APPENDICES

TABLE A1. 4 Great Lakes and L. St. Clair

(29 Cycles thru Dec 73)

Cycle beginning	Orbit	Cycle beginning	Orbit
8/1/72	124	4/10/73	3638
8/19/72	375	4/28/73	3889
9/6/72	626	5/16/73	4140
9/24/72	877	6/3/73	4391
10/12/72	1128	6/21/73	4642
10/30/72	1379	7/9/73	4893
11/17/72	1630	7/27/73	5144
12/5/72	1881	8/14/73	5395
12/23/72	2132	9/1/73	5646
1/10/73	2383	9/19/73	5897
1/28/73	2634	10/7/73	6148
2/15/73	2885	10/25/73	6399
3/5/73	3136	11/12/73	6650
3/23/73	3387	11/30/73	6901
		12/18/73	7152

ORIGINAL PAGE IS
OF POOR QUALITY

TABLE A2. SOUTHERN LAKE MICHIGAN SURFACE WIND DATA
(tens of degrees, mph) X = missing data

Date	Station	T_0	T_{-6}	T_{-12}	T_{-18}	T_{-24}	T_{-48}	T_{-72}	Resultant Wind
9 Aug 72	Dunne Crib	0113	3218	X	3025	2418	3214	2210	NW 15
25 Aug 72	"	1813	1609	X	2309	2510	1411	1810	S 8
14 Sep 72	"	0215	3029	X	2508	2020	0404	2213	W 11
1 Oct 72	"	2220	2118	X	2610	3208	3215	1816	W 9
2 Oct 72	"	1111	1908	X	2408	X	X	X	SW 10
19 Oct 72	"	3005	3214	X	3618	3415	3315	2215	NW 13
6 Nov 72	"	1411	1520	X	3022	1811	2911	0205	SW 7
24 Nov 72	"	2016	2016		2415	2518	3210	2905	W 9
13 Dec 72	"	2408	2714	X	2515	1407	2709	3016	W 12
16 Jan 73	"	2025	2022	X	2010	3406	2212	2217	SW 14
4 Feb 73	X	2207	X	2215	2215	2913	2210	1418	W 10
23 Feb 73	"	3419	3415	X	2911	2722	3426	3211	SW 14
11 Mar 73	"	2025	1822	X	0912	0712	0716	0710	E 10
30 Mar 73	"	3408	X	3222	3417	0210	1109	0710	N 10
17 Apr 73	"	1809	2010	X	2520	2528	1820	2010	SW 14
4 May 73	"	0509	3218	X	3226	3220	2530	1825	W 17
5 May 73	"	0711	0508	X	0710	0509	X	X	NW 6
24 May 73	"	0506	3607	X	3414	3418	1114	1602	NE 5
9 Jun 73	"	0706	2510	X	2028	2220	2518	0912	SW 14
10 Jun 73	"	2518	2210	X	0910	0706	X	X	SW 6
15 Jun 73	"	0515	3410	X	3607	3208	2225	2223	W 9
16 Jul 73	"	0509	0210	X	0515	0515	X	X	N 7
17 Jul 73	"	0510	1410	X	0512	0509	X	X	NE 6
3 Aug 73	"	2908	X	0208	0212	3215	2413	X	NW 9
21 Aug 73	"	0521	X	0212	3618	3415	2005	X	N 11
14 Oct 73	"	2512	X	2918	2718	2016	2016	X	SW 13
7 Dec 73	"	3417	X	2915	2914	2520	1622	X	W 11

TABLE A3. SOUTHERN LAKE HURON SURFACE WIND DATA
(tens of degrees, mph) X = missing data

Date	Station	T_0	T_{-6}	T_{-12}	T_{-18}	T_{-24}	T_{-48}	T_{-72}	Resultant Wind NW 15
9 Sep 72	Port Huron	3620	3210	3214	0220	0218	1810	2207	NW 4
28 Sep 72	"	1608	1408	0511	3615	3418	2010	2010	SE 1
20 Nov 72	"	1606	0725	0720	0917	0910	2006	1607	E 10
31 Jan 73	"	1118	0715	2705	2717	2715	3420	3606	N 8
18 Feb 73	"	2208	2208	2208	2506	2006	3627	0223	N 8
26 Mar 73	"	0220	0214	0216	3611	0508	0503	0503	NE 9
27 Mar 73	"	0208	X	3620	3628	X	X	X	N 13
13 Apr 73	"	3212	3205	0209	0214	0215	3208	2212	NW 6
14 Apr 73	"	2207	1807	X	3414	3212	X	X	W 5
19 May 73	"	0205	1610	1606	0512	0508	2708	2019	S 4
20 May 73	"	0210	0206	0208	0209	X	X	X	NE 1
7 Jun 73	"	2008	2206	X	2007	1808	2012	2008	S 7
25 Jun 73	"	0205	X	0505	0507	3209	2705	2207	N 4
13 Jul 73	"	2509	1808	1607	2205	X	3210	X	SW 5
18 Aug 73	"	3405	3408	0505	0510	1410	0205	0518	NE 3
23 Sep 73	"	2210	2211	2211	2210	1418	1408	X	S 9
11 Oct 73	"	1610	1610	1608	1605	1808	1606	X	S 8

ORIGINAL PAGE IS
OF POOR QUALITY

TABLE A4. LAKE ST. CLAIR SURFACE WIND DATA
(tens of degrees, mph) X = missing data

Date	Station	T_0	T_{-6}	T_{-12}	T_{-18}	T_{-24}	T_{-48}	T_{-72}	Resultant Wind
									NW 15
28 Sep 72	Selfridge AFB	1405	X	calm	0410	0110	2206	2108	SW 1
	Port Huron	1608	1408	0511	3615	3418	2010	2010	SE 1
	Detroit R. Light	1404	0703	0503	0504	3605	1804	2204	E 1
15 Oct 72	Selfridge AFB	3207	X	3508	3611	2609	calm	3612	NW 6
	Port Huron	X	X	X	X	X	X	X	---
	Detroit R. Light	calm	2709	3220	3215	2215	2702	3213	W 9
18 Feb 73	Selfridge AFB	2310	X	2305	2502	calm	3520	3614	NW 7
	Port Huron	2208	2208	2208	2506	2206	3627	0223	NW 8
	Detroit R. Light	X	X	X	X	X	X	X	---
8 Mar 73	Selfridge AFB	2808	X	2306	2710	1814	1401	0813	SW 3
	Port Huron	X	X	X	X	X	X	X	---
	Detroit R. Light	2205	2205	2207	1415	1415	calm	0520	SE 3
26 Mar 73	Selfridge AFB	0415	X	0204	1105	0707	0802	1002	NE 4
	Port Huron	0220	0214	0216	3611	0508	0503	0504	NE 9
	Detroit R. Light	0520	0510	0510	0910	0715	0910	calm	NE 8
27 Mar 73	Selfridge AFB	0805	X	0106	0218	0415	0707	0802	NE 7
	Port Huron	0208	X	3620	3628	X	X	X	NE 13
	Detroit R. Light	0708	3610	3615	3615	X	X	X	NE 10
13 Apr 73	Selfridge AFB	0506	X	calm	3612	0410	3011	2710	NW 6
	Port Huron	3212	3205	0209	0214	0215	3208	2212	NW 6
	Detroit R. Light	3210	3410	0508	0210	0210	2912	2210	NW 6
14 Apr 73	Selfridge AFB	2905	X	calm	0207	3506	0410	3011	N 4
	Port Huron	2207	1807	X	3414	X	X	X	NW 5
	Detroit R. Light	1805	1802	1808	2205	X	X	X	NW 3
20 May 73	Selfridge AFB	0209	X	calm	1509	1103	0305	2509	E 1
	Port Huron	0210	0206	0208	0209	0205	0508	2708	NE 3
	Detroit R. Light	3605	3610	0515	1410	1110	1405	3205	NE 4
7 Jun 73	Selfridge AFB	2404	X	calm	calm	1806	2412	3008	W 5
	Port Huron	2008	2208	X	2007	1808	2012	2008	SW 7
	Detroit R. Light	1808	2210	calm	calm	1808	1818	1805	S 9

ORIGINAL PAGE IS
OF POOR QUALITY

TABLE A4. (Continued)

Date	Station	T_0	T_{-6}	T_{-12}	T_{-18}	T_{-24}	T_{-48}	T_{-72}	Resultant Wind NW 15
24 Jun 73	Selfridge AFB	calm	X	calm	2603	2908	3107	2302	W 3
	Port Huron	3209	2505	0205	1805	2705	2207	X	SW 3
	Detroit R. Light	calm	2205	1815	1805	2705	calm	calm	S 4
25 Jun 73	Selfridge AFB	1101	X	0302	1606	calm	2908	e107	W 3
	Port Huron	0205	X	0505	0507	X	X	X	NW 4
	Detroit R. Light	0905	0905	0208	1612	X	X	X	SE 1
18 Aug 73	Selfridge AFB	3603	calm	calm	1806	0904	calm	0108	NE 1
	Port Huron	3405	3408	0505	0510	1410	0205	0518	NW 3
	Detroit R. Light	calm	calm	calm	1610	3204	calm	3415	NW 1

ORIGINAL PAGE IS OF POOR QUALITY

TABLE A5. LAKE ERIE SURFACE WIND DATA (WESTERN HALF)
(tens of degrees, mph) X = missing data

Date	Station	T_0	T_{-6}	T_{-12}	T_{-18}	T_{-24}	T_{-48}	T_{-72}	Resultant Wind NW 15
21 Aug 72	Cleveland	2211	1609	0705	0510	1811	0903	2710	SE 2
	Lorain	X	X	X	X	X	X	X	---
	Detroit R. Light	X	X	X	X	X	X	X	---
9 Sep 72	Cleveland	X	X	X	X	X	X	X	---
	Lorain	X	X	X	X	X	X	X	---
	Detroit R. Light	3602	3405	0504	calm	0204	1805	2204	NW 1
27 Sep 72	Cleveland	0522	3615	1810	2214	1810	1810	1808	S 5
	Lorain	X	X	X	X	X	X	X	---
	Detroit R. Light	X	X	X	X	X	X	X	---
28 Sep 72	Cleveland	X	X	X	X	X	X	X	---
	Lorain	X	X	X	X	X	X	X	---
	Detroit R. Light	1404	0703	0503	0504	3605	1804	2204	E 1
15 Oct 72	Cleveland	3416	3420	3623	3620	2218	3215	2914	NW 16
	Lorain	3214	3423	2508	2210	1804	2907	2710	NW 8
	Detroit R. Light	calm	2709	3220	3215	2215	2707	3213	W 9
1 Nov 72	Cleveland	0908	1109	0708	0511	0910	3610	3615	NE 7
	Lorain	X	X	X	X	X	X	X	---
	Detroit R. Light	X	X	X	X	X	X	X	---
20 Nov 72	Cleveland	X	X	X	X	X	X	X	---
	Lorain	0219	0220	0214	0907	1405	2206	0709	NE 7
	Detroit R. Light	3212	3618	0515	0719	0715	2212	3612	( )
13 Jan 73	Cleveland	1815	2208	2208	2215	2512	2515	2216	SW 12
	Lorain	1809	1409	1808	2209	2514	2218	2012	SW 10
	Detroit R. Light	X	X	X	X	X	X	X	---
31 Jan 73	Cleveland	1408	1805	2205	2215	2210	3624	3208	NW 6
	Lorain	0912	1408	1808	2212	2212	3233	0208	W 8
	Detroit R. Light	X	X	X	X	X	X	X	---
17 Feb 73	Cleveland	3410	0211	0218	3615	3615	0207	1405	N 10
	Lorain	X	X	X	X	X	X	X	---
	Detroit R. Light	X	X	X	X	X	X	X	---

ORIGINAL PAGE IS
OF POOR QUALITY

ORIGINAL PAGE IS
OF POOR QUALITY

TABLE A5. Continued

Date	Station	T_0	T_{-6}	T_{-12}	T_{-18}	T_{-24}	T_{-48}	T_{-72}	Resultant Wind NW 15
18 Feb 73	Cleveland	1808	1608	2503	3205	3410	3615	0207	N 4
	Lorain	1810	1607	1809	2705	2906	2923	3414	W 7
	Detroit R. Light	X	X	X	X	X	X	X	---
8 March 73	Cleveland	2205	2005	2712	1820	1620	1614	1408	S 9
	Lorain	2505	1809	2210	2217	1419	1609	0709	S 8
	Detroit R. Light	X	X	X	X	X	X	X	S 3
26 Mar 73	Cleveland	0510	0710	1405	1810	0505	2205	3608	E 2
	Lorain	0519	0519	0513	0710	0907	0209	0509	NE 12
	Detroit R. Light	X	X	X	X	X	X	X	NE 8
27 Mar 73	Cleveland	X	X	X	X	X	X	X	---
	Lorain	0517	0215	0915	0516	0519	X	X	NE 15
	Detroit R. Light	X	X	X	X	X	X	X	NE 10
12 Apr 73	Cleveland	0707	2209	2209	2916	3215	2518	1812	W 11
	Lorain	X	X	X	X	X	X	X	---
	Detroit R. Light	X	X	X	X	X	X	X	---
13 Apr 73	Cleveland	3612	2910	0510	0211	0707	3215	2518	NW 8
	Lorain	3412	3611	0905	3407	0214	2719	2016	NE 6
	Detroit R. Light	3210	3410	0508	0210	0210	2912	2210	NW 6
14 Apr 73	Cleveland	X	X	X	X	X	X	X	---
	Lorain	1609	1409	1605	3409	3412	X	X	N 4
	Detroit R. Light	1805	1802	1808	2205	3210	X	X	NW 3
29 Apr 73	Cleveland	3209	3214	2920	2921	2924	0425	0516	N 12
	Lorain	X	X	X	X	X	X	X	---
	Detroit R. Light	X	X	X	X	X	X	X	---
30 Apr 73	Cleveland	2010	1808	1810	0503	3209	2924	0525	W 5
	Lorain	X	X	X	X	X	X	X	---
	Detroit R. Light	X	X	X	X	X	X	X	---
18 May 73	Cleveland	3607	0208	2918	3210	0208	2216	2510	W 8
	Lorain	X	X	X	X	X	X	X	---
	Detroit R. Light	X	X	X	X	X	X	X	---

TABLE A5. Continued

Date	Station	T_0	T_{-6}	T_{-12}	T_{-18}	T_{-24}	T_{-48}	T_{-72}	Resultant Wind NW 15
19 May 73	Cleveland	1610	1411	1405	0507	3607	0208	2216	E 3
	Lorain	X	X	X	X	X	X	X	---
	Detroit R. Light	X	X	X	X	X	X	X	---
20 May 73	Cleveland	X	X	X	X	X	X	X	---
	Lorain	0520	0517	0713	0710	1614	3609	3214	NE 9
	Detroit R. Light	3605	3610	0515	1410	1110	1405	3205	NE 4
5 Jun 73	Cleveland	2215	1611	2725	3406	2512	1809	0504	SW 6
	Lorain	X	X	X	X	X	X	X	---
	Detroit R. Light	X	X	X	X	X	X	X	---
7 Jun 73	Cleveland	X	X	X	X	X	X	X	---
	Lorain	1809	2010	1607	1610	1809	1616	2007	S 10
	Detroit R. Light	1808	2210	calm	calm	1808	1818	1805	S 9
23 Jun 73	Cleveland	2909	3214	calm	3208	2510	2507	1610	W 5
	Lorain	X	X	X	X	X	X	X	---
	Detroit R. Light	X	X	X	X	X	X	X	---
24 Jun 73	Cleveland	X	X	X	X	X	X	X	---
	Lorain	2710	1608	1609	0205	2708	2507	2509	SW 4
	Detroit R. Light	calm	2205	1815	1805	2705	calm	calm	E 4
25 Jun 73	Cleveland	X	X	X	X	X	X	X	---
	Lorain	3612	0909	0707	0508	2710	X	X	S 4
	Detroit R. Light	0905	0908	0208	1612	calm	X	X	SE 1
29 Jul 73	Cleveland	3610	3415	2715	2518	2210	2514	1808	W 10
	Lorain	X	X	X	X	X	X	X	---
	Detroit R. Light	X	X	X	X	X	X	X	---
18 Aug 73	Cleveland	X	X	X	X	X	X	X	---
	Lorain	X	X	X	X	X	X	X	---
	Detroit R. Light	calm	calm	calm	1610	3204	calm	3415	NW 1
3 Sep 73	Cleveland	X	X	X	X	X	X	X	---
	Lorain	1804	1410	0907	0710	1610	2704	3605	E 3
	Detroit R. Light	1106	calm	1410	1408	calm	1408	2004	SE 5

ORIGINAL PAGE IS
OF POOR QUALITY

TABLE A5. Continued

Date	Station	T_0	T_{-6}	T_{-12}	T_{-18}	T_{-24}	T_{-48}	T_{-72}	Resultant Wind NW 15
4 Sep 73	Cleveland	X	X	X	X	X	X	X	---
	Lorain	3205	1610	1409	0510	1804	1610	2704	SE 6
	Detroit R. Light	X	1410	1410	0910	1106	calm	1408	SE 6
9 Oct 73	Cleveland	X	X	X	X	X	X	X	---
	Lorain	2505	0904	0905	3411	2205	1607	1113	E 4
	Detroit R. Light	calm	3605	1405	1410	0208	0904	1808	E 3
10 Oct 73	Cleveland	X	X	X	X	X	X	X	---
	Lorain	2505	1407	1405	0510	2505	2205	1607	SE 3
	Detroit R. Light	calm	calm	0905	1108	calm	0208	0904	NE 4
2 Dec 73	Cleveland	X	X	X	X	X	X	X	---
	Lorain	1411	1110	0910	0510	3612	2217	2722	SW 3
	Detroit R. Light	1415	1415	0914	0908	3615	2215	2715	S 5
3 Dec 73	Cleveland	X	X	X	X	X	X	X	---
	Lorain	2012	1817	1413	1612	1411	3612	2217	S 5
	Detroit R. Light	1817	1812	1812	1812	1415	3615	2215	S 4
21 Dec 73	Cleveland	X	X	X	X	X	X	X	---
	Lorain	3230	2924	2925	0707	0707	0714	0512	NW 5
	Detroit R. Light	2918	2915	2915	3210	3620	0720	3205	N 7

ORIGINAL PAGE IS OF POOR QUALITY

TABLE A6. LAKE ERIE SURFACE WIND DATA (EASTERN HALF)
(tens of degrees, mph) X = missing data

Date	Station	T_0	T_{-6}	T_{-12}	T_{-18}	T_{-24}	T_{-48}	T_{-72}	Resultant Wind NW 15
21 Aug 72	Buffalo, N.Y.	2007	1104	0905	X	X	2004	2012	SE 4
	Erie, Pa.	2509	1810	1809	0506	0207	0709	2515	S 4
	Ashtabula, O.	1810	1413	0905	0206	1805	2004	2514	SE 3
9 Sep 72	Buffalo, N.Y.	3617	3410	3611	0203	2210	2212	2205	W 4
	Erie, Pa.	X	X	X	X	X	X	X	---
	Ashtabula, O.	X	X	X	X	X	X	X	---
27 Sep 72	Buffalo, N.Y.	X	X	X	X	X	X	X	---
	Erie, Pa.	X	X	X	X	X	X	X	---
	Ashtabula, O.	3618	2513	2015	2010	1815	2010	1810	S 11
15 Oct 72	Buffalo, N.Y.	3610	2912	3217	2925	2225	1403	3412	W 10
	Erie, Pa.	3212	3410	3415	2725	2220	3607	2708	NW 9
	Ashtabula, O.	3225	3424	3625	2528	1810	1808	2715	NW 9
1 Nov 72	Buffalo, N.Y.	X	X	X	X	X	X	X	---
	Erie, Pa.	1106	1406	0710	0506	1106	3610	3610	NE 5
	Ashtabula, O.	0909	0711	0913	0708	1112	3605	3626	NE 8
20 Nov 72	Buffalo, N.Y.	3614	0212	0709	0909	0906	2907	2203	NE 4
	Erie, Pa.	3610	0220	0508	0507	1408	1804	calm	NE 6
	Ashtabula, O.	X	X	X	X	X	X	X	---
13 Jan 73	Buffalo, N.Y.	2010	2010	2712	2710	2725	3213	2530	W 12
	Erie, Pa.	X	X	X	X	X	X	X	---
	Ashtabula, O.	X	X	X	X	X	X	X	---
31 Jan 73	Buffalo, N.Y.	0915	0508	2914	2718	2530	3420	0507	NW 10
	Erie, Pa.	X	X	X	X	X	X	X	---
	Ashtabula, O.	X	X	X	X	X	X	X	---
17 Feb 73	Buffalo, N.Y.	2908	3611	3615	3417	3618	0204	calm	N 9
	Erie, Pa.	X	X	X	X	X	X	X	---
	Ashtabula, O.	3615	3622	3625	3621	3620	0905	1405	N 13
18 Feb 73	Buffalo, N.Y.	2515	2215	2215	2710	2908	X	X	W 6
	Erie, Pa.	X	X	X	X	X	X	X	---
	Ashtabula, O.	1810	1806	calm	3208	3615	3620	0905	N 6
8 Mar 73	Buffalo, N.Y.	2706	2708	2507	1818	1620	2503	0915	S 4
	Erie, Pa.	X	X	X	X	X	X	X	---
	Ashtabula, O.	1805	2205	2705	1420	1835	1805	0505	S 6
24 Mar 73	Buffalo, N.Y.	2505	2007	1807	2710	0206	0209	0908	N 2
	Erie, Pa.	X	X	X	X	X	X	X	---
	Ashtabula, O.	X	X	X	X	X	X	X	---
26 Mar 73	Buffalo, N.Y.	0510	0505	calm	calm	1107	X	X	E 1
	Erie, Pa.	X	X	X	X	X	X	X	---
	Ashtabula	0501	0501	0912	0510	0710	1405	3605	NE 5

TABLE A6. Continued

Date	Station	T_0	T_{-6}	T_{-12}	T_{-18}	T_{-24}	T_{-48}	T_{-72}	Resultant Wind NW 15
12 Apr 73	Buffalo, N.Y.	3209	1606	3408	3415	3218	2715	0911	W 5
	Erie, Pa.	X	X	X	X	X	X	X	---
	Ashtabula, O.	1806	2008	2716	2725	3622	2515	0912	W 9
13 Apr 73	Buffalo, N.Y.	3210	3210	3210	3215	3209	X	X	W 6
	Erie, Pa.	X	X	X	X	X	X	X	---
	Ashtabula, O.	3413	3615	3613	0207	1806	3622	2515	N 12
29 Apr 73	Buffalo, N.Y.	2512	3412	2710	2912	2910	0515	0910	N 8
	Erie, Pa.	X	X	X	X	X	X	X	---
	Ashtabula, O.	2717	2714	3215	2722	2725	0722	0520	N 6
30 Apr 73	Buffalo, N.Y.	1106	1605	2205	2515	X	X	X	NW 3
	Erie, Pa.	X	X	X	X	X	X	X	---
	Ashtabula, O.	1810	1406	calm	2511	2712	2725	0722	W 6
18 May 73	Buffalo, N.Y.	2709	3212	2907	2515	3209	2508	2905	W 8
	Erie, Pa.	X	X	X	X	X	X	X	---
	Ashtabula, O.	3412	3211	2910	2507	3407	2015	2509	W 7
19 May 73	Buffalo, N.Y.	2205	1805	2710	2715	2709	X	X	W 6
	Erie, Pa.	X	X	X	X	X	X	X	---
	Ashtabula, O.	1811	2012	0707	2510	3412	3407	2015	SW 3
5 Jun 73	Buffalo, N.Y.	2205	1803	2505	2008	2709	2703	2705	SW 4
	Erie, Pa.	X	X	X	X	X	X	X	---
	Ashtabula, O.	1812	1810	2207	2508	2009	1812	0905	S 8
23 Jun 73	Buffalo, N.Y.	2511	2007	2208	2512	2008	2206	2704	SW 7
	Erie, Pa.	X	X	X	X	X	X	X	---
	Ashtabula, O.	2712	2510	calm	2517	2212	2510	calm	SW 3
24 Jun 73	Buffalo, N.Y.	2214	2010	1404	2512	X	X	X	SW 7
	Erie, Pa.	X	X	X	X	X	X	X	---
	Ashtabula, O.	X	X	X	X	X	X	X	---
11 Jul 73	Buffalo, N.Y.	3410	0208	3609	2210	2207	2508	2510	W 4
	Erie, Pa.	X	X	X	X	X	X	X	---
	Ashtabula, O.	X	X	X	X	X	X	X	---
29 Jul 73	Buffalo, N.Y.	3206	2708	2708	2020	2213	2224	2205	SW 13
	Erie, Pa.	X	X	X	X	X	X	X	---
	Ashtabula, O.	3415	3412	2520	3620	2016	2220	1812	W 9
30 Jul 73	Buffalo, N.Y.	X	2005	2510	2712	X	X	X	SW 9
	Erie, Pa.	X	X	X	X	X	X	X	---
	Ashtabula	X	X	X	X	X	X	X	---

TABLE A7. LAKE ONTARIO SURFACE WIND DATA (COMPLETE)
(tens of degrees, mph) X = missing data

Date	Station	T_0	T_{-6}	T_{-12}	T_{-18}	T_{-24}	T_{-48}	T_{-72}	Resultant Wind NW 15
19 Aug 72	Oswego	X	X	X	X	X	X	X	---
	Rochester	2209	2209	3206	3210	1604	1605	0506	SW 2
	Fort Niagara	X	X	X	X	X	X	X	---
20 Aug 72	Oswego	X	X	X	X	X	X	X	---
	Rochester	3607	3607	3409	2909	2209	1604	1605	NW 2
	Fort Niagara	X	X	X	X	X	X	X	---
6 Sep 72	Oswego	X	X	X	X	X	X	X	---
	Rochester	2008	2010	2710	3608	2009	2209	3408	SW 6
	Fort Niagara	3605	3110	2712	2908	2507	3410	3415	SW 9
7 Sep 72	Oswego	X	X	X	X	X	X	X	---
	Rochester	1808	1604	0508	1605	2008	2009	2209	S 4
	Fort Niagara	2511	2507	2510	3613	3605	2507	3410	W 6
13 Oct 72	Oswego	X	X	X	X	X	X	X	---
	Rochester	X	X	X	X	X	X	X	---
	Fort Niagara	2507	3613	3215	3220	3210	2510	2510	NW 10
29 Jan 73	Oswego	X	X	X	X	X	X	X	---
	Rochester	X	X	X	X	X	X	X	---
	Fort Niagara	3423	3430	3420	3616	3607	3613	2705	N 17
23 Mar 73	Oswego	X	X	X	X	X	X	X	---
	Rochester	X	X	X	X	X	X	X	---
	Fort Niagara	3205	0904	0904	0514	0520	0915	0528	NE 11
24 Mar 73	Oswego	X	X	X	X	X	X	X	---
	Rochester	X	X	X	X	X	X	X	---
	Fort Niagara	calm	2703	0905	3208	3205	0520	0915	NE 7
12 Apr 73	Oswego	3210	3412	0525	3225	2725	2707	3610	N 10
	Rochester	X	X	X	X	X	X	X	---
	Fort Niagara	calm	2705	2714	3620	3620	2910	3610	NW 9
29 Apr 73	Oswego	3225	2927	1810	3210	calm	0912	0505	NW 3
	Rochester	X	X	X	X	X	X	X	---
	Fort Niagara	3210	3218	2517	3620	3617	2720	0912	NW 12
16 May 73	Oswego	calm	2508	2710	3215	0505	3205	2715	W 8
	Rochester	X	X	X	X	X	X	X	---
	Fort Niagara	2214	2710	2712	3205	3208	3605	2219	W 7
2 Jun 73	Oswego	0508	3608	3610	2710	2715	3205	calm	NW 6
	Rochester	X	X	X	X	X	X	X	---
	Fort Niagara	2505	2505	2502	2708	2514	2710	3405	W 6
3 Jun 73	Oswego	1810	1805	calm	2705	0508	2715	3205	W 5
	Rochester	X	X	X	X	X	X	X	---
	Fort Niagara	3603	2512	3609	3614	2505	2514	2710	W 8

ORIGINAL PAGE IS
OF POOR QUALITY

ORIGINAL PAGE IS
OF POOR QUALITY

TABLE A7. Continued

Date	Station	T_0	T_{-6}	T_{-12}	T_{-18}	T_{-24}	T_{-48}	T_{-72}	Resultant Wind NW 15
20 Jun 73	Oswego	1807	calm	1803	calm	calm	2710	0508	W 2
	Rochester	X	X	X	X	X	X	X	---
	Fort Niagara	2510	2902	3610	3618	3610	27072	3605	NW 6
23 Jun 73	Oswego	calm	calm	1802	1805	1805	1805	1807	S 4
	Rochester	X	X	X	X	X	X	X	---
	Fort Niagara	2505	2510	2705	2923	2507	2205	2510	W 8
8 Jul 73	Oswego	2708	2205	2708	3210	calm	3210	2910	W 7
	Rochester	X	X	X	X	X	X	X	---
	Fort Niagara	2510	2510	2515	2515	2510	2505	2910	W 10
9 Jul 73	Oswego	3207	2905	2705	2210	2708	calm	3210	W 4
	Rochester	X	X	X	X	X	X	X	---
	Fort Niagara	2908	2705	2515	2510	2510	2510	2505	W 9
11 Jul 73	Oswego	X	X	X	X	X	X	X	---
	Rochester	X	X	X	X	X	X	X	---
	Fort Niagara	3419	3413	3210	2703	2205	2908	2510	NW 8
27 Jul 73	Oswego	1808	1810	calm	1805	3605	1805	calm	S 4
	Rochester	X	X	X	X	X	X	X	---
	Fort Niagara	2515	2510	2508	2510	2509	2205	2210	SW 8
28 Jul 73	Oswego	1810	1805	2210	2708	1808	3605	1805	SW 3
	Rochester	X	X	X	X	X	X	X	---
	Fort Niagara	2509	2510	2513	2728	2515	2509	2205	W 12
29 Jul 73	Oswego	X	X	X	X	X	X	X	---
	Rochester	X	X	X	X	X	X	X	---
	Fort Niagara	2711	2710	2712	2510	2509	2515	2509	W 10
15 Aug 73	Oswego	1405	1805	1805	1806	1806	3210	3207	W 3
	Rochester	3605	1603	1605	0505	1405	2211	2510	SW 5
	Fort Niagara	3615	3413	3610	3611	2507	2508	2908	NW 7
2 Sep 73	Oswego	2705	1805	1805	3202	calm	1808	2710	S 5
	Rochester	2208	1807	1804	0905	1810	2004	2010	S 5
	Fort Niagara	1807	1609	1607	3405	1604	1806	1610	S 6
19 Sep 73	Oswego	2208	1805	3210	3215	3220	1409	3218	NW 4
	Rochester	1808	2208	2210	2512	3225	1408	3212	SW 5
	Fort Niagara	X	X	X	X	X	X	X	---
25 Oct 73	Oswego	1807	1805	1805	calm	2007	2205	calm	S 4
	Rochester	0703	1607	1403	3604	1805	2705	1808	S 3
	Fort Niagara	calm	2203	0505	3602	1804	calm	1605	SE 1
26 Oct 73	Oswego	3209	1805	1810	1807	1807	2007	2205	S 7
	Rochester	2210	1812	2005	2008	0703	1805	2705	S 6
	Fort Niagara	1810	1615	1405	1414	calm	1804	calm	SE 7